博 士 論 文

(Doctoral Thesis)

A Theoretical Study on the Mechanism for the Reduction of Effective g-factor in Graphene

グラフェンにおける有効g因子の減少のメカニズムに関する理論的研究

Shrestha Amit

広島大学大学院先端物質科学研究科

Graduate School of Advanced Sciences of Matter
Hiroshima University

2022 年 3月
(March 2022)

目　　次
(Table of Contents)

主 論 文

(Main thesis)

Contents

List of Tables

List of Figures

Chapter 1

Introduction

Graphene is two-dimensional layer of carbon atoms arranged in a hexagonal lattice, a thinnest material at one atom thick, and also incredibly strong. Graphene is a remarkable material that is getting a lot of attention and rapidly rising on the horizon of material science and condensed matter physics due to its unusual properties in a magnetic field [1–30]. Such a astonishing properties are strong orbital diamagnetism [1–13], unconventional oscillation of magnetization [14–16], and half integer quantum Hall effect [17–27, 30]. Graphene represents a conceptually new class of materials that offers new inroads into low-dimensional physics which provide a fertile ground for many applications such as electronic and spintronic devices [28–37].

Few years back, our group has developed the magnetic field containing relativistic tight-binding approximation (MFRTB) method [38] which allows us to calculate the electronic structure of materials taking effects of magnetic field, periodic potential and relativistic effects such as the spin-orbit (SO) interaction into consideration. With MFRTB method, we can revisit the several phenomenon like dHvA oscillation [39–41], magnetic breakdown [41] and can also predict additional oscillation peaks of the magnetization [40] which the conventional LK formula [42] can't explain. In this method the effect of magnetic field is taken as the perturbation and the hopping integrals are evaluated using perturbation theory [38]. The effect of magnetic field is appeared in so-called Peierls phase factor which multiplies the hopping integral in the absence of a magnetic field giving the approximated form of magnetic hopping integral [38]. However, there are some rooms to increase the accuracy of the magnetic hopping integrals. In order to address this discrepancy, our group also developed the nonperturbative MFRTB method [43], in which the effect of magnetic field is incorporated by using the nonperturbative method. With this method, the approximated form of magnetic hopping integrals that goes beyond the approximation of using the Peierls phase factor [43] are obtained successfully. Thus, this method is suitable for describing and investigating magnetic properties of graphene.

Among various physical quantities which determine electronic properties, optical properties, chemical properties and thermal conductivity, the g-factor of graphene is the key-quantity on determining magnetic properties of materials like spin-related properties such as the spin relaxation time. Recently, a reduction in the g-factor of graphene has been reported in the experiments on electron spin resonance (ESR) [28, 29] when graphene is subjected to an external magnetic field. The observed g-factor is about 3.1 percent smaller than that of a free electron (g=2.0023). The g-factor is evaluated in these experiments

by taking effect of an external magnetic field in to account to estimate the gap between the lowest unoccupied state (LUS) and highest occupied state (HOS), which exists at the K-point of the Brillouin Zone in case of graphene [44–46]. Usually, the SO interaction, which is related to the spatially symmetric potential of the honeycomb lattice, causes this HOS-LUS gap in graphene. In the absence of SO interactions, the energy bands of graphene are described at low energies by a two-dimensional Dirac equation with linear dispersion centered on the hexagonal corners of the honeycomb lattice Brillouin zone [47]. Such a SO interaction apparently does not depend on the external magnetic field [48]. Hence, the g-factor is expected to be constant (g=2.0023) regardless of the external magnetic field [28, 29]. However, it is clearly shown that the reduction in g-factor is about 3.1 percent in experiments [28, 29] for external magnetic field of 1 T. This is not just of scientific importance, but knowing the cause of the reduction offers up a new pathway for graphene's emerging popularity, such as in spin electronics applications.

This thesis is aimed at theoretically elucidating the mechanism of the reduced g-factor in graphene. As one of the causes, it is expected that the internal magnetic field induced by the strong orbital diamagnetism [1–9, 49, 50] might affect on the splitting of the HOS-LUS gap in graphene. This may cause the reduction of the effective g-factor in graphene. In the present work, the nonperturbative MFRTB method is used in order to evaluate the effect of the strong orbital diamagnetism of graphene on the effective g-factor. By means of nonperturbative method we may revisit the strong orbital diamagnetism of graphene and we may confirm theoretically that one of the sources for the reduction in g-factor of graphene is diamagnetism. In addition, the magnetic field dependence of the bulk SO interaction can be investigated by means of the nonperturbative MFRTB method, so that we may check whether the bulk SO interaction affects on the HOS-LUS gap or not.

In recent ESR experiments [28, 29], graphene sheet is deposited on the SiC substrate. Due to the existence of substrate breaking of space inversion symmetry occurs. So, there exists an asymmetric potential along the direction perpendicular to the graphene sheet. This causes the effective magnetic field parallel to the plane of graphene sheet. This is Rashba effect and it has grown tremendous interest in the field of spintronics [51, 52]. In the nonperturbative MFRTB method, the effect of the substrate is not considered and hence there is no breaking of space inversion symmetry in the system. This implies that the Rashba-type SO interaction [50] is ignored in the nonperturbative MFRTB method.

Rashba effect gives rise to the additional Hamiltonian that is so called as the Rashba Hamiltonian and modifies the energy spectrum of the electrons and introduces a splitting on the electronic band [53]. Precisely, the work function causes this asymmetric potential. Near the surface, electrons are controlled by this work function which spatially spread in the region determine by electron density. Since, the magnetic field is the cross product between the gradient of the asymmetric potential and the momentum of the electron [51], this work function causes magnetic field which is in-plane direction of the graphene sheet. This magnetic field is coupled with the spin magnetic moment, which forms a kind of SO interaction. The spin magnetic moment may tilt towards the in-plane direction in the presence of external magnetic field applied perpendicular to the graphene sheet. This tilting of spin magnetic moment depends on strength of Rashba effect. Hence, Rashba effect could be another potential source for the reduction of the g-factor in graphene [51].

In this thesis, initially, nonperturbative MFRTB method is used to investigate the magnetic properties of graphene. We found that the sheet magnetization, the magnetic moment per unit area, shows a characteristic dependence on the magnetic field. Investigation on effect of the orbital diamagnetism and SO interaction in effective g-factor has been made to quest for the reason why effective g-factor is smaller than that of a free electron. As will be shown later, this method alone does not fully account for the reduction of g-factor in graphene. In order to address shortcoming of this method, we discuss the reduction of effective g-factor by Rashba-type SO interaction by using empty lattice model. As shown later, it explains satisfactorily that the primary cause for the reduction of g-factor in graphene is the Rashba effect. As an extended work, we reformulate the MFRTB method by incorporating Rashba effect in order to include the effects of the orbital magnetic moment which is ignored in empty lattice model and then to re-evaluate the diamagnetism of graphene.

This thesis is organized as follows. In chapter 2, nonperturbative MFRTB method is described taking overlap integral into account. The shortcoming of Hofstadter and MFRTB methods are addressed by the application range of nonperturbative MFRTB method from the low to high magnetic field region by evaluating energy eigenvalue, hopping and overlap integrals by means of nonperturbative method. In chapter 3, we apply nonperturbative MFRTB method to graphene immersed in magnetic field. The magnetic properties of graphene are investigated. Namely, the non-monotonic dependence of sheet magnetization on magnetic field and the effect of orbital diamagnetism and SO interaction on effective g-factor are discussed. The effect of the Rashba effect on the g-factor is discussed in chapter 4. An empty lattice model mainly focusing on Rashba effect is utilized for this purpose. Specifically, a procedure to calculate the reduction of the g-factor due to Rashba effect is presented in section 4.1. Then an energy splitting at the K-point caused by the Rashba effect is discussed in section 4.2. This energy splitting directly modifies the energy band structure of graphene and reflects on the magnitude of the g-factor. The details of the energy band structure are also described in section 4.3. Calculation of the reduction of the g-factor carried out in section 4.4 based on a method that is appropriate for the analysis of the results of the previously mentioned experiments on ESR. In order to incorporate the Rashba effect into the nonpertubative MFRTB method, we need to calculate the matrix elements of the Rashba Hamiltonian. In chapter 5, the nonperturbative MFRTB method is reformulated to incorporate the Rashba effect. Finally, the significance of this work and issues for future work that need to address are discussed in chapter 6 .

Chapter 2

Nonperturbative Magnetic Field Containing Relativistic Tight Binding (MFRTB) Method

In this chapter, we reformulate the MFRTB method by incorporating overlap integral. For the approximation of matrix element of Hamiltonian and overlap matrices, the accuracy of magnetic hopping integrals and overlap integrals has been improved by non-perturbative method. The variational principle is used to calculate the eigenfunctions and eigenvalues in the nonperturbative method.

2.1 Nonperturbative Magnetic Field Containing Relativistic Tight Binding (MFRTB) Method taking overlap integral into account

When crystalline material is immersed in an uniform magnetic field, the electrons in the system are influenced by both periodic potential of the crystal and the magnetic field.

The Dirac equation for an electron is given by [54]

$$H\Phi_{\mathbf{k}}(\mathbf{r}) = E_{\mathbf{k}}\Phi_{\mathbf{k}}(\mathbf{r}). \tag{2.1}$$

with

$$H = c\alpha \cdot [\mathbf{p} + eA(\mathbf{r})] + \beta mc^2 + \sum_{\mathbf{R_n}} \sum_{i} V_{a_i}(\mathbf{r} - \mathbf{R_n} - \mathbf{d_i}), \tag{2.2}$$

where $V_{a_i}(\mathbf{r} - \mathbf{R_n} - \mathbf{d_i})$ denotes the scalar potential caused by nucleus of an atom a_i located at $\mathbf{R_n} + \mathbf{d_i}$, $\mathbf{R_n}$ is translational vector of lattice, $\mathbf{d_i}$ is position vector of an atom a_i, $\mathbf{A}(\mathbf{r})$ is vector potential of uniform magnetic field, and c, e, and m denotes the velocity of light, elementary charge and rest mass of an electron respectively. The matrices $\alpha = (\alpha_x, \alpha_y, \alpha_z)$ and β stand for 4×4 matrices.

For a uniform magnetic field $\mathbf{B} = (0, 0, B)$ applied along the z-axis, the Landau gauge used for $\mathbf{A}(\mathbf{r})$ is given by

$$\mathbf{A}(\mathbf{r}) = (0, Bx, 0), \tag{2.3}$$

where B is magnitude of magnetic field. $\Phi_{\mathbf{k}}$ is four component wave function for an electron in the uniform magnetic field where the subscript '$\mathbf{k}$' is the wave vector that belongs to the magnetic first Brillouin Zone [38].

In the nonperturbative MFRTB method, $\Phi_{\mathbf{k}}$ is expanded by using relativistic atomic orbitals $\psi_{\xi}^{a_i,\mathbf{R_n}+\mathbf{d_i}}(\mathbf{r})$ for constituent atoms immersed in the uniform magnetic field. Relativistic atomic orbitals obey the Dirac equation of an isolated atom located at $\mathbf{R_n} + \mathbf{d_i}$ and immersed in the uniform magnetic field. That is to say,

$$[c\alpha \cdot \{\mathbf{p} + e\mathbf{A}(\mathbf{r})\} + \beta mc^2 + V_{a_i}(\mathbf{r} - \mathbf{R_n} - \mathbf{d_i})]\psi_{\xi}^{a_i,\mathbf{R_n}+\mathbf{d_i}}(\mathbf{r}) = \varepsilon_{\xi}^{a_i,\mathbf{R_n}+\mathbf{d_i}}\psi_{\xi}^{a_i,\mathbf{R_n}+\mathbf{d_i}}(\mathbf{r}), \tag{2.4}$$

where $\psi_{\xi}^{a_i,\mathbf{R_n}+\mathbf{d_i}}$ and $\varepsilon_{\xi}^{a_i,\mathbf{R_n}+\mathbf{d_i}}$ denote the relativistic atomic orbital and atomic spectrum in the uniform magnetic field. The subscript 'ξ' is the quantum number in atomic system.

Expanding $\Phi_{\mathbf{k}}(\mathbf{r})$ in terms of relativistic wave function $\psi_{\xi}^{a_i,\mathbf{R_n}+\mathbf{d_i}}(\mathbf{r})$ of atoms immersed in the uniform magnetic field as a basis function , we have

$$\Phi_{\mathbf{k}}(\mathbf{r}) = \sum_{\mathbf{R_n}} \sum_{i} \sum_{\xi} C_{\mathbf{k}}^{\xi}(\mathbf{R_n} + \mathbf{d_i})\psi_{\xi}^{a_i,\mathbf{R_n}+\mathbf{d_i}}(\mathbf{r}), \tag{2.5}$$

where $C_{\mathbf{k}}^{\xi}(\mathbf{R_n} + \mathbf{d_i})$ is expansion coefficient which is to be determined. Substituting Eq.(2.5) in Eq.(2.1), we get

$$\sum_{\mathbf{R_n}} \sum_{i} \sum_{\xi} C_{\mathbf{k}}^{\xi}(\mathbf{R_n} + \mathbf{d_i}) H\psi_{\xi}^{a_i,\mathbf{R_n}+\mathbf{d_i}}(\mathbf{r}) = E_{\mathbf{k}} \sum_{\mathbf{R_n}} \sum_{i} \sum_{\xi} C_{\mathbf{k}}^{\xi}(\mathbf{R_n} + \mathbf{d_i})\psi_{\xi}^{a_i,\mathbf{R_n}+\mathbf{d_i}}(\mathbf{r}). \tag{2.6}$$

Multiplying by $\psi_{\eta}^{a_j,\mathbf{R_m}+\mathbf{d_j}}(\mathbf{r})^{\dagger}$ on both sides of Eq.(2.6) and integrating with respect to $\mathbf{r}$, we get,

$$\sum_{\mathbf{R_n}} \sum_{i} \sum_{\xi} C_{\mathbf{k}}^{\xi}(\mathbf{R_n} + \mathbf{d_i})\mathcal{H}_{\mathbf{R_m}j\eta,\mathbf{R_n}i\xi} = E_{\mathbf{k}} \sum_{\mathbf{R_n}} \sum_{i} \sum_{\xi} C_{\mathbf{k}}^{\xi}(\mathbf{R_n} + \mathbf{d_i})\mathcal{S}_{\mathbf{R_m}j\eta,\mathbf{R_n}i\xi}, \tag{2.7}$$

where $\mathcal{H}_{\mathbf{R_m}j\eta,\mathbf{R_n}i\xi}$ and $\mathcal{S}_{\mathbf{R_m}j\eta,\mathbf{R_n}i\xi}$ are Hamiltonian and Overlap matrices, respectively, and they are given by

$$\mathcal{H}_{\mathbf{R_m}j\eta,\mathbf{R_n}i\xi} = \int \psi_{\eta}^{a_j,\mathbf{R_m}+\mathbf{d_j}}(\mathbf{r})^{\dagger} H \psi_{\xi}^{a_i,\mathbf{R_n}+\mathbf{d_i}}(\mathbf{r}) d^3r, \tag{2.8}$$

$$\mathcal{S}_{\mathbf{R_m}j\eta,\mathbf{R_n}i\xi} = \int \psi_{\eta}^{a_j,\mathbf{R_m}+\mathbf{d_j}}(\mathbf{r})^{\dagger} \psi_{\xi}^{a_i,\mathbf{R_n}+\mathbf{d_i}}(\mathbf{r}) d^3r. \tag{2.9}$$

Next, we rewrite, $\mathcal{H}_{\mathbf{R_m}j\eta,\mathbf{R_n}i\xi}$ and $\mathcal{S}_{\mathbf{R_m}j\eta,\mathbf{R_n}i\xi}$. For this purpose, let's rewrite Dirac Hamiltonian given by Eq.(2.2) in an uniform magnetic field as

$$H_{\mathbf{R_m}j\eta,\mathbf{R_n}i\xi} = \frac{1}{2}[c\alpha\cdot\{\mathbf{p}+e\mathbf{A}\mathbf{r}\}+\beta m_0c^2+V_{a_j}(\mathbf{r}-\mathbf{R_m}-\mathbf{d_j})+\sum_{l\neq j}V_{a_l}(\mathbf{r}-\mathbf{R_m}-\mathbf{d_l})$$
$$+\sum_{k\neq m}\sum_{l}V_{a_l}(\mathbf{r}-\mathbf{R_{\boldsymbol{k}}}-\mathbf{d_l})]+\frac{1}{2}[c\alpha\cdot\{\mathbf{p}+e\mathbf{A}\mathbf{r}\}+\beta m_0c^2+V_{a_i}(\mathbf{r}-\mathbf{R_n}-\mathbf{d_i})$$
$$+\sum_{l\neq i}V_{a_l}(\mathbf{r}-\mathbf{R_n}-\mathbf{d_l})+\sum_{k\neq n}\sum_{l}V_{a_l}(\mathbf{r}-\mathbf{R_{\boldsymbol{k}}}-\mathbf{d_l})] \tag{2.10}$$

Substituting Eq.(2.10) in Eq.(2.8), we have

$$H_{\mathbf{R_m}j\eta,\mathbf{R_n}i\xi} = \frac{1}{2}\{\varepsilon_\eta^{a_j,\mathbf{R_m}+\mathbf{d_j}}+\varepsilon_\xi^{a_i,\mathbf{R_n}+\mathbf{d_i}}\}\mathcal{S}_{\mathbf{R_m}j\eta,\mathbf{R_n}i\xi}$$
$$+\frac{1}{2}\sum_{l\neq j}\int\psi_\eta^{a_j,\mathbf{R_m}+\mathbf{d_j}}(\mathbf{r})^\dagger V_{a_l}(\mathbf{r}-\mathbf{R_m}-\mathbf{d_l})\psi_\xi^{a_i,\mathbf{R_n}+\mathbf{d_i}}(\mathbf{r})d^3r$$
$$+\frac{1}{2}\sum_{l\neq i}\int\psi_\eta^{a_j,\mathbf{R_m}+\mathbf{d_j}}(\mathbf{r})^\dagger V_{a_l}(\mathbf{r}-\mathbf{R_n}-\mathbf{d_l})\psi_\xi^{a_i,\mathbf{R_n}+\mathbf{d_i}}(\mathbf{r})d^3r$$
$$+\frac{1}{2}\sum_{k\neq m}\sum_{l}\int\psi_\eta^{a_j,\mathbf{R_m}+\mathbf{d_j}}(\mathbf{r})^\dagger V_{a_l}(\mathbf{r}-\mathbf{R_{\boldsymbol{k}}}-\mathbf{d_l})\psi_\xi^{a_i,\mathbf{R_n}+\mathbf{d_i}}(\mathbf{r})d^3r$$
$$+\frac{1}{2}\sum_{k\neq n}\sum_{l}\int\psi_\eta^{a_j,\mathbf{R_m}+\mathbf{d_j}}(\mathbf{r})^\dagger V_{a_l}(\mathbf{r}-\mathbf{R_{\boldsymbol{k}}}-\mathbf{d_l})\psi_\xi^{a_i,\mathbf{R_n}+\mathbf{d_i}}(\mathbf{r})d^3r. \tag{2.11}$$

We consider the matrix element in two cases.

(i) $\mathbf{R_m}+\mathbf{d_j}=\mathbf{R_n}+\mathbf{d_i}$

In this case, Eq.(2.11) becomes

$$\mathcal{H}_{\mathbf{R_m}j\eta,\mathbf{R_n}i\xi} = \varepsilon_\xi^{a_i,\mathbf{R_n}+\mathbf{d_i}}\delta_{\eta,\xi}+\sum_{l\neq i}\int\psi_\eta^{a_i,\mathbf{R_n}+\mathbf{d_i}}(\mathbf{r})^\dagger V_{a_l}(\mathbf{r}-\mathbf{R_m}-\mathbf{d_l})\psi_\xi^{a_i,\mathbf{R_n}+\mathbf{d_i}}(\mathbf{r})d^3r$$
$$+\sum_{k\neq n}\sum_{l}\int\psi_\eta^{a_i,\mathbf{R_n}+\mathbf{d_i}}(\mathbf{r})^\dagger V_{a_l}(\mathbf{r}-\mathbf{R_{\boldsymbol{k}}}-\mathbf{d_l})\psi_\xi^{a_i,\mathbf{R_n}+\mathbf{d_i}}(\mathbf{r})d^3r. \tag{2.12}$$

The second and third terms of RHS of above equation represents the energy of crystal field. So, above equation can be written as

$$\mathcal{H}_{\mathbf{R_m}j\eta,\mathbf{R_n}i\xi} = \varepsilon_\xi^{a_i,\mathbf{R_n}+\mathbf{d_i}}\delta_{\eta,\xi}+\Delta\varepsilon_\xi^{a_i,\mathbf{R_n}+\mathbf{d_i}}\delta_{\eta,\xi}, \tag{2.13}$$

where $\Delta\varepsilon_\xi^{a_i,\mathbf{R_n}+\mathbf{d_i}}$ denotes the energy of crystal field and is given by

$$\Delta\varepsilon_\xi^{a_i,\mathbf{R_n}+\mathbf{d_i}}\delta_{\eta,\xi} = \int\psi_\eta^{a_i,\mathbf{R_n}+\mathbf{d_i}}(\mathbf{r})^\dagger\left\{\sum_{\substack{\mathbf{R_{\boldsymbol{k}}}\\ \mathbf{R_{\boldsymbol{k}}}+\mathbf{d_l}\neq\mathbf{R_n}+\mathbf{d_i}}}\sum_{l}V_{a_l}(\mathbf{r}-\mathbf{R_{\boldsymbol{k}}}-\mathbf{d_l})\right\}$$
$$\times\psi_\xi^{a_i,\mathbf{R_n}+\mathbf{d_i}}(\mathbf{r})d^3r. \tag{2.14}$$

(ii) $\mathbf{R_m} + \mathbf{d_j} \neq \mathbf{R_n} + \mathbf{d_i}$

In this case, Eq.(2.11) becomes

$$\begin{aligned}
\mathcal{H}_{\mathbf{R_m}j\eta,\mathbf{R_n}i\xi} &= \frac{1}{2}\{\varepsilon_\eta^{a_j,\mathbf{R_m}+\mathbf{d_j}} + \varepsilon_\xi^{a_i,\mathbf{R_n}+\mathbf{d_i}}\}\mathcal{S}_{\mathbf{R_m}j\eta,\mathbf{R_n}i\xi} \\
&\quad + \frac{1}{2}\sum_{l\neq j}\int \psi_\eta^{a_j,\mathbf{R_m}+\mathbf{d_j}}(\mathbf{r})^\dagger V_{a_l}(\mathbf{r}-\mathbf{R_m}-\mathbf{d_l})\psi_\xi^{a_i,\mathbf{R_n}+\mathbf{d_i}}(\mathbf{r})d^3r \\
&\quad + \frac{1}{2}\sum_{l\neq i}\int \psi_\eta^{a_j,\mathbf{R_m}+\mathbf{d_j}}(\mathbf{r})^\dagger V_{a_l}(\mathbf{r}-\mathbf{R_n}-\mathbf{d_l})\psi_\xi^{a_i,\mathbf{R_n}+\mathbf{d_i}}(\mathbf{r})d^3r \\
&\quad + \frac{1}{2}\sum_{k\neq m}\sum_{l}\int \psi_\eta^{a_j,\mathbf{R_m}+\mathbf{d_j}}(\mathbf{r})^\dagger V_{a_l}(\mathbf{r}-\mathbf{R_k}-\mathbf{d_l})\psi_\xi^{a_i,\mathbf{R_n}+\mathbf{d_i}}(\mathbf{r})d^3r \\
&\quad + \frac{1}{2}\sum_{k\neq n}\sum_{l}\int \psi_\eta^{a_j,\mathbf{R_m}+\mathbf{d_j}}(\mathbf{r})^\dagger V_{a_l}(\mathbf{r}-\mathbf{R_k}-\mathbf{d_l})\psi_\xi^{a_i,\mathbf{R_n}+\mathbf{d_i}}(\mathbf{r})d^3r \\
&= \frac{1}{2}\{\varepsilon_\eta^{a_j,\mathbf{R_m}+\mathbf{d_j}} + \varepsilon_\xi^{a_i,\mathbf{R_n}+\mathbf{d_i}}\}\int \psi_\eta^{a_j,\mathbf{R_m}+\mathbf{d_j}}(\mathbf{r})^\dagger \psi_\xi^{a_i,\mathbf{R_n}+\mathbf{d_i}}(\mathbf{r})d^3r \\
&\quad + \frac{1}{2}\sum_{l\neq j}\int \psi_\eta^{a_j,\mathbf{R_m}+\mathbf{d_j}}(\mathbf{r})^\dagger V_{a_l}(\mathbf{r}-\mathbf{R_m}-\mathbf{d_l})\psi_\xi^{a_i,\mathbf{R_n}+\mathbf{d_i}}(\mathbf{r})d^3r \\
&\quad + \frac{1}{2}\sum_{l\neq i}\int \psi_\eta^{a_j,\mathbf{R_m}+\mathbf{d_j}}(\mathbf{r})^\dagger V_{a_l}(\mathbf{r}-\mathbf{R_n}-\mathbf{d_l})\psi_\xi^{a_i,\mathbf{R_n}+\mathbf{d_i}}(\mathbf{r})d^3r \\
&\quad + \frac{1}{2}\sum_{k\neq m}\sum_{l}\int \psi_\eta^{a_j,\mathbf{R_m}+\mathbf{d_j}}(\mathbf{r})^\dagger V_{a_l}(\mathbf{r}-\mathbf{R_k}-\mathbf{d_l})\psi_\xi^{a_i,\mathbf{R_n}+\mathbf{d_i}}(\mathbf{r})d^3r \\
&\quad + \frac{1}{2}\sum_{k\neq n}\sum_{l}\int \psi_\eta^{a_j,\mathbf{R_m}+\mathbf{d_j}}(\mathbf{r})^\dagger V_{a_l}(\mathbf{r}-\mathbf{R_k}-\mathbf{d_l})\psi_\xi^{a_i,\mathbf{R_n}+\mathbf{d_i}}(\mathbf{r})d^3r. \quad (2.15)
\end{aligned}$$

The second and third terms corresponds to the integral involving three centers. Since, these integrals are generally smaller than other integral hence can be neglected.

Now, let us take third integral

$$\begin{aligned}
&\frac{1}{2}\sum_{k\neq m}\sum_{l}\int \psi_\eta^{a_j,\mathbf{R_m}+\mathbf{d_j}}(\mathbf{r})^\dagger V_{a_l}(\mathbf{r}-\mathbf{R_k}-\mathbf{d_l})\psi_\xi^{a_i,\mathbf{R_n}+\mathbf{d_i}}(\mathbf{r})d^3r \\
&\qquad = \frac{1}{2}\int \psi_\eta^{a_j,\mathbf{R_m}+\mathbf{d_j}}(\mathbf{r})^\dagger V_{a_i}(\mathbf{r}-\mathbf{R_n}-\mathbf{d_i})\psi_\xi^{a_i,\mathbf{R_n}+\mathbf{d_i}}(\mathbf{r})d^3r \\
&\qquad\quad + \frac{1}{2}\sum_{k\neq m,n}\sum_{\nu\neq i}\int \psi_\eta^{a_j,\mathbf{R_m}+\mathbf{d_j}}(\mathbf{r})^\dagger V_{a_l}(\mathbf{r}-\mathbf{R_k}-\mathbf{d}_\nu)\psi_\xi^{a_i,\mathbf{R_n}+\mathbf{d_i}}(\mathbf{r})d^3r \\
&\qquad\quad + \frac{1}{2}\sum_{k\neq m}\sum_{l\neq i,\nu}\int \psi_\eta^{a_j,\mathbf{R_m}+\mathbf{d_j}}(\mathbf{r})^\dagger V_{a_l}(\mathbf{r}-\mathbf{R_k}-\mathbf{d_l})\psi_\xi^{a_i,\mathbf{R_n}+\mathbf{d_i}}(\mathbf{r})d^3r. \quad (2.16)
\end{aligned}$$

Last two integrals of Eq.(2.16) are three center integral and can be neglected compared to first. Then

$$\frac{1}{2}\sum_{k\neq m}\sum_{l}\int \psi_{\eta}^{a_j,\mathbf{R_m}+\mathbf{d_j}}(\mathbf{r})^{\dagger}V_{a_l}(\mathbf{r}-\mathbf{R_k}-\mathbf{d_l})\psi_{\xi}^{a_i,\mathbf{R_n}+\mathbf{d_i}}(\mathbf{r})d^3r$$
$$\approx \frac{1}{2}\int \psi_{\eta}^{a_j,\mathbf{R_m}+\mathbf{d_j}}(\mathbf{r})^{\dagger}V_{a_i}(\mathbf{r}-\mathbf{R_n}-\mathbf{d_i})\psi_{\xi}^{a_i,\mathbf{R_n}+\mathbf{d_i}}(\mathbf{r})d^3r. \quad (2.17)$$

Similarly, let us take fourth integral of Eq.(2.15), we have

$$\frac{1}{2}\sum_{k\neq n}\sum_{l}\int \psi_{\eta}^{a_j,\mathbf{R_m}+\mathbf{d_j}}(\mathbf{r})^{\dagger}V_{a_l}(\mathbf{r}-\mathbf{R_k}-\mathbf{d_l})\psi_{\xi}^{a_i,\mathbf{R_n}+\mathbf{d_i}}(\mathbf{r})d^3r$$
$$= \frac{1}{2}\int \psi_{\eta}^{a_j,\mathbf{R_m}+\mathbf{d_j}}(\mathbf{r})^{\dagger}V_{a_i}(\mathbf{r}-\mathbf{R_m}-\mathbf{d_j})\psi_{\xi}^{a_i,\mathbf{R_n}+\mathbf{d_i}}(\mathbf{r})d^3r$$
$$+ \frac{1}{2}\sum_{k\neq m,n}\sum_{\mu\neq i}\int \psi_{\eta}^{a_j,\mathbf{R_m}+\mathbf{d_j}}(\mathbf{r})^{\dagger}V_{a_\mu}(\mathbf{r}-\mathbf{R_k}-\mathbf{d}_{\mu})\psi_{\xi}^{a_i,\mathbf{R_n}+\mathbf{d_i}}(\mathbf{r})d^3r$$
$$+ \frac{1}{2}\sum_{k\neq m}\sum_{l\neq i,\mu}\int \psi_{\eta}^{a_j,\mathbf{R_m}+\mathbf{d_j}}(\mathbf{r})^{\dagger}V_{a_l}(\mathbf{r}-\mathbf{R_k}-\mathbf{d_l})\psi_{\xi}^{a_i,\mathbf{R_n}+\mathbf{d_i}}(\mathbf{r})d^3r. \quad (2.18)$$

Again, we neglect the three center integrals of Eq.(2.18), then we have

$$\frac{1}{2}\sum_{k\neq n}\sum_{l}\int \psi_{\eta}^{a_j,\mathbf{R_m}+\mathbf{d_j}}(\mathbf{r})^{\dagger}V_{a_l}(\mathbf{r}-\mathbf{R_k}-\mathbf{d_l})\psi_{\xi}^{a_i,\mathbf{R_n}+\mathbf{d_i}}(\mathbf{r})d^3r$$
$$\approx \frac{1}{2}\int \psi_{\eta}^{a_j,\mathbf{R_m}+\mathbf{d_j}}(\mathbf{r})^{\dagger}V_{a_j}(\mathbf{r}-\mathbf{R_m}-\mathbf{d_j})\psi_{\xi}^{a_i,\mathbf{R_n}+\mathbf{d_i}}(\mathbf{r})d^3r. \quad (2.19)$$

Thus, from Eqs.(2.15), (2.17) and (2.19), we have

$$\mathcal{H}_{\mathbf{R_m}j\eta,\mathbf{R_n}i\xi} \approx \frac{1}{2}\{\varepsilon_{\eta}^{a_j,\mathbf{R_m}+\mathbf{d_j}}+\varepsilon_{\xi}^{a_i,\mathbf{R_n}+\mathbf{d_i}}\}\int \psi_{\eta}^{a_j,\mathbf{R_m}+\mathbf{d_j}}(\mathbf{r})^{\dagger}\psi_{\xi}^{a_i,\mathbf{R_n}+\mathbf{d_i}}(\mathbf{r})d^3r$$
$$+ \frac{1}{2}\int \psi_{\eta}^{a_j,\mathbf{R_m}+\mathbf{d_j}}(\mathbf{r})^{\dagger}V_{a_i}(\mathbf{r}-\mathbf{R_n}-\mathbf{d_i})\psi_{\xi}^{a_i,\mathbf{R_n}+\mathbf{d_i}}(\mathbf{r})d^3r$$
$$+ \frac{1}{2}\int \psi_{\eta}^{a_j,\mathbf{R_m}+\mathbf{d_j}}(\mathbf{r})^{\dagger}V_{a_j}(\mathbf{r}-\mathbf{R_m}-\mathbf{d_j})\psi_{\xi}^{a_i,\mathbf{R_n}+\mathbf{d_i}}(\mathbf{r})d^3r.$$

Rearranging the above equation, we get

$$\mathcal{H}_{\mathbf{R_m}j\eta,\mathbf{R_n}i\xi} \approx \int \psi_{\eta}^{a_j,\mathbf{R_m}+\mathbf{d_j}}(\mathbf{r})^{\dagger}\left[\frac{V_{a_j}^{\eta}(\mathbf{r}-\mathbf{R_m}-\mathbf{d_j})+V_{a_i}^{\xi}(\mathbf{r}-\mathbf{R_n}-\mathbf{d_i})}{2}\right]$$
$$\times\psi_{\xi}^{a_i,\mathbf{R_n}+\mathbf{d_i}}(\mathbf{r})d^3r, \quad (2.20)$$

where

$$V_{a_j}^{\eta}(\mathbf{r}-\mathbf{R_m}-\mathbf{d_j}) = \varepsilon_{\eta}^{a_j,\mathbf{R_m}+\mathbf{d_j}}+V_{a_j}(\mathbf{r}-\mathbf{R_m}-\mathbf{d_j}), \quad (2.21)$$
$$V_{a_i}^{\xi}(\mathbf{r}-\mathbf{R_n}-\mathbf{d_i}) = \varepsilon_{\xi}^{a_i,\mathbf{R_n}+\mathbf{d_i}}+V_{a_i}(\mathbf{r}-\mathbf{R_n}-\mathbf{d_i}). \quad (2.22)$$

Finally, summarizing above two cases, Eq.(2.8) becomes

$$\mathcal{H}_{\mathbf{R_m}j\eta,\mathbf{R_n}i\xi} \approx (\varepsilon_{\xi}^{a_i,\mathbf{R_n}+\mathbf{d_i}}+\Delta\varepsilon_{\xi}^{a_i,\mathbf{R_n}+\mathbf{d_i}})\delta_{\mathbf{R_m},\mathbf{R_n}}\delta_{j,i}\delta_{\eta,\xi}+(1-\delta_{\mathbf{R_m},\mathbf{R_n}}\delta_{j,i})$$
$$\times\int \psi_{\eta}^{a_j,\mathbf{R_m}+\mathbf{d_j}}(\mathbf{r})^{\dagger}\left[\frac{V_{a_j}^{\eta}(\mathbf{r}-\mathbf{R_m}-\mathbf{d_j})+V_{a_i}^{\xi}(\mathbf{r}-\mathbf{R_n}-\mathbf{d_i})}{2}\right]$$
$$\times\psi_{\xi}^{a_i,\mathbf{R_n}+\mathbf{d_i}}(\mathbf{r})d^3r. \quad (2.23)$$

Similarly, for same cases, the overlap matrix given by Eq.(2.9) becomes

(i) $\mathbf{R_m} + \mathbf{d_j} = \mathbf{R_n} + \mathbf{d_i}$

$$\mathcal{S}_{\mathbf{R_m}j\eta,\mathbf{R_n}i\xi} = \delta_{\mathbf{R_m},\mathbf{R_n}}\delta_{j,i}\delta_{\eta,\xi}. \tag{2.24}$$

(ii) $\mathbf{R_m} + \mathbf{d_j} \neq \mathbf{R_n} + \mathbf{d_i}$

$$\mathcal{S}_{\mathbf{R_m}j\eta,\mathbf{R_n}i\xi} = \int \psi_\eta^{a_j,\mathbf{R_m}+\mathbf{d_j}}(\mathbf{r})^\dagger \psi_\xi^{a_i,\mathbf{R_n}+\mathbf{d_i}}(\mathbf{r}) d^3r. \tag{2.25}$$

Summarizing these two cases, we have the overlap matrix as

$$\mathcal{S}_{\mathbf{R_m}j\eta,\mathbf{R_n}i\xi} = \delta_{\mathbf{R_m},\mathbf{R_n}}\delta_{j,i}\delta_{\eta,\xi} + (1-\delta_{\mathbf{R_m},\mathbf{R_n}}\delta_{j,i}) \int \psi_\eta^{a_j,\mathbf{R_m}+\mathbf{d_j}}(\mathbf{r})^\dagger \psi_\xi^{a_i,\mathbf{R_n}+\mathbf{d_i}}(\mathbf{r}) d^3r. \tag{2.26}$$

From Eq.(2.4), Dirac equation for an atom immersed in uniform magnetic field and located at origin is given by

$$\left[c\alpha\cdot\{\mathbf{p}+e\mathbf{A}(\mathbf{r})\} + \beta mc^2 + V_{a_i}(\mathbf{r})\right]\psi_\xi^{a_i,0}(\mathbf{r}) = \epsilon_\xi^{a_i,0}\psi_\xi^{a_i,0}(\mathbf{r}). \tag{2.27}$$

Changing variables $\mathbf{r}$ to $\mathbf{r}-\mathbf{R_n}-\mathbf{d_i}$, we have

$$\begin{aligned}\left[c\alpha\cdot\{\mathbf{p}+e\mathbf{A}(\mathbf{r}-\mathbf{R_n}-\mathbf{d_i})\} + \beta mc^2 + V_{a_i}(\mathbf{r}-\mathbf{R_n}-\mathbf{d_i})\right]\psi_\xi^{a_i,0}(\mathbf{r}-\mathbf{R_n}-\mathbf{d_i}) \\ = \varepsilon_\xi^{a_i,0}\psi_\xi^{a_i,0}(\mathbf{r}-\mathbf{R_n}-\mathbf{d_i}).\end{aligned} \tag{2.28}$$

As $\mathbf{A}(\mathbf{r}-\mathbf{R_n}-\mathbf{d_i})$ and $\mathbf{A}(\mathbf{r})$ yield same magnetic field $\mathbf{B}$, they can be related by a gauge transformation as

$$\mathbf{A}(\mathbf{r}-\mathbf{R_n}-\mathbf{d_i}) = \mathbf{A}(\mathbf{r}) + \nabla\chi(\mathbf{r},\mathbf{R_n}+\mathbf{d_i}). \tag{2.29}$$

From Eqs.(2.3) and (2.29), we have

$$\chi(\mathbf{r},\mathbf{R_n}+\mathbf{d_i}) = -B(R_{nx}+d_{ix})y. \tag{2.30}$$

Vector potentials at Eqs.(2.4) and (2.28) are different from each other by the choice of the gauge given by Eq.(2.28). So, eigenfunctions and eigenvalues of each Eqs.(2.4) and (2.28) are related as

$$\psi_\xi^{a_i,0}(\mathbf{r}-\mathbf{R_n}-\mathbf{d_i}) = e^{-i\frac{e}{\hbar}\chi(\mathbf{r},\mathbf{R_n}+\mathbf{d_i})}\psi_\xi^{a_i,\mathbf{R_n}+\mathbf{d_i}}(\mathbf{r}) \tag{2.31}$$

and

$$\varepsilon_\xi^{a_i,0} = \varepsilon_\xi^{a_i,\mathbf{R_n}+\mathbf{d_i}}. \tag{2.32}$$

In addition, we have from Eqs.(2.14) and (2.31),

$$\Delta\varepsilon_\xi^{a_i,d_i} = \Delta\varepsilon_\xi^{a_i,\mathbf{R_n}+\mathbf{d_i}} = \Delta\epsilon_\xi^{a_i,0}. \tag{2.33}$$

Using Eqs.(2.31), (2.32) and (2.33), the Hamiltonian matrix is given by Eq.(2.23) becomes

$$\mathcal{H}_{\mathbf{R_m}j\eta,\mathbf{R_n}i\xi} = (\varepsilon_{\xi}^{a_i,0} + \Delta\varepsilon_{\xi}^{a_i,d_i})\delta_{\mathbf{R}_m,\mathbf{R}_n}\delta_{j,i}\delta_{\eta,\xi} + (1-\delta_{\mathbf{R_m},\mathbf{R_n}}\delta_{j,i}) \times e^{-i\frac{eB}{\hbar}(R_{nx}+d_{ix}-R_{mx}-d_{jx})(R_{my}+d_{jy})}\tilde{T}_{\eta,\xi}^{a_j,a_i}(\mathbf{R_n}-\mathbf{R_m}+\mathbf{d_i}-\mathbf{d_j}), \quad (2.34)$$

with

$$\tilde{T}_{\eta,\xi}^{a_j,a_i}(\mathbf{R_n}-\mathbf{R_m}+\mathbf{d_i}-\mathbf{d_j}) = \int \psi_{\eta}^{a_j,\mathbf{R_m}+\mathbf{d_j}}(\mathbf{r})^{\dagger}\left(\frac{V_{a_j}^{\eta}(\mathbf{r}-\mathbf{R_m}-\mathbf{d_j})+V_{a_i}^{\xi}(\mathbf{r}-\mathbf{R_n}-\mathbf{d_i})}{2}\right) \times \psi_{\xi}^{a_i,\mathbf{R_n}+\mathbf{d_i}}(\mathbf{r})d^3r. \quad (2.35)$$

Changing the variables $\mathbf{r} \to \mathbf{r}' - \mathbf{R_m} - \mathbf{d_j}$ with $\mathbf{R_l} \to \mathbf{R_n} - \mathbf{R_m}$, Eq.(2.35) becomes

$$\tilde{T}_{\eta,\xi}^{a_j,a_i}(\mathbf{R_l}+\mathbf{d_i}-\mathbf{d_j}) = \int \psi_{\eta}^{a_j,0}(\mathbf{r})^{\dagger}\left[\frac{V_{a_j}^{\eta}(\mathbf{r})+V_{a_i}^{\xi}(\mathbf{r}-\mathbf{R_l}-\mathbf{d_i}+\mathbf{d_j})}{2}\right]\psi_{\xi}^{a_i,\mathbf{R_l}+\mathbf{d_i}-\mathbf{d_j}}(\mathbf{r})d^3r. \quad (2.36)$$

Using Eqs.(2.21), (2.22) and (2.32), Eq.(2.36) becomes

$$\tilde{T}_{\eta,\xi}^{a_j,a_i}(\mathbf{R_l}+\mathbf{d_i}-\mathbf{d_j}) = T_{\eta,\xi}^{a_j,a_i}(\mathbf{R_l}+\mathbf{d_i}-\mathbf{d_j}) + \left(\frac{\varepsilon_{\eta}^{a_j,0}+\varepsilon_{\xi}^{a_i,0}}{2}\right)S_{\eta,\xi}^{a_j,a_i}(\mathbf{R_l}+\mathbf{d_i}-\mathbf{d_j}), \quad (2.37)$$

with

$$T_{\eta,\xi}^{a_j,a_i}(\mathbf{R_l}+\mathbf{d_i}-\mathbf{d_j}) = \int \psi_{\eta}^{a_j,0}(\mathbf{r})^{\dagger}\left[\frac{V_{a_j}(\mathbf{r})+V_{a_i}(\mathbf{r}-\mathbf{R_l}-\mathbf{d_i}+\mathbf{d_j})}{2}\right]\psi_{\xi}^{a_i,\mathbf{R_l}+\mathbf{d_i}-\mathbf{d_j}}(\mathbf{r})d^3r, \quad (2.38)$$

$$S_{\eta,\xi}^{a_j,a_i}(\mathbf{R_l}+\mathbf{d_i}-\mathbf{d_j}) = \int \psi_{\eta}^{a_j,0}(\mathbf{r})^{\dagger}\psi_{\xi}^{a_i,\mathbf{R_l}+\mathbf{d_i}-\mathbf{d_j}}(\mathbf{r})d^3r. \quad (2.39)$$

Eqs.(2.38) and (2.39) are the magnetic hopping integral and magnetic overlap integral respectively. Hence, the Hamiltonian matrix given by Eq.(2.34) becomes

$$\mathcal{H}_{\mathbf{R_m}j\eta,\mathbf{R_n}i\xi} = (\varepsilon_{\xi}^{a_i,0} + \Delta\varepsilon_{\xi}^{a_i,d_i})\delta_{\mathbf{R}_m,\mathbf{R}_n}\delta_{j,i}\delta_{\eta,\xi} + (1-\delta_{\mathbf{R_m},\mathbf{R_n}}\delta_{j,i}) \times e^{-i\frac{eB}{\hbar}(R_{lx}+d_{ix}-d_{jx})(R_{my}+d_{jy})}\tilde{T}_{\eta,\xi}^{a_j,a_i}(\mathbf{R_l}+\mathbf{d_i}-\mathbf{d_j}). \quad (2.40)$$

Similarly, the overlap matrix given by Eq.(2.26) can be written as

$$\mathcal{S}_{\mathbf{R_m}j\eta,\mathbf{R_n}i\xi} = \delta_{\mathbf{R_m},\mathbf{R_n}}\delta_{j,i}\delta_{\eta,\xi} + (1-\delta_{\mathbf{R_m},\mathbf{R_n}}\delta_{j,i}) \times e^{-i\frac{eB}{\hbar}(R_{lx}+d_{ix}-d_{jx})(R_{my}+d_{jy})}S_{\eta,\xi}^{a_j,a_i}(\mathbf{R}_l+\mathbf{d_i}-\mathbf{d_j}). \quad (2.41)$$

Substituting Eqs.(2.40) and (2.41) in Eq.(2.7), we get

$$
\begin{aligned}
(\varepsilon_{\eta}^{a_j,\mathbf{0}} + \Delta\varepsilon_{\eta}^{a_j,\mathbf{d_j}})C_{\mathbf{k}}^{\eta}(\mathbf{R_m}+\mathbf{d_j}) + \sum_{i}\sum_{\mathbf{R_n}}\sum_{\xi}(1-\delta_{\mathbf{R_m},\mathbf{R_n}}\delta_{j,i}) \\
\times e^{-i\frac{eB}{\hbar}(R_{lx}+d_{ix}-d_{jx})(R_{my}+d_{jy})}\tilde{T}_{\eta,\xi}^{a_j,a_i}(\mathbf{R_l}+\mathbf{d_i}-\mathbf{d_j})C_{\mathbf{k}}^{\xi}(\mathbf{R_n}+\mathbf{d_i}) \\
= E_{\mathbf{k}}\Bigg[C_{\mathbf{k}}^{\eta}(\mathbf{R_m}+\mathbf{d_j}) + \sum_{i}\sum_{\mathbf{R_n}}\sum_{\xi}(1-\delta_{\mathbf{R_m},\mathbf{R_n}}\delta_{j,i}) \\
\times e^{-i\frac{eB}{\hbar}(R_{lx}+d_{ix}-d_{jx})(R_{my}+d_{jy})}S_{\eta,\xi}^{a_j,a_i}(\mathbf{R_l}+\mathbf{d_i}-\mathbf{d_j})\Bigg]C_{\mathbf{k}}^{\xi}(\mathbf{R_n}+\mathbf{d_i}).
\end{aligned}
\tag{2.42}
$$

For convenience, let $\mathbf{T}_{W}(\mathbf{d_j})$ is the vectors connecting a_j atom to a_i atom which is independent of $\mathbf{R_m}$ but depends on $\mathbf{d_j}$. $\{W = 1, 2, 3...\}$. By using this symbol Eq.(2.42) becomes

$$
\begin{aligned}
(\varepsilon_{\eta}^{a_j,\mathbf{0}} + \Delta\varepsilon_{\eta}^{a_j,\mathbf{d_j}})C_{\mathbf{k}}^{\eta}(\mathbf{R_m}+\mathbf{d_j}) + \sum_{W}\sum_{\eta} e^{-i\frac{eB}{\hbar}\mathbf{T}_{Wx}(\mathbf{d_j})(R_{my}+d_{jy})} \\
\times \tilde{T}_{\eta,\xi}^{a_j,a_i}\{\mathbf{T}_{W}(\mathbf{d_j})\}C_{\mathbf{k}}^{\xi}\{\mathbf{T}_{W}(\mathbf{d_j})+\mathbf{R_m}+\mathbf{d_j}\} \\
= E_{\mathbf{k}}\left[C_{\mathbf{k}}^{\eta}(\mathbf{R_m}+\mathbf{d_j}) + \sum_{W}\sum_{\eta} e^{-i\frac{eB}{\hbar}\mathbf{T}_{Wx}(\mathbf{d_j})(R_{my}+d_{jy})}S_{\eta,\xi}^{a_j,a_i}\{\mathbf{T}_{W}(\mathbf{d_j})\}\right] \\
\times C_{\mathbf{k}}^{\xi}\{\mathbf{T}_{W}(\mathbf{d_j})+\mathbf{R_m}+\mathbf{d_j}\}.
\end{aligned}
\tag{2.43}
$$

Solving this simultaneous equation, the energy eigenvalue $E_{\mathbf{k}}$ and the coefficient $C_{\mathbf{k}}^{nlJM}(\mathbf{R_n}+\mathbf{d_i})$ can be obtained. In order to solve this equation, we need the values of $T_{\eta,\xi}^{a_j,a_i}\{\mathbf{T}_{W}(\mathbf{d_j})\}$ and $S_{\eta,\xi}^{a_j,a_i}\{\mathbf{T}_{W}(\mathbf{d_j})\}$. In the following section, the approximation of these matrix elements will be discussed.

2.2 Approximation of the matrix elements

Matrix elements of Hamiltonian matrix Eq.(2.40) and Overlap matrix Eq.(2.41) can be calculated with the estimation of $T_{\eta,\xi}^{a_j,a_i}(\mathbf{R}_l+\mathbf{d_i}-\mathbf{d_j})$, $S_{\eta,\xi}^{a_j,a_i}(\mathbf{R}_l+\mathbf{d_i}-\mathbf{d_j})$ and $\varepsilon_{\xi}^{a_i,0}$ and $\Delta\varepsilon_{\xi}^{a_i,d_i}$ by using nonperturbative method. In order to estimate these parameters, let's consider the Dirac equation Eq.(2.4), for an isolated atom that is located at origin and immersed in uniform magnetic field:

$$
\left[c\alpha\cdot\{\mathbf{p}+e\mathbf{A}(\mathbf{r})\}+\beta mc^2+V_{a_i}(\mathbf{r})\right]\psi_{\xi}^{a_i,0}(\mathbf{r}) = \varepsilon_{\xi}^{a_i,0}\psi_{\xi}^{a_i,0}(\mathbf{r}). \tag{2.44}
$$

The variational principle is used to evaluate the eigenfunctions and eigenvalues of Eq.(2.44) in the nonperturbative MFRTB method [43]. In particular, we consider matrix elements of the Hamiltonian of Eq.(2.44) by using finite number of relativistic atomic orbitals $\{\phi_{nlJM}^{a_i}(\mathbf{r})\}$ as a basis function [43], where $\{\phi_{nlJM}^{a_i}(\mathbf{r})\}$ denotes the relativistic atomic orbital for the atom a_i in the absence of the magnetic field.

The Dirac equation for an isolated atom is given by

$$
H_0\phi_{nlJM}^{a_i}(\mathbf{r}) = \bar{\varepsilon}_{nlJ}^{a_i}\phi_{nlJM}^{a_i}(\mathbf{r}), \tag{2.45}
$$

where

$$H_0 = c\alpha \cdot \mathbf{p} + \beta mc^2 + V_{a_i}(\mathbf{r}). \tag{2.46}$$

Let us consider the following matrix,

$$\begin{aligned} H_{n'l'J'M',nlJM} &= \int \phi^{a_i}_{n'l'J'M'}(\mathbf{r})^\dagger \left[c\alpha \cdot \{\mathbf{p} + e\mathbf{A}_{sym}(\mathbf{r})\} + \beta mc^2 + V_{a_i}(\mathbf{r})\right] \phi^{a_i}_{nlJM}(\mathbf{r}) d^3r \\ &= \int \phi^{a_i}_{n'l'J'M'}(\mathbf{r})^\dagger \left[c\alpha \cdot \mathbf{p} + \beta mc^2 + V_{a_i}(\mathbf{r})\right] \phi^{a_i}_{nlJM}(\mathbf{r}) d^3r \\ &\qquad + \int \phi^{a_i}_{n'l'J'M'}(\mathbf{r})^\dagger \{ce\alpha \cdot \mathbf{A}_{sym}(\mathbf{r})\} \phi^{a_i}_{nlJM}(\mathbf{r}) d^3r \\ &= \bar{\varepsilon}^{a_i}_{nlJ} \delta_{n',n} \delta_{l',l} \delta_{J',J} + H'_{n'l'J'M',nlJM}, \end{aligned} \tag{2.47}$$

with

$$H'_{n'l'J'M',nlJM} = \int \phi^{a_i}_{n'l'J'M'}(\mathbf{r})^\dagger \{ce\alpha \cdot \mathbf{A}_{sym}(\mathbf{r})\} \phi^{a_i}_{nlJM}(\mathbf{r}) d^3r, \tag{2.48}$$

where $\mathbf{A}_{sym}(\mathbf{r})$ is the vector potential in the symmetric gauge, and is given by $\left(-\frac{B}{2}y, \frac{B}{2}x, 0\right)$ Also we have, Pauli's spin matrices as:

$$\alpha_x = \begin{pmatrix} 0 & \sigma_x \\ \sigma_x & 0 \end{pmatrix}, \quad \alpha_y = \begin{pmatrix} 0 & \sigma_y \\ \sigma_y & 0 \end{pmatrix} \quad \text{and} \quad \alpha_z = \begin{pmatrix} 0 & \sigma_z \\ \sigma_z & 0 \end{pmatrix}. \tag{2.49}$$

From Eq.(2.48) and Eq.(2.49),we have

$$H'_{n'l'J'M',nlJM} = ce \int \phi^{a_i}_{\eta}(\mathbf{r})^\dagger \left\{ \mathbf{A}_{sym}(\mathbf{r}) \cdot \begin{pmatrix} 0 & \sigma \\ \sigma & 0 \end{pmatrix} \right\} \phi^{a_i}_{\xi}(\mathbf{r}) d^3r. \tag{2.50}$$

The eigenfunction of H_0 is given as the relativistic atomic orbital;

$$\phi^{a_i}_{nlJM} = \frac{1}{r} \begin{pmatrix} f^{a_i}_{nlJM}(\mathbf{r}) \\ g^{a_i}_{nlJM}(\mathbf{r}) \end{pmatrix} \tag{2.51}$$

with

$$f^{a_i}_{nlJM}(\mathbf{r}) = \frac{1}{r} F^{a_i}_{nlJM}(\mathbf{r}) y^M_{l,J}(\theta, \phi), \tag{2.52}$$

$$g^{a_i}_{nlJM}(\mathbf{r}) = \frac{1}{r} G^{a_i}_{nlJM}(\mathbf{r}) y^M_{l,J}(\theta, \phi). \tag{2.53}$$

Eqs.(2.52) and (2.53) are large and small components of unperturbed wave function $\varphi^{a_i}_{nlJM}(\mathbf{r})$. The function $y^M_{l,J}(\theta, \phi)$ denotes the spinor spherical harmonics:

$$y^M_{l,J}(\theta, \phi) = \begin{cases} \left.\begin{array}{l} \sqrt{\dfrac{J+M}{2J}} Y_{l,M-\frac{1}{2}}(\theta, \phi) \\ \sqrt{\dfrac{J-M}{2J}} Y_{l,M+\frac{1}{2}}(\theta, \phi) \end{array}\right\} \text{for} \quad J = l + \dfrac{1}{2} \\ \left.\begin{array}{l} -\sqrt{\dfrac{J+1-M}{2(J+1)}} Y_{l,M-\frac{1}{2}}(\theta, \phi) \\ \sqrt{\dfrac{J+1+M}{2(J+1)}} Y_{l,M+\frac{1}{2}}(\theta, \phi) \end{array}\right\} \text{for} \quad J = l - \dfrac{1}{2} \end{cases} \tag{2.54}$$

The small component of $\phi^{a_i}_{nlJM}(\mathbf{r})$ can be approximated by [54]

$$g^{a_i}_{nlJM}(\mathbf{r}) \approx \frac{1}{2mc}(\sigma \cdot \mathbf{p}) f^{a_i}_{nlJM}(\mathbf{r}). \tag{2.55}$$

Under this approximation, Eq.(2.50) reduces to

$$H'_{n'l'J'M',nlJM} \approx \frac{e}{2m} \int f^{a_j}_{n'l'J'M'}(\mathbf{r})^\dagger \left\{\mathbf{B}.(\mathbf{L}+2\mathbf{S})\right\} f^{a_i}_{nlJM}(\mathbf{r}) d^3r \tag{2.56}$$

with $\mathbf{S} = \frac{\hbar}{2}\sigma$.

Since magnetic field is along z-axis, we have

$$\mathbf{B} \cdot (\mathbf{L}+2\mathbf{S}) = B \begin{pmatrix} L_z + \hbar & 0 \\ 0 & L_z - \hbar \end{pmatrix}. \tag{2.57}$$

Let's calculate the matrix element of the $H'_{n'l'J'M',nlJM}$ for following cases:

$$\text{(i)}\ \ J' = l' + \frac{1}{2} \text{ and } J = l + \frac{1}{2},$$

$$\text{(ii)}\ \ J' = l' + \frac{1}{2} \text{ and } J = l - \frac{1}{2},$$

$$\text{(iii)}\ \ J' = l' - \frac{1}{2} \text{ and } J = l + \frac{1}{2},$$

$$\text{(iv)}\ \ J' = l' - \frac{1}{2} \text{ and } J = l - \frac{1}{2}.$$

Using Eqs.(2.54), (2.55), (2.56) and (2.57), we calculate the matrix element for above mentioned cases:

(i) $J' = l' + \frac{1}{2}$ and $J = l + \frac{1}{2}$ Using Eqs.(2.54), (2.55), (2.56) and (2.57), we have

$$\begin{aligned} H'_{n'l'J'M',nlJM} = \frac{eB\hbar}{2m} \Bigg\{ & \sqrt{\frac{(J'+M')(J+M)}{4J'J}} \left(M + \frac{1}{2}\right) \\ & + \sqrt{\frac{(J'-M')(J-M)}{4J'J}} \left(M - \frac{1}{2}\right) \Bigg\} \delta_{l',l}\delta_{J',J}\delta_{M',M} \\ & \times \int_0^\infty F^{a_i}_{n'l'J'}(r)^\dagger F^{a_i}_{nlJ}(r) dr. \end{aligned} \tag{2.58}$$

Taking in mind the fact that $J' = J$ if $l' = l$, the integral in Eq.(2.58) is approximated as $\delta_{n',n}$ due to orthogonality of $\phi^{a_i}_{nlJM}(\mathbf{r})$

So, Eq.(2.58) becomes,

$$H'_{n'l'J'M',nlJM} = \frac{eB\hbar}{2m_0} \left(\frac{2J+1}{2J}\right) M \delta_{n',n}\delta_{l',l}\delta_{J',J}\delta_{M',M}. \tag{2.59}$$

From Eqs.(2.47) and (2.59), we finally have the matrix element of the total Hamiltonian as

$$H_{n'l'J'M',nlJM} = \bar{\varepsilon}^{a_i}_{nlJ}\delta_{n',n}\delta_{l',l}\delta_{J',J} + \frac{eB\hbar}{2m} \left(\frac{2J+1}{2J}\right) M \delta_{n',n}\delta_{l',l}\delta_{J',J}\delta_{M',M}. \tag{2.60}$$

(ii) $J' = l' + \frac{1}{2}$ and $J = l - \frac{1}{2}$

In a way similar to case (i), we have

$$H'_{n'l'J'M',nlJM} = \frac{eB\hbar}{2m}\left\{-\sqrt{\frac{(J'+M')(J+1-M)}{4J'(J+1)}}\left(M+\frac{1}{2}\right)\right.$$
$$\left.+\sqrt{\frac{(J'-M')(J+1+M)}{4J'(J+1)}}\left(M-\frac{1}{2}\right)\right\}\delta_{l',l}\delta_{M',M}$$
$$\times\int_0^\infty F^{a_i}_{n'l'J'}(r)^\dagger F^{a_i}_{nlJ}(r)dr. \quad (2.61)$$

In the case where $l' = l$, we have $J' = J+1$. So, Eq.(2.61) becomes

$$H'_{n'l'J'M',nlJM} = \frac{eB\hbar}{2m}\left\{\frac{1}{2(J+1)}\left[-\sqrt{(J+1+M')(J+1-M)}\left(M+\frac{1}{2}\right)\right.\right.$$
$$\left.\left.+\sqrt{(J+1-M')(J+1+M)}\left(M-\frac{1}{2}\right)\right]\right\}$$
$$\times\delta_{l',l}\delta_{J',J+1}\delta_{M',M}S_{nlJ}, \quad (2.62)$$

where

$$S_{nlJ} = \int_0^\infty F^{a_i}_{nlJ+1}(r)^\dagger F^{a_i}_{nlJ}(r)dr. \quad (2.63)$$

From Eqs.(2.47), (2.62) and (2.63), we have the matrix element of the total Hamiltonian as

$$H_{n'l'J'M',nlJM} = \bar{\varepsilon}^{a_i}_{nlJ}\delta_{n',n}\delta_{l',l}\delta_{J',J} - \frac{eB\hbar}{2m}\left\{\frac{1}{2(J+1)}\left[\sqrt{(J+1+M')(J+1-M)}\right]\right\}$$
$$\times\delta_{l',l}\delta_{J'+1,J}\delta_{M',M}S_{nlJ}. \quad (2.64)$$

(iii) $J' = l' - \frac{1}{2}$ and $J = l + \frac{1}{2}$

In a way similar to the case (i), we have

$$H'_{n'l'J'M',nlJM} = \frac{eB\hbar}{2m}\left\{-\sqrt{\frac{(J+M)(J'+1-M')}{4J(J'+1)}}\left(M+\frac{1}{2}\right)\right.$$
$$\left.+\sqrt{\frac{(J-M)(J'+1+M')}{4J(J'+1)}}\left(M-\frac{1}{2}\right)\right\}\delta_{l',l}\delta_{M',M}$$
$$\times\int_0^\infty F^{a_i}_{n'l'J'}(r)^\dagger F^{a_i}_{nlJ}(r)dr. \quad (2.65)$$

In the case where $l' = l$, we have $J' = J - 1$ So, Eq.(2.65) becomes

$$H'_{n'l'J'M',nlJM} = \frac{eB\hbar}{2m}\left\{\frac{1}{2J}\left[-\sqrt{(J+M)(J-M')}\left(M+\frac{1}{2}\right)\right.\right.$$
$$\left.\left.+\sqrt{(J-M)(J+M')}\left(M-\frac{1}{2}\right)\right]\right\}\delta_{l',l}\delta_{J',J-1}\delta_{M',M}S^*_{nlJ}. \quad (2.66)$$

From Eqs.(2.47) and (2.66), we have the matrix element of the total Hamiltonian as

$$H_{n'l'J'M',nlJM} = \bar{\varepsilon}^{a_i}_{nlJ}\delta_{n',n}\delta_{l',l}\delta_{J',J} - \frac{eB\hbar}{2m}\left\{\frac{1}{2J}\left[\sqrt{(J+M)(J-M')}\right]\right\}$$
$$\times\,\delta_{l',l}\delta_{J',J-1}\delta_{M',M}S^*_{nlJ}. \quad (2.67)$$

(iv) $J' = l' - \frac{1}{2}$ and $J = l - \frac{1}{2}$

In a way similar to the case (i), we have

$$H'_{n'l'J'M',nlJM} = \frac{eB\hbar}{2m}\left\{\sqrt{\frac{(J'+1-M')(J+1-M)}{4(J'+1)(J+1)}}\left(M+\frac{1}{2}\right)\right.$$
$$\left.+\sqrt{\frac{(J'+1+M')(J+1+M)}{4(J'+1)(J+1)}}\left(M-\frac{1}{2}\right)\right\}\delta_{l',l}\delta_{M',M}$$
$$\times\int_0^\infty F^{a_i}_{n'l'J'}(r)^\dagger F^{a_i}_{nlJ}(r)dr. \quad (2.68)$$

If $l' = l$, then we have $J' = J$. So, Eq.(2.68) becomes,

$$H'_{n'l'J'M',nlJM} = \frac{eB\hbar}{2m}\left\{\frac{(2J+1)}{2(J+1)}\right\}M\delta_{n',n}\delta_{l',l}\delta_{J',J}\delta_{M',M}. \quad (2.69)$$

From Eqs.(2.47 and 2.69), we have the matrix element of the total Hamiltonian as

$$H_{n'l'J'M',nlJM} = \bar{\varepsilon}^{a_i}_{nlJ}\delta_{n',n}\delta_{l',l}\delta_{J',J} + \frac{eB\hbar}{2m}\left\{\frac{(2J+1)}{2(J+1)}\right\}M\delta_{n',n}\delta_{l',l}\delta_{J',J}\delta_{M',M}. \quad (2.70)$$

Now, to derive the matrix elements of Hamiltonian $H_{nlJM',nlJM}$, only the outermost atomic orbitals are taken into consideration. First, let's obtain the matrix elements corresponding to the following unperturbed atomic states:
(a) (n, l, J, M) with $J = l + \frac{1}{2}$, $M = \pm J$ for all l,
(b) $(n, l, J-1, M)$ and (n, l, J, M) with $J = l + \frac{1}{2}$, $M \neq \pm J$ for $l \neq 0$.

(a) Matrix elements of Hamiltonian $H_{nlJM',nlJM}$ corresponding to unperturbed atomic states (n, l, J, M) with $J = l + \frac{1}{2}$, $M = \pm J$ for all l.

For this case, Matrix elements of Hamiltonian $H_{nlJM',nlJM}$ can be obtained by considering the interaction between (n', l', J', M') and (n, l, J, M) atomic states and by using Eq.(2.60).

Since $J' = J$ and $M' = M$, Eq.(2.60) can be written as

$$H_{n'l'J'M',nlJM} = \bar{\varepsilon}^{a_i}_{nlJ} + \frac{eB\hbar}{2m}\left(\frac{2J+1}{2J}\right)M$$
$$= \bar{\varepsilon}^{a_i}_{nlJ} \pm \frac{eB\hbar}{4m}(2J+1)\,. \tag{2.71}$$

(b) Matrix elements of Hamiltonian $H_{nlJM',nlJM}$ corresponding to $(n, l, J-1, M)$ and (n, l, J, M) with $J = l + \frac{1}{2}$; $M \neq \pm J$ for $l \neq 0$.

We may have following interactions in general: $(n', l', J'-1, M')$ and $(n, l, J-1, M)$, $(n', l', J'-1, M')$ and (n, l, J, M), (n', l', J', M') and $(n, l, J-1, M)$ and (n', l', J', M') and (n, l, J, M). The matrix elements from the interactions between these unperturbed atomic states are shown in the Table 2.1. In the table, we use following symbol:

$$Z = \frac{eB\hbar}{2m} \tag{2.72}$$

Table 2.1: Matrix element of Hamiltonian corresponding to $(n, l, J-1, M)$ and (n, l, J, M) with $J = l + \frac{1}{2}$; $M \neq \pm J$ for $l \neq 0$.

	$(n, l, J-1, M)$	(n, l, J, M)
$(n', l', J'-1, M')$	$\bar{\varepsilon}^{a_i}_{nlJ} + Z\frac{(2J-1)}{2J}M$	$-Z\frac{\sqrt{J^2-M^2}}{2J}S_{nlJ}$
(n', l', J', M')	$-Z\frac{\sqrt{J^2-M^2}}{2J}S^*_{nlJ}$	$\bar{\varepsilon}^{a_i}_{nlJ} + Z\frac{(2J+1)}{2J}M$

Finally, diagonalizing the resultant matrix $H_{n'l'J'M',nlJM}$, we obtained eigenvalues and eigenfunctions corresponding to above mentioned unperturbed atomic states.

The eigenvalues corresponding to (n, l, J, M) with $J = l + \frac{1}{2}$; $M = \pm J$ for $l \neq 0$ can be obtained from Eq.(2.71) and is given by

$$\varepsilon^{a_i,0}_{\xi} = \bar{\varepsilon}^{a_i}_{nlJ} \pm \frac{eB\hbar}{4m}(2J+1)\,, \tag{2.73}$$

and corresponding eigenfunctions are given by

$$\psi^{a_i,0}_{\xi}(\mathbf{r}) = \phi^{a_i}_{nlJ\pm J}(\mathbf{r}). \tag{2.74}$$

The eigenvalues corresponding to unperturbed atomic states $(n, l, J-1, M)$ and (n, l, J, M) with $J = l + \frac{1}{2}$; $M \neq \pm J$ for $l \neq 0$ can be obtained as follows:

$$|H_{n'l'J'M',nlJM} - \lambda I| = 0$$

or

$$\begin{vmatrix} \bar{\varepsilon}^{a_i}_{nlJ-1} + Z\dfrac{(2J-1)}{2J}M - \lambda & -Z\dfrac{\sqrt{J^2-M^2}}{2J}S_{nlJ} \\ -Z\dfrac{\sqrt{J^2-M^2}}{2J}S^*_{nlJ} & \bar{\varepsilon}^{a_i}_{nlJ} + Z\dfrac{(2J+1)}{2J}M - \lambda \end{vmatrix} = 0.$$

Therefore, we have

$$\lambda^2 - \lambda\left(\bar{\varepsilon}^{a_i}_{nlJ} + \bar{\varepsilon}^{a_i}_{nlJ-1} + 2ZM\right) + \left\{\bar{\varepsilon}^{a_i}_{nlJ}\bar{\varepsilon}^{a_i}_{nlJ-1} + \frac{ZM}{2J}\left[(2J-1)\bar{\varepsilon}^{a_i}_{nlJ} + (2J+1)\bar{\varepsilon}^{a_i}_{nlJ-1}\right] + \frac{Z^2}{4J^2}\left[(4J^2-1)M^2 - (J^2-M^2)|S_{nlJ}|^2\right]\right\} = 0. \tag{2.75}$$

Solving this quadratic equation, we get the value of λ as an eigenvalues corresponding to the unperturbed atomic states $(n, l, J-1, M)$ and (n, l, J, M). So, we have,

$$\lambda = \frac{\bar{\varepsilon}^{a_i}_{nlJ} + \bar{\varepsilon}^{a_i}_{nlJ-1}}{2} + \frac{eB\hbar}{2m}M \pm \frac{\bar{\varepsilon}^{a_i}_{nlJ} - \bar{\varepsilon}^{a_i}_{nlJ-1}}{2}\sqrt{1 + 2\frac{M}{J}x_{nl} + \frac{(J^2-M^2)|S_{nlJ}|^2 + M^2}{J^2}x^2_{nl}}, \tag{2.76}$$

with

$$x_{nl} = \frac{eB\hbar/2m}{\bar{\varepsilon}^{a_i}_{nlJ} - \bar{\varepsilon}^{a_i}_{nlJ-1}}. \tag{2.77}$$

Hence, the eigenvalues are:

$$\varepsilon^{a_i,0}_{\xi} = \frac{\bar{\varepsilon}^{a_i}_{nlJ} + \bar{\varepsilon}^{a_i}_{nlJ-1}}{2} + \frac{eB\hbar}{2m}M \pm \frac{\bar{\varepsilon}^{a_i}_{nlJ} - \bar{\varepsilon}^{a_i}_{nlJ-1}}{2}\sqrt{1 + 2\frac{M}{J}x_{nl} + \frac{(J^2-M^2)|S_{nlJ}|^2 + M^2}{J^2}x^2_{nl}}. \tag{2.78}$$

The plus and minus sign in Eq.(2.78) corresponds to unperturbed atomic states (n, l, J, M) and $(n, l, J-1, M)$ respectively.

Let the eigenvectors corresponding to $H_{n'l'J'M',nlJM}$ be $\begin{pmatrix} a \\ b \end{pmatrix}$. Then we have

$$\left(H_{n'l'J'M',nlJM} - \lambda I\right)\begin{pmatrix} a \\ b \end{pmatrix} = 0.$$

Then, we obtain the following equations:

$$\left\{\varepsilon^{a_i}_{nlJ-1} + Z\frac{(2J-1)}{2J}M\right\}a - \left\{Z\frac{\sqrt{J^2-M^2}}{2J}S_{nlJ}\right\}b = \lambda a, \tag{2.79}$$

$$\left\{-Z\frac{\sqrt{J^2-M^2}}{2J}S_{nlJ}\right\}a + \left\{\varepsilon^{a_i}_{nlJ} + Z\frac{(2J+1)}{2J}M\right\}b = \lambda b. \tag{2.80}$$

First, let us consider the plus sign in Eq.(2.76). Taking Eqs.(2.76 and 2.80), we have

$$\begin{aligned}
\frac{a}{b} &= \frac{2J}{ZS_{nlJ}\sqrt{J^2-M^2}}\left\{\bar{\varepsilon}^{a_i}_{nlJ} + Z\frac{(2J+1)}{2J}M - \frac{\bar{\varepsilon}^{a_i}_{nlJ}}{2} - \frac{\bar{\varepsilon}^{a_i}_{nlJ-1}}{2} - ZM \right. \\
&\qquad \left. -\frac{(\bar{\varepsilon}^{a_i}_{nlJ} - \bar{\varepsilon}^{a_i}_{nlJ-1})}{2}\sqrt{1+2\frac{M}{J}x_{nl} + \frac{(J^2-M^2)S^2_{nlJ}+M^2}{J^2}x^2_{nl}}\right\} \\
&= \frac{2J}{ZS_{nlJ}\sqrt{J^2-M^2}}\left\{\frac{\bar{\varepsilon}^{a_i}_{nlJ} - \bar{\varepsilon}^{a_i}_{nlJ-1}}{2} + \frac{ZM}{2J} - \frac{\bar{\varepsilon}^{a_i}_{nlJ} - \bar{\varepsilon}^{a_i}_{nlJ-1}}{2} \right. \\
&\qquad \left. \times\sqrt{1+2\frac{M}{J}x_{nl} + \frac{(J^2-M^2)S^2_{nlJ}+M^2}{J^2}x^2_{nl}}\right\} \\
&= \frac{J}{S_{nlJ}\sqrt{J^2-M^2}}\frac{(\bar{\varepsilon}^{a_i}_{nlJ} - \bar{\varepsilon}^{a_i}_{nlJ-1})}{Z}\left\{1 + \frac{M}{J}\frac{Z}{(\bar{\varepsilon}^{a_i}_{nlJ} - \bar{\varepsilon}^{a_i}_{nlJ-1})} \right. \\
&\qquad \left. -\sqrt{1+2\frac{M}{J}x_{nl} + \frac{(J^2-M^2)S^2_{nlJ}+M^2}{J^2}x^2_{nl}}\right\} \\
&= \frac{J}{S_{nlJ}\sqrt{J^2-M^2}x_{nl}}\left\{1 + \frac{M}{J}x_{nl} - \sqrt{1+2\frac{M}{J}x_{nl} + \frac{(J^2-M^2)S^2_{nlJ}+M^2}{J^2}x^2_{nl}}\right\}.
\end{aligned} \tag{2.81}$$

Here, we introduce the symbol $\eta^{a_i}_{nlJM}$ defined by

$$\eta^{a_i}_{nlJM} = \frac{J}{S_{nlJ}\sqrt{J^2-M^2}x_{nl}}\left\{1 + \frac{M}{J}x_{nl} - \sqrt{1+2\frac{M}{J}x_{nl} + \frac{(J^2-M^2)S^2_{nlJ}+M^2}{J^2}x^2_{nl}}\right\} \tag{2.82}$$

which hereafter is referred to the mixing coefficient.

From Eqs.(2.81) and (2.82), we have

$$a = \eta^{a_i}_{nlJM} b. \tag{2.83}$$

Hence, the normalized eigenvectors are given by

$$\begin{pmatrix} a \\ b \end{pmatrix} = \frac{1}{\sqrt{1+(\eta^{a_i}_{nlJM})^2}}\begin{pmatrix} \eta^{a_i}_{nlJM} \\ 1 \end{pmatrix}. \tag{2.84}$$

Hence, the corresponding eigenfunction is linear combination of eigenvectors. i.e.

$$\psi^{a_i,0}_{\xi}(\mathbf{r}) = \frac{\phi^{a_i}_{nlJM}(\mathbf{r}) + \eta^{a_i}_{nlJM}\phi^{a_i}_{nlJ-1M}(\mathbf{r})}{\sqrt{1+(\eta^{a_i}_{nlJM})^2}}. \tag{2.85}$$

Now, let us consider the minus sign in Eq.(2.76). From Eqs.(2.76) and (2.79), we have

$$\begin{aligned}
\frac{b}{a} &= \frac{2J}{ZS_{nlJ}\sqrt{J^2-M^2}}\left\{\bar{\varepsilon}^{a_i}_{nlJ-1}+Z\frac{(2J-1)}{2J}M-\frac{\bar{\varepsilon}^{a_i}_{nlJ}}{2}-\frac{\bar{\varepsilon}^{a_i}_{nlJ-1}}{2}-ZM\right. \\
&\qquad \left.+\frac{(\bar{\varepsilon}^{a_i}_{nlJ}-\bar{\varepsilon}^{a_i}_{nlJ-1})}{2}\sqrt{1+2\frac{M}{J}x_{nl}+\frac{(J^2-M^2)S^2_{nlJ}+M^2}{J^2}x^2_{nl}}\right\} \\
&= \frac{2J}{ZS_{nlJ}\sqrt{J^2-M^2}}\left\{\frac{-(\bar{\varepsilon}^{a_i}_{nlJ}-\bar{\varepsilon}^{a_i}_{nlJ-1})}{2}+ZM\left(\frac{2J-1}{2J}-1\right)+\frac{\bar{\varepsilon}^{a_i}_{nlJ}-\bar{\varepsilon}^{a_i}_{nlJ-1}}{2}\right. \\
&\qquad \left.\times\sqrt{1+2\frac{M}{J}x_{nl}+\frac{(J^2-M^2)S^2_{nlJ}+M^2}{J^2}x^2_{nl}}\right\} \\
&= -\frac{J}{S_{nlJ}\sqrt{J^2-M^2}}\frac{(\bar{\varepsilon}^{a_i}_{nlJ}-\bar{\varepsilon}^{a_i}_{nlJ-1})}{Z}\left\{1+\frac{M}{J}\frac{Z}{(\bar{\varepsilon}^{a_i}_{nlJ}-\bar{\varepsilon}^{a_i}_{nlJ-1})}\right. \\
&\qquad \left.-\sqrt{1+2\frac{M}{J}x_{nl}+\frac{(J^2-M^2)S^2_{nlJ}+M^2}{J^2}x^2_{nl}}\right\} \\
&= -\frac{J}{S_{nlJ}\sqrt{J^2-M^2}x_{nl}}\left\{1+\frac{M}{J}x_{nl}-\sqrt{1+2\frac{M}{J}x_{nl}+\frac{(J^2-M^2)S^2_{nlJ}+M^2}{J^2}x^2_{nl}}\right\}.
\end{aligned} \tag{2.86}$$

Here we introduce the symbol $\eta^{a_i}_{nlJ-1M}$ that is defined as

$$\eta^{a_i}_{nlJ-1M} = -\frac{J}{S_{nlJ}\sqrt{J^2-M^2}x_{nl}}\left\{1+\frac{M}{J}x_{nl}-\sqrt{1+2\frac{M}{J}x_{nl}+\frac{(J^2-M^2)S^2_{nlJ}+M^2}{J^2}x^2_{nl}}\right\}. \tag{2.87}$$

This implies that

$$\eta^{a_i}_{nlJM} = -\eta^{a_i}_{nlJ-1M} \tag{2.88}$$

$$= \frac{J}{S_{nlJ}\sqrt{J^2-M^2}x_{nl}}\left\{1+\frac{M}{J}x_{nl}-\sqrt{1+2\frac{M}{J}x_{nl}+\frac{(J^2-M^2)S^2_{nlJ}+M^2}{J^2}x^2_{nl}}\right\}. \tag{2.89}$$

From Eqs.(2.86) and (2.87), we have

$$b = \eta^{a_i}_{nlJ-1M}a. \tag{2.90}$$

Hence, the normalized eigenvectors are given by

$$\begin{pmatrix}a\\b\end{pmatrix} = \frac{1}{\sqrt{1+(\eta^{a_i}_{nlJ-1M})^2}}\begin{pmatrix}1\\ \eta^{a_i}_{nlJ-1M}\end{pmatrix}. \tag{2.91}$$

Hence, the corresponding eigenfunction is linear combination of eigenvectors. i.e.

$$\psi^{a_i,0}_{\xi}(\mathbf{r}) = \frac{\phi^{a_i}_{nlJ-1M}(\mathbf{r})+\eta^{a_i}_{nlJ-1M}\phi^{a_i}_{nlJM}(\mathbf{r})}{\sqrt{1+(\eta^{a_i}_{nlJ-1M})^2}}. \tag{2.92}$$

In summary, the eigenfunction is given by

$$\psi_{\xi}^{a_i,0}(\mathbf{r}) = \begin{cases} \dfrac{\phi_{nlJM}^{a_i}(\mathbf{r}) + \eta_{nlJM}^{a_i}\phi_{nlJ-1M}^{a_i}(\mathbf{r})}{\sqrt{1+(\eta_{nlJM}^{a_i})^2}} & \text{for } (n,l,J,M), M \neq J \\ \dfrac{\phi_{nlJ-1M}^{a_i}(\mathbf{r}) + \eta_{nlJ-1M}^{a_i}\phi_{nlJM}^{a_i}(\mathbf{r})}{\sqrt{1+(\eta_{nlJ-1M}^{a_i})^2}} & \text{for } (n,l,J-1,M). \end{cases} \tag{2.93}$$

Evidently, in low magnetic field, i.e. $x_{nl} \ll 1$, Eqs.(2.73), (2.74), (2.78), (2.89) and (2.93) produce the same results of perturbation theory. Substituting Eqs.(2.74) and (2.93) in to Eqs.(2.38) and (2.39), approximated form of magnetic hopping and overlap integral can be obtained. Both $T_{\eta,\xi}^{a_j a_i}(\mathbf{R_l} + \mathbf{d_i} - \mathbf{d_j})$ and $S_{\eta,\xi}^{a_j a_i}(\mathbf{R_l} + \mathbf{d_i} - \mathbf{d_j})$ can be expressed as a linear combination of relativistic hopping integrals and overlap integrals in the absence of magnetic field. The approximated form of $T_{\eta,\xi}^{a_j a_i}(\mathbf{R_l} + \mathbf{d_i} - \mathbf{d_j})$ for $l = 0$ and 1 are summarized in Table I of Ref. [43]. The derivation of some of hopping integrals are presented in Appendix:A. Similarly, the approximated form of $S_{\eta,\xi}^{a_j a_i}(\mathbf{R_l} + \mathbf{d_i} - \mathbf{d_j})$ can easily be obtained by replacing hopping integrals by overlap integrals in Table I of Ref. [43].

Moreover, for $x_{nl} \gg 1$ (high magnetic field), Eq.(2.78) can be approximated as

$$\varepsilon_{\xi}^{a_i,0} \approx \frac{(\bar{\varepsilon}_{nlJ}^{a_i} - \bar{\varepsilon}_{nlJ-1}^{a_i})}{2} + \frac{e\hbar B}{2m}\left(M \pm \frac{1}{2}\right). \tag{2.94}$$

The second terms of Eq.(2.73) and Eq.(2.94) corresponds to the energy shift due to Paschen-Back effect [55]. Therefore, Eqs.(2.73) and (2.78) and magnetic hopping integrals listed in the Table I of Ref. [43] are treated as the corrected expressions which include both Zeeman effect and Paschen-Back effect. Thus, the nonperturbative MFRTB method enables us to calculate electronic structure of the material not only in low magnetic field (Zeeman effect) but also in high magnetic field case (Paschen-Back effect).

Hence, under the approximation that neglecting atomic orbitals other than the outermost ones, we obtained energy eigenvalue $\varepsilon_{\xi}^{a_i,0}$ and eigenfunction $\psi_{\xi}^{a_i,0}(\mathbf{r})$ as given by Eqs.(2.78) and (2.93). Furthermore, their approximated form for $s(l = 0)$ and $p(l = 1)$ orbitals [see, Appendix B] are given by

$$\varepsilon_{\xi}^{a_i,0} = \begin{cases} \bar{\varepsilon}_{n0\frac{1}{2}}^{a_i} \pm \dfrac{e\hbar B}{2m_0} \\ \dfrac{\bar{\varepsilon}_{n1\frac{3}{2}}^{a_i} + \bar{\varepsilon}_{n1\frac{1}{2}}^{a_i}}{2} + \dfrac{e\hbar B}{4m} + \dfrac{\bar{\varepsilon}_{n1\frac{3}{2}}^{a_i} - \bar{\varepsilon}_{n1\frac{1}{2}}^{a_i}}{2}\sqrt{1 + \dfrac{2}{3}x_{nl} + \dfrac{1+8S_{nl}^2}{9}x_{nl}^2} \\ \dfrac{\bar{\varepsilon}_{n1\frac{3}{2}}^{a_i} + \bar{\varepsilon}_{n1\frac{1}{2}}^{a_i}}{2} + \dfrac{e\hbar B}{4m} - \dfrac{\bar{\varepsilon}_{n1\frac{3}{2}}^{a_i} - \bar{\varepsilon}_{n1\frac{1}{2}}^{a_i}}{2}\sqrt{1 + \dfrac{2}{3}x_{nl} + \dfrac{1+8S_{nl}^2}{9}x_{nl}^2} \\ \dfrac{\bar{\varepsilon}_{n1\frac{3}{2}}^{a_i} + \bar{\varepsilon}_{n1\frac{1}{2}}^{a_i}}{2} - \dfrac{e\hbar B}{4m} + \dfrac{\bar{\varepsilon}_{n1\frac{3}{2}}^{a_i} - \bar{\varepsilon}_{n1\frac{1}{2}}^{a_i}}{2}\sqrt{1 - \dfrac{2}{3}x_{nl} + \dfrac{1+8S_{nl}^2}{9}x_{nl}^2} \\ \dfrac{\bar{\varepsilon}_{n1\frac{3}{2}}^{a_i} + \bar{\varepsilon}_{n1\frac{1}{2}}^{a_i}}{2} - \dfrac{e\hbar B}{4m} - \dfrac{\bar{\varepsilon}_{n1\frac{3}{2}}^{a_i} - \bar{\varepsilon}_{n1\frac{1}{2}}^{a_i}}{2}\sqrt{1 - \dfrac{2}{3}x_{nl} + \dfrac{1+8S_{nl}^2}{9}x_{nl}^2} \\ \bar{\varepsilon}_{n1\frac{3}{2}}^{a_i} \pm \dfrac{e\hbar B}{m} \end{cases} \tag{2.95}$$

and

$$\psi_{\xi}^{a_i,0} = \begin{cases} \phi^{a_i}_{n0\frac{1}{2}\pm\frac{1}{2}}(\mathbf{r}) \\ \dfrac{\phi^{a_i}_{n1\frac{3}{2}\frac{1}{2}}(\mathbf{r}) + \eta_+^{a_i}\phi^{a_i}_{n1\frac{1}{2}\frac{1}{2}}(\mathbf{r})}{\sqrt{1+{\eta_+^{a_i}}^2}} \\ \dfrac{-\eta_+^{a_i}\phi^{a_i}_{n1\frac{3}{2}\frac{1}{2}}(\mathbf{r}) + \phi^{a_i}_{n1\frac{1}{2}\frac{1}{2}}(\mathbf{r})}{\sqrt{1+{\eta_+^{a_i}}^2}} \\ \dfrac{\phi^{a_i}_{n1\frac{3}{2}-\frac{1}{2}}(\mathbf{r}) + \eta_-^{a_i}\phi^{a_i}_{n1\frac{1}{2}-\frac{1}{2}}(\mathbf{r})}{\sqrt{1+{\eta_-^{a_i}}^2}} \\ \dfrac{-\eta_-^{a_i}\phi^{a_i}_{n1\frac{3}{2}-\frac{1}{2}}(\mathbf{r}) + \phi^{a_i}_{n1\frac{1}{2}-\frac{1}{2}}(\mathbf{r})}{\sqrt{1+{\eta_-^{a_i}}^2}} \\ \phi^{a_i}_{n1\frac{3}{2}\pm\frac{1}{2}}(\mathbf{r}), \end{cases} \tag{2.96}$$

with

$$\eta_{\pm}^{a_i} = \frac{3}{2\sqrt{2}S_{nl}x_{nl}}\left\{1 \pm \frac{x_{nl}}{3} - \sqrt{1 \pm \frac{2}{3}x_{nl} + \frac{1+8S_{nl}^2}{9}x_{nl}^2}\right\} \tag{2.97}$$

and

$$x_{nl} = \frac{e\hbar B/2m}{\bar{\varepsilon}^{a_i}_{n1\frac{3}{2}} - \bar{\varepsilon}^{a_i}_{n1\frac{1}{2}}}, \tag{2.98}$$

where $\bar{\varepsilon}^{a_i}_{nlJ}$ and S_{nl} denote the atomic spectrum in the absence of magnetic field and inner product between $\phi^{a_i}_{n1\frac{3}{2}M}(\mathbf{r})$ and $\phi^{a_i}_{n1\frac{1}{2}M}(\mathbf{r})$ respectively. Here, note that Eqs.(2.95, 2.96, 2.97, and 2.98) are reduced to results of the perturbation theory in the low magnetic field so that magnetic hopping integral calculated via Eqs.(2.96, 2.97, and 2.98) are regarded as an improved version of magnetic hopping integrals calculated by Peierls Phase [43].

Hopping integrals and overlap integrals in the absence of magnetic field can be expressed in terms of several relativistic tight-binding (TB) parameters, which is summarized in the relativistic version of the Slater-Koster table [38]. Specific values of relativistic TB parameters for graphene are given in Sec.3.4.

Chapter 3

Application of Nonperturbative Magnetic Field Containing Relativistic Tight Binding (MFRTB) Method to graphene

In this chapter, we apply the nonperturbative MFRTB method to graphene immersed in uniform magnetic field to investigate its magnetic property. First we reduce the simultaneous Eq.(2.43) via magnetic Bloch theorem to obtain the concrete equation with finite number of expansion coefficients. As an application of nonperturbative MFRTB mehod, we calculate the diamagnetic property of graphene using this method and find out the cause of the reduction in g-factor of graphene.

3.1 Magnetic Bloch theorem for graphene

Let us take two-dimensional honeycomb lattice of graphene with lattice constant a as shown in Fig. 3.1. The lattice vector is given by

$$\mathbf{R_n} = n_1\mathbf{a_1} + n_2\mathbf{a_2}, \tag{3.1}$$

where n_1 and n_2 are integers.

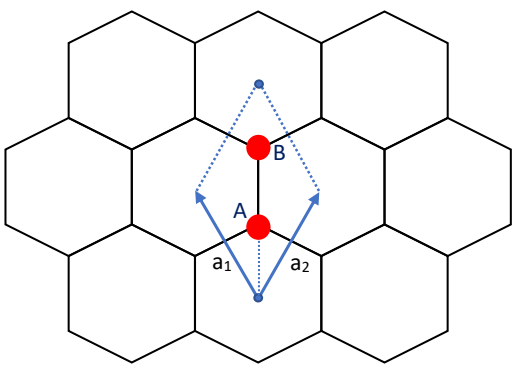

Figure 3.1: Honeycomb lattice of graphene

The vectors $\mathbf{a_1}$ and $\mathbf{a_2}$ are the primitive vectors of honeycomb lattice that are defined as

$$\mathbf{a_1} = \frac{a}{2}\mathbf{e}_x + \frac{\sqrt{3}a}{2}\mathbf{e}_y, \tag{3.2}$$

$$\mathbf{a_2} = -\frac{a}{2}\mathbf{e}_x + \frac{\sqrt{3}a}{2}\mathbf{e}_y. \tag{3.3}$$

The unit cell of graphene has two atoms, say at A and B positions. So, the vectors $\mathbf{d_i}$ (i=A or B) are given by

$$\mathbf{d_A} = (0, \frac{a}{\sqrt{3}}) = \frac{a}{\sqrt{3}}\mathbf{e_y}, \tag{3.4}$$

$$\mathbf{d_B} = (0, \frac{2a}{\sqrt{3}}) = \frac{2a}{\sqrt{3}}\mathbf{e_y}. \tag{3.5}$$

Let us consider the set of magnetic translation operators that commute with each other. The magnetic translation operator $U(\mathbf{R_n})$ is defined by [38]

$$U(\mathbf{R_n}) = e^{i\frac{e}{\hbar}\chi(\mathbf{r},\mathbf{R_n})}T(\mathbf{R_n}), \tag{3.6}$$

where $T(\mathbf{R_n})$ denotes the usual translation operator which is given by [56]

$$T(\mathbf{R_n}) = e^{-i\mathbf{R_n}\cdot\frac{\mathbf{p}}{\hbar}}. \tag{3.7}$$

and $\chi(\mathbf{r}, \mathbf{R_n})$ is the gauge transformation function, which is given by

$$\mathbf{A}(\mathbf{r} - \mathbf{R_n}) = \mathbf{A}(\mathbf{r}) + \nabla\chi(\mathbf{r}, \mathbf{R_n}). \tag{3.8}$$

Referring to the Eq.(2.3), in case of landau gauge, $\chi(\mathbf{r}, \mathbf{R_n})$ can be written as

$$\chi(\mathbf{r}, \mathbf{R_n}) = -BR_{nx}y. \tag{3.9}$$

It is evident that $U(\mathbf{R_n})$ commutes with the Hamiltonian Eq.(2.2) [38]. Which means

$$[U(\mathbf{R_n}), H] = 0. \tag{3.10}$$

Using Eqs.(2.30) and (3.6), multiplication of two magnetic translation operators $U(\mathbf{R_n})$ and $U(\mathbf{R_m})$ yields

$$U(\mathbf{R_n})U(\mathbf{R_m}) = e^{i\frac{e}{\hbar}[\chi(\mathbf{r},\mathbf{R_n})+\chi(\mathbf{r}-\mathbf{R_n},\mathbf{R_m})-\chi(\mathbf{r},\mathbf{R_n}+\mathbf{R_m})]}U(\mathbf{R_n}+\mathbf{R_m}). \tag{3.11}$$

Using Eq.(3.9), Eq.(3.11) leads to

$$U(\mathbf{R_n})U(\mathbf{R_m}) = e^{i\frac{e}{\hbar}BR_{mx}R_{ny}}U(\mathbf{R_n}+\mathbf{R_m}), \tag{3.12}$$

$$U(\mathbf{R_m})U(\mathbf{R_n}) = e^{i\frac{e}{\hbar}BR_{nx}R_{my}}U(\mathbf{R_m}+\mathbf{R_n}). \tag{3.13}$$

From Eqs.(3.12) and (3.13), we have

$$U(\mathbf{R_n})U(\mathbf{R_m}) = e^{i\frac{e}{\hbar}B(R_{mx}R_{ny}-R_{nx}R_{my})}U(\mathbf{R_m})U(\mathbf{R_n}). \tag{3.14}$$

In order to form a set of an Abelian group of magnetic translation operators, the magnitude of magnetic field is supposed to be expressed by

$$B = \frac{8\pi\hbar}{\sqrt{3}ea^2}\frac{p}{q}, \tag{3.15}$$

Where p and q are relatively prime integers [57–59].

Substituting the value of B in Eq.(3.14), we have

$$U(\mathbf{R_n})U(\mathbf{R_m}) = e^{2\pi i\frac{p}{q}[(m_1-m_2)(n_1+n_2)-(n_1-n_2)(m_1+m_2)]}U(\mathbf{R_m})U(\mathbf{R_n}). \tag{3.16}$$

Let us consider the set of magnetic translation operators such as,

$$\{U(\mathbf{t_n})|t_n = n_1{\mathbf{a_1}}^M + n_2{\mathbf{a_2}}^M\}, \tag{3.17}$$

with ${\mathbf{a_1}}^M = a\mathbf{e_x}$ and ${\mathbf{a_2}}^M = q\mathbf{a_2}$, then it is shown that from Eq.(3.16), this set forms an abelian group with a maximal order [38]. The vectors ${\mathbf{a_1}}^M$ and ${\mathbf{a_2}}^M$ are primitive vectors of magnetic unit cell. Therefore, the area of the magnetic unit cell is q times as large as that of the unit cell.

Consequently, we have

$$U(\mathbf{t_n})U(\mathbf{t_m}) = U(\mathbf{t_m})U(\mathbf{t_n}). \tag{3.18}$$

In general the eigenfunctions of the Hamiltonian, $\Phi_k(\mathbf{r})$, which belongs to a degenerate level, form basis functions of the irreducible representation (IRs) of the symmetric group of Hamiltonian [60]. This symmetric group of Hamiltonian contains an operator that commutes with the Hamiltonian. So, eigenfunction of Hamiltonian can be the basis functions of IRs of the Abelian group Eq.(3.17) [38]. we have

$$U(\mathbf{t_n})\Phi_\mathbf{k}(\mathbf{r}) = C(\mathbf{t_n})\Phi_\mathbf{k}(\mathbf{r}), \tag{3.19}$$

where $C(\mathbf{t_n})$ is the IR of Abelian group.

Since it is clear that $H, U(\mathbf{t_n}), U(\mathbf{t'_n}), U(\mathbf{t''_n})$..... all commutes with each other , they must have simultaneous eigenfunction, $\Phi_\mathbf{k}(\mathbf{r})$. Then we have from Eq.(2.1)

$$H\Phi_\mathbf{k}(\mathbf{r}) = E\Phi_\mathbf{k}(\mathbf{r}). \tag{3.20}$$

Operating by $U(\mathbf{t_n})$ on both sides of Eq.(3.20), we have

$$U(\mathbf{t_n})H\Phi_\mathbf{k}(\mathbf{r}) = E\{U(\mathbf{t_n})\Phi_\mathbf{k}(\mathbf{r})\}. \tag{3.21}$$

As we know $[H, U(\mathbf{t_n})] = 0$, above Eq.(3.21) can be written as

$$H\{U(\mathbf{t_n})\Phi_\mathbf{k}(\mathbf{r})\} = E\{U(\mathbf{t_n})\Phi_\mathbf{k}(\mathbf{r})\}. \tag{3.22}$$

This shows that $U(\mathbf{t_n})\Phi_\mathbf{k}(\mathbf{r})$ is also an eigenfunction of Hamiltonian H. So, $\Phi_\mathbf{k}(\mathbf{r})$ and $U(\mathbf{t_n})\Phi_\mathbf{k}(\mathbf{r})$ are related to each other by gauge transformation.

Normalization of Eq.(3.19) yields

$$C(\mathbf{t_n}) = e^{-2\pi ik_i}, \tag{3.23}$$

where k_i is a real number. So, Eq.(3.19) becomes

$$U(\mathbf{t_n})\Phi_{\mathbf{k}}(\mathbf{r}) = e^{-2\pi i k_i}\Phi_{\mathbf{k}}(\mathbf{r}). \tag{3.24}$$

The magnetic first Brillouin zone is defined as the Wigner-Seitz cell in the reciprocal lattice spanned by magnetic reciprocal lattice vectors, say $\mathbf{b_1}^M$ and $\mathbf{b_2}^M$. Then, the wave vector $\mathbf{k}$ is defined by

$$\mathbf{k} = k_1\mathbf{b_1}^M + k_2\mathbf{b_2}^M, \tag{3.25}$$

with

$$\mathbf{b_1}^M = \frac{2\pi}{a}\left(\mathbf{e_x} + \frac{1}{\sqrt{3}}\mathbf{e_y}\right), \tag{3.26}$$

$$\mathbf{b_2}^M = \frac{4\pi}{\sqrt{3}aq}\mathbf{e_y}. \tag{3.27}$$

The schematic view of magnetic first Brillouin zone spanned by magnetic reciprocal lattice vectors $\mathbf{b_1}^M$ and $\mathbf{b_2}^M$of graphene immersed in magnetic field is shown in Fig. 3.2.

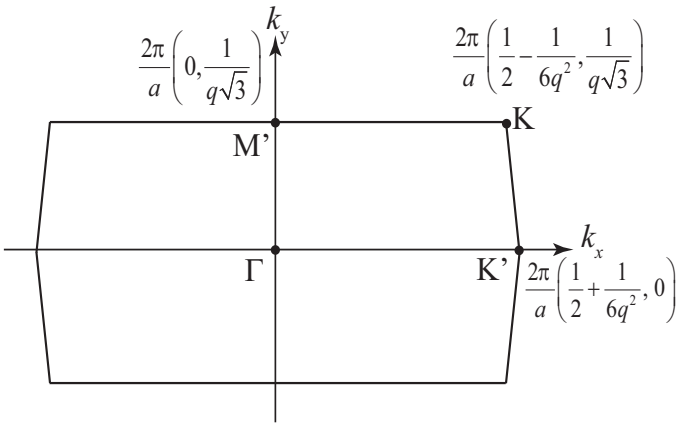

Figure 3.2: Schematic view of magnetic first Brillouin zone of graphene [61].

Let us take translation vectors $\mathbf{t_n} = n_1\mathbf{a_1}^M + n_2\mathbf{a_2}^M$ as given by Eq.(3.17) , then Eq.(3.24) becomes

$$U(\mathbf{a_1}^M)\Phi_{\mathbf{k}}(\mathbf{r}) = e^{-2\pi i k_1}\Phi_{\mathbf{k}}(\mathbf{r}), \tag{3.28}$$

$$U(\mathbf{a_2}^M)\Phi_{\mathbf{k}}(\mathbf{r}) = e^{-2\pi i k_2}\Phi_{\mathbf{k}}(\mathbf{r}), \tag{3.29}$$

where k_1 and k_2 are real numbers. Hence, we have

$$U(\mathbf{t_n})\Phi_{\mathbf{k}}(\mathbf{r}) = e^{-2\pi i(n_1k_1 + n_2k_2)}\Phi_{\mathbf{k}}(\mathbf{r}). \tag{3.30}$$

Also, we may write

$$\mathbf{k}\cdot\mathbf{t_n} = 2\pi(n_1k_1 + n_2k_2). \tag{3.31}$$

From Eqs.(3.30) and (3.31), we get

$$U(\mathbf{t_n})\Phi_{\mathbf{k}}(\mathbf{r}) = e^{-i\boldsymbol{k}\cdot\mathbf{t_n}}\Phi_{\mathbf{k}}(\mathbf{r}). \tag{3.32}$$

Furthermore, we have from Eq.(3.6)

$$U(\mathbf{t_n})\Phi_{\mathbf{k}}(\mathbf{r}) = e^{i\frac{e}{\hbar}\chi(\mathbf{r},\mathbf{t_n})}T(\mathbf{t_n})\Phi_{\mathbf{k}}(\mathbf{r}) = e^{i\frac{e}{\hbar}\chi(\mathbf{r},\mathbf{t_n})}\Phi_{\mathbf{k}}(\mathbf{r}-\mathbf{t_n}). \tag{3.33}$$

From Eqs.(3.32) and (3.33), we have

$$\Phi_{\mathbf{k}}(\mathbf{r}-\mathbf{t_n}) = e^{-i\mathbf{k}\cdot\mathbf{t_n}}e^{-i\frac{e}{\hbar}\chi(\mathbf{r},\mathbf{t_n})}\Phi_{\mathbf{k}}(\mathbf{r}). \tag{3.34}$$

Using Eq.(3.9), Eq.(3.34) becomes

$$\Phi_{\mathbf{k}}(\mathbf{r}-\mathbf{t_n}) = e^{-i\mathbf{k}\cdot\mathbf{t_n}}e^{i\frac{e}{\hbar}Bt_{nx}y}\Phi_{\mathbf{k}}(\mathbf{r}). \tag{3.35}$$

Eq.(3.35) represents the magnetic Bloch theorem which is an extension of the Bloch theorem for an electron that moves in an uniform magnetic field under the influence of a periodic potential of the crystal. It is evident that form Eq.(3.35), in the absence of magnetic field (i.e. B=0), it reduces to conventional Bloch theorem.

3.2 Reduction of simultaneous equations using Magnetic Bloch theorem

Now, we can express all the lattice vectors $\mathbf{R_n}$ in terms of translation vector $\mathbf{t_n}$ as

$$\mathbf{R_n} = \mathbf{t_n} + I'\mathbf{a_2}, \tag{3.36}$$

where $I' = 0, 1, 2, ..., q-1$.

Using Eq.(3.36), Eq.(2.5) can be written as

$$\Phi_{\mathbf{k}}(\mathbf{r}) = \sum_{\mathbf{t_n}}\sum_{i}\sum_{\xi}\sum_{I=0}^{q-1} C_{\mathbf{k}}^{\xi}(\mathbf{t_n}+I'\mathbf{a_2}+\mathbf{d_i})\psi_{\xi}^{a_i,\mathbf{t_n}+I'\mathbf{a_2}+\mathbf{d_i}}(\mathbf{r}). \tag{3.37}$$

In the similar manner, we have

$$\Phi_{\mathbf{k}}(\mathbf{r}-\mathbf{t_m}) = \sum_{\mathbf{t_n}}\sum_{i}\sum_{\xi}\sum_{I'=0}^{q-1} C_{\mathbf{k}}^{\xi}(\mathbf{t_n}+I'\mathbf{a_2}+\mathbf{d_i})\psi_{\xi}^{a_i,\mathbf{t_n}+I'\mathbf{a_2}+\mathbf{d_i}}(\mathbf{r}-\mathbf{t_m}). \tag{3.38}$$

Substituting Eqs.(3.37) and (3.38) in to Eq.(3.34), we get

$$\sum_{\mathbf{t_n}}\sum_{i}\sum_{\xi}\sum_{I'=0}^{q-1} C_{\mathbf{k}}^{\xi}(\mathbf{t_n}+I'\mathbf{a_2}+\mathbf{d_i})\psi_{\xi}^{a_i,\mathbf{t_n}+I'\mathbf{a_2}+\mathbf{d_i}}(\mathbf{r}-\mathbf{t_m}) = e^{-i\mathbf{k}\cdot\mathbf{t_m}}e^{-i\frac{e}{\hbar}\chi(\mathbf{r},\mathbf{t_m})}\sum_{\mathbf{t_n}}\sum_{i}\sum_{\xi}\sum_{I'=0}^{q-1} C_{\mathbf{k}}^{\xi}(\mathbf{t_n}+I'\mathbf{a_2}+\mathbf{d_i})\psi_{\xi}^{a_i,\mathbf{t_n}+I'\mathbf{a_2}+\mathbf{d_i}}(\mathbf{r}). \tag{3.39}$$

Now at first, let us establish the relation between $\psi_{\xi}^{a_i,\mathbf{t_n}+I'\mathbf{a_2}+\mathbf{d_i}}(\mathbf{r}-\mathbf{t_m})$ and $\psi_{\xi}^{a_i,\mathbf{t_n}+I'\mathbf{a_2}+\mathbf{d_i}}(\mathbf{r})$.

For this, let us assume that $\psi_{\xi}^{a_i,\mathbf{t_n}+I'\mathbf{a_2}+\mathbf{d_i}}(\mathbf{r})$ obeys the following Dirac equation:

$$\left[c\alpha\cdot\{\mathbf{p}+e\mathbf{A}(\mathbf{r})\}+\beta m_0c^2+V_{a_i}(\mathbf{r}-\mathbf{t_n}-I'\mathbf{a_2}-\mathbf{d_i})\right]\psi_{\xi}^{a_i,\mathbf{t_n}+I'\mathbf{a_2}+\mathbf{d_i}}(\mathbf{r}) = E_{\xi}^{\mathbf{t_n}+I'\mathbf{a_2}+\mathbf{d_i}}\psi_{\xi}^{a_i,\mathbf{t_n}+I'\mathbf{a_2}+\mathbf{d_i}}(\mathbf{r}). \tag{3.40}$$

Let us change the variables $\mathbf{r}$ to $\mathbf{r}' - \mathbf{t_m}$, we have

$$\big[c\alpha \cdot \{\mathbf{p}' + e\mathbf{A}(\mathbf{r}' - \mathbf{t_m})\} + \beta m_0 c^2 + V_{a_i}(\mathbf{r}' - \mathbf{t_m} - \mathbf{t_n} - I'\mathbf{a_2} - \mathbf{d_i})\big] \times \psi_\xi^{a_i, \mathbf{t_n} + I'\mathbf{a_2} + \mathbf{d_i}}(\mathbf{r}' - \mathbf{t_m}) = E_\xi^{\mathbf{t_n} + I'\mathbf{a_2} + \mathbf{d_i}} \psi_\xi^{a_i, \mathbf{t_n} + I'\mathbf{a_2} + \mathbf{d_i}}(\mathbf{r}' - \mathbf{t_m}). \quad (3.41)$$

According to gauge transformation, $\mathbf{A}(\mathbf{r}')$ and $\mathbf{A}(\mathbf{r}' - \mathbf{t_m})$ are related as

$$\mathbf{A}(\mathbf{r}' - \mathbf{t_m}) = \mathbf{A}(\mathbf{r}') + \nabla\chi(\mathbf{r}', \mathbf{t_m}) \quad (3.42)$$

Using Eq.(3.42), we have

$$\big[c\alpha \cdot \{\mathbf{p} + e\mathbf{A}(\mathbf{r}) + e\nabla\chi(\mathbf{r}, \mathbf{t_m})\} + \beta m_0 c^2 + V_{a_i}(\mathbf{r} - \mathbf{t_m} - \mathbf{t_n} - I'\mathbf{a_2} - \mathbf{d_i})\big] \times \psi_\xi^{a_i, \mathbf{t_n} + I'\mathbf{a_2} + \mathbf{d_i}}(\mathbf{r} - \mathbf{t_m}) = E_\xi^{\mathbf{t_n} + I'\mathbf{a_2} + \mathbf{d_i}} \psi_\xi^{a_i, \mathbf{t_n} + I'\mathbf{a_2} + \mathbf{d_i}}(\mathbf{r} - \mathbf{t_m}). \quad (3.43)$$

Here we have changed primed variable to unprimed variable. It is clear that, $\psi_\xi^{a_i, \mathbf{t_n} + \mathbf{t_m} + I'\mathbf{a_2} + \mathbf{d_i}}(\mathbf{r})$ also obeys the following Dirac equation:

$$\big[c\alpha \cdot \{\mathbf{p} + e\mathbf{A}(\mathbf{r})\} + \beta m_0 c^2 + V_{a_i}(\mathbf{r} - \mathbf{t_m} - \mathbf{t_n} - I'\mathbf{a_2} - \mathbf{d_i})\big] \times \psi_\xi^{a_i, \mathbf{t_n} + \mathbf{t_m} + I'\mathbf{a_2} + \mathbf{d_i}}(\mathbf{r}) = E_\xi^{\mathbf{t_n} + \mathbf{t_m} + I'\mathbf{a_2} + \mathbf{d_i}} \psi_\xi^{a_i, \mathbf{t_n} + \mathbf{t_m} + I'\mathbf{a_2} + \mathbf{d_i}}(\mathbf{r}). \quad (3.44)$$

Comparison of Eqs.(3.43) and (3.44) leads us to the fact that the gauge transformation of the wave functions $\psi_\xi^{a_i, \mathbf{t_n} + I'\mathbf{a_2} + \mathbf{d_i}}(\mathbf{r} - \mathbf{t_m})$ and $\psi_\xi^{a_i, \mathbf{t_n} + \mathbf{t_m} + I'\mathbf{a_2} + \mathbf{d_i}}(\mathbf{r})$ relates both the wave functions of respective equations as

$$\psi_\xi^{a_i, \mathbf{t_n} + I'\mathbf{a_2} + \mathbf{d_i}}(\mathbf{r} - \mathbf{t_m}) = e^{-i\frac{e}{\hbar}\chi(\mathbf{r}, \mathbf{t_m})} \psi_\xi^{a_i, \mathbf{t_n} + \mathbf{t_m} + I'\mathbf{a_2} + \mathbf{d_i}}(\mathbf{r}). \quad (3.45)$$

Substituting Eq.(3.45) in to Eq.(3.39), we get

$$\sum_{\mathbf{t_n}} \sum_i \sum_\xi \sum_{I'=0}^{q-1} C_{\mathbf{k}}^\xi(\mathbf{t_n} + I'\mathbf{a_2} + \mathbf{d_i}) e^{-i\frac{e}{\hbar}\chi(\mathbf{r}, \mathbf{t_m})} \psi_\xi^{a_i, \mathbf{t_n} + \mathbf{t_m} + I'\mathbf{a_2} + \mathbf{d_i}}(\mathbf{r}) = e^{-i\mathbf{k}\cdot\mathbf{t_m}} e^{-i\frac{e}{\hbar}\chi(\mathbf{r}, \mathbf{t_m})} \sum_{\mathbf{t_n}} \sum_i \sum_\xi \sum_{I'=0}^{q-1} C_{\mathbf{k}}^\xi(\mathbf{t_n} + I'\mathbf{a_2} + \mathbf{d_i}) \psi_\xi^{a_i, \mathbf{t_n} + I'\mathbf{a_2} + \mathbf{d_i}}(\mathbf{r}). \quad (3.46)$$

Change of variables $\mathbf{t_n} + \mathbf{t_m}$ to $\mathbf{t_l}$ in LHS of Eq.(3.46) yields

$$\sum_{\mathbf{t_l}} \sum_i \sum_\xi \sum_{I'=0}^{q-1} C_{\mathbf{k}}^\xi(\mathbf{t_l} - \mathbf{t_m} + I'\mathbf{a_2} + \mathbf{d_i}) \psi_\xi^{a_i, \mathbf{t_l} + I'\mathbf{a_2} + \mathbf{d_i}}(\mathbf{r}) = e^{-i\mathbf{k}\cdot\mathbf{t_m}} \sum_{\mathbf{t_n}} \sum_i \sum_\xi \sum_{I'=0}^{q-1} C_{\mathbf{k}}^\xi(\mathbf{t_n} + I'\mathbf{a_2} + \mathbf{d_i}) \psi_\xi^{a_i, \mathbf{t_n} + I'\mathbf{a_2} + \mathbf{d_i}}(\mathbf{r}). \quad (3.47)$$

Again, changing the variables $\mathbf{t_l}$ to $\mathbf{t_n}$ in LHS of Eq.(3.47), we have

$$\sum_{\mathbf{t_n}} \sum_i \sum_\xi \sum_{I=0}^{q-1} \Big\{ C_{\mathbf{k}}^\xi(\mathbf{t_n} - \mathbf{t_m} + I'\mathbf{a_2} + \mathbf{d_i}) - e^{-i\mathbf{k}\cdot\mathbf{t_m}} C_{\mathbf{k}}^\xi(\mathbf{t_n} + I'\mathbf{a_2} + \mathbf{d_i}) \Big\} \times \psi_\xi^{a_i, \mathbf{t_n} + I'\mathbf{a_2} + \mathbf{d_i}}(\mathbf{r}) = 0. \quad (3.48)$$

Multiplying both sides of Eq.(3.48) by $\psi_{\xi}^{a_j,\mathbf{t_{n'}}+I'\mathbf{a_2}+\mathbf{d_j}}(\mathbf{r})^{\dagger}$ and integrating , we get

$$\sum_{\mathbf{t_n}}\sum_{i}\sum_{\xi}\sum_{I'=0}^{q-1}\Big\{C_{\mathbf{k}}^{\xi}(\mathbf{t_n}-\mathbf{t_m}+I'\mathbf{a_2}+\mathbf{d_i})-e^{-i\mathbf{k}\cdot\mathbf{t_m}}C_{\mathbf{k}}^{\xi}(\mathbf{t_n}+I'\mathbf{a_2}+\mathbf{d_i})\Big\}$$
$$\times\int\psi_{\xi}^{a_j,\mathbf{t_{n'}}+I'\mathbf{a_2}+\mathbf{d_j}}(\mathbf{r})^{\dagger}\psi_{\xi}^{a_i,\mathbf{t_n}+I'\mathbf{a_2}+\mathbf{d_i}}(\mathbf{r})=0. \quad (3.49)$$

Using orthogonality of basis function, the relation between coefficients is obtained as

$$C_{\mathbf{k}}^{\xi}(\mathbf{t_n}-\mathbf{t_m}+I'\mathbf{a_2}+\mathbf{d_i})=e^{-i\mathbf{k}\cdot\mathbf{t_m}}C_{\mathbf{k}}^{\xi}(\mathbf{t_n}+I'\mathbf{a_2}+\mathbf{d_i}). \quad (3.50)$$

Putting $\mathbf{t_l}$ back instead of $\mathbf{t_n}-\mathbf{t_m}$, we get

$$C_{\mathbf{k}}^{\xi}(\mathbf{t_l}+I'\mathbf{a_2}+\mathbf{d_i})=e^{-i\mathbf{k}\cdot(\mathbf{t_n}-\mathbf{t_l})}C_{\mathbf{k}}^{\xi}(\mathbf{t_n}+I'\mathbf{a_2}+\mathbf{d_i}). \quad (3.51)$$

If $\mathbf{t_l}=0$, then we get

$$C_{\mathbf{k}}^{\xi}(\mathbf{t_n}+I'\mathbf{a_2}+\mathbf{d_i})=e^{i\mathbf{k}\cdot\mathbf{t_n}}C_{\mathbf{k}}^{\xi}(I'\mathbf{a_2}+\mathbf{d_i}). \quad (3.52)$$

This is an alternative expression of magnetic Bloch theorem. The Eq.(3.52) means that all coefficients $C_{\mathbf{k}}^{\xi}(\mathbf{t_n}+I'\mathbf{a_2}+\mathbf{d_i})$ can be obtained by using Eq.(3.52) if we get 2q-coefficients $\{C_{\mathbf{k}}^{\xi}(I'\mathbf{a_2}+\mathbf{d_i})|I'=0,1,2,.....,q-1;i=A,B;\xi=nlJM\}$.

Using Eq.(3.52) to the simultaneous Eq.(2.43), we get

$$\begin{aligned}(\varepsilon_{\eta}^{a_j,\mathbf{0}}+\Delta\varepsilon_{\eta}^{a_j,\mathbf{d_j}})C_{\mathbf{k}}^{\eta}(\mathbf{I'a_2}+\mathbf{d_j})+\sum_{W}\sum_{\xi}e^{-i\frac{eB}{\hbar}\mathbf{T}_{Wx}(\mathbf{d_j})(R_{my}+d_{jy})}&\\ \times\tilde{T}_{\eta,\xi}\{\mathbf{T}_{W}(\mathbf{d_j})\}C_{\mathbf{k}}^{\xi}\{\mathbf{T}_{W}(\mathbf{d_j})+\mathbf{I'a_2}+\mathbf{d_j}\}&\\ =E_{\mathbf{k}}\left[C_{\mathbf{k}}^{\xi}(\mathbf{I'a_2}+\mathbf{d_j})+\sum_{W}\sum_{\xi}e^{-i\frac{eB}{\hbar}\mathbf{T}_{Wx}(\mathbf{d_j})(R_{my}+d_{jy})}S_{\eta,\xi}\{\mathbf{T}_{W}(\mathbf{d_j})\}\right]&\\ \times C_{\mathbf{k}}^{\xi}\{\mathbf{T}_{W}(\mathbf{d_j})+\mathbf{I'a_2}+\mathbf{d_j}\}.&\end{aligned} \quad (3.53)$$

Since all the lattice points are occupied by carbon atoms, we remove the superscripts of the magnetic hopping and magnetic overlap integrals. We know that the vectors $\mathbf{T}_{W}(\mathbf{d_j})+\mathbf{I'a_2}+\mathbf{d_j}$ in Eq.(3.53) denote the positions of C-atom. So, using Eq.(3.52), these vectors can be rewritten in the form of $\mathbf{t'_n}+\mathbf{I''a_2}+\mathbf{d'_j}$ as

$$\begin{aligned}C_{\mathbf{k}}^{nlJM}\{\mathbf{T}_{W}(\mathbf{d_j})+\mathbf{I'a_2}+\mathbf{d_j}\}&=\mathbf{t'_n}+\mathbf{I''a_2}+\mathbf{d'_j}\\ &=e^{i\mathbf{k}\cdot\mathbf{t'_n}}C_{\mathbf{k}}^{nlJM}(\mathbf{I''a_2}+\mathbf{d'_j}).\end{aligned} \quad (3.54)$$

The phase factor $e^{-i\frac{eB}{\hbar}\mathbf{T}_{W}(\mathbf{d_j})\mathbf{t_{my}}}$ that appeared in Eq.(3.53) would be approximated to unity for the magnetic field of magnitude given by Eq.(3.15). This leads us to the solutions of Eq.(3.53) which are consistent with the Magnetic Bloch Theorem. Taking this fact in

to consideration, the Eq.(3.53) can be rewritten as

$$(\varepsilon_{\eta}^{a_j,\mathbf{0}} + \Delta\varepsilon_{\eta}^{a_j,\mathbf{d_j}})C_{\mathbf{k}}^{\eta}(\mathbf{I'a_2} + \mathbf{d_j}) + \sum_{W}\sum_{\xi} e^{-i\frac{eB}{\hbar}\mathbf{T}_{Wx}(\mathbf{d_j})(R_{my}+d_{jy})} \times \tilde{T}_{\eta,\xi}\{\mathbf{T}_{W}(\mathbf{d_j})\}C_{\mathbf{k}}^{\xi}\{\mathbf{T}_{W}(\mathbf{d_j}) + \mathbf{I'a_2} + \mathbf{d_j}\}$$
$$= E_{\boldsymbol{k}}\left[C_{\mathbf{k}}^{\eta}(\mathbf{I'a_2} + \mathbf{d_j}) + \sum_{W}\sum_{\xi} e^{-i\frac{eB}{\hbar}\mathbf{T}_{Wx}(\mathbf{d_j})(R_{my}+d_{jy})}S_{\eta,\xi}\{\mathbf{T}_{W}(\mathbf{d_j})\}\right] \times C_{\mathbf{k}}^{\xi}\{\mathbf{T}_{W}(\mathbf{d_j}) + \mathbf{I'a_2} + \mathbf{d_j}\}. \tag{3.55}$$

This is the simultaneous equation with finite number of coefficients $\{C_{\mathbf{k}}^{\xi}(\mathbf{I'a_2} + \mathbf{d_j})|I' = 0, 1, 2, ...q-1; i = A \text{ or } B; \xi = nlJM\}$.

3.3 Concrete expression of the simultaneous equation

Let us look at the concrete formulation for the simultaneous equation that we employ for our calculations. To examine the electronic states near the Fermi level, we consider only outermost $s(l = 0)$ and $p(l = 1)$ orbitals of C atom. Under these assumption, magnetic hopping and magnetic overlap integrals are calculated. Specifically, we chose magnetic hopping and magnetic overlap integrals between following eight shells:

$$(n, l, J, M) = \left(2, 0, \frac{1}{2}, \pm\frac{1}{2}\right), \left(2, 1, \frac{1}{2}, \pm\frac{1}{2}\right), \left(2, 1, \frac{3}{2}, \pm\frac{1}{2}\right), \left(2, 1, \frac{3}{2}, \pm\frac{3}{2}\right). \tag{3.56}$$

We only chose the electron hopping between the first nearest neighbor atoms. Namely, three vectors $\mathbf{T}_{W}(\mathbf{d_j})|_{W=1,2,3}$ are taken in to consideration.

The phase factors $e^{-i\frac{eB}{\hbar}\mathbf{T}_{W}(\mathbf{d_j})(R_{my}+d_{jy})}$ and the coefficients $C_{\mathbf{k}}^{nlJM}\{\mathbf{T}_{W}(\mathbf{d_j}) + \mathbf{I'a_2} + \mathbf{d_j}\}$ of Eq.(3.55) for the atoms located at $\mathbf{d_{(j=A)}} = \left(0, \frac{a}{\sqrt{3}}\right)$ and $\mathbf{d_{(j=B)}} = \left(0, \frac{2a}{\sqrt{3}}\right)$ are listed in Tables 3.1 and 3.2 respectively.

Table 3.1: The phase factors $e^{-i\frac{eB}{\hbar}\mathbf{T}_{W}(\mathbf{d_j})(R_{my}+d_{jy})}$ and the coefficients $C_{\mathbf{k}}^{nlJM}\{\mathbf{T}_{W}(\mathbf{d_j}) + \mathbf{I'a_2} + \mathbf{d_A}\}$.

W	$\mathbf{T}_{W}(\mathbf{d_j})$	$e^{-i\frac{eB}{\hbar}\mathbf{T}_{W}(\mathbf{d_j})(R_{my}+d_{jy})}$	$C_{\mathbf{k}}^{\xi}\{\mathbf{T}_{W}(\mathbf{d_j}) + \mathbf{I'a_2} + \mathbf{d_A}\}$
1	$\left(0, \frac{a}{\sqrt{3}}\right)$	1	$C_{\mathbf{k}}^{\xi}(\mathbf{I'a_2} + \mathbf{d_B})$
2	$\left(\frac{a}{2}, -\frac{a}{2\sqrt{3}}\right)$	$e^{-2\pi i\frac{p}{q}\left(I'+\frac{2}{3}\right)}$	$C_{\mathbf{k}}^{\xi}\{(\mathbf{I'}-\mathbf{1})\mathbf{a_2} + \mathbf{d_B}\}$
3	$\left(-\frac{a}{2}, -\frac{a}{\sqrt{3}}\right)$	$e^{2\pi i\frac{p}{q}\left(I'+\frac{2}{3}\right)}$	$e^{-ik_x a}C_{\mathbf{k}}^{\xi}\{(\mathbf{I'}-\mathbf{1})\mathbf{a_2} + \mathbf{d_B}\}$

Using the values of phase factors and coefficients from Tables 3.1 and 3.2, we have the following two sets of concrete equations:

Table 3.2: The phase factors $e^{-i\frac{eB}{\hbar}\mathbf{T}_W(\mathbf{d_j})(R_{my}+d_{jy})}$ and the coefficients $C_{\mathbf{k}}^{nlJM}\{\mathbf{T}_W(\mathbf{d_j}) + \mathbf{I'a_2} + \mathbf{d_B}\}$

W	$\mathbf{T}_W(\mathbf{d_j})$	$e^{-i\frac{eB}{\hbar}\mathbf{T}_W(\mathbf{d_j})(R_{my}+d_{jy})}$	$C_{\mathbf{k}}^{\xi}\{\mathbf{T}_W(\mathbf{d_j}) + \mathbf{I'a_2} + \mathbf{d_B}\}$
1	$\left(0, -\frac{a}{\sqrt{3}}\right)$	1	$C_{\mathbf{k}}^{\xi}(\mathbf{I'a_2} + \mathbf{d_A})$
2	$\left(-\frac{a}{2}, \frac{a}{2\sqrt{3}}\right)$	$e^{2\pi i\frac{p}{q}\left(I'+\frac{4}{3}\right)}$	$C_{\mathbf{k}}^{\xi}\{(\mathbf{I'}-\mathbf{1})\mathbf{a_2} + \mathbf{d_A}\}$
3	$\left(\frac{a}{2}, \frac{a}{\sqrt{3}}\right)$	$e^{-2\pi i\frac{p}{q}\left(I'+\frac{4}{3}\right)}$	$e^{ik_x a}C_{\mathbf{k}}^{\xi}\{(\mathbf{I'}-\mathbf{1})\mathbf{a_2} + \mathbf{d_A}\}$

(i) For $d_j = d_A$,

$$\begin{aligned}
&(\varepsilon_{\eta}^{a_j,\mathbf{0}} + \Delta\varepsilon_{\eta}^{a_j,\mathbf{d_j}})C_{\mathbf{k}}^{\eta}(\mathbf{I'a_2} + \mathbf{d_A}) + \sum_{\xi}\tilde{T}_{\eta,\xi}\{\mathbf{T}_1(\mathbf{d_A})\}C_{\mathbf{k}}^{\xi}\{\mathbf{I'a_2} + \mathbf{d_B}\} \\
&\quad + \sum_{\xi}\left(e^{-2\pi i\frac{p}{q}\left(I'+\frac{2}{3}\right)}\tilde{T}_{\eta,\xi}\{\mathbf{T}_2(\mathbf{d_A})\} + e^{2\pi i\frac{p}{q}\left(I'+\frac{2}{3}\right)}e^{-ik_x a}\tilde{T}_{\eta,\xi}\{\mathbf{T}_3(\mathbf{d_A})\}\right) \\
&\qquad\qquad \times C_{\mathbf{k}}^{\xi}\{(\mathbf{I'}-\mathbf{1})\mathbf{a_2} + \mathbf{d_B}\} \\
&= E_{\mathbf{k}}\Bigg[C_{\mathbf{k}}^{\eta}(\mathbf{I'a_2} + \mathbf{d_A}) + \sum_{\xi}S_{\eta,\xi}\{\mathbf{T}_1(\mathbf{d_A})\}C_{\mathbf{k}}^{\xi}\{\mathbf{I'a_2} + \mathbf{d_B}\} \\
&\quad + \sum_{\xi}\left(e^{-2\pi i\frac{p}{q}\left(I'+\frac{2}{3}\right)}S_{\eta,\xi}\{\mathbf{T}_2(\mathbf{d_A})\} + e^{2\pi i\frac{p}{q}\left(I'+\frac{2}{3}\right)}e^{-ik_x a}S_{\eta,\xi}\{\mathbf{T}_3(\mathbf{d_A})\}\right)\Bigg] \\
&\qquad\qquad \times C_{\mathbf{k}}^{\xi}\{(\mathbf{I'}-\mathbf{1})\mathbf{a_2} + \mathbf{d_B}\},
\end{aligned} \tag{3.57}$$

with

$$C_{\mathbf{k}}^{\xi}\{(\mathbf{I'}-\mathbf{1})\mathbf{a_2} + \mathbf{d_B}\} = \begin{cases} e^{i\mathbf{k}.\mathbf{qa_2}}C_{\mathbf{k}}^{2lJM}\{(\mathbf{I'}-\mathbf{1})\mathbf{a_2} + \mathbf{d_B}\} & \text{for} \quad I' = 0, \\ C_{\mathbf{k}}^{2lJM}\{(\mathbf{I'}-\mathbf{1})\mathbf{a_2} + \mathbf{d_B}\} & \text{for} \quad I' \neq 0. \end{cases} \tag{3.58}$$

(ii) For $d_j = d_B$,

$$\begin{aligned}
&(\varepsilon_{\eta}^{a_j,\mathbf{0}} + \Delta\varepsilon_{\eta}^{a_j,\mathbf{d_j}})C_{\mathbf{k}}^{\eta}(\mathbf{I'a_2} + \mathbf{d_B}) + \sum_{\xi}\tilde{T}_{\eta,\xi}\{\mathbf{T}_1(\mathbf{d_B})\}C_{\mathbf{k}}^{\xi}\{\mathbf{I'a_2} + \mathbf{d_A}\} \\
&\quad + \sum_{\xi}\left(e^{2\pi i\frac{p}{q}\left(I'+\frac{4}{3}\right)}\tilde{T}_{\eta,\xi}\{\mathbf{T}_2(\mathbf{d_B})\} + e^{-2\pi i\frac{p}{q}\left(I'+\frac{4}{3}\right)}e^{ik_x a}\tilde{T}_{\eta,\xi}\{\mathbf{T}_3(\mathbf{d_B})\}\right) \\
&\qquad\qquad \times C_{\mathbf{k}}^{\xi}\{(\mathbf{I'}+\mathbf{1})\mathbf{a_2} + \mathbf{d_A}\} \\
&= E_{\mathbf{k}}\Bigg[C_{\mathbf{k}}^{\eta}(\mathbf{I'a_2} + \mathbf{d_B}) + \sum_{\xi}S_{\eta,\xi}\{\mathbf{T}_1(\mathbf{d_B})\}C_{\mathbf{k}}^{\xi}\{\mathbf{I'a_2} + \mathbf{d_A}\} \\
&\quad + \sum_{\xi}\left(e^{2\pi i\frac{p}{q}\left(I'+\frac{4}{3}\right)}S_{\eta,\xi}\{\mathbf{T}_2(\mathbf{d_B})\} + e^{-2\pi i\frac{p}{q}\left(I'+\frac{4}{3}\right)}e^{ik_x a}S_{\eta,\xi}\{\mathbf{T}_3(\mathbf{d_B})\}\right)\Bigg] \\
&\qquad\qquad \times C_{\mathbf{k}}^{\xi}\{(\mathbf{I'}+\mathbf{1})\mathbf{a_2} + \mathbf{d_A}\},
\end{aligned} \tag{3.59}$$

with

$$C^{\xi}_{\mathbf{k}}\{(\mathbf{I}'+\mathbf{1})\mathbf{a_2}+\mathbf{d_A}\} = \begin{cases} e^{-i\mathbf{k}.\mathbf{q}\mathbf{a_2}} C^{2lJM}_{\mathbf{k}}\{\mathbf{d_A}\} & \text{for} \quad I' = q-1, \\ C^{2lJM}_{\mathbf{k}}\{(\mathbf{I}'+\mathbf{1})\mathbf{a_2}+\mathbf{d_A}\} & \text{for} \quad I' \neq q-1. \end{cases} \tag{3.60}$$

The summation on l, J and M in Eqs.(3.57 and 3.59) are taken over eight states described in Eq.(3.56). Hence, Eqs.(3.57-3.59) are the simultaneous equations with $16q$-coefficients.

3.4 Relativistic TB parameters for graphene

The energy-band structure estimated using the relativistic TB approximation approach for the case of $B = 0$ must coincide with that of the reference data to determine relativistic TB parameters. We make use of the energy-band structure calculated by Win2K code [62] as the reference data which use the linear augmented plane wave technique together with SO interaction. We ignore $\Delta\varepsilon^{C,\mathbf{d_i}}_{nlJM}$ and the atomic spectrum, which is calculated using the density functional theory with the local density approximation, because the energy of the crystal field is assumed to be considerably less than the atomic spectrum. Table 3.3 shows the numerical values of $\varepsilon^{a_j,\mathbf{0}}_{\eta} + \Delta\varepsilon^{a_j,\mathbf{d_j}}_{\eta}$ and relativistic TB parameters that were calculated under above mentioned assumption. The resultant energy band structure for the case of $B = 0$ is given in Fig. 3.3. The Fermi energy is about 5.53 (meV). The magnified view around K point is shown in the inset. A minor gap approximately 24 (μeV) emerges at the K point due to SO interaction, which is consistent with earlier results [23, 46]. In the next section, we use the nonperturbative MFRTB method with the parameters specified in Table 3.3 to calculate the energy-band structure and magnetic properties of graphene immersed in a magnetic field. The magnitude of the magnetic field in this calculation ranges from 1.57 to 200 (T).

3.5 Results and Discussion

3.5.1 Relation between energy-bands obtained from nonperturbative MFRTB method and the so-called Landau levels

Fig. 3.4 illustrates the energy-band structure of graphene immersed in a magnetic field of about $B = 195$ (T) ($p = 1, q = 809$). The horizontal axis denotes special $\mathbf{k}$ points of the magnetic first Brillouin zone that is drawn in Fig. 3.2. It is found that $E - \mathbf{k}$ curves depends little on $\mathbf{k}$. This is similar to the case of the two-dimensional square lattice immersed in a magnetic field [38]. These nearly flat energy-bands relate to the quantization of electron orbital motion in a magnetic field [38]. We will describe the relationship between the nearly flat energy-band and the so-called Landau level in detail for the convenience in the following discussion. The eigenvalues of a nearly flat energy-band are approximately degenerate, as shown in Fig. 3.4. In other words, a nearly flat energy-band approximately corresponds to a degenerate energy level. The degree degeneracy is equal to the total number of $\mathbf{k}$ points contained in the magnetic first Brillouin zone. According to the theorem given in ref. [38], the total number of $\mathbf{k}$ points contained in a magnetic first Brillouin zone coincides with that of the magnetic unit cells contained in the system. The area of the magnetic unit cell is q times as large as that of the unit cell as mentioned in Sec.3.1. If we denote the number of the unit cell contained in the

Table 3.3: Relativistic TB parameters between the nearest neighboring atoms for graphene. $K_1(n'l'J', nlJ)_{|M|}$ and $S_1(n'l'J', nlJ)_{|M|}$ denote relativistic TB parameters for hopping integrals and overlap integrals respectively[61].

(n, l, J, M)	Numerical values (eV)
$\bar{\varepsilon}^C_{20\frac{1}{2}} + \Delta\bar{\varepsilon}^{C,\mathbf{d_i}}_{20\frac{1}{2}M}$	-8.370
$\bar{\varepsilon}^C_{21\frac{1}{2}} + \Delta\bar{\varepsilon}^{C,\mathbf{d_i}}_{21\frac{1}{2}M}$	0.000
$\bar{\varepsilon}^C_{21\frac{3}{2}} + \Delta\bar{\varepsilon}^{C,\mathbf{d_i}}_{21\frac{3}{2}M}$	8.305×10^{-3}
$K_1(20\frac{1}{2}, 20\frac{1}{2})_{\frac{1}{2}}$	-5.727
$K_1(20\frac{1}{2}, 21\frac{1}{2})_{\frac{1}{2}}$	-3.226
$K_1(20\frac{1}{2}, 21\frac{3}{2})_{\frac{1}{2}}$	4.587
$K_1(21\frac{1}{2}, 21\frac{1}{2})_{\frac{1}{2}}$	-1.810×10^{-2}
$K_1(21\frac{1}{2}, 21\frac{3}{2})_{\frac{1}{2}}$	-4.298
$K_1(21\frac{3}{2}, 21\frac{3}{2})_{\frac{1}{2}}$	3.010
$K_1(21\frac{3}{2}, 21\frac{3}{2})_{\frac{3}{2}}$	-3.064
$S_1(20\frac{1}{2}, 20\frac{1}{2})_{\frac{1}{2}}$	1.012×10^{-1}
$S_1(20\frac{1}{2}, 21\frac{1}{2})_{\frac{1}{2}}$	9.739×10^{-2}
$S_1(20\frac{1}{2}, 21\frac{3}{2})_{\frac{1}{2}}$	-1.392×10^{-1}
$S_1(21\frac{1}{2}, 21\frac{1}{2})_{\frac{1}{2}}$	-7.904×10^{-2}
$S_1(21\frac{1}{2}, 21\frac{3}{2})_{\frac{1}{2}}$	2.081×10^{-1}
$S_1(21\frac{3}{2}, 21\frac{3}{2})_{\frac{1}{2}}$	-2.289×10^{-1}
$S_1(21\frac{3}{2}, 21\frac{3}{2})_{\frac{3}{2}}$	6.802×10^{-2}

system as N_0, then that of the magnetic primitive unit cell is $\frac{N_0}{q}$. Therefore, we can say that a nearly flat energy-band approximately represents $\frac{N_0}{q}$-fold degenerate energy level. Note that N_0 is given by $\frac{2S}{\sqrt{3}a^2}$ in case of graphene, where S denotes the area of the system.

Next, we consider two cases where the magnetic field is nearly equal to each other. Specifically, the ratio $\frac{p}{q}$ in Eq.(3.15) is nearly equal to $\frac{1}{q'}$, i.e., $\frac{p}{q} \sim \frac{1}{q'}$. Because of $q \sim pq'$, the period of $\mathbf{t_n}$ along the a_2-direction in the case of $\frac{p}{q}$ is p times longer than that in case of $\frac{1}{q'}$. Therefore, p energy gaps may be induced at the boundaries of the magnetic first Brillouin zone due to the folding of the magnetic first Brillouin zone [38]. Namely, an energy band in the case of $\frac{1}{q'}$ is divided into p energy bands in the case of $\frac{p}{q}$. In the previous work [38–41], we refer to the set of p energy bands as a cluster. The energy width of the cluster is nearly equal to that of the energy band of the case of $\frac{1}{q'}$ [38]. As shown in Fig. 3.4, the energy band of the case of $\frac{1}{q'}$ is nearly flat, so the p energy-bands approximately overlap to each other. Since, each energy band is nearly flat and approximately regarded as a $\frac{N_0}{q}$-fold degenerate energy level, we can say that the cluster is approximately regarded as a $N_0\frac{p}{q}$-fold degenerate energy level. The approximately degenerate factor $N_0\frac{p}{q}$ is proportional to the magnetic field. Thus, the cluster corresponds to the so-called the

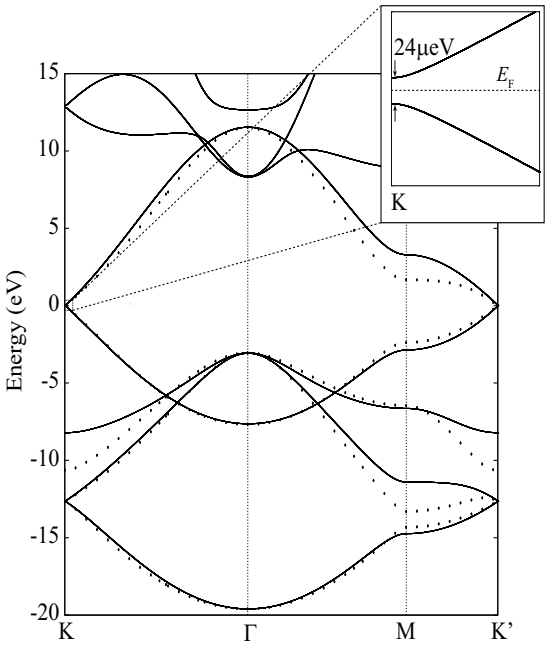

Figure 3.3: Energy band structure of graphene. The circle denote the reference data calculated by the Wien2k code [61].

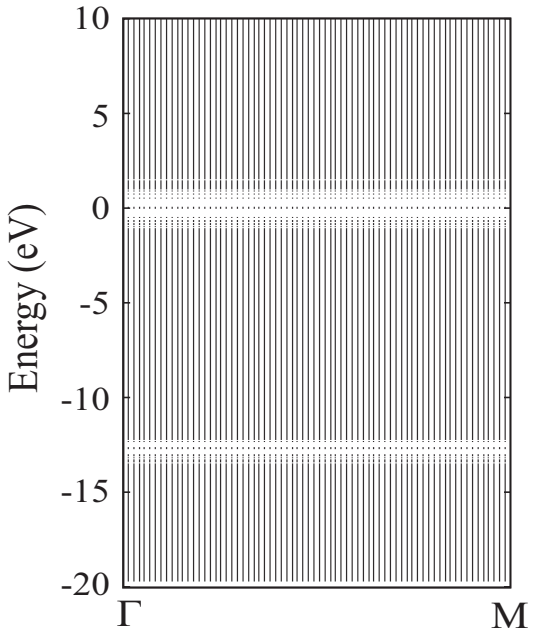

Figure 3.4: Energy band structure of graphene immersed in a uniform magnetic field about 195 (T). Values of p and q are 1 and 809 respectively [61].

Landau level, the degree of degeneracy of which is proportional to the magnetic field. The number of energy bands obtained by the nonperturbative MFRTB method is equal to $16q$ as mentioned in Sec 3.1. Therefore, the number of clusters is approximately given by $16\frac{q}{p}(\approx 16q')$. That means that the number of clusters, which is corresponds to the number of the so-called Landau levels, decreases with increasing B. Since the energy level of the cluster is approximately $N_0\frac{p}{q}$-fold ($\approx \frac{N_0}{q'}$-fold) degenerate as mentioned above, we obtain $16N_0$ energy states total. For simplicity, we consider the case of $p = 1$ in the following discussion because the clusters in the case of $\frac{1}{q'}$ approximately corresponds to those in the case of $\frac{p}{q}$ from the viewpoint of the number of clusters and their degeneracy.

3.5.2 Energy spectrum

Fig. 3.5 shows overview and Figs. 3.6, 3.7 and 3.8 show magnified views of the magnetic field dependence of the energy spectrum, respectively. It is reported by previous works [1, 2] that the energy spectrum near the Fermi energy is approximately proportional to $\pm\sqrt{nB}$ $(n = 0, 1, 2, ...)$ for graphene immersed in a magnetic field. As shown in Figs. 3.5 and 3.6, the square-root dependence of the energy spectrum on B is revisited by the nonperturbative MFRTB method. In addition, each energy level splits in to two levels due to Zeeman effect. Especially, energy levels corresponding to Landau levels with $(n = 0)$ increases or decreases with magnetic field, so that the energy gap appears and increases with the magnetic field. The splitting of energy levels near the Fermi energy is observed experimentally [20].

It is found from Fig. 3.7 that the energy spacing strongly depends on energy. Namely, the energy spacing becomes narrow gradually with the decrease of the energy down to

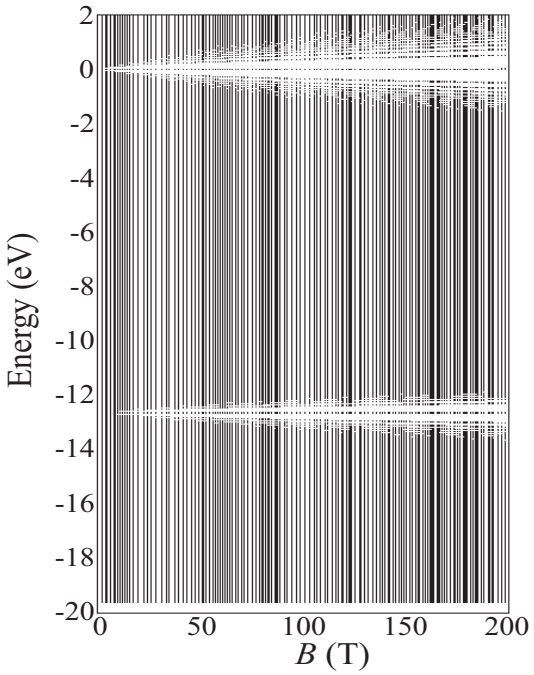

Figure 3.5: Overall view of magnetic field dependence of the energy spectrum of graphene [61].

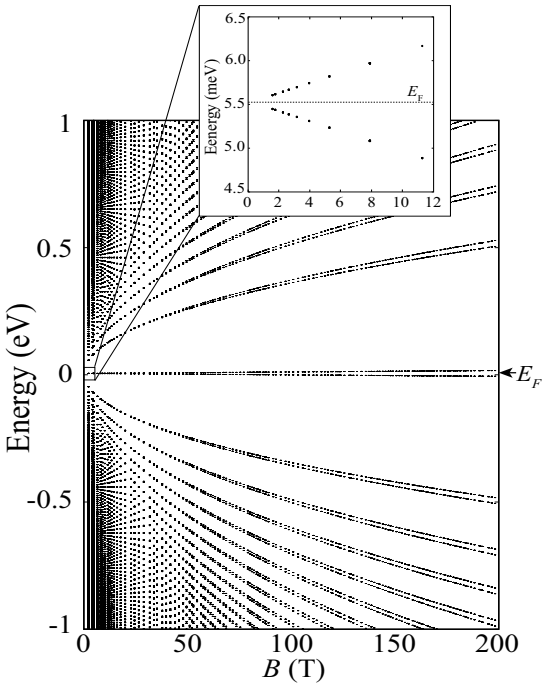

Figure 3.6: Magnified view of energy spectrum within range between -1 (eV) to 1 (eV) [61].

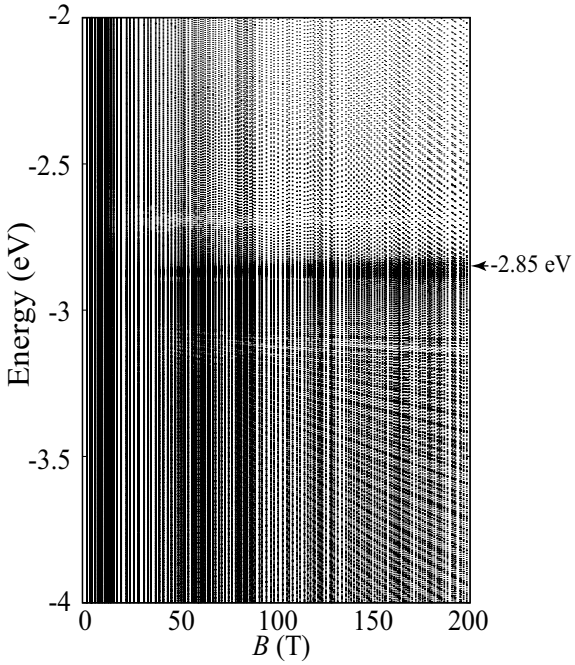

Figure 3.7: Magnified view of energy spectrum within range between -4 (eV) to -2 (eV) [61].

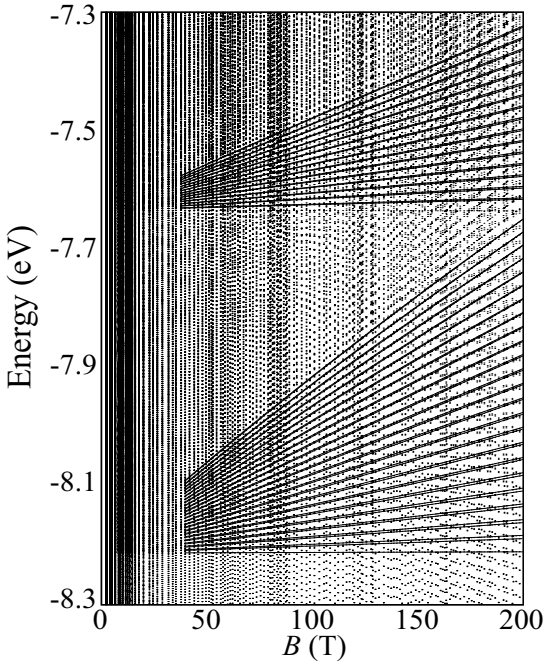

Figure 3.8: Magnified view of energy spectrum within range between -8.3 (eV) to -7.3 (eV) [61].

about -2.8 (eV), as is expected from the square-root dependence. The energy spacing becomes narrow rapidly in the energy around -2.85 (eV). This can be explained on the basis of the energy band structure for the case of $B = 0$ (Fig. 3.3). The cross-sectional area of the constant energy plane increases rapidly around -2.85 (eV) as is expected from

the flat $E - \mathbf{k}$ curves between K' and M points of Fig. 3.3, so that the cyclotron mass becomes large around -2.85 (eV). Therefore, the energy spacing becomes narrow around -2.85 (eV). In addition, it is expected from Fig.(3.3) that hole orbits centering around Γ point appear below about -3.0 (eV). Corresponding to the hole orbits, a lot of energy levels that decreases with B appear below about -3.0 (eV) as shown in Fig. 3.7.
Fig. 3.8 shows that magnetic field dependence of the energy spectrum in the other energy range. As indicated by lines in Fig. 3.8, two sets of energy levels that increase with B are found in energy range around -7.6 and -8.2 (eV). According to the energy band shown in Fig. 3.3, two sets of electron orbits are expected to appear around Γ point [-7.6 (eV)] and around K (K') point [-8.2 (eV)]. These electron orbits corresponds to energy levels found in Fig 3.8. In addition, there are many energy levels that come from electron orbits. Thus, the present method can predict the complicated but realistic energy levels of graphene immersed in magnetic field.

3.5.3 Diamagnetism

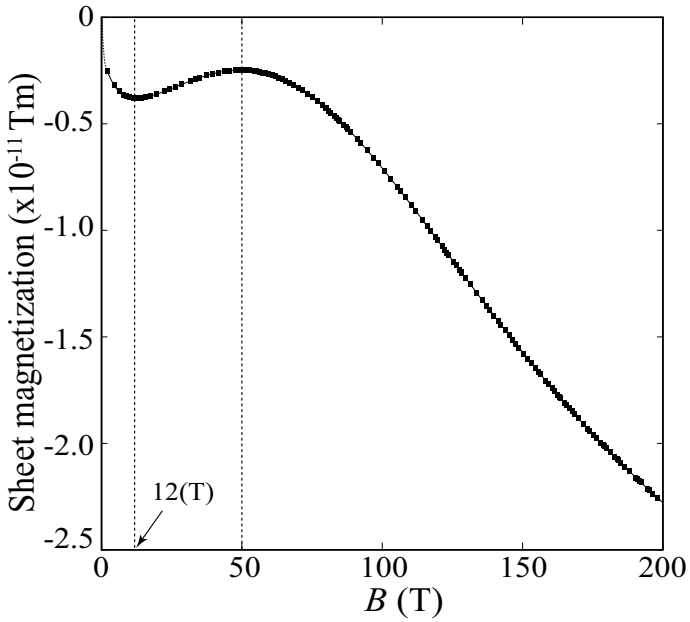

Figure 3.9: Magnetic field dependence of sheet magnetization [61].

The sheet magnetization is calculated by the derivative of the total energy with respect to the magnetic field. Fig. 3.9 shows the magnetic field dependence of the sheet magnetization. The sheet magnetization rapidly decreases with B in the low magnetic-field region [$B < 12$ (T)], which leads to the high magnetic susceptibility. This means that the orbital diamagnetism is stronger than the Pauli paramagnetism in graphene. Thus, the nonperturbative MFRTB method can revisit the strong orbital diamagnetism of graphene [1]-[13]. The sheet magnetization shows a characteristic dependence on B on other magnetic field regions. Namely, the sheet magnetization upturns at about 12 (T) and turns down again at about 50 (T) as shown in Fig. 3.9.

In order to consider the magnetic-field dependence of the sheet magnetization (Fig. 3.9), we shall consider the magnetic field dependence of the total energy. As mentioned in

subsec. 3.5.1, we obtain $16N_0$ energy states in total by means of the nonperturbative MFRTB method. There are $8N_0$ electrons in the system because tow carbon atoms are contained in the unit cell. Since each cluster is approximately $\frac{N_0}{q'}$-fold degenerate, the lower half of clusters ($8q'$ clusters) are occupied by electrons. The $8q'$-th cluster from the bottom corresponds to the so-called Landau level with $n = 0$ that lies immediately below the Fermi energy in Fig. 3.6.

Since the number of clusters decreases with B as mentioned in subsec. 3.5.1, some clusters disappear with increasing B. On the other hand, the degree of degeneracy of the remaining clusters increases with B as mentioned in subsec. 3.5.1. Therefore, electrons that occupy the disappeared clusters are redistributed to remaining clusters. In this case, the energy of the redistributed electron sometimes increases (diamagnetic effect) or decreases (paramagnetic effect). In addition, the energy level of the remaining cluster increases (diamagnetic effect) or decreases (paramagnetic effect) with B as shown in Fig. 3.5-3.8, depending on whether the cluster corresponds to the Landau level originating from electron orbitals or from hole orbitals. In other words, the cluster corresponding to electron orbitals (hole orbitals) contributes to the diamagnetism (paramagnetism).

Thus, the magnetic-field dependences of the total energy and also of the magnetization are complexly determined by the above mentioned factors, so that we can describe the magnetic field dependence only by the energy band calculation for graphene immersed in a magnetic field.

It is found in Fig. 3.9, that the sheet magnetization is diamagnetic for the whole region of the magnetic field. This means that the above mentioned diamagnetic effects are superior to the paramagnetic ones in the whole region of the magnetic field. The balance of these competitive effects changes with B, which leads to the characteristics magnetic field dependence of the diamagnetism. For instance, the derivative of the magnetic field dependence of the total energy is positive but the second derivative is negative in the region ranging from 12 to 15 (T).

In the low magnetic field region [< 12 (T)], the strong orbital diamagnetism of graphene can be revisited as shown in Fig. 3.9. On the other hand, it is shown in previous works [1]-[13] that the massless Dirac electrons causes a strong orbital susceptibility. This implies that the above mentioned diamagnetic effects caused by electrons, which occupy the energy states near the Fermi energy and are like a massless Dirac electron, would be dominant in the low magnetic field region.

In the high magnetic field [> 50 (T)], the sheet magnetization turns down again at about 50 (T). In this region, the sheet magnetization decreases in proportion to about B^2. This dependence is different from the magnetic field dependence found in low magnetic field [< 12 (T)] of Fig. 3.9. Therefore, we can say the the dominant diamagnetic effects in the high magnetic field region would be different from those in the low magnetic field regions.

Thus, the complicated but realistic energy levels of graphene immersed in a magnetic field [Figs. 3.5-3.8] cause a characteristic magnetic field dependence of the diamagnetism.

3.5.4 Effective g-factor

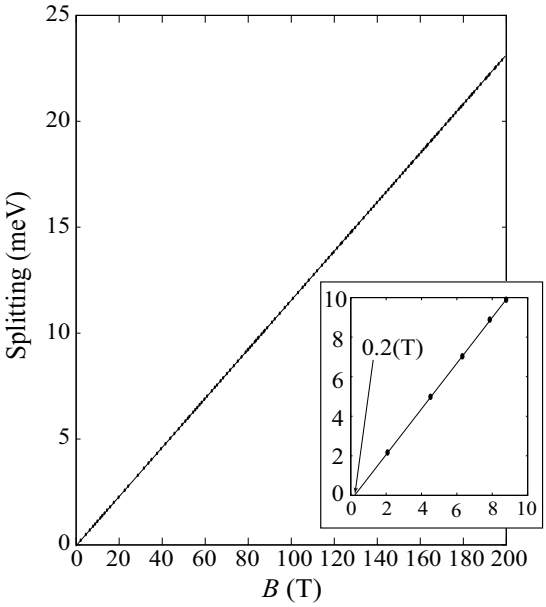

Figure 3.10: Magnetic field dependence of the splitting between the highest occupied and lowest unoccupied energy levels [61].

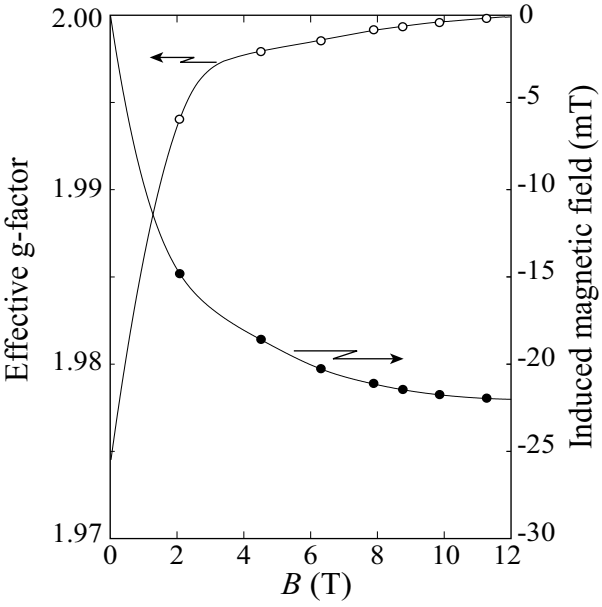

Figure 3.11: Magnetic-field dependence of the effective g-factor and induced magnetic field [61].

As observed in experiments of the electron spin resonance [28, 29], the effective g-factor of the electron in graphene is lower than that of the free electron. It is pointed out by Yafet that the Zeeman splitting of the energy level is affected by the effective magnetic field caused by the SO interaction [63]. Since, we do not consider the effect of the substrate in the present calculations, the space inversion symmetry is not broken in the system. This means that the Rashba-type SO interaction [51], which causes the effective magnetic field parallel to the plane of the graphene, is not taken into account in the present calculations. Therefore, it is reasonable to suppose that the effective magnetic field is perpendicular to the plane of the graphene. If the effective magnetic field is denoted as B_{SO}, then the Zeeman splitting between the highest occupied state and the lowest unoccupied one (ΔE) is given by $\Delta E = g\frac{e\hbar}{2m_0}(B + B_{SO})$, where g denotes the g-factor and is given by $g \simeq 2.0$. Thus, the effective magnetic field caused by the SO interaction changes the Zeeman splitting. In the experiments of Ref. [28] and [29], the magnetic field dependence of ΔE is measured, and the effective g-factor is estimated from the slop of $\Delta E - B$ curve. Similar to the estimation method of the experiments, we calculate the magnetic field dependence of ΔE that is shown in Fig. 3.10. If B_{SO} is independent of B, then the slop of $\Delta E - B$ curve is $g\frac{e\hbar}{2m_0}$. If B_{SO} dependents on B, then slop of $\Delta E - B$ curve deviates from $g\frac{e\hbar}{2m_0}$. It is found from Fig. 3.10 that the slope of $\Delta E - B$ curve is nearly equal to $g\frac{e\hbar}{2m_0}$. This means that B_{SO} is independent of B, i.e., the SO interaction is independent of B. The value of B_{SO} can be obtained from the intersection point of the horizontal axis. It is found from Fig. 3.10 that the intersection point of the horizontal axis is about 0.2 (T). Fig. 3.12 is the magnified view of magnetic field dependence of the energy spectrum in a low magnetic field region. It is found from Fig. 3.12 that the highest occupied energy

level and lowest unoccupied energy level intersect at about 0.2 (T). This also suggests that the value of B_{SO} is about 0.2 (T). Therefore, we can say that B_{SO} is antiparallel to the applied magnetic field and its magnitude is about 0.2 (T). Therefore, we can say that B_{SO} is anti parallel to the applied magnetic field and its magnitude is about 0.2 (T). Thus, the experimentally observed small g-factor is not due to the SO interaction because the slop of the linear dependence is 2.0 as shown in Fig. 3.10.

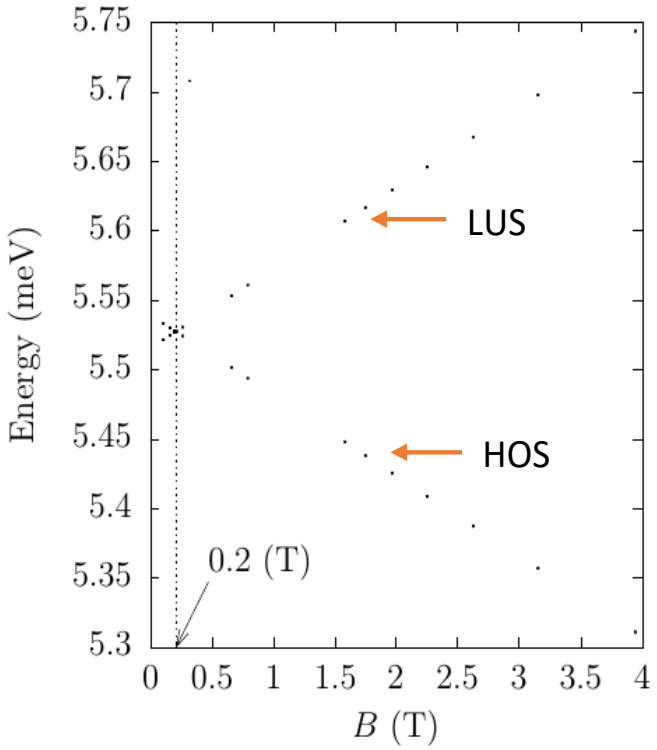

Figure 3.12: Magnified view of Magnetic field dependence of the splitting between the highest occupied and lowest unoccupied energy levels within the range between 5.3 to 5.75 (meV).

In order to clarify the origin of the small g-factor, we investigated the magnetic field induced by the diamagnetism of graphene. The induced magnetic field is estimated as follows. The magnetic moment per one carbon atom can be calculated as the product of the sheet magnetization and the area covered by one carbon atom. Note that the area is regarded as that of the equilateral triangle with sides a. Since the magnitude of the magnetic moment is equivalent to the product of the loop current and the area of the loop, we can obtain the current flowing along the edge of the equilateral triangle. The current generates the magnetic field that can be calculated by Biot-Savart law. The induced magnetic field is estimated as the magnetic field at the position of the carbon atom. The induced magnetic fields thus obtained are shown in Fig. 3.11. The actual magnetic field is smaller than the applied magnetic field due to the induced magnetic field. Therefore, the effective g-factor is reduced due to the reduction of the magnetic field as shown in Fig. 3.11. It is found that the estimated g-factor strongly depends on the applied magnetic field. Due to induced magnetic field, Zeeman splitting between HOS and LUS is given by $\Delta E = g\frac{e\hbar}{2m}(B_{ext} + B_{ind})$. The effective g-factor is calculated

from the slope of $\Delta E - B_{ext}$ and it is given by $g_{\text{eff}} = g\left(1 + \dfrac{dB_{ind}}{dB_{ext}}\right)$. The calculated value of $\dfrac{dB_{ind}}{dB_{ext}}$ is -6.548057×10^{-3} when $B_{ext} = 1$ (T). The estimated value of the effective g-factor is about 1.986 at $B_{ext} = 1$ (T). Following the same calculation, the value of effective g-factor at $B_{ext} = 2$ (T) is found to be 1.993. Thus the magnetic field induced by the strong diamagnetism is one of the cause why the effective g-factor of the electron in graphene is lower than that of the free electron.

It should be noted that the experimental value of the effective g-factor is about 1.94 [28, 29] at the magnetic field of about 1 (T), while theoretically estimated value is 1.986 as mentioned above. This implies that there exist other mechanisms that reduce the value of effective g-factor. The Rashba-type SO interaction is considered as a possibility of reducing the value of effective g-factor. Namely, since there exist the substrate, space inversion symmetry is broken in the real system [28, 29]. Therefore, in the graphene, the gradient of the scalar potential has a component that is perpendicular to the two dimensional plane. The perpendicular component would cause the effective magnetic field that is parallel to the two dimensional plane. This is known as Rashba effect [51, 52] and is not incorporated in present calculations. Due to Rashba effect, the orientation of the spin would be tiled from the z-axis in graphene. The tilting of the spin orientation leads to the reduction of the Zeeman splitting. Suppose that the average of the angle between z-axis and the spin is given by θ, the Zeeman splitting would be reduced by the factor $cos\theta$. If the discrepancy between experimentally observed value of the effective g-factor ($g = 1.94$) and the theoretical one ($g = 1.986$) comes from the tilting of the spin orientation, then the angle θ is estimated to be $\frac{12.3\pi}{180}$(rad) at the magnetic field of 1 (T). Although the tilting of spin orientation due to the Rashba effect is not taken into consideration in the present calculations, it would be one of the cause for small value of the effective g-factor that is observed experimentally [28, 29]

Chapter 4

Reduction of g-factor due to Rashba effect in graphene

In chapter 3, we demonstrated that the diamagnetism is the one of sources for the reduction in g-factor of graphene. However, the cause of the reduction in g-factor observed in the experiments is not completely explained by diamagnetic property of graphene alone. Therefore, in this chapter, we focused on the Rashba effect which is caused by work function existing in the vicinity of graphene surface to account remaining reduction in g-factor of graphene. In this chapter, we use empty lattice model by incorporating Rashba effect.

4.1 Calculation scheme

A. **Calculation procedure**

In graphene, the energy band exists at K point. Let us assume that this band gap (HOS-LUS) still exits at K point when Rashba effect is considered and external magnetic field is applied. This means only small modification occurs in the electronic structure of graphene. This is reasonable assumption because the magnitude of external magnetic field is at most 1 (T) and magnetic field due caused by Rashba effect is much smaller than the external magnetic field.

For intrinsic case (Zero magnetic field), the energy bands of usual graphene possess double degeneracy at any wave number $\mathbf{k} = (k_x, k_y)$ due to the presence of time reversal and space inversion symmetry. The energy degeneracy consists of two bands mixed up by up-spin and down-spin states and is resolved by the Rashba effect and/or the external magnetic field. This energy splitting results in the modification of the HOS-LUS gap.

The calculation scheme is as follows:

(i) First the energy splitting is calculated in a model system that has a free-electron Hamiltonian with the Rashba term, spin Zeeman term and an asymmetric potential caused by the work function are added. The energy splitting, whose explicit form is described in coming section, is dependent on the wavenumber $\mathbf{k} = (k_x, k_y)$. It is hereafter denoted as $\Delta_{k_x k_y}$, and its value at K-point is specif-

ically denoted as Δ_k. Note that we employ a free-electron Hamiltonian only for the calculation of the energy splitting.

(ii) Next, the obtained energy splitting $\Delta_{k_x k_y}$ is added to energy bands of the usual graphene [46]. Consequently, the original two bands, which are degenerate with each other [34], shifted by $+\Delta_{k_x k_y}$ and $-\Delta_{k_x k_y}$ respectively. In particular, the HOS and LUS are modified by Δ_K. The resultant energy levels of the HOS and LUS are, respectively given by

$$\varepsilon_{LUS} = \varepsilon_K + E_{SO} - \Delta_K, \tag{4.1}$$
$$\varepsilon_{HOS} = \varepsilon_K - \Delta_K. \tag{4.2}$$

where ε_K is the energy level of the HOS and E_{SO} is the SO interaction energy caused by the spatially symmetric potential of the hexagonal lattice of the graphene sheet. The HOS-LUS gap is given by

$$\begin{aligned}\Delta\varepsilon|_{atK} &= \varepsilon_{LUS} - \varepsilon_{HOS} \\ &= E_{SO} - 2\Delta_K.\end{aligned} \tag{4.3}$$

Since the reduction to the g-factor in graphene has experimentally observed [28, 29], this reduction must be calculated by a method that can suitably enable the analysis of those ESR experimental results. To achieve this, we perform the following calculations.

(iii) From the dependence of the HOS-LUS gap on the external magnetic field, the g-factor is observed as if it were reduced [28, 29]. Let the reduced g-factor be called effective g-factor. To facilitate the analysis of the experimental value observed in ESR experiment [28, 29], the effective g-factor g_{eff} is defined as

$$g_{\text{eff}} = \frac{1}{\mu_B}\left|\frac{d}{dB_{ext}}\Delta\varepsilon|_{atK}\right|, \tag{4.4}$$

where μ_B is the Bohr magneton and B_{ext} is the external magnetic field. The details are described in Section 4.4.

As mentioned above, we first calculate the energy splitting caused by the Rashba and spin Zeeman effects at the K point by treating graphene lattice as an empty one. Next, we add the thus-obtained energy splitting estimated at the K point of the Brillouin zone of graphene. This idea of calculating the Rashba effect of graphene in our scheme is similar to that of treating the exchange-correlation (xc) effects in the local density approximation (LDA) of the density functional theory (DFT) [58, 64–70]. In LDA, the xc effects are considered on the basis of the model of a homogeneous electron liquid, referred to as the jellium model, and the results are applied to the inhomogeneous electron system such as atoms, molecules, and solid [64]. In general terms, the idea of LDA is that xc effects are considered on the basis of a simplified model, and the result are extensively applied to more general cases. This idea is also used in developing the kinetic energy functional of the pair-density functional theory [71–87]. There are other good examples such as BCS theory, Pauli paramagnetism, Landau diamagnetism, and so on. Similarly, in our present scheme, the Rashba effect is treated in a model system, and the results are applied to actual graphene. Thus, the idea of this scheme is analogous to that of the LDA-DFT.

As a final note in this section, we comment briefly on the second of the two kinds of magnetic moments (the first being the spin magnetic moment) that electrons in metals primarily possess, the orbital magnetic moment [88–91]. The orbital magnetic moment generally appears when an external magnetic field is applied to metals. In our study with graphene, the magnitude of the orbital magnetic moment for the state of K point would be small, since the orbital motion on the constant energy surface of the k space is point like at the K point [44–46]. Consequently,when solving the eigenvalue problem at the K point, we can neglect the effect of the orbital magnetic moment, and consider only the effects of the spin magnetic moment.

B. Model of an asymmetric potential

In this subsection, we shall explain the model for an asymmetric potential used. Let us consider the case where graphene is placed in vacuum. In this case, the electron at the K point is confined to the graphene sheet due to the work function that spatially spreads in the region determined by electron density. Hereafter, we refer to the potential caused by the work function as the surface potential. When graphene is placed in vacuum, the surface potential is symmetric in the direction perpendicular to the graphene sheet. Contributions to the energy splitting by the surface potential formed on both sides of the graphene sheet are canceled out each other [92]. Therefore, the energy splitting does not occur in this case.

Next, let us consider the case of the graphene sheet deposited on the substrate. We assume that the distance between the graphene and the substrate is close enough to affect the surface potential. In this case, the surface potential is asymmetric in the direction perpendicular to the graphene sheet. This is because the surface potential formed on the substrate side is different from that on the vacuum side. The former and later surface potentials are denoted as V_{sub} and V_{vac}, respectively. Since contributions of V_{vac} and V_{sub} to the energy splitting are not canceled out each other, the energy splitting occurs in this case.

It is known that the height of V_{sub} is equal to that of V_{vac} minus electron affinity of the substrate material, i.e. $V_{sub} = V_{vac} - \chi$, where χ is the electron affinity. Namely, V_{sub} is smaller than V_{vac} due to electron affinity. In addition to this fact, it is shown by the experiment that the reduction of the g-factor does not largely depend on the type of substrate [29]. This experimental results seems to indicate that V_{sub} is so small that it makes little contribution to the energy splitting. In this work, we assume that the contribution of V_{sub} to the energy splitting is negligibly small in comparison with that of V_{vac}. Under this assumption, the contribution of V_{vac} to the energy splitting is hardly canceled out by that of V_{sub} and, therefore energy splitting due to V_{vac} almost remains. In section 4.2, we employ V_{vac} as a model of the asymmetric potential and calculate the energy splitting $\Delta_{k_x k_y}$.

We shall give a brief comment on this model. It is well known that the large energy splitting due to Rashba effect is observed on the Au(111) surface [93]. The

experimentally-observed energy splitting is five orders of magnitude larger than the energy splitting expected from the electron gas model with the surface potential caused by the work function [93]. According to the first-principle calculation [94], the wave function becomes asymmetric along the vertical direction to the surface due to surface potential. The electron near the surface feels strong potential gradient caused by the nucleus rather than that of the surface potential. This is the reason why the large energy splitting is observed on the Au(111) surface [94]. It is well known that this enhancement of the Rashba effect becomes more pronounced for heavy atoms. Indeed, the Rashba effect is usually regarded as a small effect in the graphene system [95].

The present model is based on the electron gas model with the surface potential caused by the work function. That is to say, we assume that the above-mentioned enhancement of the Rashba effect is not pronounced for the graphene sheet deposited on the substrate. This assumption may underestimate the Rashba effect. However, the Rashba effect calculated under this assumption can explain the experimentally observed reduction of the g-factor as shown in Sections. 4.2-4.4.

4.2 Energy splitting $\Delta_{k_x k_y}$

In this study, we deal with the graphene sheet deposited on the substrate. Suppose that the direction perpendicular to the hexagonal lattice of graphene sheet is the z-axis and that the vacuum side is the positive direction.

Now lets calculate the energy splitting $\Delta_{k_x k_y}$ in model system, the Hamiltonian of this model system has the Rashba term H_{Rashba}, spin Zeeman term H_{Zeeman}, and Asymmetric potential $V_{asymm}(z)$ that is caused by the work function. The Hamiltonian of the model system is given by

$$H = \frac{p^2}{2m} + V(\mathbf{r}) + H_{Rashba} + H_{Zeeman}, \tag{4.5}$$

where p is momentum of an electron and $V(\mathbf{r})$ is crystal potential which can be taken as the sum of symmetric potential $V_{symm}(x, y)$ along in-plane direction and asymmetric potential $V_{asymm}(z)$ caused by the work function which exits in the vicinity of surface and is asymmetric w.r.t. z-axis due to existence of substrate. The potential $V_{asymm}(z)$ also yields the Rashba effect, which is kind of SO interaction and expressed as the following [51, 52]:

$$H_{Rashba} = -\mu_S \cdot \mathbf{B}_{SO}^{asymm}(\mathbf{r}), \tag{4.6}$$

where μ_S is spin magnetic moment of an electron given by

$$\mu_S = -g\mu_B \frac{\mathbf{S}}{\hbar}, \tag{4.7}$$

g is conventional electron g-factor given by $g = 2.0023$, μ_B is Bohr Magneton, $\mathbf{S}$ is spin angular momentum, $\hbar$ is reduced Planck's constant $(h/2\pi)$, and $\mathbf{B}_{SO}^{asymm}(\mathbf{r})$ is magnetic field caused by asymmetric potential $V_{asymm}(z)$ which is given by

$$\mathbf{B}_{SO}^{asymm}(\mathbf{r}) = \frac{2}{g\mu_B} \frac{\hbar}{4m^2c^2} \nabla V_{asymm}(z) \times \mathbf{p}, \tag{4.8}$$

where m and c are rest mass of an electron, and speed of light in vacuum, respectively. This is sometimes called the Rashba magnetic field.

From Eqs.(4.6) and (4.7), we have

$$H_{Rashba} = g\mu_B \frac{\mathbf{S}}{\hbar} \cdot \mathbf{B}_{SO}^{asymm}(\mathbf{r}), \tag{4.9}$$

Since $\mathbf{S} = \frac{\hbar}{2}\sigma$, where σ is Pauli's spin matrices, Eq.(4.9) is given by

$$\begin{aligned} H_{Rashba} &= g\mu_B \frac{\hbar}{2\hbar}\sigma \cdot \mathbf{B}_{SO}^{asymm}(\mathbf{r}) \\ &= \frac{g}{2}\mu_B \sigma \cdot \mathbf{B}_{SO}^{asymm}(\mathbf{r}). \end{aligned} \tag{4.10}$$

From Eq.(4.8), Eq.(4.10) can be written as

$$\begin{aligned} H_{Rashba} &= \frac{g}{2}\mu_B \sigma \cdot \frac{2}{g\mu_B}\frac{\hbar}{4m^2c^2}\nabla V_{asymm}(z) \times \mathbf{p} \\ &= \frac{\hbar}{4m^2c^2}\sigma \cdot \nabla V_{asymm}(z) \times \mathbf{p}. \end{aligned} \tag{4.11}$$

If the Rashba parameter is defined as

$$\alpha_{asymm}(\mathbf{r}) = \frac{\hbar}{4m^2c^2}\nabla V_{asymm}(z), \tag{4.12}$$

then, Eq.(4.11) becomes

$$H_{Rashba} = \sigma \cdot \{\alpha_{asymm}(z) \times \mathbf{p}\}. \tag{4.13}$$

Suppose, the external magnetic field B_{ext} is applied in the z-direction i.e. $\mathbf{B}_{ext} = (0, 0, B_{ext})$. The spin Zeeman effect with respect to this field is given by

$$\begin{aligned} H_{Zeeman} &= -\mu_S \cdot \mathbf{B}_{ext} \\ &= g\mu_B \frac{\mathbf{S}}{\hbar} \cdot \mathbf{B}_{ext} \\ &= g\mu_B \frac{\sigma}{2} \cdot \mathbf{B}_{ext}. \end{aligned} \tag{4.14}$$

Along z-axis,

$$H_{Zeeman} = \frac{g}{2}\mu_B \sigma_z \mathbf{B}_{ext}. \tag{4.15}$$

In order to diagonalized the Hamiltonian Eq.(4.5), let us chose the eigenfunctions of subsystem of Eq.(4.5) as a basis function, say $\varphi_{\mathbf{k}n}(\mathbf{r})$. Let us consider the Hamiltonian excluding third and forth terms of Eq.(4.5) as a subsystem and denote it by H_0. The Hamiltonian of subsystem H_0 is given by

$$\begin{aligned} H_0 &= -\frac{\hbar^2}{2m}\nabla^2 + V_{symm}(x, y) + V_{asymm}(z) \\ &= -\frac{\hbar^2}{2m}\left(\frac{\partial^2}{\partial x^2} + \frac{\partial^2}{\partial y^2} + \frac{\partial^2}{\partial z^2}\right) + V_{symm}(x, y) + V_{asymm}(z). \end{aligned} \tag{4.16}$$

If $\varphi_{\mathbf{k}n}(\mathbf{r})$ and $\varepsilon_{\mathbf{k}n}$, respectively, are eigenfunction and eigenvalue for H_0. Then system obeys the following equation:

$$H_0\varphi_{\mathbf{k}n}(\mathbf{r}) = \varepsilon_{\mathbf{k}n}\varphi_{\mathbf{k}n}(\mathbf{r}). \tag{4.17}$$

The basis function $\varphi_{\mathbf{k}n}(\mathbf{r})$ can be expressed as

$$\varphi_{\mathbf{k}n}(\mathbf{r}) = f_{k_xk_yn}(x,y)u_n(z). \tag{4.18}$$

We now require the eigenfunctions to be periodic in x, y, z with period L.

$$\varphi(x+L,y,z) = \varphi(x,y,z), \tag{4.19}$$
$$\varphi(x,y+L,z) = \varphi(x,y,z), \tag{4.20}$$
$$\varphi(x,y,z+L) = \varphi(x,y,z). \tag{4.21}$$

Eigenfunctions satisfying the free particle Schrödinger wave equation and the periodicity condition are of the form of a traveling plane. Since the motion of an electron is restricted along xy-plane, the wave function $f_{k_xk_yn}(x,y)$ can be expressed as

$$\begin{aligned} f_{k_xk_yn}(x,y) &= \frac{1}{\sqrt{N}}e^{i(\mathbf{K}\cdot\mathbf{r})} \\ &= \frac{1}{\sqrt{N}}e^{i(k_xx+k_yy)}, \end{aligned} \tag{4.22}$$

where N is normalization constant. From Eqs.(4.18 and 4.22), we have

$$\varphi_{k_xk_yn}(\mathbf{r}) = \frac{1}{\sqrt{N}}e^{i(k_xx+k_yy)}u_n(z). \tag{4.23}$$

Taking the boundary conditions given by Eqs.(4.19), (4.20), and (4.21), We have the normalized wave function as

$$\varphi_{k_xk_yn}(\mathbf{r}) = \frac{1}{\sqrt{L^2}}e^{i(k_xx+k_yy)}u_n(z). \tag{4.24}$$

From Eqs. (4.16), (4.17), and (4.24), we have

$$\begin{aligned} &\left\{-\frac{\hbar^2}{2m}\left(\frac{\partial^2}{\partial x^2}+\frac{\partial^2}{\partial y^2}\right)+V_{symm}(x,y)\right\}e^{i(k_xx+k_yy)}u_n(z) \\ &\quad+\left\{-\frac{\hbar^2}{2m}\frac{\partial^2}{\partial z^2}+V_{asymm}(z)\right\}e^{i(k_xx+k_yy)}u_n(z) = \varepsilon_{k_xk_yn}e^{i(k_xx+k_yy)}u_n(z). \end{aligned} \tag{4.25}$$

For empty lattice model, $V_{symm}(x,y) = 0$, so, Eq.(4.25) becomes

$$\begin{aligned} &\left\{-\frac{\hbar^2}{2m}\left(\frac{\partial^2}{\partial x^2}+\frac{\partial^2}{\partial y^2}\right)\right\}e^{i(k_xx+k_yy)}u_n(z)+\left\{-\frac{\hbar^2}{2m}\frac{\partial^2}{\partial z^2}+V_{asymm}(z)\right\}e^{i(k_xx+k_yy)}u_n(z) \\ &\qquad = \varepsilon_{k_xk_yn}e^{i(k_xx+k_yy)}u_n(z) \end{aligned}$$

or

$$\frac{\hbar^2}{2m}(k_x^2+k_y^2)u_n(z)+\xi_nu_n(z) = \varepsilon_{k_xk_yn}u_n(z), \tag{4.26}$$

where

$$\xi_n = -\frac{\hbar^2}{2m}(k_x^2 + k_y^2)\frac{\partial^2}{\partial z^2} + V_{asymm}(z). \tag{4.27}$$

Hence, the eigenvalue of Eq.(4.17) is given by

$$\varepsilon_{k_x k_y n} = \frac{\hbar^2}{2m}(k_x^2 + k_y^2) + \xi_n, \tag{4.28}$$

where $u_n(z)$ and ξ_n satisfy following equation:

$$\left\{-\frac{\hbar^2}{2m}\frac{\partial^2}{\partial z^2} + V_{asymm}(z)\right\} u_n(z) = \xi_n u_n(z). \tag{4.29}$$

Here, we employ an approximation such that the Rashba parameter Eq.(4.12) is spatially constant. Specifically, $\alpha_{asymm}(\mathbf{r})$ is approximated in to $\tilde{\alpha}_z \hat{\mathbf{e}}_z$, where $\hat{\mathbf{e}}_z$ is a unit vector along z axis. This approximation implies that the electric field in the z direction, i.e., $\nabla V_{asymm}(z)$, is assumed to be constant [96]. The approximation corresponds to the assumption that $\nabla V_{asymm}(z)$ is linearly proportional to z in the vicinity of the surface, which is reasonable [96]. Furthermore, this approximation does not disturb the original symmetry of the system given by Eq.(4.5) in which spatial inversion symmetry does not exit. Since the second and third terms of Eq.(4.5) are spin dependent, we utilize the set of eigenfunction $\varphi_{k_x k_y n}(\mathbf{r}, \sigma)$ as the basis function to diagonalized the Hamiltonian Eq.(4.5).

$$\varphi_{k_x k_y n}(\mathbf{r}, \sigma) = \varphi_{k_x k_y n}(\mathbf{r})\chi_\sigma, \tag{4.30}$$

where χ_σ is spin function. From Eqs. (4.24) and (4.30), we have

$$\varphi_{k_x k_y n}(\mathbf{r}, \sigma) = \frac{1}{\sqrt{L}} e^{i(k_x + k_y y)} u_n(z)\chi_\sigma. \tag{4.31}$$

If eigenvalue and eigenfunction of the Hamiltonian H of Eq.(4.5) are denoted by $E_{k_x k_y n}$ and $\varphi_{k_x k_y n}(\mathbf{r}, \sigma)$, respectively, then the system of Hamiltonian H obeys following equation:

$$H\varphi_{k_x k_y n}(\mathbf{r}, \sigma) = E_{k_x k_y n}\varphi_{k_x k_y n}(\mathbf{r}, \sigma). \tag{4.32}$$

Applying Eq.(4.30) and multiplying with $\varphi_{k'_x k'_y n'}(\mathbf{r})\chi'_\sigma$ on both sides of Eq.(4.32), we have

$$\langle \varphi_{k'_x k'_y n'}(\mathbf{r})\chi'_\sigma | H | \varphi_{k_x k_y n}(\mathbf{r})\chi_\sigma \rangle = E_{k_x k_y n}\langle \varphi|_{k'_x k'_y n'}(\mathbf{r})\chi'_\sigma | \varphi_{k_x k_y n}(\mathbf{r})\chi_\sigma \rangle. \tag{4.33}$$

Using Eqs.(4.5), (4.30), and (4.33), we have

$$\begin{aligned}\langle \varphi_{k'_x k'_y n'}(\mathbf{r})\chi'_\sigma | H_0 + H_{Rashba} + H_{Zeeman} | \varphi_{k_x k_y n}(\mathbf{r})\chi_\sigma \rangle \\ = E_{k_x k_y n}\langle \varphi_{k'_x k'_y n'}(\mathbf{r}) | \varphi_{k_x k_y n}(\mathbf{r}) \rangle \langle \chi'_\sigma | \chi_\sigma \rangle.\end{aligned} \tag{4.34}$$

From Eqs.(4.31) and (4.34), we have

$$\begin{aligned}&\langle e^{-i(k'_x x' + k'_y y')} u_{n'}(z)\chi_{\sigma'} | H_0 | e^{i(k_x x + k_y y)} u_n(z)\chi_\sigma \rangle \\ &\quad + \langle e^{-i(k'_x x' + k'_y y')} u_{n'}(z)\chi_{\sigma'} | H_{Rashba} | e^{i(k_x x + k_y y)} u_n(z)\chi_\sigma \rangle \\ &\quad\quad + \langle e^{-i(k'_x x' + k'_y y')} u_{n'}(z)\chi_{\sigma'} | H_{Zeeman} | e^{i(k_x x + k_y y)} u_n(z)\chi_\sigma \rangle \\ &\quad\quad\quad = E_{k_x k_y n}\langle \varphi_{k'_x k'_y n'}(\mathbf{r}) | \varphi_{k_x k_y n}(\mathbf{r}) \rangle \langle \chi_{\sigma'} | \chi_\sigma \rangle.\end{aligned} \tag{4.35}$$

Using Eq.(4.28) and Eq.(4.35), we have

$$
\begin{aligned}
e^{-i(k'_x x'+k'_y y')} e^{i(k_x x+k_y y)} \left\{ \frac{\hbar^2}{2m}(k_x^2+k_y^2)+\xi_n \right\} \langle u_{n'}(z)|u_n(z)\rangle \langle \chi_{\sigma'}|\chi_\sigma\rangle \\
+ e^{-i(k'_x x'+k'_y y')} e^{i(k_x x+k_y y)} \langle u_{n'}(z)|u_n(z)\rangle \langle \chi_{\sigma'}|H_{Rashba}|\chi_\sigma\rangle \\
+ e^{-i(k'_x x'+k'_y y')} e^{i(k_x x+k_y y)} \langle u_{n'}(z)|u_n(z)\rangle \langle \chi_{\sigma'}|H_{Zeeman}|\chi_\sigma\rangle \\
= E_{k_x k_y n} \langle \varphi_{k'_x k'_y n'}(\mathbf{r})|\varphi_{k_x k_y n}(\mathbf{r})\rangle \langle \chi_{\sigma'}|\chi_\sigma\rangle
\end{aligned}
$$

or

$$
\begin{aligned}
\left\{ \frac{\hbar^2}{2m}(k_x^2+k_y^2)+\xi_n \right\} \delta_{k_{x'}k_x}\delta_{k_{y'}k_y}\delta_{n'n} \\
+ \langle \chi_{\sigma'}|\tilde{\alpha}_z \hbar(-k_y\sigma_x + k_x\sigma_y)|\chi_\sigma\rangle \delta_{k_{x'}k_x}\delta_{k_{y'}k_y}\delta_{n'n} \\
+ \langle \chi_{\sigma'}|\frac{g}{2}\mu_B B_{ext}\sigma_z|\chi_\sigma\rangle \delta_{k_{x'}k_x}\delta_{k_{y'}k_y}\delta_{n'n} \\
= E_{k_x k_y n}\delta_{k_{x'}k_x}\delta_{k_{y'}k_y}\delta_{n'n}\delta_{\sigma'\sigma}. \quad (4.36)
\end{aligned}
$$

Hence, we have matrix elements of Eq.(4.36) as

$$
\begin{aligned}
H_{k'_x k'_y n'\sigma', k_x k_y n\sigma} = \left\{ \frac{\hbar^2}{2m}(k_x^2+k_y^2)+\xi_n \right\} \delta_{k_{x'}k_x}\delta_{k_{y'}k_y}\delta_{n'n} \\
+ \{-\tilde{\alpha}_z\hbar k_y \langle \chi_{\sigma'}|\sigma_x|\chi_\sigma\rangle + \tilde{\alpha}_z \hbar k_x \langle \chi_{\sigma'}|\sigma_y|\chi_\sigma\rangle\} \delta_{k_{x'}k_x}\delta_{k_{y'}k_y}\delta_{n'n} \\
+ \frac{g}{2}\mu_B B_{ext}\langle \chi_{\sigma'}|\sigma_z|\chi_\sigma\rangle \delta_{k_{x'}k_x}\delta_{k_{y'}k_y}\delta_{n'n}, \quad (4.37)
\end{aligned}
$$

with

$$
\sigma_x = \begin{pmatrix} 0 & 1 \\ 1 & 0 \end{pmatrix};\ \sigma_y = \begin{pmatrix} 0 & -i \\ i & 0 \end{pmatrix} \text{ and } \sigma_z = \begin{pmatrix} 1 & 0 \\ 0 & -1 \end{pmatrix}. \quad (4.38)
$$

The diagonalization can be performed in each block matrix with the same (k_x, k_y) and n. The block matrix is a 2×2 matrix and is given by

$$
h(k_x,k_y,n) = \begin{pmatrix} \frac{\hbar^2}{2m}(k_x^2+k_y^2)+\xi_n+\frac{g}{2}\mu_B B_{ext} & -\tilde{\alpha}_z\hbar(k_x+ik_y) \\ -\tilde{\alpha}_z\hbar(k_x-ik_y) & \frac{\hbar^2}{2m}(k_x^2+k_y^2)+\xi_n-\frac{g}{2}\mu_B B_{ext} \end{pmatrix}. \quad (4.39)
$$

Diagonalizing Eq.(4.39), we get

$$
|h(k_x,k_y,n)-\lambda I| = 0
$$

or

$$
\begin{vmatrix} \varepsilon_{k_x k_y n}+\frac{g}{2}\mu_B B_{ext}-\lambda & -\tilde{\alpha}_z\hbar(k_x+ik_y) \\ -\tilde{\alpha}_z\hbar(k_x-ik_y) & \varepsilon_{k_x k_y n}-\frac{g}{2}\mu_B B_{ext}-\lambda \end{vmatrix} = 0.
$$

Therefore, we have

$$
\lambda = \varepsilon_{k_x k_y n} \pm \sqrt{\left(\frac{g}{2}\mu_B B_{ext}\right)^2 + (\tilde{\alpha}_z\hbar)^2(k_x^2+k_y^2)}. \quad (4.40)
$$

Hence, the energy eigenvalue of the block matrix $h(k_x, k_y, n)$ is

$$E_{\pm}(k_x, k_y, n) = \varepsilon_{k_x k_y n} \pm \sqrt{\left(\frac{g}{2}\mu_B B_{ext}\right)^2 + (\tilde{\alpha}_z\hbar)^2(k_x^2 + k_y^2)}$$

or

$$E_{\pm}(k_x, k_y, n) = \varepsilon_{k_x k_y n} \pm \Delta_{k_x k_y}, \tag{4.41}$$

where

$$\Delta_{k_x k_y} = \pm\sqrt{\left(\frac{g}{2}\mu_B B_{ext}\right)^2 + (\tilde{\alpha}_z\hbar)^2(k_x^2 + k_y^2)}$$

or

$$\Delta_{k_x k_y} = \pm\sqrt{\delta\left(B_{ext}\right)^2 + (\tilde{\alpha}_z\hbar)^2(k_x^2 + k_y^2)}, \tag{4.42}$$

where,

$$\delta(B_{ext}) = \frac{g}{2}\mu_B B_{ext}. \tag{4.43}$$

From Eq.(4.41), it is clear that $\Delta_{k_x k_y}$, the energy splitting consists of both Zeeman effect $\delta(B_{ext})$ and energy splitting due to Rashba effect, i.e., $\tilde{\alpha}_z^2(k_x^2 + k_y^2)$. It is also shown from Eq.(4.42) that $\Delta_{k_x k_y}$ shows the dependency on wavenumber $\mathbf{K} = (k_x, k_y)$.

Eq.(4.42) can be rewritten as

$$\Delta_{k_x k_y} = \pm\left[\delta\left(B_{ext}\right)^2 + (\tilde{\alpha}_z\hbar)^2(k_x^2 + k_y^2)\right]^{\frac{1}{2}}. \tag{4.44}$$

If the magnitude of B_{ext} is greater than magnitude magnetic field due to Rashba effect, Eq.(4.44) can be approximated as

$$\Delta_{k_x k_y} \approx |\delta(B_{ext})| + \frac{(\tilde{\alpha}_z\hbar)^2(k_x^2 + k_y^2)}{2|\delta(B_{ext})|}. \tag{4.45}$$

The assumption that Eq.(4.45) is valid for the case of graphene because the magnitude of the Rashba magnetic field given by Eq.(4.8) is about one-fourth of that of the external magnetic field if the later is 1 (T).

4.3 Energy band structure

In the Hamiltonian Eq.(4.5), the spatial inversion symmetry is lost to an asymmetric potential and/or Rashba term. In addition, the time reversal symmetry is lost due to spin Zeeman term. However, the rotational symmetry with respect to any angle around z-axis is preserve in Eq.(4.5). As a result, the energy splitting $\Delta_{k_x k_y}$ is invariant under a transformation that does not change the magnitude of $\mathbf{k} = (k_x, k_y)$. In other words, the energy splitting $\Delta_{k_x k_y}$ is symmetric with respect to the origin of $\mathbf{k}$. This is easily confirmed in Eq.(4.45).

In our present scheme, as mentioned in Sec. 4.1, the energy splitting $\pm\Delta_{k_xk_y}$ are simply added to the original energy band of usual graphene [46]. As a result, the original degenerate bands, which correspond to two bands mixed up by up-spin and down-spin bands, shift by $+\Delta_{k_xk_y}$ and $-\Delta_{k_xk_y}$, respectively. The schematic diagram of energy bands around the K point is illustrated in Fig. 4.1. Fig. 4.1 reveals that the HOS, LUS, and HOS-LUS gap are given by Eqs.(4.1), (4.2), and (4.3) respectively. Then, with reference to Fig. (4.1), we can write

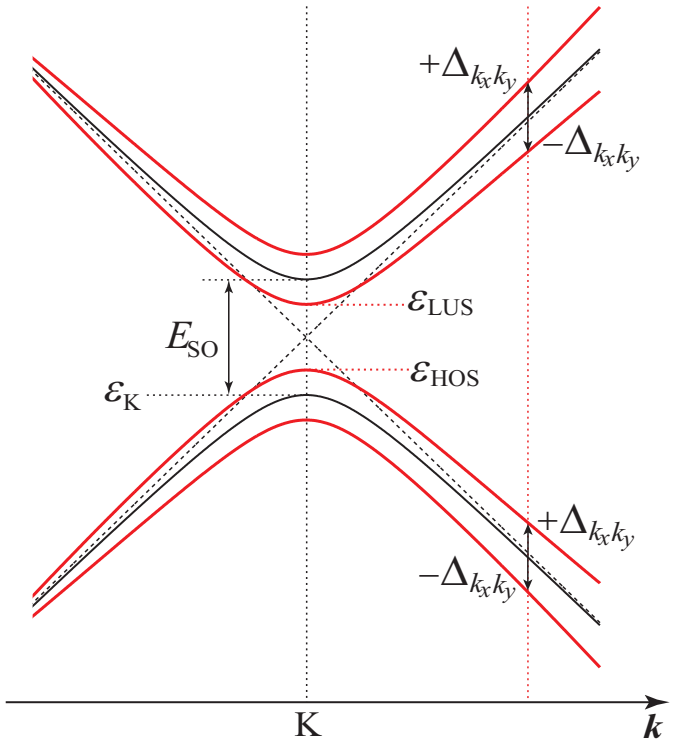

Figure 4.1: schematic diagram of energy bands around K point. Solid lines indicate degenerated bands mixed by up-spin and down-spin states. Red lines indicate the bands shifted by the Rashba effect and external magnetic field. Dashed lines indicate the energy bands in the case neglecting SO interaction [97].

$$\varepsilon_{LUS} = \varepsilon_K + E_{SO} - \Delta_{k_xk_y}, \tag{4.46}$$
$$\varepsilon_{HOS} = \varepsilon_K + \Delta_{k_xk_y}. \tag{4.47}$$

where ε_K is energy level of highest occupied state (HOS) and E_{SO} is SO interaction energy caused by spatially symmetric potential.

From Eqs. (4.46) and (4.47), the resultant HOS-LUS gap is given by

$$\begin{aligned}\Delta\varepsilon|_{at\ K} &= \varepsilon_{LUS} - \varepsilon_{HOS} \\ \Delta\varepsilon|_{at\ K} &= \varepsilon_K + E_{SO} - \Delta_{k_xk_y} - \varepsilon_K - \Delta_{k_xk_y} \\ \Delta\varepsilon|_{at\ K} &= E_{SO} - 2\Delta_{k_xk_y} \end{aligned} \tag{4.48}$$

From Eqs.(4.45) and (4.48), the resultant HOS-LUS gap is rewritten as

$$\Delta\varepsilon|_{at\ K} = E_{SO} - \left\{ 2|\delta(B_{ext})| + \frac{(\tilde{\alpha}_z\hbar)^2(k_x^2+k_y^2)}{|\delta(B_{ext})|}\Big|_{at\ K} \right\}. \tag{4.49}$$

The second term of the RHS of Eq.(4.49) plays a vital role for the modification of HOS-LUS gap. Since this second term depends on external magnetic field, it directly affects the reduction of g-factor.

4.4 Effective g-factor

A. Estimation of the effective g-factor

In the previous experiments on ESR [28, 29], the effective g-factor is derived by using the dependence of the HOS-LUS gap on the external magnetic field. Specially, in this experiments, $\Delta\varepsilon|_{\text{at } K}$ is regarded as the spin Zeeman energy and the proportional coefficient to the external magnetic field is derived by differentiating $\Delta\varepsilon|_{atK}$ with respect to the external magnetic field. This method of derivation is different from the one that has been previously used in the literature, in which the SO interaction energy E_{SO} explicitly changes the value of the effective g-factor [63], while in this method E_{SO} does not affect the effective g-factor [28, 29]. It is, therefore, possible to exclude the effect of E_{SO} from the effective g-factor in this derivation. Thus, as given by Eq.(4.4), the effective g-factor can be define as

$$g_{eff} = \frac{1}{\mu_B}\left|\frac{d}{dB_{ext}}\Delta\varepsilon|_{at\ K}\right|. \tag{4.50}$$

Now, from Eqs.(4.49) and (4.50), we have

$$g_{eff} = \frac{1}{\mu_B}\left|\frac{d}{dB_{ext}}\left[E_{SO} - 2|\delta B_{ext}| + \frac{\tilde{\alpha}_z\hbar)^2(k_x^2+k_y^2)}{\delta(B_{ext})}\right]\Big|_{at\ K}\right|.$$

Since SO interaction energy E_{SO} is independent of external magnetic field B_{ext}, we get an expression for effective g-factor as

$$g_{eff} = g\left\{1 - 2\left(\frac{\tilde{\alpha}_z\hbar}{g\mu_B B_{ext}}\right)^2 (k_x^2+k_y^2)\Big|_{at\ K}\right\}. \tag{4.51}$$

The expression Eq.(4.51) can also be derived in a more intuitive manner. In order to estimate the tilting angle of the spin magnetic moment from the z-axis to the x-y plane, it is sufficient to calculate the ratio of the Rashba field $\mathbf{B}_{SO}^{asymm}$ to the external field $\mathbf{B}_{ext}$. From Eqs. (4.8) and (4.12), we have

$$\mathbf{B}_{SO}^{asymm}(\mathbf{r}) = \frac{2}{g\mu_B}\left\{\alpha_{asymm}(\mathbf{r}) \times \mathbf{p}\right\}. \tag{4.52}$$

Since from the approximation

$$\alpha_{asymm}(\mathbf{r}) \approx \tilde{\alpha_z}\hat{e}_z \tag{4.53}$$

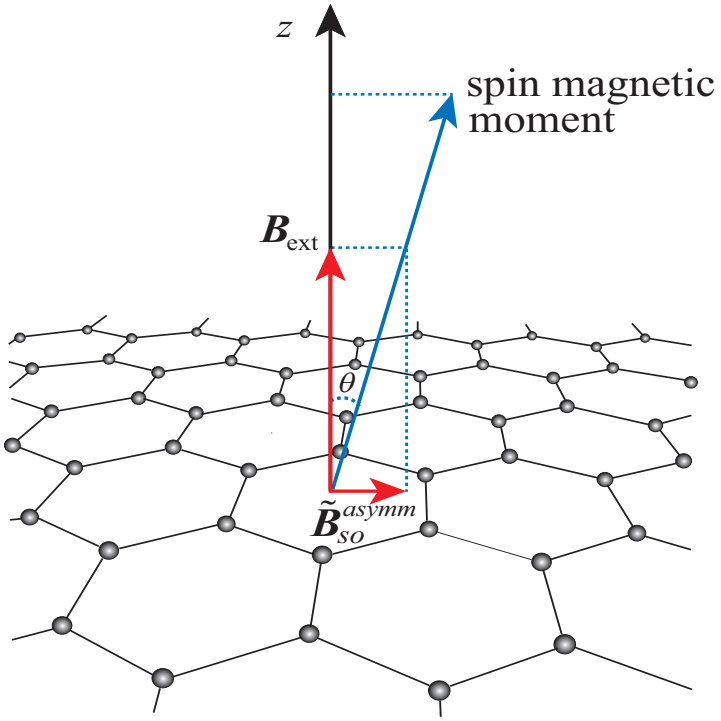

Figure 4.2: Schematic view of the Rashba magnetic field, external magnetic field and spin magnetic moment. The tilting angle θ of the spin magnetic moment is given by equation 4.59 [97].

and

$$\mathbf{p} = \hbar\mathbf{k}. \tag{4.54}$$

Eq.(4.52) becomes

$$\mathbf{B}_{SO}^{asymm}(\mathbf{r}) = \frac{2}{g\mu_B}\tilde{\alpha}_z\hbar\left(\hat{e}_z \times \mathbf{p}\right)$$

or

$$\mathbf{B}_{SO}^{asymm}(\mathbf{r}) = \frac{2}{g\mu_B}\tilde{\alpha}_z\hbar\left(k_x\hat{e}_y - k_y\hat{e}_x\right). \tag{4.55}$$

Hence, the magnitude of the Rashba field $\mathbf{B}_{SO}^{asymm}(\mathbf{r})$ is given by

$$|\mathbf{B}_{SO}^{asymm}(\mathbf{r})| = \frac{2\hbar}{g\mu_B}|\tilde{\alpha}_z|\sqrt{k_x^2 + k_y^2}. \tag{4.56}$$

The schematic view of the Rashba magnetic field $\mathbf{B}_{SO}^{asymm}(\mathbf{r})$, external magnetic field B_{ext} and spin magnetic moment is given in Fig. 4.2. If the angle is denoted as θ, we have

$$tan\theta = \frac{|\mathbf{B}_{SO}^{asymm}(\mathbf{r})|}{|B_{ext}|}. \tag{4.57}$$

Using Eq.(4.56), the tilting angle is rewritten as

$$tan\theta = \frac{2\hbar}{g\mu_B B_{ext}} |\tilde{\alpha}_z| \sqrt{k_x^2 + k_y^2}. \tag{4.58}$$

Now, the spin magnetic moment is substantially reduced by factor $cos\theta$. If the tilting angle is small such that the Rashba effect is smaller than the spin Zeeman effect, then $cos\theta$ is given by

$$cos\theta = 1 - 2\left(\frac{\tilde{\alpha}_z \hbar}{g\mu_B B_{ext}}\right)^2 (k_x^2 + k_y^2). \tag{4.59}$$

We thus obtain the tilting angle of the spin magnetic moment. Comparing Eq.(4.59) to Eq.(4.51), we can see that the reduction of the g-factor is also explained using the ratio of Rashba field to external magnetic field. Alternatively, we can also confirm Eq.(4.59) by calculating the expectation value of the spin magnetic moment with respect to eigenfunctions of Eq.(4.39). This shows that the spin magnetic moment of the HOS tilts by θ at the K point, while that of LUS tilts by $(\pi - \theta)$ at the K point.

In order to estimate the effective g-factor quantitatively, the value of Rashba parameter $\tilde{\alpha}_z$ is needed as shown in Eq.(4.51). We calculate $\tilde{\alpha}_z$ in the following three steps and using this, we determine effective g-factor.

Step 1:
In order to calculate the Rashba parameter $\tilde{\alpha}_z$, we need the electric field $\nabla V_{asymm}(z)$, as can be seen in Eq.(4.12). An asymmetric potential $V_{asymm}(z)$ is caused by the work function. The work function generally consists of the surface term and the bulk term [96]. The surface term originates from the electrical double layer existing near the surface. Electrons seep into the vacuum side from the surface due to the tunnel effect, due to which the electrical double layer forms in the vicinity of the surface. The electrons cannot easily escape from the surface, which is the origin of the work function [96]. The bulk term corresponds to the difference between the total energy of isolated atoms and that of the jellium model of electron liquid. This term, therefore, coincides with the cohesive energy times the factor -1 [96]. In our study, we use the experimental value W=4.3 (eV), obtained from, [98] for the work function.

Step 2:
The work function spatially spreads over some region near the surface. Correspondingly, electron density may decrease in that region because the work function acts as a potential barrier for the electrons. Therefore, the decay length of the electron density can be regarded as the spread length of the work function. In this step, we evaluate the decay length of the electron density in the vicinity of the surface of graphene using the Jellium model of electron liquid [96]. Let this decay length be referred to as d.

In the paper by Lang-Kohn [96], the spatial profile of the electron density is derived for various r_s parameters. In Appendix, we calculate the r_s parameter of the graphene sheet, using effective thickness of the graphene sheet. This results in a value of $r_s = 1.93548$ for the graphene sheet. Accordingly, we borrow a result from prior work for the spatial profile of electron density of $r_s = 2$ [96]. In such a profile

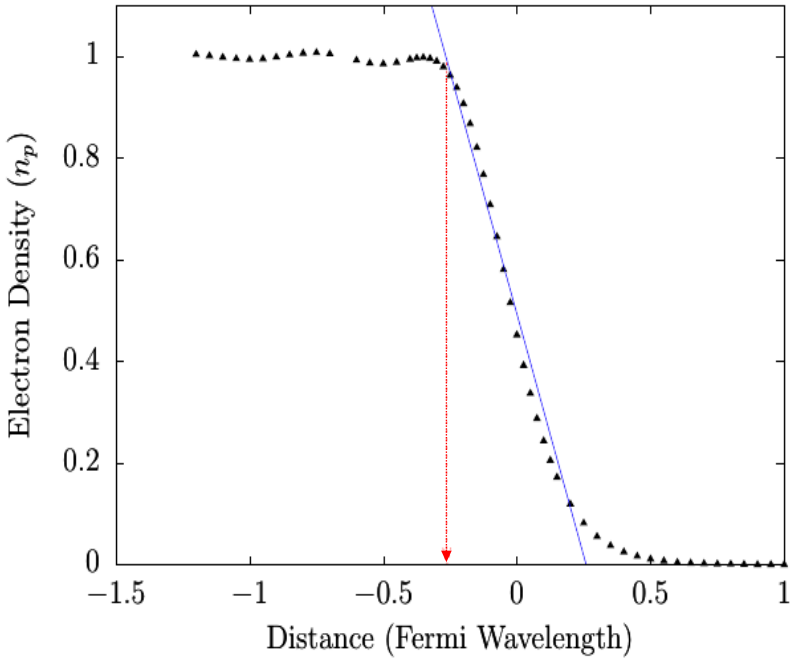

Figure 4.3: Variation of electron density between $0.95\bar{n}_p$ to $0.05\bar{n}_p$ near surface for $r_s = 2$. Blue line is the best fitted line.

[96], assume that a length decreasing the electron density from $0.95\bar{n}_p$ to $0.05\bar{n}_p$ is regarded as the decay length of the electron density as shown in Fig. 4.3, where $\bar{n}_p$ is the uniform positive charge density of the jellium model. The resulting d is 1.7604×10^{-10}(m). As mentioned above, this value of d corresponds to the spread length of the work function.

The electric field caused by work function is supposed to be constant in our present scheme as mentioned in Sec. 4.2. Using the work function W and its spread length d, the asymmetric potential is written as

$$V_{asymm}(z) = \frac{W}{d} z. \tag{4.60}$$

Using Eqs.(4.12) and (4.60), the Rashba parameter $\tilde{\alpha}_z$ is given by

$$|\tilde{\alpha}_z| = \frac{\hbar}{4m^2c^2} \frac{W}{d}, \tag{4.61}$$

where $W = 4.3$ (eV) and $d = 1.7604 \times 10^{-10}$m as shown in *step 1* and *step 2* respectively.
As a reference, the corresponding value of Rashba magnetic field $\tilde{B}_{SO}^{asymm}$ is calculated to be 0.268 (T), which is much smaller than the magnitude of the external magnetic field $B_{ext} = 1$ (T). This implies that the premise of Eq.(4.45) is correct. The relation between the Rashba magnetic field, external magnetic field, and spin magnetic moment is illustrated in Fig. 4.2.

Let us compare the magnitude of the Rashba effect with previous estimations [18, 46, 47]. The magnitude of Rashba effect is usually evaluated by the energy splitting of the Dirac cones in the case where the electric field of 1 (V/nm) is applied perpendicularly to the graphene sheet. This energy splitting is usually denoted as $2\lambda_R$. Estimated previous and present value of $2\lambda_R$ are summarized in Table 4.1. The value of $2\lambda_R$ for graphene was first estimated by Kane and Mele as $0.516(\mu\text{eVnm/V})$ [18]. Min *et al.* estimated it as $133.2(\mu\text{eVnm/V})$ by the tight binding approximation method [47]. The estimation of $2\lambda_R$ through the first-principle calculation is done by Gmitra *et al.*, and they estimated it as $9.9(\mu\text{eVnm/V})$ [46]. In order to compare these estimations with our estimation, we consider the energy splitting due to the Rashba effect in the case of $B_{ext} = 0$. The energy splitting for the case of $B_{ext} = 0$ is calculated by Eqs.(4.42 and 4.61). The estimated value of $2\lambda_R$ is $1.27(\mu\text{eVnm/V})$. This value is about 2.5 times larger than Kane and Mele's estimation, and is about 1/8 and 1/105 of the estimations by Min *et al.* and Gmitra *et al.*, respectively. Although previous numerical estimations for $2\lambda_R$ are rather controversial, our value is about in the middle of them. As described in the next step (step 3), the present estimation of energy splitting can successfully explain the experimental results of g-factor.

Table 4.1: Estimated values of $2\lambda_R$. Here, $2\lambda_R$ denotes the energy splitting of the Dirac cones due to the Rashba effect in the case where the electric field of 1 (V/nm) is applied perpendicularly to the graphene sheet [97].

	$2\lambda_R(\mu\text{eVnm/V})$
Kane and Mele [18]	0.516
Min *et al.* [47]	133.2
Gmitra *et al.* [46]	9.9
Present work	1.27

Step 3:
Finally, in order to evaluate the effective g-factor, we need the magnitude of $\mathbf{k}$ at the K point. The K point and its magnitude are given by $\mathbf{k}|_{\text{at K}} = (2\pi/a)(1/3, 1/\sqrt{3})$, and $\mathbf{k}|_{\text{at K}} = 1.70276 \times 10^{10}(\text{m}^{-1})$, respectively. Substituting the results obtained in these three steps in to Eq.(4.51) with an external magnetic field of 1 (T), we get $g_{eff} = 1.931$ (see Table 4.2). This is the effective g-factor predicted by our scheme at B_{ext} =1 (T).

This reveals that the reduction of g-factor is actually caused by the Rashba effect. The g-factor is reduced by about 3.6 percent in our scheme, while its experimentally observed value is a reduction by about 3.1 percent [28] or 2.5 percent [29] when external magnetic field is 1 (T) (Table 4.2). This establishes the fact that the Rashba effect is the primary cause for the reduction of the g-factor in graphene. As already explained, the diamagnetism of graphene is another source for the reduction of its g-factor by about 0.7 percent [48]. Additionally accounting for this factor suggests that our scheme slightly overestimates the influence of the Rashba effect on the g-factor of graphene. In section 4.4 B, we comment on the possibility of other influencing factors

that might be causing this overestimation in our scheme.

At the end of this section, we give a brief comment on the case where the external magnetic field is applied parallel to the graphene sheet. The effective magnetic field $\mathbf{B}_{SO}^{asymm}(\mathbf{r})$ caused by Rashba effect is parallel to the graphene sheet as shown in Fig. 4.2, irrespective to the direction of the external magnetic field. Namely, $\mathbf{B}_{SO}^{asymm}(\mathbf{r})$ is parallel to the external magnetic field in this case. Although the HOS-LUS gap changes with the external magnetic field, the differential of the HOS-LUS gap with respect to the external magnetic field would not change. Therefore, the g-factor is expected to be close to that of a free electron, which is consistent with the earlier experimental works of graphite [99, 100].

Table 4.2: Effective g-factor at $B_{ext} = 1$ (T) [97].

	Effective g-factor
Mani *et al.* [28] (experiment)	1.94 ± 0.024
Lyon *et al.*[29] (experiment)	1.952 ± 0.002
Present work	1.931

B. **Gate voltage dependence of the effective g-factor**

It is shown by the experiment on ESR [28] that the effective g-factor does not depend on the gate voltage, where the externally applied electric field (E_z^{ext}) perpendicular to the graphene sheet is controlled by the gate voltage. We consider the inherently-existing electric field (E_z^{in}) that comes from the work function as mentioned in section 4.1-4.3. When we consider the gate voltage dependence of the energy splitting due to Rashba effect, we should take both E_z^{ext} and E_z^{in} into consideration. The magnitude of E_z^{in} is estimated as $E_z^{in} = 24.4$(V/nm) using Eq.(4.60), $W = 4.3$ (eV) and $d = 1.7604\times10^{-10}$(m). On the other hand, $(E_z^{ext}) \sim 50$V/300nm is often used in estimating Rashba effect caused by the external applied electric field [18, 46, 47]. This value is more than two orders of magnitude smaller than E_z^{in}. It is expected that E_z^{ext} is much smaller than E_z^{in} even if teh gate voltage changes form -30 to 20 (V) like in the experiment on ESR [28]. Therefore, the Rashba effect in the graphene sheet deposited on the substrate is mainly caused by E_z^{in}. It is expected from the present scheme that the energy splitting as well as the effective g-factor is almost independent of the gate voltage. Thus, the present scheme can describe the experimental fact that the effective g-factor is almost independent of the gate voltage.

Chapter 5

Magnetic Field Containing Relativistic Tight Binding (MFRTB) Approximation incorporating Rashba effect

Even though Rashba effect is incorporated in empty lattice model while estimating effective g-factor, the orbital magnetic moment is totally ignored. This is because the magnitude of the orbital magnetic moment for the state of K point is likely to be small in graphene. The accuracy of previous calculation methods could be increased by examine the actual magnitude of effect of orbital magnetic moment on g-factor. The MFRTB method [38, 43, 48] can be used for the theoretical treatment of the effect of orbital magnetic moment. The relativistic effects like SO interaction are also incorporated by MFRTB method. Hence, in this chapter we extend the MFRTB method in order to incorporate the Rashba effect in order to apply it on graphene.

5.1 Magnetic Field Containing Relativistic Tight Binding (MFRTB) Approximation with Rashba effect

At any cystal interface or surface inversion asymmetry cause the asymmetric potential along the direction perpendicular to the graphene sheet. This causes the effective magnetic field parallel to the plane of graphene sheet. This is known as Rashba effect. Let $V_{asymm}(\mathbf{r})$ be the asymmetric potential which is added to the Hamiltonian of Eq.(2.1).

Hence, Eq.(2.1) can be rewritten as

$$\left[H + V_{asymm}(\mathbf{r})\right] \Phi_{\mathbf{k}}(\mathbf{r}) = E_{\mathbf{k}} \Phi_{\mathbf{k}}(\mathbf{r}), \tag{5.1}$$

where

$$H = c\alpha \cdot [\mathbf{p} + eA(\mathbf{r})] + \beta mc^2 + \sum_{\mathbf{R_n}} \sum_{i} V_{a_i}(\mathbf{r} - \mathbf{R_n} - \mathbf{d_i}), \tag{5.2}$$

is the Dirac Hamiltonian. The symbols have their usual meaning.

In the MFRTB method, $\Phi_{\mathbf{k}}$ is expanded by using relativistic atomic orbitals $\psi_{\xi}^{a_i,\mathbf{R_n}+\mathbf{d_i}}(\mathbf{r})$ for constituent atoms immersed in the uniform magnetic field. Relativistic atomic orbitals obey the Dirac equation of an isolated atom located at $\mathbf{R_n}+\mathbf{d_i}$ and immersed in the uniform magnetic field. That is to say

$$[c\alpha\cdot\{\mathbf{p}+e\mathbf{A}(\mathbf{r})\}+\beta mc^2+V_{a_i}(\mathbf{r}-\mathbf{R_n}-\mathbf{d_i})]\psi_{\xi}^{a_i,\mathbf{R_n}+\mathbf{d_i}}(\mathbf{r})=\varepsilon_{\xi}^{a_i,\mathbf{R_n}+\mathbf{d_i}}\psi_{\xi}^{a_i,\mathbf{R_n}+\mathbf{d_i}}(\mathbf{r}), \tag{5.3}$$

where $\psi_{\xi}^{a_i,\mathbf{R_n}+\mathbf{d_i}}$ and $\varepsilon_{\xi}^{a_i,\mathbf{R_n}+\mathbf{d_i}}$ denote the relativistic atomic orbital and atomic spectrum in the uniform magnetic field. The subscript $\xi=(nlJM)$ is the quantum number in atomic system.

Expanding $\Phi_{\mathbf{k}}(\mathbf{r})$ in terms of relativistic wave function $\psi_{\xi}^{a_i,\mathbf{R_n}+\mathbf{d_i}}(\mathbf{r})$ of atoms immersed in the uniform magnetic field as a basis function using Eq.(2.5). Then, Eq.(5.1) can be written as

$$\begin{aligned}\sum_{\mathbf{R_n}}\sum_{i}\sum_{\xi}C_{\mathbf{k}}^{\xi}(\mathbf{R_n}+\mathbf{d_i})H\psi_{\xi}^{a_i,\mathbf{R_n}+\mathbf{d_i}}(\mathbf{r})&\\ +\sum_{\mathbf{R_n}}\sum_{i}\sum_{\xi}C_{\mathbf{k}}^{\xi}(\mathbf{R_n}+\mathbf{d_i})V_{asymm}(\mathbf{r})\psi_{\xi}^{a_i,\mathbf{R_n}+\mathbf{d_i}}(\mathbf{r})&\\ =E_{\mathbf{k}}\sum_{\mathbf{R_n}}\sum_{i}\sum_{\xi}C_{\mathbf{k}}^{\xi}(\mathbf{R_n}+\mathbf{d_i})\psi_{\xi}^{a_i,\mathbf{R_n}+\mathbf{d_i}}(\mathbf{r}).&\end{aligned} \tag{5.4}$$

Multiplying by $\psi_{\eta}^{a_j,\mathbf{R_m}+\mathbf{d_j}}(\mathbf{r})^{\dagger}$ on both sides of Eq.(5.4) and integrating with respect to $\mathbf{r}$, we get,

$$\begin{aligned}\sum_{\mathbf{R_n}}\sum_{i}\sum_{\xi}C_{\mathbf{k}}^{\xi}(\mathbf{R_n}+\mathbf{d_i})\int\psi_{\eta}^{a_j,\mathbf{R_m}+\mathbf{d_j}}(\mathbf{r})^{\dagger}H\psi_{\xi}^{a_i,\mathbf{R_n}+\mathbf{d_i}}(\mathbf{r})d^3r&\\ +\sum_{\mathbf{R_n}}\sum_{i}\sum_{\xi}C_{\mathbf{k}}^{\xi}(\mathbf{R_n}+\mathbf{d_i})\int\psi_{\eta}^{a_j,\mathbf{R_m}+\mathbf{d_j}}(\mathbf{r})^{\dagger}V_{asymm}(\mathbf{r})\psi_{\xi}^{a_i,\mathbf{R_n}+\mathbf{d_i}}(\mathbf{r})d^3r&\\ =E_{\mathbf{k}}\sum_{\mathbf{R_n}}\sum_{i}\sum_{\xi}C_{\mathbf{k}}^{\xi}(\mathbf{R_n}+\mathbf{d_i})\int\psi_{\eta}^{a_j,\mathbf{R_m}+\mathbf{d_j}}(\mathbf{r})^{\dagger}\psi_{\xi}^{a_i,\mathbf{R_n}+\mathbf{d_i}}(\mathbf{r})d^3r&\end{aligned}$$

or

$$\begin{aligned}\sum_{\mathbf{R_n}}\sum_{i}\sum_{\xi}C_{\mathbf{k}}^{\xi}(\mathbf{R_n}+\mathbf{d_i})\mathcal{H}_{\mathbf{R_m}j\eta,\mathbf{R_n}i\xi}+\sum_{\mathbf{R_n}}\sum_{i}\sum_{\xi}C_{\mathbf{k}}^{\xi}(\mathbf{R_n}+\mathbf{d_i})\mathcal{H}_{\mathbf{R_m}j\eta,\mathbf{R_n}i\xi}^{asymm}&\\ =E_{\mathbf{k}}\sum_{\mathbf{R_n}}\sum_{i}\sum_{\xi}C_{\mathbf{k}}^{\xi}(\mathbf{R_n}+\mathbf{d_i})\mathcal{S}_{\mathbf{R_m}j\eta,\mathbf{R_n}i\xi},&\end{aligned} \tag{5.5}$$

where $\mathcal{H}_{\mathbf{R_m}j\eta,\mathbf{R_n}i\xi}$, $\mathcal{H}_{\mathbf{R_m}j\eta,\mathbf{R_n}i\xi}^{asymm}$, and $\mathcal{S}_{\mathbf{R_m}j\eta,\mathbf{R_n}i\xi}$ denotes the Dirac Hamiltonian, Rashba Hamiltonian and overlap matrices, respectively, and they are given by

$$\mathcal{H}_{\mathbf{R_m}j\eta,\mathbf{R_n}i\xi}=\int\psi_{\eta}^{a_j,\mathbf{R_m}+\mathbf{d_j}}(\mathbf{r})^{\dagger}H\psi_{\xi}^{a_i,\mathbf{R_n}+\mathbf{d_i}}(\mathbf{r})d^3r, \tag{5.6}$$

$$\mathcal{H}_{\mathbf{R_m}j\eta,\mathbf{R_n}i\xi}^{asymm}=\int\psi_{\eta}^{a_j,\mathbf{R_m}+\mathbf{d_j}}(\mathbf{r})^{\dagger}V_{asymm}(\mathbf{r})\psi_{\xi}^{a_i,\mathbf{R_n}+\mathbf{d_i}}(\mathbf{r})d^3r, \tag{5.7}$$

$$\mathcal{S}_{\mathbf{R_m}j\eta,\mathbf{R_n}i\xi}=\int\psi_{\eta}^{a_j,\mathbf{R_m}+\mathbf{d_j}}(\mathbf{r})^{\dagger}\psi_{\xi}^{a_i,\mathbf{R_n}+\mathbf{d_i}}(\mathbf{r})d^3r. \tag{5.8}$$

For simplicity, we use the expression for Dirac Hamiltonian matrix given by Eq.(2.23) as

$$\mathcal{H}_{\mathbf{R_m}j\eta,\mathbf{R_n}i\xi} \approx (\varepsilon_\xi^{a_i,\mathbf{R_n}+\mathbf{d_i}} + \Delta\varepsilon_\xi^{a_i,\mathbf{R_n}+\mathbf{d_i}})\delta_{\mathbf{R_m},\mathbf{R_n}}\delta_{j,i}\delta_{\eta,\xi} + (1-\delta_{\mathbf{R_m},\mathbf{R_n}}\delta_{j,i}) \times \int \psi_\eta^{a_j,\mathbf{R_m}+\mathbf{d_j}}(\mathbf{r})^\dagger \left[\frac{V_{a_j}^\eta(\mathbf{r}-\mathbf{R_m}-\mathbf{d_j}) + V_{a_i}^\xi(\mathbf{r}-\mathbf{R_n}-\mathbf{d_i})}{2}\right] \times \psi_\xi^{a_i,\mathbf{R_n}+\mathbf{d_i}}(\mathbf{r})d^3r, \quad (5.9)$$

where $\varepsilon_\xi^{a_i,\mathbf{R_n}+\mathbf{d_i}}$ is the atomic spectrum in an uniform magnetic field and $\Delta\varepsilon_\xi^{a_i,\mathbf{R_n}+\mathbf{d_i}}$ denotes the energy of crystal field and is given by

$$\Delta\varepsilon_\xi^{a_i,\mathbf{R_n}+\mathbf{d_i}}\delta_{\eta,\xi} = \int \psi_\eta^{a_i,\mathbf{R_n}+\mathbf{d_i}}(\mathbf{r})^\dagger \left\{ \sum_{\substack{\mathbf{R_k} \\ \mathbf{R_k}+\mathbf{d_l}\neq\mathbf{R_n}+\mathbf{d_i}}} \sum_l V_{a_l}(\mathbf{r}-\mathbf{R_k}-\mathbf{d_l}) \right\} \times \psi_\xi^{a_i,\mathbf{R_n}+\mathbf{d_i}}(\mathbf{r})d^3r \quad (5.10)$$

and overlap matrix given by Eq.(2.26) as

$$\mathcal{S}_{\mathbf{R_m}j\eta,\mathbf{R_n}i\xi} = \delta_{\mathbf{R_m},\mathbf{R_n}}\delta_{j,i}\delta_{\eta,\xi} + (1-\delta_{\mathbf{R_m},\mathbf{R_n}}\delta_{j,i}) \int \psi_\eta^{a_j,\mathbf{R_m}+\mathbf{d_j}}(\mathbf{r})^\dagger \psi_\xi^{a_i,\mathbf{R_n}+\mathbf{d_i}}(\mathbf{r})d^3r. \quad (5.11)$$

which are already derived in chapter 2.

From Eq.(5.3), Dirac equation for an atom immersed in uniform magnetic field and located at origin is given by

$$\left[c\alpha\cdot\{\mathbf{p}+e\mathbf{A}(\mathbf{r})\} + \beta mc^2 + V_{a_i}(\mathbf{r})\right]\psi_\xi^{a_i,0}(\mathbf{r}) = \epsilon_\xi^{a_i,0}\psi_\xi^{a_i,0}(\mathbf{r}). \quad (5.12)$$

Changing variables $\mathbf{r}$ to $\mathbf{r}-\mathbf{R_n}-\mathbf{d_i}$, we have

$$\left[c\alpha\cdot\{\mathbf{p}+e\mathbf{A}(\mathbf{r}-\mathbf{R_n}-\mathbf{d_i})\} + \beta mc^2 + V_{a_i}(\mathbf{r}-\mathbf{R_n}-\mathbf{d_i})\right]\psi_\xi^{a_i,0}(\mathbf{r}-\mathbf{R_n}-\mathbf{d_i}) = \varepsilon_\xi^{a_i,0}\psi_\xi^{a_i,0}(\mathbf{r}-\mathbf{R_n}-\mathbf{d_i}). \quad (5.13)$$

As $\mathbf{A}(\mathbf{r}-\mathbf{R_n}-\mathbf{d_i})$ and $\mathbf{A}(\mathbf{r})$ cause the same magnetic field $\mathbf{B}=(0,0,B)$, they can be related by a gauge transformation as

$$\mathbf{A}(\mathbf{r}-\mathbf{R_n}-\mathbf{d_i}) = \mathbf{A}(\mathbf{r}) + \nabla\chi(\mathbf{r},\mathbf{R_n}+\mathbf{d_i}). \quad (5.14)$$

We have the Landau gauge employed for $\mathbf{A}(\mathbf{r})$ is

$$\mathbf{A}(\mathbf{r}) = (0, Bx, 0) \quad (5.15)$$

From Eqs. (5.14) and (5.15), we have

$$\chi(\mathbf{r},\mathbf{R_n}+\mathbf{d_i}) = -B(R_{nx}+d_{ix})y. \quad (5.16)$$

Vector potentials at Eqs.(5.3) and (5.13) are different from each other by the choice of the gauge given by Eq.(5.13). So, eigenfunctions and eigenvalues of each Eqs.(5.3) and (5.13) are related as

$$\psi_\xi^{a_i,0}(\mathbf{r}-\mathbf{R_n}-\mathbf{d_i}) = e^{-i\frac{e}{\hbar}\chi(\mathbf{r},\mathbf{R_n}+\mathbf{d_i})}\psi_\xi^{a_i,\mathbf{R_n}+\mathbf{d_i}}(\mathbf{r}), \quad (5.17)$$

$$\psi_\xi^{a_i,0}(\mathbf{r}-\mathbf{R_m}-\mathbf{d_j}) = e^{-i\frac{e}{\hbar}\chi(\mathbf{r},\mathbf{R_m}+\mathbf{d_j})}\psi_\xi^{a_i,\mathbf{R_m}+\mathbf{d_j}}(\mathbf{r}) \quad (5.18)$$

and

$$\varepsilon_{\xi}^{a_i,0} = \varepsilon_{\xi}^{a_i,\mathbf{R_n}+\mathbf{d_i}}. \tag{5.19}$$

In addition, we have from Eqs.(5.10) and (5.17),

$$\Delta\varepsilon_{\xi}^{a_i,d_i} = \Delta\varepsilon_{\xi}^{a_i,\mathbf{R_n}+\mathbf{d_i}} = \Delta\epsilon_{\xi}^{a_i,0}. \tag{5.20}$$

Using Eqs. (5.16), (5.17), (5.19) and (5.20), the Hamiltonian matrix Eq.(5.9) is rewritten as

$$\mathcal{H}_{\mathbf{R_m}j\eta,\mathbf{R_n}i\xi} = (\varepsilon_{\xi}^{a_i,0} + \Delta\varepsilon_{\xi}^{a_i,d_i})\delta_{\mathbf{R}_m,\mathbf{R}_n}\delta_{j,i}\delta_{\eta,\xi} + (1-\delta_{\mathbf{R_m},\mathbf{R_n}}\delta_{j,i}) \times e^{-i\frac{eB}{\hbar}(R_{lx}+d_{ix}-d_{jx})(R_{my}+d_{jy})}\tilde{T}_{\eta,\xi}^{a_j,a_i}(\mathbf{R_l}+\mathbf{d_i}-\mathbf{d_j}), \tag{5.21}$$

Where

$$\tilde{T}_{\eta,\xi}^{a_j,a_i}(\mathbf{R_l}+\mathbf{d_i}-\mathbf{d_j}) = T_{\eta,\xi}^{a_j,a_i}(\mathbf{R_l}+\mathbf{d_i}-\mathbf{d_j}) + \left(\frac{\varepsilon_{\eta}^{a_j,0}+\varepsilon_{\xi}^{a_i,0}}{2}\right) S_{\eta,\xi}^{a_j,a_i}(\mathbf{R_l}+\mathbf{d_i}-\mathbf{d_j}), \tag{5.22}$$

with

$$T_{\eta,\xi}^{a_j,a_i}(\mathbf{R_l}+\mathbf{d_i}-\mathbf{d_j}) = \int \psi_{\eta}^{a_j,0}(\mathbf{r})^{\dagger}\left[\frac{V_{a_j}(\mathbf{r})+V_{a_i}(\mathbf{r}-\mathbf{R_l}-\mathbf{d_i}+\mathbf{d_j})}{2}\right]\psi_{\xi}^{a_i,\mathbf{R_l}+\mathbf{d_i}-\mathbf{d_j}}(\mathbf{r})d^3r, \tag{5.23}$$

$$S_{\eta,\xi}^{a_j,a_i}(\mathbf{R_l}+\mathbf{d_i}-\mathbf{d_j}) = \int \psi_{\eta}^{a_j,0}(\mathbf{r})^{\dagger}\psi_{\xi}^{a_i,\mathbf{R_l}+\mathbf{d_i}-\mathbf{d_j}}(\mathbf{r})d^3r. \tag{5.24}$$

are the magnetic hopping and magnetic overlap integrals.

Similarly, Using Eqs. (5.16) and (5.17), the overlap matrix Eq.(5.11) is rewritten as

$$\mathcal{S}_{\mathbf{R_m}j\eta,\mathbf{R_n}i\xi} = \delta_{\mathbf{R_m},\mathbf{R_n}}\delta_{j,i}\delta_{\eta,\xi} + (1-\delta_{\mathbf{R_m},\mathbf{R_n}}\delta_{j,i}) \times e^{-i\frac{eB}{\hbar}(R_{lx}+d_{ix}-d_{jx})(R_{my}+d_{jy})}S_{\eta,\xi}^{a_j,a_i}(\mathbf{R}_l+\mathbf{d_i}-\mathbf{d_j}). \tag{5.25}$$

Now, lets substitute Eqs.(5.17) and (5.18) into Eq.(5.7). Then, the Rashba Hamiltonian matrix given by Eq.(5.7) becomes

$$\mathcal{H}_{\mathbf{R_m}j\eta,\mathbf{R_n}i\xi}^{asymm} = \int e^{-i\frac{e}{\hbar}\chi(\mathbf{r},\mathbf{R_m}+\mathbf{d_j})}e^{-i\frac{e}{\hbar}\chi(\mathbf{r},\mathbf{R_n}+\mathbf{d_i})} \times \psi_{\eta}^{a_j,0}(\mathbf{r}-\mathbf{R_m}-\mathbf{d_j})^{\dagger}V_{asymm}(\mathbf{r})\psi_{\xi}^{a_i,0}(\mathbf{r}-\mathbf{R_n}-\mathbf{d_i})d^3r. \tag{5.26}$$

Using Eqs.(5.16), Eq.(5.26) becomes

$$\mathcal{H}_{\mathbf{R_m}j\eta,\mathbf{R_n}i\xi}^{asymm} = \int e^{-i\frac{eB}{\hbar}[R_{nx}+d_{ix}-R_{mx}-d_{jx}]y} \times \psi_{\eta}^{a_j,0}(\mathbf{r}-\mathbf{R_m}-\mathbf{d_j})^{\dagger}V_{asymm}(\mathbf{r})\psi_{\xi}^{a_i,0}(\mathbf{r}-\mathbf{R_n}-\mathbf{d_i})d^3r. \tag{5.27}$$

Changing variables, $\mathbf{r}'$ to $\mathbf{r}-\mathbf{R_m}-\mathbf{d_j}$, Eq.(5.17) becomes

$$\psi_{\xi}^{a_i,0}(\mathbf{r}'-\mathbf{R_l}-\mathbf{d_i}+\mathbf{d_j}) = e^{-i\frac{e}{\hbar}\chi(\mathbf{r}',\mathbf{R_l}+\mathbf{d_i}-\mathbf{d_j})}\psi_{\xi}^{a_i,\mathbf{R_l}+\mathbf{d_i}-\mathbf{d_j}}(\mathbf{r}'), \tag{5.28}$$

where $\mathbf{R_l} = \mathbf{R_n} - \mathbf{R_m}$.

From Eqs.(5.17) and (5.27), the Rashba Hamiltonian matrix is given by

$$\mathcal{H}^{asymm}_{\mathbf{R_m}j\eta,\mathbf{R_n}i\xi} = \int e^{-i\frac{eB}{\hbar}(R_{lx}+d_{ix}-d_{jx})(R_{my}+d_{jy})} \times \psi^{a_j,0}_{\eta}(\mathbf{r'})^{\dagger} V_{asymm}(\mathbf{r'} + \mathbf{R_m} + \mathbf{d_j}) \psi^{a_i,\mathbf{R_l}+\mathbf{d_i}-\mathbf{d_j}}_{\xi}(\mathbf{r'}) d^3r'. \quad (5.29)$$

In MFRTB method [38], $\psi^{a_i,\mathbf{R_l}+\mathbf{d_i}-\mathbf{d_j}}_{\xi}(\mathbf{r})$ is approximated as

$$\psi^{a_i,\mathbf{R_l}+\mathbf{d_i}-\mathbf{d_j}}_{\xi}(\mathbf{r}) = e^{-i\frac{eB}{2\hbar}(R_{ly}+d_{iy}-d_{jy})(R_{lx}+d_{ix}-d_{jx})} \phi^{a_i}_{nlJM}(\mathbf{r} - \mathbf{R_l} - \mathbf{d_i} + \mathbf{d_j}). \quad (5.30)$$

In the vicinity of origin, it would be reasonable to approximate

$$\psi^{a_j,0}_{\eta}(\mathbf{r}) \approx \phi^{a_j}_{n'l'J'M'}(\mathbf{r}), \quad (5.31)$$

where $\phi^{a_i}_{nlJM}(\mathbf{r})$ is relativistic atomic orbital in the absence of magnetic field which obeys following Dirac equation;

$$[c\alpha \cdot \mathbf{p} + \beta mc^2 + V_{a_i}(\mathbf{r})]\phi^{a_i}_{nlJM} = \bar{\varepsilon}^{a_i}_{nlJ} \phi^{a_i}_{nlJM}(\mathbf{r}), \quad (5.32)$$

where n, l, J, M are the principal, azimuthal, total angular momentum and magnetic quantum numbers respectively and $\bar{\varepsilon}^{a_i}_{nlJ}$ denotes the atomic spectrum for the zero magnetic field case.

From Eqs.(5.29), (5.30), and (5.31), finally, Rashba Hamiltonian matrix is given by

$$\mathcal{H}^{asymm}_{\mathbf{R_m}j\eta,\mathbf{R_n}i\xi} = \int e^{-i\frac{eB}{2\hbar}(R_{lx}+d_{ix}-d_{jx})(R_{ny}+d_{iy}+R_{my}+d_{jy})} \times \phi^{a_j}_{n'l'J'M'}(\mathbf{r})^{\dagger} V_{asymm}(\mathbf{r} + \mathbf{R_m} + \mathbf{d_j}) \phi^{a_i}_{nlJM}(\mathbf{r} - \mathbf{R_l} - \mathbf{d_i} + \mathbf{d_j}) d^3r. \quad (5.33)$$

In the following section, the approximation of matrix elements of Rashba Hamiltonian matrix will be discussed.

5.2 Approximation of matrix element of Rashaba Hamiltonian matrix

The relativistic atomic orbital $\phi^{a_i}_{nlJM}(\mathbf{r})$ can be expressed as

$$\phi^{a_i}_{nlJM} = \frac{1}{r} \begin{pmatrix} f^{a_i}_{nlJM}(\mathbf{r}) \\ g^{a_i}_{nlJM}(\mathbf{r}) \end{pmatrix}, \quad (5.34)$$

where $f^{a_i}_{nlJM}(\mathbf{r})$ and $g^{a_i}_{nlJM}(\mathbf{r})$ are large and small components of $\phi^{a_i}_{nlJM}$, respectively, and they are expressed as

$$f^{a_i}_{nlJM}(\mathbf{r}) = \frac{1}{r} F^{a_i}_{nlJM}(\mathbf{r}) y^M_{l,J}(\theta, \phi), \quad (5.35)$$

$$g^{a_i}_{nlJM}(\mathbf{r}) = \frac{1}{r} G^{a_i}_{nlJM}(\mathbf{r}) y^M_{l,J}(\theta, \phi). \quad (5.36)$$

From Eq.(5.34), Eq.(5.33) can be written as

$$\mathcal{H}^{asymm}_{\mathbf{R_m}j\eta,\mathbf{R_n}i\xi} = \int e^{-i\frac{eB}{2\hbar}(R_{lx}+d_{ix}-d_{jx})(R_{ny}+d_{iy}+R_{my}+d_{jy})} \times \{f^{a_j}_{n'l'J'M'}(\mathbf{r})g^{a_j}_{n'l'J'M'}(\mathbf{r})\}^{\dagger} V_{asymm}(\mathbf{r}+\mathbf{R_m}+\mathbf{d_j}) \begin{Bmatrix} f^{a_i}_{nlJM}(\mathbf{r}-\mathbf{R}) \\ g^{a_i}_{nlJM}(\mathbf{r}-\mathbf{R}) \end{Bmatrix} d^3r$$

$$= \int e^{-i\frac{eB}{2\hbar}(R_{lx}+d_{ix}-d_{jx})(R_{ny}+d_{iy}+R_{my}+d_{jy})} \times \{f^{a_j}_{n'l'J'M'}(\mathbf{r})^{\dagger} V_{asymm}(\mathbf{r}+\mathbf{R_m}+\mathbf{d_j}) f^{a_i}_{nlJM}(\mathbf{r}-\mathbf{R}) + g^{a_j}_{n'l'J'M'}(\mathbf{r})^{\dagger} V_{asymm}(\mathbf{r}+\mathbf{R_m}+\mathbf{d_j}) g^{a_i}_{nlJM}(\mathbf{r}-\mathbf{R})\} d^3r, \quad (5.37)$$

where $\mathbf{R} = \mathbf{R_l} - \mathbf{d_i} + \mathbf{d_j}$.

Introducing following approximation [54]

$$g^{a_i}_{nlJM}(\mathbf{r}) \approx \frac{1}{2mc}(\sigma \cdot \mathbf{p}) f^{a_i}_{nlJM}(\mathbf{r}), \quad (5.38)$$

Eq.(5.37) becomes

$$\mathcal{H}^{asymm}_{\mathbf{R_m}j\eta,\mathbf{R_n}i\xi} = \int e^{-i\frac{eB}{2\hbar}(R_{lx}+d_{ix}-d_{jx})(R_{ny}+d_{iy}+R_{my}+d_{jy})} \times \Big\{ f^{a_j}_{n'l'J'M'}(\mathbf{r})^{\dagger} V_{asymm}(\mathbf{r}+\mathbf{R_m}+\mathbf{d_j}) f^{a_i}_{nlJM}(\mathbf{r}-\mathbf{R}) + \frac{(\sigma\cdot\mathbf{p})}{2mc} f^{a_j}_{n'l'J'M'}(\mathbf{r})^{\dagger} V_{asymm}(\mathbf{r}+\mathbf{R_m}+\mathbf{d_j}) \frac{(\sigma\cdot\mathbf{p})}{2mc} f^{a_i}_{nlJM}(\mathbf{r}-\mathbf{R}) \Big\} d^3r$$

$$= \int e^{-i\frac{eB}{2\hbar}(R_{lx}+d_{ix}-d_{jx})(R_{ny}+d_{iy}+R_{my}+d_{jy})} \times \Big\{ f^{a_j}_{n'l'J'M'}(\mathbf{r})^{\dagger} V_{asymm}(\mathbf{r}+\mathbf{R_m}+\mathbf{d_j}) f^{a_i}_{nlJM}(\mathbf{r}-\mathbf{R}) + \frac{1}{4m^2c^2} f^{a_j}_{n'l'J'M'}(\mathbf{r})^{\dagger} (\sigma\cdot\mathbf{p}) V_{asymm}(\mathbf{r}+\mathbf{R_m}+\mathbf{d_j}) \times (\sigma\cdot\mathbf{p}) f^{a_i}_{nlJM}(\mathbf{r}-\mathbf{R}) \Big\} d^3r$$

$$= \int e^{-i\frac{eB}{2\hbar}(R_{lx}+d_{ix}-d_{jx})(R_{ny}+d_{iy}+R_{my}+d_{jy})} \times \Big\{ f^{a_j}_{n'l'J'M'}(\mathbf{r})^{\dagger} V_{asymm}(\mathbf{r}+\mathbf{R_m}+\mathbf{d_j}) f^{a_i}_{nlJM}(\mathbf{r}-\mathbf{R}) + \frac{1}{4m^2c^2} f^{a_j}_{n'l'J'M'}(\mathbf{r})^{\dagger} (\sigma\cdot -\mathbf{i}\hbar\nabla) V_{asymm}(\mathbf{r}+\mathbf{R_m}+\mathbf{d_j}) \times (\sigma\cdot\mathbf{p}) f^{a_i}_{nlJM}(\mathbf{r}-\mathbf{R}) \Big\} d^3r \quad (5.39)$$

$$
\begin{aligned}
&= \int e^{-i\frac{eB}{2\hbar}(R_{lx}+d_{ix}-d_{jx})(R_{ny}+d_{iy}+R_{my}+d_{jy})} \\
&\quad \times \Big\{ f^{a_j}_{n'l'J'M'}(\mathbf{r})^\dagger V_{asymm}(\mathbf{r}+\mathbf{R_m}+\mathbf{d_j}) f^{a_i}_{nlJM}(\mathbf{r}-\mathbf{R}) \\
&\qquad -\frac{i\hbar}{4m^2c^2} f^{a_j}_{n'l'J'M'}(\mathbf{r})^\dagger [\sigma\cdot\nabla V_{asymm}(\mathbf{r}+\mathbf{R_m}+\mathbf{d_j})](\sigma\cdot\mathbf{p}) f^{a_i}_{nlJM}(\mathbf{r}-\mathbf{R}) \\
&\qquad +\frac{1}{4m^2c^2} f^{a_j}_{n'l'J'M'}(\mathbf{r})^\dagger [\nabla V_{asymm}(\mathbf{r}+\mathbf{R_m}+\mathbf{d_j})(\sigma\cdot\mathbf{p})(\sigma\cdot\mathbf{p})] \\
&\qquad\qquad \times f^{a_i}_{nlJM}(\mathbf{r}-\mathbf{R}) \Big\} d^3r.
\end{aligned} \tag{5.40}
$$

Using the property

$$
(\sigma\cdot\mathbf{C})(\sigma\cdot\mathbf{D}) = \mathbf{C}.\mathbf{D} + i\sigma.(\mathbf{C}\times\mathbf{D}), \tag{5.41}
$$

Eq.(5.40) is written as

$$
\begin{aligned}
\mathcal{H}^{asymm}_{\mathbf{R_m}j\eta,\mathbf{R_n}i\xi} &= \int e^{-i\frac{eB}{2\hbar}(R_{lx}+d_{ix}-d_{jx})(R_{ny}+d_{iy}+R_{my}+d_{jy})} \\
&\quad \times \Big\{ f^{a_j}_{n'l'J'M'}(\mathbf{r})^\dagger V_{asymm}(\mathbf{r}+\mathbf{R_m}+\mathbf{d_j}) f^{a_i}_{nlJM}(\mathbf{r}-\mathbf{R}) \\
&\qquad -\frac{i\hbar}{4m^2c^2} f^{a_j}_{n'l'J'M'}(\mathbf{r})^\dagger [\nabla V_{asymm}(\mathbf{r}+\mathbf{R_m}+\mathbf{d_j})\cdot\mathbf{p}] f^{a_i}_{nlJM}(\mathbf{r}-\mathbf{R}) \\
&\qquad -\frac{i\hbar}{4m^2c^2} f^{a_j}_{n'l'J'M'}(\mathbf{r})^\dagger [i\sigma\cdot\{\nabla V_{asymm}(\mathbf{r}+\mathbf{R_m}+\mathbf{d_j})\times\mathbf{p}\}] f^{a_i}_{nlJM}(\mathbf{r}-\mathbf{R}) \\
&\qquad +\frac{1}{4m^2c^2} f^{a_j}_{n'l'J'M'}(\mathbf{r})^\dagger [V_{asymm}(\mathbf{r}+\mathbf{R_m}+\mathbf{d_j})p^2] f^{a_i}_{nlJM}(\mathbf{r}-\mathbf{R}) \\
&\qquad +\frac{1}{4m^2c^2} f^{a_j}_{n'l'J'M'}(\mathbf{r})^\dagger [iV_{asymm}(\mathbf{r}+\mathbf{R_m}+\mathbf{d_j})\{\sigma\cdot(\mathbf{p}\times\mathbf{p})\}] \\
&\qquad\qquad \times f^{a_i}_{nlJM}(\mathbf{r}-\mathbf{R}) \Big\} d^3r \\
&= \int e^{-i\frac{eB}{2\hbar}(R_{lx}+d_{ix}-d_{jx})(R_{ny}+d_{iy}+R_{my}+d_{jy})} \\
&\quad \times \Big\{ f^{a_j}_{n'l'J'M'}(\mathbf{r})^\dagger V_{asymm}(\mathbf{r}+\mathbf{R_m}+\mathbf{d_j}) f^{a_i}_{nlJM}(\mathbf{r}-\mathbf{R}) \\
&\qquad +\frac{i\hbar}{4m^2c^2} f^{a_j}_{n'l'J'M'}(\mathbf{r})^\dagger [-\nabla V_{asymm}(\mathbf{r}+\mathbf{R_m}+\mathbf{d_j})\cdot\mathbf{p}] f^{a_i}_{nlJM}(\mathbf{r}-\mathbf{R}) \\
&\qquad +f^{a_j}_{n'l'J'M'}(\mathbf{r})^\dagger \left[\frac{\hbar}{4m^2c^2}\sigma\cdot\{\nabla V_{asymm}(\mathbf{r}+\mathbf{R_m}+\mathbf{d_j})\times\mathbf{p}\}\right] f^{a_i}_{nlJM}(\mathbf{r}-\mathbf{R}) \\
&\qquad +f^{a_j}_{n'l'J'M'}(\mathbf{r})^\dagger \left[V_{asymm}(\mathbf{r}+\mathbf{R_m}+\mathbf{d_j})\frac{p^2}{4m^2c^2}\right] f^{a_i}_{nlJM}(\mathbf{r}-\mathbf{R}) \\
&\qquad +\frac{1}{4m^2c^2} f^{a_j}_{n'l'J'M'}(\mathbf{r})^\dagger [iV_{asymm}(\mathbf{r}+\mathbf{R_m}+\mathbf{d_j})\{\sigma\cdot(\mathbf{p}\times\mathbf{p})\}] \\
&\qquad\qquad \times f^{a_i}_{nlJM}(\mathbf{r}-\mathbf{R}) \Big\} d^3r.
\end{aligned} \tag{5.42}
$$

Eq.(5.42) shows that the Rashba Hamiltonian matrix consists of following five terms:

(i) First term consists of integral

$$\int f^{a_j}_{n'l'J'M'}(\mathbf{r})^{\dagger} V_{asymm}(\mathbf{r}+\mathbf{R_m}+\mathbf{d_j}) f^{a_i}_{nlJM}(\mathbf{r}-\mathbf{R}) d^3r$$

which corresponds to the hopping integral.

(ii) Second term consists of integral

$$\int \frac{i\hbar}{4m^2c^2} f^{a_j}_{n'l'J'M'}(\mathbf{r})^{\dagger} [-\nabla V_{asymm}(\mathbf{r}+\mathbf{R_m}+\mathbf{d_j})\cdot\mathbf{p}] f^{a_i}_{nlJM}(\mathbf{r}-\mathbf{R}) d^3r,$$

which vanishes as electric field $-\nabla V_{asymm}(\mathbf{r}+\mathbf{R_m}+\mathbf{d_j})$ due to asymmetric potential is perpendicular to the surface and to the direction of electron momentum $\mathbf{p}$

(iii) Third term consists of integral

$$\int f^{a_j}_{n'l'J'M'}(\mathbf{r})^{\dagger} \left[\frac{\hbar}{4m^2c^2}\sigma\cdot\{\nabla V_{asymm}(\mathbf{r}+\mathbf{R_m}+\mathbf{d_j})\times\mathbf{p}\}\right] f^{a_i}_{nlJM}(\mathbf{r}-\mathbf{R}) d^3r,$$

which is related to the Rashba Hamiltonian, say 'H_R' and is expressed as

$$\begin{aligned} H_R &= \frac{\hbar}{4m^2c^2}\sigma\cdot\{\nabla V_{asymm}(\mathbf{r}+\mathbf{R_m}+\mathbf{d_j})\times\mathbf{p}\} \\ &= \sigma\cdot\left\{\frac{\hbar}{4m^2c^2}\nabla V_{asymm}(\mathbf{r}+\mathbf{R_m}+\mathbf{d_j})\times\mathbf{p}\right\} \\ &= \sigma\cdot\{\boldsymbol{\alpha}_{asymm}(\mathbf{r}+\mathbf{R_m}+\mathbf{d_j})\times\mathbf{p}\}, \end{aligned} \tag{5.43}$$

where $\boldsymbol{\alpha}_{asymm}(\mathbf{r}+\mathbf{R_m}+\mathbf{d_j})$ is known as Rashba parameter and it is given by

$$\boldsymbol{\alpha}_{asymm}(\mathbf{r}+\mathbf{R_m}+\mathbf{d_j}) = \frac{\hbar}{4m^2c^2}\nabla V_{asymm}(\mathbf{r}+\mathbf{R_m}+\mathbf{d_j}). \tag{5.44}$$

(iv) Fourth term consists of integral

$$\int f^{a_j}_{n'l'J'M'}(\mathbf{r})^{\dagger} \left[V_{asymm}(\mathbf{r}+\mathbf{R_m}+\mathbf{d_j})\frac{p^2}{4m^2c^2}\right] f^{a_i}_{nlJM}(\mathbf{r}-\mathbf{R}) d^3r,$$

which can be neglected because the ratio $\dfrac{p^2/2m}{2mc^2}$ is very small.

(v) Fifth term consists of integral

$$\frac{1}{4m_0^2c^2} f^{a_j}_{n'l'J'M'}(\mathbf{r})^{\dagger} [iV_{asymm}(\mathbf{r}+\mathbf{R_m}+\mathbf{d_j})\{\sigma\cdot(\mathbf{p}\times\mathbf{p})\}] f^{a_i}_{nlJM}(\mathbf{r}-\mathbf{R})\} d^3r,$$

which vanishes due to the property $(\mathbf{p}\times\mathbf{p}) = 0$.

Hence, the Rashba Hamiltonian matrix given by Eq.(5.42) becomes

$$\begin{aligned} \mathcal{H}^{asymm}_{\mathbf{R_m}j\eta,\mathbf{R_n}i\xi} = \int & e^{-i\frac{eB}{2\hbar}(R_{lx}+d_{ix}-d_{jx})(R_{ny}+d_{iy}+R_{my}+d_{jy})} \\ & \times \Big\{ f^{a_j}_{n'l'J'M'}(\mathbf{r})^{\dagger} V_{asymm}(\mathbf{r}+\mathbf{R_m}+\mathbf{d_j}) f^{a_i}_{nlJM}(\mathbf{r}-\mathbf{R}) \\ & \qquad + f^{a_j}_{n'l'J'M'}(\mathbf{r})^{\dagger} H_R f^{a_i}_{nlJM}(\mathbf{r}-\mathbf{R}) \Big\} d^3r. \end{aligned} \tag{5.45}$$

Let us assume that the Rashba parameter given by Eq.(5.44) is constant along z-direction. i.e. $\boldsymbol{\alpha}_{asymm}(\mathbf{r}+\mathbf{R_m}+\mathbf{d_j}) \approx \tilde{\alpha}_z(|\mathbf{r}+\mathbf{R_m}+\mathbf{d_j}|\hat{\mathbf{e}}_\mathbf{z}) \approx |\tilde{\alpha}_z|\hat{\mathbf{e}}_\mathbf{z}$, where $\hat{\mathbf{e}}_\mathbf{z}$ is a unit vector along z-axis. This implies that the electric field, i.e. $\nabla V_{asymm}(z)$ assumed to be constant along z-direction. Hence, this assumption leads us to the fact that $V_{asymm}(z)$ is varies linearly with z in the vicinity of the surface.

The magnitude of asymmetric potential in terms of work function W and its spread length d is given by Eq.(4.60). This equation is rewritten as

$$V_{asymm}\{|(\mathbf{r}+\mathbf{R_m}+\mathbf{d_j})\hat{\mathbf{e}}_\mathbf{z}|\} = \frac{W}{d}z. \tag{5.46}$$

From Eqs.(5.43), (5.45), and (5.46), Rashba Hamiltonian matrix is given by

$$\begin{aligned}\mathcal{H}^{asymm}_{\mathbf{R_m}j\eta,\mathbf{R_n}i\xi} = \int e^{-i\frac{eB}{2\hbar}(R_{lx}+d_{ix}-d_{jx})(R_{ny}+d_{iy}+R_{my}+d_{jy})} \\ \times \left\{ \frac{W}{d} f^{a_j}_{n'l'J'M'}(\mathbf{r})^\dagger z f^{a_i}_{nlJM}(\mathbf{r}-\mathbf{R}) \right. \\ \left. +|\tilde{\alpha}_z| f^{a_j}_{n'l'J'M'}(\mathbf{r})^\dagger \left[\sigma.(\hat{\mathbf{e_z}}\times\mathbf{p})\right] f^{a_i}_{nlJM}(\mathbf{r}-\mathbf{R}) \right\} d^3r.\end{aligned} \tag{5.47}$$

Eq.(5.47) shows that only second term is spin dependence. Since, energy splitting is mainly caused by spin dependence term, we may consider only the second term in order to incorporate Rashba effect in MFRTB approximation. Hence, Eq.(5.47) can be approximated as

$$\begin{aligned}\mathcal{H}^{asymm}_{\mathbf{R_m}j\eta,\mathbf{R_n}i\xi} &\approx \int e^{-i\frac{eB}{2\hbar}(R_{lx}+d_{ix}-d_{jx})(R_{ny}+d_{iy}+R_{my}+d_{jy})} \\ &\qquad \times |\tilde{\alpha}_z| f^{a_j}_{n'l'J'M'}(\mathbf{r})^\dagger \left[\sigma.(\hat{\mathbf{e_z}}\times\mathbf{p})\right] f^{a_i}_{nlJM}(\mathbf{r}-\mathbf{R}) d^3r \\ &\approx e^{-i\frac{eB}{2\hbar}(R_{lx}+d_{ix}-d_{jx})(R_{ny}+d_{iy}+R_{my}+d_{jy})} \int f^{a_j}_{n'l'J'M'}(\mathbf{r})^\dagger H_R f^{a_i}_{nlJM}(\mathbf{r}-\mathbf{R}) d^3r.\end{aligned} \tag{5.48}$$

From Eq.(5.35), the integral part of of Eq.(5.48) can be written as

$$\begin{aligned}&\int f^{a_j}_{n'l'J'M'}(\mathbf{r})^\dagger H_R f^{a_i}_{nlJM}(\mathbf{r}-\mathbf{R}) d^3r \\ &\qquad = |\tilde{\alpha}_z| \int \frac{1}{r r_{_R}} F^{a_j *}_{n'l'J'}(\mathbf{r}) y^{M'*}_{l',J'}(\theta,\phi) \left[\sigma.(\hat{\mathbf{e_z}}\times\mathbf{p})\right] F^{a_i}_{nlJ}(\mathbf{r_R}) y^{M}_{l,J}(\theta_R,\phi_R) d^3r,\end{aligned} \tag{5.49}$$

where $y^M_{l,J}(\theta,\phi)$ is the spin angular function and is given by

$$y^M_{l,J}(\theta,\phi) = \begin{cases} \left.\begin{array}{l} \sqrt{\dfrac{J+M}{2J}} Y_{l,M-\frac{1}{2}}(\theta,\phi) \\ \sqrt{\dfrac{J-M}{2J}} Y_{l,M+\frac{1}{2}}(\theta,\phi) \end{array}\right\} \text{for} \quad J = l+\dfrac{1}{2} \\ \\ \left.\begin{array}{l} -\sqrt{\dfrac{J+1-M}{2(J+1)}} Y_{l,M-\frac{1}{2}}(\theta,\phi) \\ \sqrt{\dfrac{J+1+M}{2(J+1)}} Y_{l,M+\frac{1}{2}}(\theta,\phi) \end{array}\right\} \text{for} \quad J = l-\dfrac{1}{2} \end{cases}, \tag{5.50}$$

with $Y_{l,M}(\theta,\phi)$ being a Spherical harmonic function. Here, we also have

$$\sigma.(\hat{\mathbf{e}}_{\mathbf{z}}\times\mathbf{p})=\begin{pmatrix}0 & -ip_x-p_y\\ ip_x-p_y & 0\end{pmatrix}. \tag{5.51}$$

Substituting Eq.(5.51) into Eq.(5.49), we get

$$\begin{aligned}\int f^{a_j}_{n'l'J'M'}(\mathbf{r})^\dagger H_R f^{a_i}_{nlJM}(\mathbf{r}-\mathbf{R})d^3r\\ =|\tilde{\alpha}_z|\int\frac{1}{rr_{_R}}F^{a_j*}_{n'l'J'}(\mathbf{r})y^{M'*}_{l',J'}(\theta,\phi)\begin{pmatrix}0 & -ip_x-p_y\\ ip_x-p_y & 0\end{pmatrix}\\ \times F^{a_i}_{nlJ}(\mathbf{r}_{\mathbf{R}})y^{M}_{l,J}(\theta_R,\phi_R)d^3r.\end{aligned} \tag{5.52}$$

Let us compute the integral given by Eq.(5.52) for the following cases:

(a) $J'=l'+\frac{1}{2}$ and $J=l+\frac{1}{2}$,

(b) $J'=l'+\frac{1}{2}$ and $J=l-\frac{1}{2}$,

(c) $J'=l'-\frac{1}{2}$ and $J=l+\frac{1}{2}$,

(d) $J'=l'-\frac{1}{2}$ and $J=l-\frac{1}{2}$.

(a) For $J'=l'+\frac{1}{2}$ and $J=l+\frac{1}{2}$

From Eq.(5.50) for spin angular function and Eq.(5.52), we have

$$\begin{aligned}\int f^{a_j}_{n'l'J'M'}(\mathbf{r})^\dagger H_R f^{a_i}_{nlJM}(\mathbf{r}-\mathbf{R})d^3r\\ =|\tilde{\alpha}_z|\int\frac{1}{rr_{_R}}F^{a_j}_{n'l'J'}(\mathbf{r})^*\left\{\sqrt{\frac{J'+M'}{2J'}}Y_{l',M'-\frac{1}{2}}(\theta,\phi)^*\sqrt{\frac{J'-M'}{2J'}}Y^*_{l',M'+\frac{1}{2}}(\theta,\phi)\right\}\\ \times\begin{pmatrix}0 & -ip_x-p_y\\ ip_x-p_y & 0\end{pmatrix}F^{a_i}_{nlJ}(\mathbf{r}_{\mathbf{R}})\left\{\begin{array}{l}\sqrt{\frac{J+M}{2J}}Y_{l,M-\frac{1}{2}}(\theta_R,\phi_R)\\ \sqrt{\frac{J-M}{2J}}Y_{l,M+\frac{1}{2}}(\theta_R,\phi_R)\end{array}\right\}d^3r\\ =|\tilde{\alpha}_z|\left[\sqrt{\frac{J'+M'}{2J'}}\sqrt{\frac{J-M}{2J}}\int\frac{1}{rr_{_R}}F^{a_j}_{n'l'J'}(\mathbf{r})^*Y_{l',M'-\frac{1}{2}}(\theta,\phi)^*\{-ip_x-p_y\}\right.\\ \times F^{a_i}_{nlJ}(\mathbf{r}_{\mathbf{R}})Y_{l,M+\frac{1}{2}}(\theta_R,\phi_R)d^3r\\ +\sqrt{\frac{J+M}{2J}}\sqrt{\frac{J'-M'}{2J'}}\int\frac{1}{rr_{_R}}F^{a_j}_{n'l'J'}(\mathbf{r})^*Y_{l',M'+\frac{1}{2}}(\theta,\phi)^*\{ip_x-p_y\}\\ \left.\times F^{a_i}_{nlJ}(\mathbf{r}_{\mathbf{R}})Y_{l,M-\frac{1}{2}}(\theta_R,\phi_R)d^3r\right].\end{aligned} \tag{5.53}$$

In non-relativistic case, we have

$$\phi^{a_i}_{nlJM}(\mathbf{r}) \approx \frac{1}{r} F^{a_i}_{nlJ}(\mathbf{r}) Y_{l,M}(\theta,\phi). \tag{5.54}$$

Substituting Eq. (5.54) into Eq.(5.53), we get

$$\begin{aligned}
&\int f^{a_j}_{n'l'J'M'}(\mathbf{r})^\dagger H_R f^{a_i}_{nlJM}(\mathbf{r}-\mathbf{R}) d^3r \\
&= |\tilde{\alpha}_z| \left[\sqrt{\frac{J'+M'}{2J'}} \sqrt{\frac{J-M}{2J}} \int \phi^{a_j}_{n'l'J'M'-\frac{1}{2}}(\mathbf{r})^* \{-ip_x - p_y\} \phi^{a_i}_{nlJM+\frac{1}{2}}(\mathbf{r}-\mathbf{R}) d^3r \right. \\
&\quad \left. + \sqrt{\frac{J+M}{2J}} \sqrt{\frac{J'-M'}{2J'}} \int \phi^{a_j}_{n'l'J'M'+\frac{1}{2}}(\mathbf{r})^* \{ip_x - p_y\} \phi^{a_i}_{nlJM-\frac{1}{2}}(\mathbf{r}-\mathbf{R}) d^3r \right].
\end{aligned} \tag{5.55}$$

The non-relativistic wave function $\phi^{a_i}_{nlJM}(\mathbf{r})$ obeys the following Schrödinger wave equation

$$H^{\mathbf{0}}_{atom} \phi^{a_i}_{nlJM}(\mathbf{r}) = \varepsilon_{nl} \phi^{a_i}_{nlJM}(\mathbf{r}), \tag{5.56}$$

with

$$H^{\mathbf{0}}_{atom} = \frac{p^2}{2m} + V_{a_i}(\mathbf{r}), \tag{5.57}$$

where V_{a_i} is potential of an atom a_i located at origin.

From Eq(5.55), it is evident that the integral part in Rashba Hamiltonian can be regarded as momentum matrix. Hence, to calculate matrix element of Rashba Hamiltonian matrix, we have to compute the momentum matrices of Eq.(5.55).

In Heisenberg picture, for an operator $\hat{A}$, we have

$$\frac{d\hat{A}}{dt} = \frac{1}{i\hbar}[\hat{A}, H]. \tag{5.58}$$

Applying this relation to the x-co-ordinate, we obtain

$$\frac{dx}{dt} = \frac{1}{i\hbar} \left[x, H^{\mathbf{0}}_{atom} \right]. \tag{5.59}$$

Using Eq.(5.57), Eq.(5.59) becomes

$$p_x = \frac{m}{i\hbar} \left[x, H^{\mathbf{0}}_{atom} \right]. \tag{5.60}$$

Similarly, for y-coordinate, we get

$$p_y = \frac{m}{i\hbar} \left[y, H^{\mathbf{0}}_{atom} \right]. \tag{5.61}$$

With the help of Eqs.(5.60) and (5.61), we evaluate the momentum matrices of Eq.(5.55). At first, let us take the following momentum matix:

$$
\begin{aligned}
&\int \phi^{a_j}_{n'l'J'M'\mp\frac{1}{2}}(\mathbf{r})^* p_x \phi^{a_i}_{nlJM\pm\frac{1}{2}}(\mathbf{r}-\mathbf{R}) d^3r \\
&\quad = \int \phi^{a_j}_{n'l'J'M'\mp\frac{1}{2}}(\mathbf{r})^* \frac{m}{i\hbar}\left(xH^{\mathbf{0}}_{atom} - H^{\mathbf{0}}_{atom}x\right)\phi^{a_i}_{nlJM\pm\frac{1}{2}}(\mathbf{r}-\mathbf{R}) d^3r \\
&\quad = \frac{m}{i\hbar}\left\{\int \phi^{a_j}_{n'l'J'M'\mp\frac{1}{2}}(\mathbf{r})^* x H^{\mathbf{0}}_{atom}\phi^{a_i}_{nlMJ\pm\frac{1}{2}}(\mathbf{r}-\mathbf{R}) d^3r \right. \\
&\qquad\qquad \left. - \int \phi^{a_j}_{n'l'J'M'\mp\frac{1}{2}}(\mathbf{r})^* H^{\mathbf{0}}_{atom} x \phi^{a_i}_{nlJM\pm\frac{1}{2}}(\mathbf{r}-\mathbf{R}) d^3r \right\} \\
&\quad = \frac{m}{i\hbar}\left\{\int \phi^{a_j}_{n'l'J'M'\mp\frac{1}{2}}(\mathbf{r})^* x \{H^{\mathbf{R}}_{atom} + V_{atom}(\mathbf{r}) - V_{atom}(\mathbf{r}-\mathbf{R})\}\phi^{a_i}_{nlJM\pm\frac{1}{2}}(\mathbf{r}-\mathbf{R}) d^3r \right. \\
&\qquad\qquad \left. -\varepsilon_{n'l'}\int \phi^{a_j}_{n'l'J'M'\mp\frac{1}{2}}(\mathbf{r})^* x \phi^{a_i}_{nlJM\pm\frac{1}{2}}(\mathbf{r}-\mathbf{R}) d^3r \right\} \\
&\quad = \frac{m}{i\hbar}\left\{\int \phi^{a_j}_{n'l'J'M'\mp\frac{1}{2}}(\mathbf{r})^* x H^{\mathbf{R}}_{atom}\phi^{a_i}_{nlJM\pm\frac{1}{2}}(\mathbf{r}-\mathbf{R}) d^3r \right. \\
&\qquad + \int \phi^{a_j}_{n'l'JM'\mp\frac{1}{2}}(\mathbf{r})^* x \{V_{atom}(\mathbf{r}) - V_{atom}(\mathbf{r}-\mathbf{R})\}\phi^{a_i}_{nlJM\pm\frac{1}{2}}(\mathbf{r}-\mathbf{R}) d^3r \\
&\qquad\qquad \left. -\varepsilon_{n'l'}\int \phi^{a_j}_{n'l'J'M'\mp\frac{1}{2}}(\mathbf{r})^* x \phi^{a_i}_{nlJM\pm\frac{1}{2}}(\mathbf{r}-\mathbf{R}) d^3r \right\} \\
&\quad = \frac{m}{i\hbar}\left\{\varepsilon_{nl}\int \phi^{a_j}_{n'l'J'M'\mp\frac{1}{2}}(\mathbf{r})^* x \phi^{a_i}_{nlJM\pm\frac{1}{2}}(\mathbf{r}-\mathbf{R}) d^3r \right. \\
&\qquad + \int \phi^{a_j}_{n'l'J'M'\mp\frac{1}{2}}(\mathbf{r})^* x \{V_{atom}(\mathbf{r}) - V_{atom}(\mathbf{r}-\mathbf{R})\}\phi^{a_i}_{nlJM\pm\frac{1}{2}}(\mathbf{r}-\mathbf{R}) d^3r \\
&\qquad\qquad \left. -\varepsilon_{n'l'}\int \phi^{a_j}_{n'l'J'M'\mp\frac{1}{2}}(\mathbf{r})^* x \phi^{a_i}_{nlJM\pm\frac{1}{2}}(\mathbf{r}-\mathbf{R}) d^3r \right\} \\
&\quad = \frac{m}{i\hbar}\left\{(\varepsilon_{nl}-\varepsilon_{n'l'})\int \phi^{a_j}_{n'l'J'M'\mp\frac{1}{2}}(\mathbf{r})^* x \phi^{a_i}_{nlJM\pm\frac{1}{2}}(\mathbf{r}-\mathbf{R}) d^3r \right. \\
&\qquad + \int \phi^{a_j}_{n'l'J'M'\mp\frac{1}{2}}(\mathbf{r})^* x V_{atom}(\mathbf{r})\phi^{a_i}_{nlJM\pm\frac{1}{2}}(\mathbf{r}-\mathbf{R}) d^3r \\
&\qquad\qquad \left. - \int \phi^{a_j}_{n'l'J'M'\mp\frac{1}{2}}(\mathbf{r})^* x V_{atom}(\mathbf{r}-\mathbf{R})\phi^{a_i}_{nlJM\pm\frac{1}{2}}(\mathbf{r}-\mathbf{R}) d^3r \right\}.
\end{aligned}
\tag{5.62}
$$

In order to estimate first term of Eq.(5.62), let us express s and p orbitals for $n = 2$ in terms of radial and spherical harmonic functions. Then, we have the following atomic orbitals:

$$
\begin{aligned}
\phi_{20JM\pm\frac{1}{2}}(\mathbf{r}) &= R_{20}(\mathbf{r})Y_{0,0}(\theta,\phi) \\
&= 2\left(\frac{z}{2a_0}\right)^{\frac{3}{2}}\left(1-\frac{zr}{2a_0}\right)e^{-zr/2a_0}Y_{0,0}(\theta,\phi) \\
&= \frac{1}{\sqrt{2}}\left(\frac{z}{a_0}\right)^{\frac{3}{2}}\left(1-\frac{zr}{2a_0}\right)e^{-zr/2a_0}Y_{0,0}(\theta,\phi),
\end{aligned}
\tag{5.63}
$$

$$\begin{aligned}\phi_{21JM\pm\frac{1}{2}}(\mathbf{r}) &= R_{21}(\mathbf{r})Y_{1,M\pm\frac{1}{2}}(\theta,\phi)\\ &= \frac{1}{\sqrt{3}}\left(\frac{z}{2a_0}\right)^{\frac{3}{2}}\left(\frac{zr}{a_0}\right)e^{-zr/2a_0}Y_{1,M\pm\frac{1}{2}}(\theta,\phi)\\ &= \frac{1}{2\sqrt{6}}\left(\frac{z}{a_0}\right)^{\frac{3}{2}}\left(\frac{zr}{a_0}\right)e^{-zr/2a_0}Y_{1,M\pm\frac{1}{2}}(\theta,\phi),\end{aligned} \tag{5.64}$$

$$\begin{aligned}\phi_{20JM\pm\frac{1}{2}}(\mathbf{r}-\mathbf{R}) &= R_{20}(\mathbf{r}-\mathbf{R})Y_{0,0}(\theta_R,\phi_R)\\ &= 2\left(\frac{z}{2a_0}\right)^{\frac{3}{2}}\left(1-\frac{z}{2a_0}|\mathbf{r}-\mathbf{R}|\right)e^{-\frac{z}{2a_0}|\mathbf{r}-\mathbf{R}|}Y_{0,0}(\theta_R,\phi_R)\\ &= \frac{1}{\sqrt{2}}\left(\frac{z}{a_0}\right)^{\frac{3}{2}}\left(1-\frac{z}{2a_0}|\mathbf{r}-\mathbf{R}|\right)e^{-\frac{z}{2a_0}|\mathbf{r}-\mathbf{R}|}Y_{0,0}(\theta_R,\phi_R),\end{aligned} \tag{5.65}$$

$$\begin{aligned}\phi_{21JM\pm\frac{1}{2}}(\mathbf{r}-\mathbf{R}) &= R_{21}(\mathbf{r}-\mathbf{R})Y_{1,M\pm\frac{1}{2}}(\theta_R,\phi_R)\\ &= \frac{1}{\sqrt{3}}\left(\frac{z}{2a_0}\right)^{\frac{3}{2}}\left(\frac{z}{a_0}|\mathbf{r}-\mathbf{R}|\right)e^{-\frac{z}{2a_o}|\mathbf{r}-\mathbf{R}|}Y_{1,M\pm\frac{1}{2}}(\theta_R,\phi_R)\\ &= \frac{1}{2\sqrt{6}}\left(\frac{z}{a_0}\right)^{\frac{3}{2}}\left(\frac{z}{a_0}|\mathbf{r}-\mathbf{R}|\right)e^{-\frac{z}{2a_o}|\mathbf{r}-\mathbf{R}|}Y_{1,M\pm\frac{1}{2}}(\theta_R,\phi_R).\end{aligned} \tag{5.66}$$

The Spherical harmonic functions $Y_{l,M}(\theta,\phi)$ along ξ-axis as shown in Fig. 5.1 are given by

$$Y_{0,0}(\theta,\phi) = \frac{1}{\sqrt{4\pi}}, \tag{5.67}$$

$$Y_{0,0}(\theta_R,\phi_R) = \frac{1}{\sqrt{4\pi}}, \tag{5.68}$$

$$Y_{1,0}(\theta,\phi) = 0, \tag{5.69}$$

$$Y_{1,0}(\theta_R,\phi_R) = 0, \tag{5.70}$$

$$Y_{1,1}(\theta,\phi) = -\sqrt{\frac{3}{8\pi}}e^{i\alpha}, \tag{5.71}$$

$$Y_{1,1}(\theta_R,\phi_R) = -\sqrt{\frac{3}{8\pi}}e^{-i\alpha}, \tag{5.72}$$

$$Y_{1,-1}(\theta,\phi) = \sqrt{\frac{3}{8\pi}}e^{-i\alpha}, \tag{5.73}$$

$$Y_{1,-1}(\theta_R,\phi_R) = \sqrt{\frac{3}{8\pi}}e^{i\alpha}. \tag{5.74}$$

Fig. 5.1 shows that the spherical co-ordinate representation for two wave functions $\phi_{2l'J'M'}(\mathbf{r})$ and $\phi_{21JM}(\mathbf{r}-\mathbf{R})$ at origin and position $\mathbf{R}$. The product of these two wave functions, i.e., $\phi_{2l'J'M'}(\mathbf{r})^*\phi_{21JM}(\mathbf{r}-\mathbf{R})$ becomes large as we approach near $\mathbf{R}$ from origin. Fig. 5.2 shows the cylindrical region of radius $\frac{2a_0}{z}$ in the vicinity of $\mathbf{R}$ where the product of two wave functions has large value and vanishes outside of this region. Fig. 5.3 shows the representation of coordinate system in terms of ξ-coordinate.

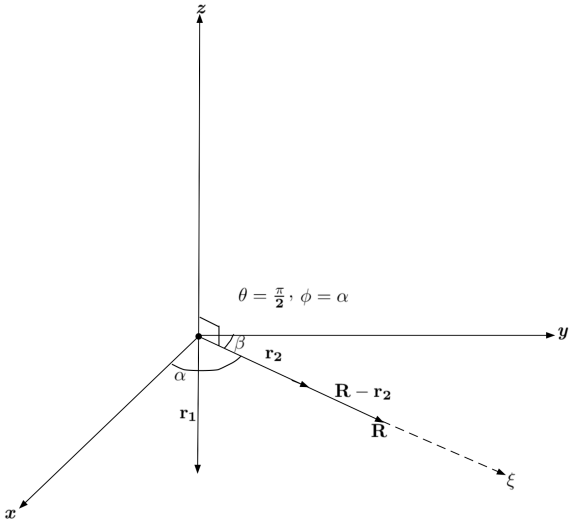

Figure 5.1: Spherical polar coordinate representation when $\mathbf{r_1}$ approaches to $\mathbf{R}$ along ξ-axis.

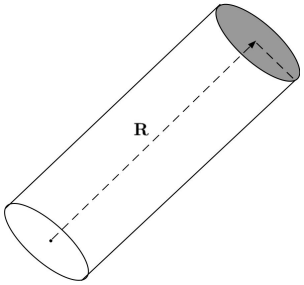

Figure 5.2: Cylindrical region in the vicinity of $\mathbf{R}$ where the product of two wave function becomes large.

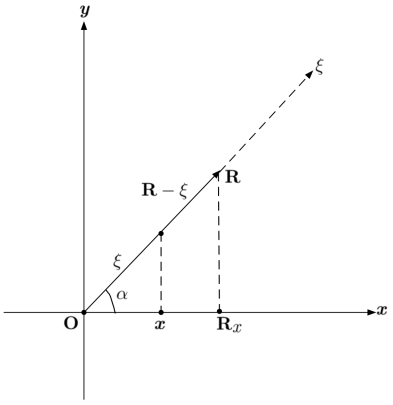

Figure 5.3: Representation of the coordinates along ξ-axis in ξ-coordinate in xy-plane.

Under these assumptions, let us calculate the product of two wave functions for following orbital interactions:

(i) $\phi_{20J'0}(\mathbf{r})^*\phi_{20J0}(\mathbf{r}-\mathbf{R})$

From Eqs.(5.63) and (5.65), we have

$$\begin{aligned}\phi_{20J'0}(\mathbf{r})^*\phi_{20J0}(\mathbf{r}-\mathbf{R}) \\ = \frac{1}{\sqrt{2}}\left(\frac{z}{a_0}\right)^{\frac{3}{2}}\left(1-\frac{zr}{2a_0}\right)e^{-\frac{zr}{2a_0}}\frac{1}{\sqrt{2}}\left(\frac{z}{a_0}\right)^{\frac{3}{2}}\left(1-\frac{z}{2a_0}|\mathbf{r}-\mathbf{R}|\right)e^{-\frac{z}{2a_0}|\mathbf{r}-\mathbf{R}|} \\ \times Y^*_{0,0}(\theta,\phi)Y_{0,0}(\theta_R,\phi_R).\end{aligned} \tag{5.75}$$

Using Eq.(5.67), Eq.(5.68), and Eq.(5.75) reduces to

$$\phi_{20J'0}(\mathbf{r})^*\phi_{20J0}(\mathbf{r}-\mathbf{R})$$
$$= \frac{1}{2}\left(\frac{z}{a_0}\right)^3\left(1-\frac{zr}{2a_0}\right)\left(1-\frac{z}{2a_0}|\mathbf{r}-\mathbf{R}|\right)e^{-\frac{zr}{2a_0}}e^{-\frac{z}{2a_0}|\mathbf{R}-\mathbf{r}|}\quad\left(\frac{1}{4\pi}\right)$$
$$= \begin{cases} \dfrac{1}{8\pi}\left(\dfrac{z}{a_0}\right)^3\left(1-\dfrac{z}{2a_0}\xi\right)\left\{1-\dfrac{z}{2a_0}(R-\xi)\right\}e^{-\frac{z}{2a_0}R} & \\ \qquad\qquad \text{(near cylinder of radius } \frac{2a_0}{z} \text{ and length } R \text{ along } \xi \text{ axis)} & \\ 0 \qquad\qquad \text{(otherwise).} & \end{cases} \tag{5.76}$$

(ii) $\phi_{20J'0}(\mathbf{r})^*\phi_{21J0}(\mathbf{r}-\mathbf{R})$

From Eqs.(5.63), (5.66), (5.67) and (5.70), we have

$$\phi_{20J'0}(\mathbf{r})^*\phi_{21J0}(\mathbf{r}-\mathbf{R}) = 0. \tag{5.77}$$

(iii) $\phi_{20J'0}(\mathbf{r})^*\phi_{21J1}(\mathbf{r}-\mathbf{R})$

From Eqs.(5.63) and (5.66), we have

$$\phi_{20J'0}(\mathbf{r})^*\phi_{21J1}(\mathbf{r}-\mathbf{R})$$
$$= \frac{1}{\sqrt{2}}\left(\frac{z}{a_0}\right)^{\frac{3}{2}}\left(1-\frac{zr}{2a_0}\right)e^{-\frac{zr}{2a_0}}\frac{1}{2\sqrt{6}}\left(\frac{z}{a_0}\right)^{\frac{3}{2}}\left(\frac{z}{a_0}|\mathbf{r}-\mathbf{R}|\right)e^{-\frac{z}{2a_0}|\mathbf{r}-\mathbf{R}|}$$
$$\times Y^*_{0,0}(\theta,\phi)Y_{1,1}(\theta_R,\phi_R). \tag{5.78}$$

Using Eqs.(5.67) and (5.72), Eq.(5.78) reduces to

$$\phi_{20J'0}(\mathbf{r})^*\phi_{21J1}(\mathbf{r}-\mathbf{R})$$
$$= \frac{1}{2\sqrt{12}}\left(\frac{z}{a_0}\right)^3\left(1-\frac{zr}{2a_0}\right)\left(\frac{z}{a_0}|\mathbf{R}-\mathbf{r}|\right)e^{-\frac{zr}{2a_0}}e^{-\frac{z}{2a_0}|\mathbf{R}-\mathbf{r}|}$$
$$\times\left(\frac{1}{\sqrt{4\pi}}\right)\left(-\sqrt{\frac{3}{8\pi}}e^{-i\alpha}\right)$$
$$= \begin{cases} -\dfrac{1}{16\pi\sqrt{2}}\left(\dfrac{z}{a_0}\right)^4\left(1-\dfrac{z}{2a_0}\xi\right)(R-\xi)e^{-\frac{z}{2a_0}R}e^{-i\alpha} & \\ \qquad\qquad \text{(near cylinder of radius } \frac{2a_0}{z} \text{ and length } R \text{ along } \xi \text{ axis)} & \\ 0 \qquad\qquad \text{(otherwise).} & \end{cases} \tag{5.79}$$

(iv) $\phi_{20J'0}(\mathbf{r})^*\phi_{21J-1}(\mathbf{r}-\mathbf{R})$

From Eqs.(5.63) and (5.66), we have

$$\begin{aligned}\phi_{20J'0}(\mathbf{r})^*\phi_{21J-1}(\mathbf{r}-\mathbf{R}) \\ = \frac{1}{\sqrt{2}}\left(\frac{z}{a_0}\right)^{\frac{3}{2}}\left(1-\frac{zr}{2a_0}\right)e^{-\frac{zr}{2a_0}}\frac{1}{2\sqrt{6}}\left(\frac{z}{a_0}\right)^{\frac{3}{2}}\left(\frac{z}{a_0}|\mathbf{r}-\mathbf{R}|\right)e^{-\frac{z}{2a_0}|\mathbf{r}-\mathbf{R}|} \\ \times Y^*_{0,0}(\theta,\phi)Y_{1,-1}(\theta_R,\phi_R).\end{aligned} \tag{5.80}$$

Using Eqs.(5.67) and (5.74), Eq.(5.80) becomes

$$\begin{aligned}\phi_{20J'0}(\mathbf{r})^*\phi_{21J\text{-}1}(\mathbf{r}-\mathbf{R}) \\ = \frac{1}{2\sqrt{12}}\left(\frac{z}{a_0}\right)^{3}\left(1-\frac{zr}{2a_0}\right)\left(\frac{z}{a_0}|\mathbf{R}-\mathbf{r}|\right)e^{-\frac{zr}{2a_0}}e^{-\frac{z}{2a_0}|\mathbf{R}-\mathbf{r}|} \\ \times\left(\frac{1}{\sqrt{4\pi}}\right)\left(\sqrt{\frac{3}{8\pi}}e^{i\alpha}\right) \\ = \begin{cases}\dfrac{1}{16\pi\sqrt{2}}\left(\dfrac{z}{a_0}\right)^4\left(1-\dfrac{z}{2a_0}\xi\right)(R-\xi)e^{-\frac{z}{2a_0}R}e^{i\alpha} \\ \qquad\text{(near cylinder of radius } \frac{2a_0}{z} \text{ and length } R \text{ along } \xi \text{ axis)} \\ 0 \qquad\text{(otherwise).}\end{cases}\end{aligned} \tag{5.81}$$

(v) $\phi_{21J'0}(\mathbf{r})^*\phi_{20J0}(\mathbf{r}-\mathbf{R})$ orbits.

From Eqs.(5.64), (5.65), (5.68) and (5.69), we have

$$\phi_{21J'0}(\mathbf{r})^*\phi_{20J0}(\mathbf{r}-\mathbf{R}) = 0. \tag{5.82}$$

(vi) $\phi_{21J'0}(\mathbf{r})^*\phi_{21J0}(\mathbf{r}-\mathbf{R})$

From Eqs.(5.64), (5.66), and (5.70), we have

$$\phi_{21J'0}(\mathbf{r})^*\phi_{21J0}(\mathbf{r}-\mathbf{R}) = 0. \tag{5.83}$$

(vii) $\phi_{21J'0}(\mathbf{r})^*\phi_{21J1}(\mathbf{r}-\mathbf{R})$

From Eqs.(5.64), (5.66), (5.69), and (5.72), we have

$$\phi_{21J'0}(\mathbf{r})^*\phi_{21J1}(\mathbf{r}-\mathbf{R}) = 0. \tag{5.84}$$

(viii) $\phi_{21J'0}(\mathbf{r})^*\phi_{21J-1}(\mathbf{r}-\mathbf{R})$

From Eqs.(5.64), (5.66), (5.67) and (5.74), we have

$$\phi_{21J'0}(\mathbf{r})^*\phi_{21J-1}(\mathbf{r}-\mathbf{R}) = 0. \tag{5.85}$$

(ix) $\phi_{21J'1}(\mathbf{r})^*\phi_{20J0}(\mathbf{r}-\mathbf{R})$

From Eqs.(5.64) and (5.65), we have

$$\begin{aligned}&\phi_{21J'1}(\mathbf{r})^*\phi_{20J0}(\mathbf{r}-\mathbf{R})\\&\quad=\frac{1}{2\sqrt{6}}\left(\frac{z}{a_0}\right)^{\frac{3}{2}}\left(\frac{zr}{a_0}\right)e^{-\frac{zr}{2a_0}}\frac{1}{\sqrt{2}}\left(\frac{z}{a_0}\right)^{\frac{3}{2}}\left(1-\frac{z}{2a_0}|\mathbf{r}-\mathbf{R}|\right)e^{-\frac{z}{2a_0}|\mathbf{r}-\mathbf{R}|}\\&\qquad\qquad\times Y^*_{1,1}(\theta,\phi)Y_{0,0}(\theta_R,\phi_R).\end{aligned}\tag{5.86}$$

Using Eqs.(5.68) and (5.71), Eq.(5.86) becomes

$$\begin{aligned}&\phi_{21J'1}(\mathbf{r})^*\phi_{20J0}(\mathbf{r}-\mathbf{R})\\&\quad=\frac{1}{2\sqrt{12}}\left(\frac{z}{a_0}\right)^{3}\left(\frac{zr}{a_0}\right)\left(1-\frac{z}{2a_0}|\mathbf{R}-\mathbf{r}|\right)e^{-\frac{zr}{2a_0}}e^{-\frac{z}{2a_0}|\mathbf{R}-\mathbf{r}|}\\&\qquad\qquad\times\left(-\sqrt{\frac{3}{8\pi}}e^{-i\alpha}\right)\left(\frac{1}{\sqrt{4\pi}}\right)\\&\quad=\begin{cases}-\dfrac{1}{16\pi\sqrt{2}}\left(\dfrac{z}{a_0}\right)^4\xi\left\{1-\dfrac{z}{2a_0}(R-\xi)\right\}e^{-\frac{z}{2a_0}R}e^{-i\alpha}\\\qquad\text{(near cylinder of radius }\frac{2a_0}{z}\text{ and length }R\text{ along }\xi\text{ axis)}\\0\qquad\qquad\text{(otherwise).}\end{cases}\end{aligned}\tag{5.87}$$

(x) $\phi_{21J'1}(\mathbf{r})^*\phi_{21J0}(\mathbf{r}-\mathbf{R})$

From Eqs.(5.64), (5.66), (5.70) and (5.71), we have

$$\phi_{21J'1}(\mathbf{r})^*\phi_{21J0}(\mathbf{r}-\mathbf{R})=0.\tag{5.88}$$

(xi) $\phi_{21J'1}(\mathbf{r})^*\phi_{21J1}(\mathbf{r}-\mathbf{R})$

From Eqs.(5.64) and (5.66), we have

$$\begin{aligned}&\phi_{21J'1}(\mathbf{r})^*\phi_{21J1}(\mathbf{r}-\mathbf{R})\\&\quad=\frac{1}{2\sqrt{6}}\left(\frac{z}{a_0}\right)^{\frac{3}{2}}\left(\frac{zr}{a_0}\right)e^{-\frac{zr}{2a_0}}\frac{1}{2\sqrt{6}}\left(\frac{z}{a_0}\right)^{\frac{3}{2}}\left(\frac{z}{a_0}|\mathbf{r}-\mathbf{R}|\right)e^{-\frac{z}{2a_0}|\mathbf{r}-\mathbf{R}|}\\&\qquad\qquad\times Y^*_{1,1}(\theta,\phi)Y_{1,1}(\theta_R,\phi_R).\end{aligned}\tag{5.89}$$

Using Eqs.(5.71) and (5.72), Eq.(5.89) becomes

$$\phi_{21J'1}(\mathbf{r})^*\phi_{21J1}(\mathbf{r}-\mathbf{R})$$
$$= \frac{1}{24}\left(\frac{z}{a_0}\right)^3\left(\frac{zr}{2a_0}\right)\left(\frac{z}{a_0}|\mathbf{R}-\mathbf{r}|\right)e^{-\frac{zr}{2a_0}}e^{-\frac{z}{2a_0}|\mathbf{R}-\mathbf{r}|}$$
$$\times\left(-\sqrt{\frac{3}{8\pi}}e^{-i\alpha}\right)\left(-\sqrt{\frac{3}{8\pi}}e^{-i\alpha}\right)$$
$$= \begin{cases} \dfrac{1}{64\pi}\left(\dfrac{z}{a_0}\right)^5\xi(R-\xi)e^{-\frac{z}{2a_0}R}e^{-2i\alpha} \\ \qquad\qquad \text{(near cylinder of radius } \frac{2a_0}{z} \text{ and length } R \text{ along } \xi \text{ axis)} \\ 0 \qquad\qquad \text{(otherwise).} \end{cases} \tag{5.90}$$

(xii) $\phi_{21J'1}(\mathbf{r})^*\phi_{21J-1}(\mathbf{r}-\mathbf{R})$

From Eqs.(5.64) and (5.66), we have

$$\phi_{21J'1}(\mathbf{r})^*\phi_{21J-1}(\mathbf{r}-\mathbf{R})$$
$$= \frac{1}{2\sqrt{6}}\left(\frac{z}{a_0}\right)^{\frac{3}{2}}\left(\frac{zr}{a_0}\right)e^{-\frac{zr}{2a_0}}\frac{1}{2\sqrt{6}}\left(\frac{z}{a_0}\right)^{\frac{3}{2}}\left(\frac{z}{a_0}|\mathbf{r}-\mathbf{R}|\right)e^{-\frac{z}{2a_0}|\mathbf{r}-\mathbf{R}|}$$
$$\times Y^*_{1,1}(\theta,\phi)Y_{1,-1}(\theta_R,\phi_R). \tag{5.91}$$

Using Eqs.(5.71) and (5.74), Eq.(5.91) becomes

$$\phi_{21J'1}(\mathbf{r})^*\phi_{21J-1}(\mathbf{r}-\mathbf{R})$$
$$= \frac{1}{24}\left(\frac{z}{a_0}\right)^3\left(\frac{zr}{2a_0}\right)\left(\frac{z}{a_0}|\mathbf{R}-\mathbf{r}|\right)e^{-\frac{zr}{2a_0}}e^{-\frac{z}{2a_0}|\mathbf{R}-\mathbf{r}|}$$
$$\times\left(-\sqrt{\frac{3}{8\pi}}e^{-i\alpha}\right)\left(\sqrt{\frac{3}{8\pi}}e^{i\alpha}\right)$$
$$= \begin{cases} -\dfrac{1}{64\pi}\left(\dfrac{z}{a_0}\right)^5\xi(R-\xi)e^{-\frac{z}{2a_0}R} \\ \qquad\qquad \text{(near cylinder of radius } \frac{2a_0}{z} \text{ and length } R \text{ along } \xi \text{ axis)} \\ 0 \qquad\qquad \text{(otherwise).} \end{cases} \tag{5.92}$$

(xiii) $\phi_{21J'-1}(\mathbf{r})^*\phi_{20J0}(\mathbf{r}-\mathbf{R})$

From Eqs.(5.64) and (5.65), we get

$$\phi_{21J'-1}(\mathbf{r})^*\phi_{20J0}(\mathbf{r}-\mathbf{R})$$
$$= \frac{1}{2\sqrt{6}}\left(\frac{z}{a_0}\right)^{\frac{3}{2}}\left(\frac{zr}{a_0}\right)e^{-\frac{zr}{2a_0}}\frac{1}{\sqrt{2}}\left(\frac{z}{a_0}\right)^{\frac{3}{2}}\left(1-\frac{z}{2a_0}|\mathbf{r}-\mathbf{R}|\right)e^{-\frac{z}{2a_0}|\mathbf{r}-\mathbf{R}|} \times Y^*_{1,-1}(\theta,\phi)Y_{0,0}(\theta_R,\phi_R). \tag{5.93}$$

Using Eqs.(5.68) and (5.73), Eq.(5.93) becomes

$$= \frac{1}{2\sqrt{12}}\left(\frac{z}{a_0}\right)^{3}\left(\frac{zr}{a_0}\right)\left(1-\frac{z}{2a_0}|\mathbf{R}-\mathbf{r}|\right)e^{-\frac{zr}{2a_0}}e^{-\frac{z}{2a_0}|\mathbf{R}-\mathbf{r}|} \times \left(\sqrt{\frac{3}{8\pi}}e^{i\alpha}\right)\left(\sqrt{\frac{1}{4\pi}}\right)$$
$$= \begin{cases} \dfrac{1}{16\pi\sqrt{2}}\left(\dfrac{z}{a_0}\right)^4\xi\left\{1-\dfrac{z}{2a_0}(R-\xi)\right\}e^{-\frac{z}{2a_0}R}e^{i\alpha} \\ \qquad\qquad \text{(near cylinder of radius } \frac{2a_0}{z} \text{ and length } R \text{ along } \xi \text{ axis)} \\ \\ 0 \qquad\qquad \text{(otherwise).} \end{cases} \tag{5.94}$$

(xiv) $\phi_{21J'-1}(\mathbf{r})^*\phi_{21J0}(\mathbf{r}-\mathbf{R})$ orbits.

From Eqs.(5.64), (5.66), (5.70), and (5.73), we have

$$\phi_{21J'-1}(\mathbf{r})^*\phi_{21J0}(\mathbf{r}-\mathbf{R}) = 0. \tag{5.95}$$

(xv) $\phi_{21J'-1}(\mathbf{r})^*\phi_{21J1}(\mathbf{r}-\mathbf{R})$ orbits.

From Eqs.(5.64) and (5.66), we have

$$\phi_{21J'-1}(\mathbf{r})^*\phi_{21J1}(\mathbf{r}-\mathbf{R})$$
$$= \frac{1}{2\sqrt{6}}\left(\frac{z}{a_0}\right)^{\frac{3}{2}}\left(\frac{zr}{a_0}\right)e^{-\frac{zr}{2a_0}}\frac{1}{2\sqrt{6}}\left(\frac{z}{a_0}\right)^{\frac{3}{2}}\left(\frac{z}{a_0}|\mathbf{r}-\mathbf{R}|\right)e^{-\frac{z}{2a_0}|\mathbf{r}-\mathbf{R}|} \times Y^*_{1,-1}(\theta,\phi)Y_{1,1}(\theta_R,\phi_R). \tag{5.96}$$

Using Eqs.(5.72) and (5.73), Eq.(5.96) becomes

$$\phi_{21J'-1}(\mathbf{r})^*\phi_{21J1}(\mathbf{r}-\mathbf{R})$$
$$= \frac{1}{24}\left(\frac{z}{a_0}\right)^{3}\left(\frac{zr}{2a_0}\right)\left(\frac{z}{a_0}|\mathbf{R}-\mathbf{r}|\right)e^{-\frac{zr}{2a_0}}e^{-\frac{z}{2a_0}|\mathbf{R}-\mathbf{r}|} \times \left(\sqrt{\frac{3}{8\pi}}e^{i\alpha}\right)\left(-\sqrt{\frac{3}{8\pi}}e^{-i\alpha}\right)$$

$$= \begin{cases} -\dfrac{1}{64\pi}\left(\dfrac{z}{a_0}\right)^5 \xi(R-\xi)e^{-\frac{z}{2a_0}R} \\ \qquad\qquad \text{(near cylinder of radius } \frac{2a_0}{z} \text{ and length } R \text{ along } \xi \text{ axis)} \\ \\ 0 \qquad\qquad \text{(otherwise).} \end{cases} \tag{5.97}$$

(xvi) $\phi_{21J'-1}(\mathbf{r})^*\phi_{21J-1}(\mathbf{r}-\mathbf{R})$

From Eqs.(5.64) and (5.66), we get

$$\begin{aligned} &\phi_{21J'-1}(\mathbf{r})^*\phi_{21J-1}(\mathbf{r}-\mathbf{R}) \\ &\quad = \frac{1}{2\sqrt{6}}\left(\frac{z}{a_0}\right)^{\frac{3}{2}}\left(\frac{zr}{a_0}\right)e^{-\frac{zr}{2a_0}}\frac{1}{2\sqrt{6}}\left(\frac{z}{a_0}\right)^{\frac{3}{2}}\left(\frac{z}{a_0}|\mathbf{r}-\mathbf{R}|\right)e^{-\frac{z}{2a_0}|\mathbf{r}-\mathbf{R}|} \\ &\qquad\qquad \times Y^*_{1,-1}(\theta,\phi)Y_{1,-1}(\theta_R,\phi_R). \end{aligned} \tag{5.98}$$

Using Eqs.(5.73) and (5.74), Eq.(5.98) becomes

$$\begin{aligned} &\phi_{21J'-1}(\mathbf{r})^*\phi_{21J-1}(\mathbf{r}-\mathbf{R}) \\ &\quad = \frac{1}{24}\left(\frac{z}{a_0}\right)^3\left(\frac{zr}{2a_0}\right)\left(\frac{z}{a_0}|\mathbf{R}-\mathbf{r}|\right)e^{-\frac{zr}{2a_0}}e^{-\frac{z}{2a_0}|\mathbf{R}-\mathbf{r}|} \\ &\qquad\qquad \times\left(\sqrt{\frac{3}{8\pi}}e^{i\alpha}\right)\left(\sqrt{\frac{3}{8\pi}}e^{i\alpha}\right) \\ &\quad = \begin{cases} \dfrac{1}{64\pi}\left(\dfrac{z}{a_0}\right)^5 \xi(R-\xi)e^{-\frac{z}{2a_0}R}e^{2i\alpha} \\ \qquad\qquad \text{(near cylinder of radius } \frac{2a_0}{z} \text{ and length } R \text{ along } \xi \text{ axis)} \\ \\ 0 \qquad\qquad \text{(otherwise).} \end{cases} \end{aligned} \tag{5.99}$$

With these orbital product, we approximate the first term of Eq.(5.62) for the respective cases as follows:

(i) For $(n'l'J'M') = (20J'0), (nlJM) = (20J0)$

$$\begin{aligned} &\frac{m}{i\hbar}(\varepsilon_{nl}-\varepsilon_{n'l'})\int \phi^{a_j}_{n'l'J'M'\mp\frac{1}{2}}(\mathbf{r})^* x \phi^{a_i}_{nlJM\pm\frac{1}{2}}(\mathbf{r}-\mathbf{R})d^3r \\ &\quad = \frac{m}{i\hbar}(\varepsilon_{20}-\varepsilon_{20})\int \phi^{a_j}_{20J'0}(\mathbf{r})^* x \phi^{a_i}_{20J0}(\mathbf{r}-\mathbf{R})d^3r \\ &\quad = 0. \end{aligned} \tag{5.100}$$

(ii) For $(n'l'J'M') = (20J'0), (nlJM) = (21J0)$.

$$\begin{aligned} &\frac{m}{i\hbar}(\varepsilon_{nl}-\varepsilon_{n'l'})\int \phi^{a_j}_{n'l'J'M'\mp\frac{1}{2}}(\mathbf{r})^* x \phi^{a_i}_{nlJM\pm\frac{1}{2}}(\mathbf{r}-\mathbf{R})d^3r \\ &\quad = \frac{m}{i\hbar}(\varepsilon_{20}-\varepsilon_{21})\int \phi^{a_j}_{20J'0}(\mathbf{r})^* x \phi^{a_i}_{21J0}(\mathbf{r}-\mathbf{R})d^3r. \end{aligned}$$

From Eq.(5.74), we have

$$\frac{m}{i\hbar}(\varepsilon_{nl}-\varepsilon_{n'l'})\int \phi^{a_j}_{n'l'J'M'\mp\frac{1}{2}}(\mathbf{r})^* x \phi^{a_i}_{nlJM\pm\frac{1}{2}}(\mathbf{r}-\mathbf{R})d^3r = 0. \tag{5.101}$$

(iii) For $(n'l'J'M') = (20J'0), (nlJM) = (21J1)$

$$\frac{m}{i\hbar}(\varepsilon_{nl}-\varepsilon_{n'l'})\int \phi^{a_j}_{n'l'J'M'\mp\frac{1}{2}}(\mathbf{r})^* x \phi^{a_i}_{nlJM\pm\frac{1}{2}}(\mathbf{r}-\mathbf{R})d^3r = \frac{m}{i\hbar}(\varepsilon_{20}-\varepsilon_{21})\int\limits_{\text{cylinder}} \phi^{a_j}_{20J'0}(\mathbf{r})^* x \phi^{a_i}_{21J1}(\mathbf{r}-\mathbf{R})d^3r. \tag{5.102}$$

with $x = \xi cos\alpha$ and volume of cylinder$(d^3r) = \left(\frac{2a_0}{z}\right)^2 \pi d\xi$.From Eqs.(5.79) and (5.102), we have

$$\begin{aligned}
&\frac{m}{i\hbar}(\varepsilon_{20}-\varepsilon_{21})\int\limits_{\text{cylinder}} \phi^{a_j}_{20J'0}(\mathbf{r})^* x \phi^{a_i}_{21J1}(\mathbf{r}-\mathbf{R})d^3r \\
&= \frac{m}{i\hbar}(\varepsilon_{20}-\varepsilon_{21})\int_0^R -\frac{1}{16\pi\sqrt{2}}\left(\frac{z}{a_0}\right)^4\left(1-\frac{z}{2a_0}\xi\right)(R-\xi)e^{-\frac{z}{2a_0}R}e^{-i\alpha} \\
&\qquad \times \xi cos\alpha\left(\frac{2a_0}{z}\right)^2\pi d\xi \\
&= \frac{m}{i\hbar}(\varepsilon_{20}-\varepsilon_{21})\left\{-\frac{1}{16\pi\sqrt{2}}\left(\frac{z}{a_0}\right)^4 e^{-\frac{z}{2a_0}R}e^{-i\alpha}cos\alpha\left(\frac{2a_0}{z}\right)^2\pi\right\} \\
&\qquad \times \int_0^R \xi(R-\xi)\left(1-\frac{z}{2a_0}\xi\right)d\xi \\
&= \frac{m}{i\hbar}(\varepsilon_{20}-\varepsilon_{21})\left\{-\frac{1}{16\pi\sqrt{2}}\left(\frac{z}{a_0}\right)^4 e^{-\frac{z}{2a_0}R}e^{-i\alpha}cos\alpha\left(\frac{2a_0}{z}\right)^2\pi\right\}\frac{R^3}{6}\left(1-\frac{z}{4a_0}R\right) \\
&= \frac{m}{i\hbar}(\varepsilon_{21}-\varepsilon_{20})\frac{1}{24\sqrt{2}}\left(\frac{z}{a_0}\right)^2\left(1-\frac{z}{4a_0}R\right)e^{-\frac{z}{2a_0}R}e^{-i\alpha}R^3cos\alpha \\
&= \frac{m}{i\hbar}(\varepsilon_{21}-\varepsilon_{20})\frac{1}{24\sqrt{2}}\left(\frac{z}{a_0}\right)^2\left(1-\frac{z}{4a_0}R\right)e^{-\frac{z}{2a_0}R}R(Rcos\alpha-iRsin\alpha)Rcos\alpha \\
&= \frac{m}{i\hbar}(\varepsilon_{21}-\varepsilon_{20})\frac{1}{24\sqrt{2}}\left(\frac{z}{a_0}\right)^2\left(1-\frac{z}{4a_0}R\right)e^{-\frac{z}{2a_0}R}R(R_x-iR_y)R_x \\
&= \frac{mR}{i\hbar}(R_x^2-iR_xR_y)(\varepsilon_{21}-\varepsilon_{20})\frac{1}{24\sqrt{2}}\left(\frac{z}{a_0}\right)^2\left(1-\frac{z}{4a_0}R\right)e^{-\frac{z}{2a_0}R.}.
\end{aligned} \tag{5.103}$$

(iv) For $(n'l'J'M') = (20J'0), (nlJM) = (21J\text{-}1)$.

$$\frac{m}{i\hbar}(\varepsilon_{nl}-\varepsilon_{n'l'})\int \phi^{a_j}_{n'l'J'M'\mp\frac{1}{2}}(\mathbf{r})^* x \phi^{a_i}_{nlJM\pm\frac{1}{2}}(\mathbf{r}-\mathbf{R})d^3r = \frac{m}{i\hbar}(\varepsilon_{20}-\varepsilon_{21})\int\limits_{\text{cylinder}} \phi^{a_j}_{20J'0}(\mathbf{r})^* x \phi^{a_i}_{21J-1}(\mathbf{r}-\mathbf{R})d^3r. \tag{5.104}$$

We have, $x = \xi cos\alpha$ and $d^3r = \left(\frac{2a_0}{z}\right)^2 \pi d\xi$. From Eqs.(5.81) and (5.104), we get

$$\begin{aligned}
&\frac{m}{i\hbar}(\varepsilon_{20} - \varepsilon_{21}) \int\limits_{\text{cylinder}} \phi^{a_j}_{20J'0}(\mathbf{r})^* x \phi^{a_i}_{21J-1}(\mathbf{r} - \mathbf{R}) d^3r \\
&\quad = \frac{m}{i\hbar}(\varepsilon_{20} - \varepsilon_{21}) \int\limits_{\text{cylinder}} \frac{1}{16\pi\sqrt{2}} \left(\frac{z}{a_0}\right)^4 \left(1 - \frac{z}{2a_0}\xi\right)(R - \xi) e^{-\frac{z}{2a_0}R} e^{i\alpha} \\
&\qquad\qquad \times \xi cos\alpha \left(\frac{2a_0}{z}\right)^2 \pi d\xi \\
&\quad = \frac{m}{i\hbar}(\varepsilon_{20} - \varepsilon_{21}) \left\{ \frac{1}{4\sqrt{2}} \left(\frac{z}{a_0}\right)^2 e^{-\frac{z}{2a_0}R} e^{i\alpha} cos\alpha \right\} \int_0^R \xi(R - \xi) \left(1 - \frac{z}{2a_0}\xi\right) d\xi \\
&\quad = \frac{m}{i\hbar}(\varepsilon_{20} - \varepsilon_{21}) \left\{ \frac{1}{4\sqrt{2}} \left(\frac{z}{a_0}\right)^2 e^{-\frac{z}{2a_0}R} e^{i\alpha} cos\alpha \right\} \frac{R^3}{6} \left(1 - \frac{z}{2a_0}R\right) \\
&\quad = \frac{m}{i\hbar}(\varepsilon_{20} - \varepsilon_{21}) \frac{1}{24\sqrt{2}} \left(\frac{z}{a_0}\right)^2 \left(1 - \frac{z}{2a_0}R\right) e^{-\frac{z}{2a_0}R} e^{i\alpha} R^3 cos\alpha \\
&\quad = \frac{m}{i\hbar}(\varepsilon_{20} - \varepsilon_{21}) \frac{1}{24\sqrt{2}} \left(\frac{z}{a_0}\right)^2 \left(1 - \frac{z}{4a_0}R\right) e^{-\frac{z}{2a_0}R} R(R_x + iR_y) R_x \\
&\quad = \frac{mR}{i\hbar}(R_x^2 + iR_xR_y)(\varepsilon_{20} - \varepsilon_{21}) \frac{1}{24\sqrt{2}} \left(\frac{z}{a_0}\right)^2 \left(1 - \frac{z}{4a_0}R\right) e^{-\frac{z}{2a_0}R}. \qquad (5.105)
\end{aligned}$$

(v) For $(n'l'J'M') = (21J'1), (nlJM) = (20J0)$.

$$\begin{aligned}
&\frac{m}{i\hbar}(\varepsilon_{nl} - \varepsilon_{n'l'}) \int \phi^{a_j}_{n'l'J'M'\mp\frac{1}{2}}(\mathbf{r})^* x \phi^{a_i}_{nlJM\pm\frac{1}{2}}(\mathbf{r} - \mathbf{R}) d^3r \\
&\qquad\qquad = \frac{m}{i\hbar}(\varepsilon_{21} - \varepsilon_{20}) \int\limits_{\text{cylinder}} \phi^{a_j}_{21J'1}(\mathbf{r})^* x \phi^{a_i}_{20J0}(\mathbf{r} - \mathbf{R}) d^3r. \qquad (5.106)
\end{aligned}$$

From Eqs.(5.87) and (5.106), we have

$$\begin{aligned}
&\frac{m}{i\hbar}(\varepsilon_{21} - \varepsilon_{20}) \int\limits_{\text{cylinder}} \phi^{a_j}_{21J'1}(\mathbf{r})^* x \phi^{a_i}_{20J0}(\mathbf{r} - \mathbf{R}) d^3r \\
&\quad = \frac{m}{i\hbar}(\varepsilon_{21} - \varepsilon_{20}) \int_0^R -\frac{1}{16\pi\sqrt{2}} \left(\frac{z}{a_0}\right)^4 \xi \left\{1 - \frac{z}{2a_0}(R - \xi)\right\} e^{-\frac{z}{2a_0}R} e^{-i\alpha} \\
&\qquad\qquad \times \xi cos\alpha \left(\frac{2a_0}{z}\right)^2 \pi d\xi \\
&\quad = \frac{m}{i\hbar}(\varepsilon_{20} - \varepsilon_{21}) \frac{1}{4\sqrt{2}} \left(\frac{z}{a_0}\right)^2 e^{-\frac{z}{2a_0}R} e^{-i\alpha} cos\alpha \int_0^R \xi^2 \left\{1 - \frac{z}{2a_0}(R - \xi)\right\} d\xi \\
&\quad = \frac{m}{i\hbar}(\varepsilon_{20} - \varepsilon_{21}) \frac{1}{4\sqrt{2}} \left(\frac{z}{a_0}\right)^2 e^{-\frac{z}{2a_0}R} e^{-i\alpha} cos\alpha \frac{R^3}{3} \left(1 - \frac{z}{8a_0}R\right) \\
&\quad = \frac{mR}{i\hbar}(R_x^2 - iR_xR_y)(\varepsilon_{20} - \varepsilon_{21}) \frac{1}{12\sqrt{2}} \left(\frac{z}{a_0}\right)^2 \left(1 - \frac{z}{8a_0}R\right) e^{-\frac{z}{2a_0}R}. \qquad (5.107)
\end{aligned}$$

(vi) For $(n'l'J'M') = (21J'1), (nlJM) = (21J1)$

$$\begin{aligned}
&\frac{m}{i\hbar}(\varepsilon_{nl} - \varepsilon_{n'l'}) \int \phi^{a_j}_{n'l'J'M'\mp\frac{1}{2}}(\mathbf{r})^* x \phi^{a_i}_{nlJM\pm\frac{1}{2}}(\mathbf{r}-\mathbf{R}) d^3r \\
&\quad = \frac{m}{i\hbar}(\varepsilon_{21} - \varepsilon_{21}) \int\limits_{\text{cylinder}} \phi^{a_j}_{21J'1}(\mathbf{r})^* x \phi^{a_i}_{21J1}(\mathbf{r}-\mathbf{R}) d^3r \\
&\quad = 0. \qquad (5.108)
\end{aligned}$$

(vii) For$(n'l'J'M') = (20J'0), (nlJM) = (21J\text{-}1)$

$$\begin{aligned}
&\frac{m}{i\hbar}(\varepsilon_{nl} - \varepsilon_{n'l'}) \int \phi^{a_j}_{n'l'J'M'\mp\frac{1}{2}}(\mathbf{r})^* x \phi^{a_i}_{nlJM\pm\frac{1}{2}}(\mathbf{r}-\mathbf{R}) d^3r \\
&\quad = \frac{m}{i\hbar}(\varepsilon_{21} - \varepsilon_{21}) \int\limits_{\text{cylinder}} \phi^{a_j}_{21J'1}(\mathbf{r})^* x \phi^{a_i}_{21J\text{-}1}(\mathbf{r}-\mathbf{R}) d^3r \\
&\quad = 0. \qquad (5.109)
\end{aligned}$$

(viii) For $(n'l'J'M') = (21J'\text{-}1), (nlJM) = (20J0)$.

$$\begin{aligned}
&\frac{m}{i\hbar}(\varepsilon_{nl} - \varepsilon_{n'l'}) \int \phi^{a_j}_{n'l'J'M'\mp\frac{1}{2}}(\mathbf{r})^* x \phi^{a_i}_{nlJM\pm\frac{1}{2}}(\mathbf{r}-\mathbf{R}) d^3r \\
&\qquad\qquad = \frac{m}{i\hbar}(\varepsilon_{21} - \varepsilon_{20}) \int\limits_{\text{cylinder}} \phi^{a_j}_{21J'\text{-}1}(\mathbf{r})^* x \phi^{a_i}_{20J0}(\mathbf{r}-\mathbf{R}) d^3r. \qquad (5.110)
\end{aligned}$$

From Eqs.(5.94) and (5.110), we have

$$\begin{aligned}
&\frac{m}{i\hbar}(\varepsilon_{21} - \varepsilon_{20}) \int\limits_{\text{cylinder}} \phi^{a_j}_{21J'\text{-}1}(\mathbf{r})^* x \phi^{a_i}_{20J0}(\mathbf{r}-\mathbf{R}) d^3r \\
&\quad = \frac{m}{i\hbar}(\varepsilon_{21} - \varepsilon_{20}) \int_0^R \frac{1}{16\pi\sqrt{2}} \left(\frac{z}{a_0}\right)^4 \xi \left\{1 - \frac{z}{2a_0}(R-\xi)\right\} e^{-\frac{z}{2a_0}R} e^{i\alpha} \\
&\qquad\qquad \times \xi cos\alpha \left(\frac{2a_0}{z}\right) \pi d\xi \\
&\quad = \frac{m}{i\hbar}(\varepsilon_{21} - \varepsilon_{20}) \frac{1}{4\sqrt{2}} \left(\frac{z}{a_0}\right)^2 e^{-\frac{z}{2a_0}R} e^{i\alpha} cos\alpha \int_0^R \xi^2 \left\{1 - \frac{z}{2a_0}(R-\xi)\right\} d\xi \\
&\quad = \frac{m}{i\hbar}(\varepsilon_{21} - \varepsilon_{20}) \frac{1}{4\sqrt{2}} \left(\frac{z}{a_0}\right)^2 e^{-\frac{z}{2a_0}R} e^{i\alpha} cos\alpha \, \frac{R^3}{3} \left(1 - \frac{z}{8a_0}R\right) \\
&\quad = \frac{mR}{i\hbar}(R_x^2 + iR_xR_y)(\varepsilon_{21} - \varepsilon_{20}) \frac{1}{12\sqrt{2}} \left(\frac{z}{a_0}\right)^2 \left(1 - \frac{z}{8a_0}R\right) e^{-\frac{z}{2a_0}R}. \qquad (5.111)
\end{aligned}$$

(ix) For $(n'l'J'M') = (21J'\text{-}1), (nlJM) = (21J1)$

$$\begin{aligned}
&\frac{m}{i\hbar}(\varepsilon_{nl} - \varepsilon_{n'l'}) \int \phi^{a_j}_{n'l'J'M'\mp\frac{1}{2}}(\mathbf{r})^* x \phi^{a_i}_{nlJM\pm\frac{1}{2}}(\mathbf{r}-\mathbf{R}) d^3r \\
&\quad = \frac{m}{i\hbar}(\varepsilon_{21} - \varepsilon_{21}) \int\limits_{\text{cylinder}} \phi^{a_j}_{21J'\text{-}1}(\mathbf{r})^* x \phi^{a_i}_{21J1}(\mathbf{r}-\mathbf{R}) d^3r \\
&\quad = 0. \qquad (5.112)
\end{aligned}$$

(x) For $(n'l'J'M') = (21J'\text{-}1), (nlJM) = (21J\text{-}1)$.

$$\begin{aligned}
&\frac{m}{i\hbar}(\varepsilon_{nl} - \varepsilon_{n'l'}) \int \phi^{a_j}_{n'l'J'M'\mp\frac{1}{2}}(\mathbf{r})^* x \phi^{a_i}_{nlJM\pm\frac{1}{2}}(\mathbf{r}-\mathbf{R}) d^3r \\
&\quad = \frac{m}{i\hbar}(\varepsilon_{21} - \varepsilon_{21}) \int\limits_{\text{cylinder}} \phi^{a_j}_{21J'\text{-}1}(\mathbf{r})^* x \phi^{a_i}_{21J\text{-}1}(\mathbf{r}-\mathbf{R}) d^3r \\
&\quad = 0.
\end{aligned} \tag{5.113}$$

The second term of the Eq.(5.62) is estimated as

$$\begin{aligned}
&\frac{m}{i\hbar} \int \phi^{a_j}_{n'l'J'M'\mp\frac{1}{2}}(\mathbf{r})^* x V_{atom}(\mathbf{r}) \phi^{a_i}_{nlJM\pm\frac{1}{2}}(\mathbf{r}-\mathbf{R}) d^3r \\
&\qquad = \frac{m}{i\hbar} \int\limits_{\text{cylinder}} \phi^{a_j}_{n'l'J'M'\mp\frac{1}{2}}(\mathbf{r})^* \xi cos\alpha \frac{ze^2}{4\pi\epsilon_0 \xi} \phi^{a_i}_{nlJM\pm\frac{1}{2}}(\mathbf{r}-\mathbf{R}) d^3r \\
&\qquad = \frac{m}{i\hbar} \frac{ze^2}{4\pi\epsilon_0} cos\alpha \int\limits_{\text{cylinder}} \phi^{a_j}_{n'l'J'M'\mp\frac{1}{2}}(\mathbf{r})^* \phi^{a_i}_{nlJM\pm\frac{1}{2}}(\mathbf{r}-\mathbf{R}) d^3r \\
&\qquad = \frac{m}{i\hbar} \frac{ze^2}{4\pi\epsilon_0 \mathbf{R}} R_x \; s^{a_j,a_i}_{n'l'J'M'\mp\frac{1}{2},nlJM\pm\frac{1}{2}}(\mathbf{R}),
\end{aligned} \tag{5.114}$$

where $s^{a_j,a_i}_{n'l'J'M'\mp\frac{1}{2},nlJM\pm\frac{1}{2}}(\mathbf{R})$ is the non-relativistic overlap integral, which is given by

$$s^{a_j,a_i}_{n'l'J'M'\mp\frac{1}{2},nlJM\pm\frac{1}{2}}(\mathbf{R}) = \int\limits_{\text{cylinder}} \phi^{a_j}_{n'l'J'M'\mp\frac{1}{2}}(\mathbf{r})^* \phi^{a_i}_{nlJM\pm\frac{1}{2}}(\mathbf{r}-\mathbf{R}) d^3r. \tag{5.115}$$

Here, we have used $R_x = \mathbf{R} cos\alpha$ (from Fig. 5.3).

The third term of the Eq.(5.62) is estimated as

$$\begin{aligned}
&\frac{m}{i\hbar} \int \phi^{a_j}_{n'l'J'M'\mp\frac{1}{2}}(\mathbf{r})^* x V_{atom}(\mathbf{r}-\mathbf{R}) \phi^{a_i}_{nlJM\pm\frac{1}{2}}(\mathbf{r}-\mathbf{R}) d^3r \\
&\qquad = \frac{m}{i\hbar} \int \phi^{a_j}_{n'l'J'M'\mp\frac{1}{2}}(\mathbf{r})^* (x - R_x) V_{atom}(\mathbf{r}-\mathbf{R}) \phi^{a_i}_{nlJM\pm\frac{1}{2}}(\mathbf{r}-\mathbf{R}) d^3r \\
&\qquad\qquad + \frac{m}{i\hbar} R_x \int \phi^{a_j}_{n'l'J'M'\mp\frac{1}{2}}(\mathbf{r})^* V_{atom}(\mathbf{r}-\mathbf{R}) \phi^{a_i}_{nlJM\pm\frac{1}{2}}(\mathbf{r}-\mathbf{R}) d^3r \\
&\qquad = \frac{m}{i\hbar} \int\limits_{\text{cylinder}} \phi^{a_j}_{n'l'J'M'\mp\frac{1}{2}}(\mathbf{r})^* (\xi - R) cos\alpha \frac{ze^2}{4\pi\epsilon_0 (R-\xi)} \phi^{a_i}_{nlJM\pm\frac{1}{2}}(\mathbf{r}-\mathbf{R}) d^3r \\
&\qquad\qquad + \frac{m}{i\hbar} R_x \int\limits_{\text{cylinder}} \phi^{a_j}_{n'l'J'M'\mp\frac{1}{2}}(\mathbf{r})^* V_{atom}(\mathbf{r}-\mathbf{R}) \phi^{a_i}_{nlJM\pm\frac{1}{2}}(\mathbf{r}-\mathbf{R}) d^3r \\
&\qquad = -\frac{m}{i\hbar} \frac{ze^2}{4\pi\epsilon_0 R} R_x \int\limits_{\text{cylinder}} \phi^{a_j}_{n'l'J'M'\mp\frac{1}{2}}(\mathbf{r})^* \phi^{a_i}_{nlJM\pm\frac{1}{2}}(\mathbf{r}-\mathbf{R}) d^3r \\
&\qquad\qquad + \frac{m}{i\hbar} R_x \int\limits_{\text{cylinder}} \phi^{a_j}_{n'l'J'M'\mp\frac{1}{2}}(\mathbf{r})^* V_{atom}(\mathbf{r}-\mathbf{R}) \phi^{a_i}_{nlJM\pm\frac{1}{2}}(\mathbf{r}-\mathbf{R}) d^3r
\end{aligned}$$

$$= -\frac{m}{i\hbar}\frac{ze^2}{4\pi\epsilon_0 R}R_x\, s^{a_j,a_i}_{n'l'J'M'\mp\frac{1}{2},nlJM\pm\frac{1}{2}}(\mathbf{R}) + \frac{m}{i\hbar}R_x\, t^{a_j,a_i}_{n'l'J'M'\mp\frac{1}{2},nlJM\pm\frac{1}{2}}(\mathbf{R}), \tag{5.116}$$

where $t^{a_j,a_i}_{n'l'J'M'\mp\frac{1}{2},nlJM\pm\frac{1}{2}}(\mathbf{R})$ is non-relativistic hopping integral and is given by

$$t^{a_j,a_i}_{n'l'J'M'\mp\frac{1}{2},nlJM\pm\frac{1}{2}}(\mathbf{R}) = \int_{\text{cylinder}} \phi^{a_j}_{n'l'J'M'\mp\frac{1}{2}}(\mathbf{r})^* V_{atom}(\mathbf{r}-\mathbf{R})\phi^{a_i}_{nlJM\pm\frac{1}{2}}(\mathbf{r}-\mathbf{R})d^3r. \tag{5.117}$$

Hence, From the Eqs.(5.114) and (5.116), the momentum matrix of Eq.(5.62) can be written as

$$\begin{aligned}
&\int \phi^{a_j}_{n'l'J'M'\mp\frac{1}{2}}(\mathbf{r})^* p_x \phi^{a_i}_{nlJM\pm\frac{1}{2}}(\mathbf{r}-\mathbf{R})d^3r \\
&\quad = \frac{m}{i\hbar}(\varepsilon_{nl}-\varepsilon_{n'l'})\int \phi^{a_j}_{n'l'J'M'\mp\frac{1}{2}}(\mathbf{r})^* x \phi^{a_i}_{nlJM\pm\frac{1}{2}}(\mathbf{r}-\mathbf{R})d^3r \\
&\quad\quad + \frac{m}{i\hbar}R_x\left\{2\frac{ze^2}{4\pi\epsilon_0\mathbf{R}}\, s^{a_j,a_i}_{n'l'J'M'\mp\frac{1}{2},nlJM\pm\frac{1}{2}}(\mathbf{R}) - t^{a_j,a_i}_{n'l'J'M'\mp\frac{1}{2},nlJM\pm\frac{1}{2}}(\mathbf{R})\right\}.
\end{aligned} \tag{5.118}$$

Following the similar calculation steps, the momentum matrix $\int \phi^{a_j}_{n'l'J'M'\mp\frac{1}{2}}(\mathbf{r})^* p_y \phi^{a_i}_{nlJM\pm\frac{1}{2}}(\mathbf{r}-\mathbf{R})d^3r$ can be calculated. Then, we have

$$\begin{aligned}
&\int \phi^{a_j}_{n'l'J'M'\mp\frac{1}{2}}(\mathbf{r})^* p_y \phi^{a_i}_{nlJM\pm\frac{1}{2}}(\mathbf{r}-\mathbf{R})d^3r \\
&\quad = \int \phi^{a_j}_{n'l'J'M'\mp\frac{1}{2}}(\mathbf{r})^* \frac{m}{i\hbar}\left(yH^{\mathbf{0}}_{atom} - H^{\mathbf{0}}_{atom}y\right)\phi^{a_i}_{nlJM\pm\frac{1}{2}}(\mathbf{r}-\mathbf{R})d^3r \\
&\quad = \frac{m}{i\hbar}\left\{\int \phi^{a_j}_{n'l'J'M'\mp\frac{1}{2}}(\mathbf{r})^* y H^{\mathbf{0}}_{atom}\phi^{a_i}_{nlJM\pm\frac{1}{2}}(\mathbf{r}-\mathbf{R})d^3r\right. \\
&\qquad\qquad \left. - \int \phi^{a_j}_{n'l'J'M'\mp\frac{1}{2}}(\mathbf{r})^* H^{\mathbf{0}}_{atom} y \phi^{a_i}_{nlJM\pm\frac{1}{2}}(\mathbf{r}-\mathbf{R})d^3r\right\} \\
&\quad = \frac{m}{i\hbar}\left\{\int \phi^{a_j}_{n'l'J'M'\mp\frac{1}{2}}(\mathbf{r})^* y\{H^{\mathbf{R}}_{atom} + V_{atom}(\mathbf{r}) - V_{atom}(\mathbf{r}-\mathbf{R})\}\phi^{a_i}_{nlJM\pm\frac{1}{2}}(\mathbf{r}-\mathbf{R})d^3r\right. \\
&\qquad\qquad \left. -\varepsilon_{n'l'}\int \phi^{a_j}_{n'l'J'M'\mp\frac{1}{2}}(\mathbf{r})^* y \phi^{a_i}_{nlJM\pm\frac{1}{2}}(\mathbf{r}-\mathbf{R})d^3r\right\} \\
&\quad = \frac{m}{i\hbar}\left\{\int \phi^{a_j}_{n'l'J'M'\mp\frac{1}{2}}(\mathbf{r})^* y H^{\mathbf{R}}_{atom}\phi^{a_i}_{nlJM\pm\frac{1}{2}}(\mathbf{r}-\mathbf{R})d^3r\right. \\
&\qquad\qquad + \int \phi^{a_j}_{n'l'J'M'\mp\frac{1}{2}}(\mathbf{r})^* y\{V_{atom}(\mathbf{r}) - V_{atom}(\mathbf{r}-\mathbf{R})\}\phi^{a_i}_{nlJM\pm\frac{1}{2}}(\mathbf{r}-\mathbf{R})d^3r \\
&\qquad\qquad \left. -\varepsilon_{n'l'}\int \phi^{a_j}_{n'l'J'M'\mp\frac{1}{2}}(\mathbf{r})^* y \phi^{a_i}_{nlJM\pm\frac{1}{2}}(\mathbf{r}-\mathbf{R})d^3r\right\} \\
&\quad = \frac{m}{i\hbar}\left\{\varepsilon_{nl}\int \phi^{a_j}_{n'l'J'M'\mp\frac{1}{2}}(\mathbf{r})^* y \phi^{a_i}_{nlJM\pm\frac{1}{2}}(\mathbf{r}-\mathbf{R})d^3r\right. \\
&\qquad\qquad + \int \phi^{a_j}_{n'l'J'M'\mp\frac{1}{2}}(\mathbf{r})^* y\{V_{atom}(\mathbf{r}) - V_{atom}(\mathbf{r}-\mathbf{R})\}\phi^{a_i}_{nlJM\pm\frac{1}{2}}(\mathbf{r}-\mathbf{R})d^3r \\
&\qquad\qquad \left. -\varepsilon_{n'l'}\int \phi^{a_j}_{n'l'J'M'\mp\frac{1}{2}}(\mathbf{r})^* y \phi^{a_i}_{nlJM\pm\frac{1}{2}}(\mathbf{r}-\mathbf{R})d^3r\right\}
\end{aligned}$$

$$= \frac{m}{i\hbar}\left\{(\varepsilon_{nl}-\varepsilon_{n'l'})\int \phi^{a_j}_{n'l'J'M'\mp\frac{1}{2}}(\mathbf{r}) * y\phi^{a_i}_{nlJM\pm\frac{1}{2}}(\mathbf{r}-\mathbf{R})d^3r \right.$$
$$+\int \phi^{a_j}_{n'l'J'M'\mp\frac{1}{2}}(\mathbf{r})^* y V_{atom}(\mathbf{r})\phi^{a_i}_{nlJM\pm\frac{1}{2}}(\mathbf{r}-\mathbf{R})d^3r$$
$$\left.-\int \phi^{a_j}_{n'l'J'M'\mp\frac{1}{2}}(\mathbf{r})^* y V_{atom}(\mathbf{r}-\mathbf{R})\phi^{a_i}_{nlJM\pm\frac{1}{2}}(\mathbf{r}-\mathbf{R})d^3r\right\}. \tag{5.119}$$

First term of Eq.(5.119) can be evaluated following similar calculation method which is carried out with first term of Eq.(5.62). For the respective orbital products, the first term of Eq.(5.119) is given as follows:

(i) For $(n'l'J'M') = (20J'0), (nlJM) = (20J0)$

$$\frac{m}{i\hbar}(\varepsilon_{nl}-\varepsilon_{n'l'})\int \phi^{a_j}_{n'l'J'M'\mp\frac{1}{2}}(\mathbf{r})^* y\phi^{a_i}_{nlJM\pm\frac{1}{2}}(\mathbf{r}-\mathbf{R})d^3r$$
$$= \frac{m}{i\hbar}(\varepsilon_{20}-\varepsilon_{20})\int\limits_{\text{cylinder}} \phi^{a_j}_{20J'0}(\mathbf{r})^* y\phi^{a_i}_{20J0}(\mathbf{r}-\mathbf{R})d^3r$$
$$= 0. \tag{5.120}$$

(ii) For $(n'l'J'M') = (20J'0), (nlJM) = (21J1)$

$$\frac{m}{i\hbar}(\varepsilon_{nl}-\varepsilon_{n'l'})\int \phi^{a_j}_{n'l'J'M'\mp\frac{1}{2}}(\mathbf{r})^* y\phi^{a_i}_{nlJM\pm\frac{1}{2}}(\mathbf{r}-\mathbf{R})d^3r$$
$$= \frac{m}{i\hbar}(\varepsilon_{20}-\varepsilon_{21})\int\limits_{\text{cylinder}} \phi^{a_j}_{20J'0}(\mathbf{r})^* y\phi^{a_i}_{21J1}(\mathbf{r}-\mathbf{R})d^3r.$$

Form Eq.(5.79), we have

$$\frac{m}{i\hbar}(\varepsilon_{20}-\varepsilon_{21})\int\limits_{\text{cylinder}} \phi^{a_j}_{20J'0}(\mathbf{r})^* y\phi^{a_i}_{21J1}(\mathbf{r}-\mathbf{R})d^3r$$
$$= \frac{mR}{i\hbar}(R_y^2 - iR_xR_y)(\varepsilon_{21}-\varepsilon_{20})\frac{1}{24\sqrt{2}}\left(\frac{z}{a_0}\right)^2\left(1-\frac{z}{4a_0}R\right)e^{-\frac{z}{2a_0}R}. \tag{5.121}$$

Here, we employed $y = \xi sin\alpha$ and $R_y = Rsin\alpha$ (from Fig. 5.3).

(iii) For $(n'l'J'M') = (20J'0), (nlJM) = (21J\text{-}1)$

$$\frac{m}{i\hbar}(\varepsilon_{nl}-\varepsilon_{n'l'})\int \phi^{a_j}_{n'l'J'M'\mp\frac{1}{2}}(\mathbf{r})^* y\phi^{a_i}_{nlJM\pm\frac{1}{2}}(\mathbf{r}-\mathbf{R})d^3r$$
$$= \frac{m}{i\hbar}(\varepsilon_{20}-\varepsilon_{21})\int\limits_{\text{cylinder}} \phi^{a_j}_{20J'0}(\mathbf{r})^* y\phi^{a_i}_{21J\text{-}1}(\mathbf{r}-\mathbf{R})d^3r.$$

From Eq.(5.81), we have

$$\frac{m}{i\hbar}(\varepsilon_{20}-\varepsilon_{21})\int\limits_{\text{cylinder}} \phi^{a_j}_{20J'0}(\mathbf{r})^* y\phi^{a_i}_{21J\text{-}1}(\mathbf{r}-\mathbf{R})d^3r$$
$$= \frac{mR}{i\hbar}(R_y^2 + iR_xR_y)(\varepsilon_{20}-\varepsilon_{21})\frac{1}{24\sqrt{2}}\left(\frac{z}{a_0}\right)^2\left(1-\frac{z}{4a_0}R\right)e^{-\frac{z}{2a_0}R}. \tag{5.122}$$

(iv) $(n'l'J'M') = (21J'1), (nlJM) = (20J0)$

$$\frac{m}{i\hbar}(\varepsilon_{nl} - \varepsilon_{n'l'}) \int \phi^{a_j}_{n'l'J'M'\mp\frac{1}{2}}(\mathbf{r})^* y \phi^{a_i}_{nlJM\pm\frac{1}{2}}(\mathbf{r}-\mathbf{R}) d^3r$$
$$= \frac{m}{i\hbar}(\varepsilon_{21} - \varepsilon_{20}) \int\limits_{\text{cylinder}} \phi^{a_j}_{21J'1}(\mathbf{r})^* y \phi^{a_i}_{20J0}(\mathbf{r}-\mathbf{R}) d^3r.$$

From Eq.(5.81), we have

$$\frac{m}{i\hbar}(\varepsilon_{21} - \varepsilon_{20}) \int\limits_{\text{cylinder}} \phi^{a_j}_{21J'1}(\mathbf{r})^* y \phi^{a_i}_{20J0}(\mathbf{r}-\mathbf{R}) d^3r$$
$$= \frac{mR}{i\hbar}(R_y^2 - iR_xR_y)(\varepsilon_{20} - \varepsilon_{21}) \frac{1}{12\sqrt{2}} \left(\frac{z}{a_0}\right)^2 \left(1 - \frac{z}{8a_0}R\right) e^{-\frac{z}{2a_0}R}. \quad (5.123)$$

(v) For $(n'l'J'M') = (21J'1), (nlJM) = (21J1)$

$$\frac{m}{i\hbar}(\varepsilon_{nl} - \varepsilon_{n'l'}) \int \phi^{a_j}_{n'l'J'M'\mp\frac{1}{2}}(\mathbf{r})^* y \phi^{a_i}_{nlJM\pm\frac{1}{2}}(\mathbf{r}-\mathbf{R}) d^3r$$
$$= \frac{m}{i\hbar}(\varepsilon_{21} - \varepsilon_{21}) \int\limits_{\text{cylinder}} \phi^{a_j}_{21J'1}(\mathbf{r})^* y \phi^{a_i}_{21J1}(\mathbf{r}-\mathbf{R}) d^3r$$
$$= 0. \quad (5.124)$$

(vi) For $(n'l'J'M') = (21J'1), (nlJM) = (21J\text{-}1)$

$$\frac{m}{i\hbar}(\varepsilon_{nl} - \varepsilon_{n'l'}) \int \phi^{a_j}_{n'l'J'M'\mp\frac{1}{2}}(\mathbf{r})^* y \phi^{a_i}_{nlJM\pm\frac{1}{2}}(\mathbf{r}-\mathbf{R}) d^3r$$
$$= \frac{m}{i\hbar}(\varepsilon_{21} - \varepsilon_{21}) \int\limits_{\text{cylinder}} \phi^{a_j}_{21J'1}(\mathbf{r})^* y \phi^{a_i}_{21J-1}(\mathbf{r}-\mathbf{R}) d^3r$$
$$= 0. \quad (5.125)$$

(vii) $(n'l'J'M') = (21J'\text{-}1), (nlJM) = (2J0)$

$$\frac{m}{i\hbar}(\varepsilon_{nl} - \varepsilon_{n'l'}) \int \phi^{a_j}_{n'l'J'M'\mp\frac{1}{2}}(\mathbf{r})^* y \phi^{a_i}_{nlJM\pm\frac{1}{2}}(\mathbf{r}-\mathbf{R}) d^3r$$
$$= \frac{m}{i\hbar}(\varepsilon_{21} - \varepsilon_{20}) \int\limits_{\text{cylinder}} \phi^{a_j}_{21J'-1}(\mathbf{r})^* y \phi^{a_i}_{20J0}(\mathbf{r}-\mathbf{R}) d^3r$$

From Eq.(5.81), we have

$$\frac{m}{i\hbar}(\varepsilon_{21} - \varepsilon_{20}) \int\limits_{\text{cylinder}} \phi^{a_j}_{21J'-1}(\mathbf{r})^* y \phi^{a_i}_{20J0}(\mathbf{r}-\mathbf{R}) d^3r$$
$$= \frac{mR}{i\hbar}(R_y^2 + iR_xR_y)(\varepsilon_{21} - \varepsilon_{20}) \frac{1}{12\sqrt{2}} \left(\frac{z}{a_0}\right)^2 \left(1 - \frac{z}{8a_0}R\right) e^{-\frac{z}{2a_0}R}. \quad (5.126)$$

(viii) For $(n'l'J'M') = (21J'\text{-}1), (nlJM) = (21J1)$

$$\begin{aligned}
&\frac{m}{i\hbar}(\varepsilon_{nl} - \varepsilon_{n'l'}) \int \phi^{a_j}_{n'l'J'M'\mp\frac{1}{2}}(\mathbf{r})^* y \phi^{a_i}_{nlJM\pm\frac{1}{2}}(\mathbf{r}-\mathbf{R}) d^3r \\
&\quad = \frac{m}{i\hbar}(\varepsilon_{21} - \varepsilon_{21}) \int_{\text{cylinder}} \phi^{a_j}_{21J'\text{-}1}(\mathbf{r})^* y \phi^{a_i}_{21J1}(\mathbf{r}-\mathbf{R}) d^3r \\
&\quad = 0. \qquad . \quad (5.127)
\end{aligned}$$

(ix) For $(n'l'J'M') = (21J'\text{-}1), (nlJM) = (21J\text{-}1)$

$$\begin{aligned}
&\frac{m}{i\hbar}(\varepsilon_{nl} - \varepsilon_{n'l'}) \int \phi^{a_j}_{n'l'J'M'\mp\frac{1}{2}}(\mathbf{r})^* y \phi^{a_i}_{nlJM\pm\frac{1}{2}}(\mathbf{r}-\mathbf{R}) d^3r \\
&\quad = \frac{m}{i\hbar}(\varepsilon_{21} - \varepsilon_{21}) \int_{\text{cylinder}} \phi^{a_j}_{21J'\text{-}1}(\mathbf{r})^* y \phi^{a_i}_{21J\text{-}1}(\mathbf{r}-\mathbf{R}) d^3r \\
&\quad = 0. \qquad (5.128)
\end{aligned}$$

Similarly, the second and third terms of Eq.(5.119) are given by

$$\int \phi^{a_j}_{n'l'J'M'\mp\frac{1}{2}}(\mathbf{r})^* y V_{atom}(\mathbf{r}) \phi^{a_i}_{nlJM\pm\frac{1}{2}}(\mathbf{r}-\mathbf{R}) d^3r \;=\; \frac{m}{i\hbar}\frac{ze^2}{4\pi\epsilon_0 R} R_y \, s^{a_j,a_i}_{n'l'J'M'\mp\frac{1}{2},nlJM\pm\frac{1}{2}}(\mathbf{R}) \qquad (5.129)$$

and

$$\begin{aligned}
&\int \phi^{a_j}_{n'l'J'M'\mp\frac{1}{2}}(\mathbf{r})^* y V_{atom}(\mathbf{r}-\mathbf{R}) \phi^{a_i}_{nlJM\pm\frac{1}{2}}(\mathbf{r}-\mathbf{R}) d^3r \\
&\quad = -\frac{m}{i\hbar}\frac{ze^2}{4\pi\epsilon_0 R} R_y \, s^{a_j,a_i}_{n'l'J'M'\mp\frac{1}{2},nlJM\pm\frac{1}{2}}(\mathbf{R}) + \frac{m}{i\hbar} R_y \, t^{a_j,a_i}_{n'l'J'M'\mp\frac{1}{2},nlJM\pm\frac{1}{2}}(\mathbf{R}). \qquad (5.130)
\end{aligned}$$

Hence, from Eqs. (5.129) and (5.130), the momentum matrix of Eq.(5.119) can be written as

$$\begin{aligned}
&\int \phi^{a_j}_{n'l'J'M'\mp\frac{1}{2}}(\mathbf{r})^* p_y \phi^{a_i}_{nlJM\pm\frac{1}{2}}(\mathbf{r}-\mathbf{R}) d^3r \\
&\quad = \frac{m}{i\hbar}(\varepsilon_{nl} - \varepsilon_{n'l'}) \int \phi^{a_j}_{n'l'J'M'\mp\frac{1}{2}}(\mathbf{r})^* y \phi^{a_i}_{nlJM\pm\frac{1}{2}}(\mathbf{r}-\mathbf{R}) d^3r \\
&\qquad + \frac{m}{i\hbar} R_y \left\{ 2\frac{ze^2}{4\pi\epsilon_0 \mathbf{R}} \, s^{a_j,a_i}_{n'l'J'M'\mp\frac{1}{2},nlJM\pm\frac{1}{2}}(\mathbf{R}) - t^{a_j,a_i}_{n'l'J'M'\mp\frac{1}{2},nlJM\pm\frac{1}{2}}(\mathbf{R}) \right\}. \qquad (5.131)
\end{aligned}$$

From Eqs.(5.118 and 5.131), we have momentum matrices in each terms from Eq.(5.55) as

$$\begin{aligned}
&\int \phi^{a_j}_{n'l'J'M'\mp\frac{1}{2}}(\mathbf{r})^* \{\mp i p_x - p_y\} \phi^{a_i}_{nlJM\pm\frac{1}{2}}(\mathbf{r}-\mathbf{R}) d^3r \\
&\quad = \frac{m}{i\hbar}(\varepsilon_{nl} - \varepsilon_{n'l'}) \int \phi^{a_j}_{n'l'J'M'\mp\frac{1}{2}}(\mathbf{r})^* (\mp i x - y) \phi^{a_i}_{nlJM\pm\frac{1}{2}}(\mathbf{r}-\mathbf{R}) d^3r \\
&\qquad + \frac{m}{i\hbar}(\mp i R_x - R_y) \left\{ 2\frac{ze^2}{4\pi\epsilon_0 \mathbf{R}} \, s^{a_j,a_i}_{n'l'J'M'\mp\frac{1}{2},nlJM\pm\frac{1}{2}}(\mathbf{R}) - t^{a_j,a_i}_{n'l'J'M'\mp\frac{1}{2},nlJM\pm\frac{1}{2}}(\mathbf{R}) \right\}. \qquad (5.132)
\end{aligned}$$

Finally, from Eqs.(5.48), (5.55), and (5.132), Rashba Hamiltonian matrix for $J' = l' + \frac{1}{2}$ and $J = l + \frac{1}{2}$ is given by

$$\begin{aligned}
&\mathcal{H}^{asymm}_{\mathbf{R_m}j\eta,\mathbf{R_n}i\xi} \\
&\quad\approx e^{-i\frac{eB}{2\hbar}(R_{lx}+d_{ix}-d_{jx})(R_{ny}+d_{iy}+R_{my}+d_{jy})|\tilde{\alpha}_z|}\left(\tfrac{m}{i\hbar}\right) \\
&\quad\times\Bigg[\sqrt{\frac{J'+M'}{2J'}}\sqrt{\frac{J-M}{2J}}\Big\{(\varepsilon_{nl}-\varepsilon_{n'l'})\int\phi^{a_j}_{n'l'J'M'-\frac{1}{2}}(\mathbf{r})^*\{-ix-y\}\phi^{a_i}_{nlJM+\frac{1}{2}}(\mathbf{r}-\mathbf{R})d^3r \\
&\qquad\qquad+(-iR_x-R_y)\left(\frac{ze^2}{2\pi\epsilon_0\mathbf{R}}\,s^{a_j,a_i}_{n'l'J'M'-\frac{1}{2},nlJM+\frac{1}{2}}(\mathbf{R})-t^{a_j,a_i}_{n'l'J'M'-\frac{1}{2},nlJM+\frac{1}{2}}(\mathbf{R})\right)\Big\} \\
&\qquad+\sqrt{\frac{J+M}{2J}}\sqrt{\frac{J'-M'}{2J'}}\Big\{(\varepsilon_{nl}-\varepsilon_{n'l'})\int\phi^{a_j}_{n'l'J'M'+\frac{1}{2}}(\mathbf{r})^*\{ix-y\}\phi^{a_i}_{nlJM-\frac{1}{2}}(\mathbf{r}-\mathbf{R})d^3r \\
&\qquad\qquad+(+iR_x-R_y)\left(\frac{ze^2}{2\pi\epsilon_0\mathbf{R}}\,s^{a_j,a_i}_{n'l'J'M'+\frac{1}{2},nlJM-\frac{1}{2}}(\mathbf{R})-t^{a_j,a_i}_{n'l'J'M'+\frac{1}{2},nlJM-\frac{1}{2}}(\mathbf{R})\right)\Big\}\Bigg].
\end{aligned} \tag{5.133}$$

Let $\mathbf{T}_{W}(\mathbf{d_j})$ is the vectors connecting a_j atom to a_i atom which is independent of $\mathbf{R_m}$ but depends on $\mathbf{d_j}$. $\{W = 1, 2, 3...\}$. Then, Eq.(5.133) becomes

$$\begin{aligned}
&\mathcal{H}^{asymm}_{\mathbf{R_m}j\eta,\mathbf{R_n}i\xi} \\
&\quad\approx e^{-i\frac{eB}{2\hbar}\mathbf{T}_{Wx}\left[\mathbf{T}_{Wy}(\mathbf{d_j})+2R_{my}+2d_{jy}\right]}\left(\tfrac{m}{i\hbar}|\tilde{\alpha}_z|\right) \\
&\quad\times\Bigg[\sqrt{\frac{J'+M'}{2J'}}\sqrt{\frac{J-M}{2J}}\Big\{(\varepsilon_{nl}-\varepsilon_{n'l'})\int\phi^{a_j}_{n'l'J'M'-\frac{1}{2}}(\mathbf{r})^*\{-ix-y\}\phi^{a_i}_{nlJM+\frac{1}{2}}(\mathbf{r}-\mathbf{R})d^3r \\
&\qquad\qquad-(iR_x+R_y)\left(\frac{ze^2}{2\pi\epsilon_0\mathbf{R}}\,s^{a_j,a_i}_{n'l'J'M'-\frac{1}{2},nlJM+\frac{1}{2}}(\mathbf{R})-t^{a_j,a_i}_{n'l'J'M'-\frac{1}{2},nlJM+\frac{1}{2}}(\mathbf{R})\right)\Big\} \\
&\qquad+\sqrt{\frac{J+M}{2J}}\sqrt{\frac{J'-M'}{2J'}}\Big\{(\varepsilon_{nl}-\varepsilon_{n'l'})\int\phi^{a_j}_{n'l'J'M'+\frac{1}{2}}(\mathbf{r})^*\{ix-y\}\phi^{a_i}_{nlJM-\frac{1}{2}}(\mathbf{r}-\mathbf{R})d^3r \\
&\qquad\qquad+(iR_x-R_y)\left(\frac{ze^2}{2\pi\epsilon_0\mathbf{R}}\,s^{a_j,a_i}_{n'l'J'M'+\frac{1}{2},nlJM-\frac{1}{2}}(\mathbf{R})-t^{a_j,a_i}_{n'l'J'M'+\frac{1}{2},nlJM-\frac{1}{2}}(\mathbf{R})\right)\Big\}\Bigg].
\end{aligned} \tag{5.134}$$

Hence, Rashba Hamiltonian matrix for remaining three cases are as follows:
(b) For $J' = l' + \frac{1}{2}$ and $J = l - \frac{1}{2}$

$$\begin{aligned}
&\mathcal{H}^{asymm}_{\mathbf{R_m}j\eta,\mathbf{R_n}i\xi} \\
&\quad\approx e^{-i\frac{eB}{2\hbar}\mathbf{T}_{Wx}\left[\mathbf{T}_{Wy}(\mathbf{d_j})+2R_{my}+2d_{jy}\right]}\left(\tfrac{m}{i\hbar}|\tilde{\alpha}_z|\right) \\
&\quad\times\Bigg[\sqrt{\frac{J'+M'}{2J'}}\sqrt{\frac{J+1+M}{2(J+1)}}\Big\{(\varepsilon_{nl}-\varepsilon_{n'l'})\int\phi^{a_j}_{n'l'J'M'-\frac{1}{2}}(\mathbf{r})^*\{-ix-y\}\phi^{a_i}_{nlJM+\frac{1}{2}}(\mathbf{r}-\mathbf{R})d^3r \\
&\qquad\qquad-(iR_x+R_y)\left(\frac{ze^2}{2\pi\epsilon_0\mathbf{R}}\,s^{a_j,a_i}_{n'l'J'M'-\frac{1}{2},nlJM+\frac{1}{2}}(\mathbf{R})-t^{a_j,a_i}_{n'l'J'M'-\frac{1}{2},nlJM+\frac{1}{2}}(\mathbf{R})\right)\Big\} \\
&\qquad-\sqrt{\frac{J+1-M}{2(J+1)}}\sqrt{\frac{J'-M'}{2J'}}\Big\{(\varepsilon_{nl}-\varepsilon_{n'l'})\int\phi^{a_j}_{n'l'J'M'+\frac{1}{2}}(\mathbf{r})^*\{ix-y\}\phi^{a_i}_{nlJM-\frac{1}{2}}(\mathbf{r}-\mathbf{R})d^3r \\
&\qquad\qquad+(iR_x-R_y)\left(\frac{ze^2}{2\pi\epsilon_0\mathbf{R}}\,s^{a_j,a_i}_{n'l'J'M'+\frac{1}{2},nlJM-\frac{1}{2}}(\mathbf{R})-t^{a_j,a_i}_{n'l'J'M'+\frac{1}{2},nlJM-\frac{1}{2}}(\mathbf{R})\right)\Big\}\Bigg].
\end{aligned} \tag{5.135}$$

(c) For $J' = l' - \frac{1}{2}$ and $J = l + \frac{1}{2}$

$$\begin{aligned}
&\mathcal{H}^{asymm}_{\mathbf{R_m}j\eta,\mathbf{R_n}i\xi} \\
&\approx e^{-i\frac{eB}{2\hbar}\mathbf{T}_{Wx}\left[\mathbf{T}_{Wy}(\mathbf{d_j})+2R_{my}+2d_{jy}\right]}\left(\frac{m}{i\hbar}|\tilde{\alpha}_z|\right) \\
&\times\Bigg[-\sqrt{\frac{J'+1-M'}{2(J'+1)}}\sqrt{\frac{J-M}{2(J)}}\Bigg\{(\varepsilon_{nl}-\varepsilon_{n'l'})\int\phi^{a_j}_{n'l'J'M'-\frac{1}{2}}(\mathbf{r})^*\{-ix-y\}\phi^{a_i}_{nlJM+\frac{1}{2}}(\mathbf{r}-\mathbf{R})d^3r \\
&\qquad -(iR_x+R_y)\left(\frac{ze^2}{2\pi\epsilon_0\mathbf{R}}\,s^{a_j,a_i}_{n'l'J'M'-\frac{1}{2},nlJM+\frac{1}{2}}(\mathbf{R})-t^{a_j,a_i}_{n'l'J'M'-\frac{1}{2},nlJM+\frac{1}{2}}(\mathbf{R})\right)\Bigg\} \\
&\quad+\sqrt{\frac{J'+1+M'}{2(J'+1)}}\sqrt{\frac{J+M}{2J}}\Bigg\{(\varepsilon_{nl}-\varepsilon_{n'l'})\int\phi^{a_j}_{n'l'J'M'+\frac{1}{2}}(\mathbf{r})^*\{ix-y\}\phi^{a_i}_{nlJM-\frac{1}{2}}(\mathbf{r}-\mathbf{R})d^3r \\
&\qquad +(iR_x-R_y)\left(\frac{ze^2}{2\pi\epsilon_0\mathbf{R}}\,s^{a_j,a_i}_{n'l'J'M'+\frac{1}{2},nlJM-\frac{1}{2}}(\mathbf{R})-t^{a_j,a_i}_{n'l'J'M'+\frac{1}{2},nlJM-\frac{1}{2}}(\mathbf{R})\right)\Bigg\}\Bigg].
\end{aligned} \tag{5.136}$$

(d) For $J' = l' - \frac{1}{2}$ and $J = l - \frac{1}{2}$

$$\begin{aligned}
&\mathcal{H}^{asymm}_{\mathbf{R_m}j\eta,\mathbf{R_n}i\xi} \\
&\approx e^{-i\frac{eB}{2\hbar}\mathbf{T}_{Wx}\left[\mathbf{T}_{Wy}(\mathbf{d_j})+2R_{my}+2d_{jy}\right]}\left(\frac{m}{i\hbar}|\tilde{\alpha}_z|\right) \\
&\times\Bigg[-\sqrt{\frac{J'+1-M'}{2(J'+1)}}\sqrt{\frac{J+1+M}{2(J+1)}}\Bigg\{(\varepsilon_{nl}-\varepsilon_{n'l'})\int\phi^{a_j}_{n'l'J'M'-\frac{1}{2}}(\mathbf{r})^*\{-ix-y\}\phi^{a_i}_{nlJM+\frac{1}{2}}(\mathbf{r}-\mathbf{R})d^3r \\
&\qquad -(iR_x+R_y)\left(\frac{ze^2}{2\pi\epsilon_0\mathbf{R}}\,s^{a_j,a_i}_{n'l'M'-\frac{1}{2},nlJM+\frac{1}{2}}(\mathbf{R})-t^{a_j,a_i}_{n'l'J'M'-\frac{1}{2},nlJM+\frac{1}{2}}(\mathbf{R})\right)\Bigg\} \\
&\quad-\sqrt{\frac{J'+1+M'}{2(J'+1)}}\sqrt{\frac{J+1-M}{2(J+1)}}\Bigg\{(\varepsilon_{nl}-\varepsilon_{n'l'})\int\phi^{a_j}_{n'l'J'M'+\frac{1}{2}}(\mathbf{r})^*\{ix-y\}\phi^{a_i}_{nlJM-\frac{1}{2}}(\mathbf{r}-\mathbf{R})d^3r \\
&\qquad +(iR_x-R_y)\left(\frac{ze^2}{2\pi\epsilon_0\mathbf{R}}\,s^{a_j,a_i}_{n'l'J'M'+\frac{1}{2},nlJM-\frac{1}{2}}(\mathbf{R})-t^{a_j,a_i}_{n'l'J'M'+\frac{1}{2},nlJM-\frac{1}{2}}(\mathbf{R})\right)\Bigg\}\Bigg].
\end{aligned} \tag{5.137}$$

It is evident that Eqs.(5.134), (5.135), (5.136), and (5.137) are the matrix elements of Rashba Hamiltonian matrix. $\mathcal{H}^{asymm}_{\mathbf{R_m}j\eta,\mathbf{R_n}i\xi}$ Hence, according to Eq.(5.5), these matrix elements of Rashba Hamiltonian matrix $\mathcal{H}^{asymm}_{\mathbf{R_m}j\eta,\mathbf{R_n}i\xi}$ for respective cases contribute to the diagonal block matrix of the total Hamiltonian matrix of the system. Hence, with the reference of Eq.(2.43), the resultant simultaneous equation including Rashba Hamiltonian matrix is given by

$$\begin{aligned}
&(\varepsilon^{a_j,\mathbf{0}}_{\eta}+\Delta\varepsilon^{a_j,\mathbf{d_j}}_{\eta})C^{\eta}_{\mathbf{k}}(\mathbf{R_m}+\mathbf{d_j})+\sum_W\sum_\eta e^{-i\frac{eB}{\hbar}\mathbf{T}_{Wx}(\mathbf{d_j})(R_{my}+d_{jy})} \\
&\quad\times\tilde{T}^{a_j,a_i}_{\eta,\xi}\{\mathbf{T}_W(d_j)\}C^{\xi}_{\mathbf{k}}\{\mathbf{T}_W(d_j)+\mathbf{R_m}+\mathbf{d_j}\}+\mathcal{H}^{asymm}_{\mathbf{R_m}j\eta,\mathbf{R_n}i\xi}C^{\xi}_{\mathbf{k}}\{\mathbf{T}_W(d_j)+\mathbf{R_m}+\mathbf{d_j}\} \\
&\qquad=E^R_{\mathbf{k}}\left[C^{\eta}_{\mathbf{k}}(\mathbf{R_m}+\mathbf{d_j})+\sum_W\sum_\eta e^{-i\frac{eB}{\hbar}\mathbf{T}_{Wx}(\mathbf{d_j})(R_{my}+d_{jy})}S^{a_j,a_i}_{\eta,\xi}\{\mathbf{T}_W(d_j)\}\right] \\
&\qquad\qquad\times C^{\xi}_{\mathbf{k}}\{\mathbf{T}_W(d_j)+\mathbf{R_m}+\mathbf{d_j}\}.
\end{aligned} \tag{5.138}$$

In order to get the complete solution of this resultant simultaneous equation, we need to estimate $(\varepsilon_{\eta}^{a_j,\mathbf{0}}+\Delta\varepsilon_{\eta}^{a_j,\mathbf{d_j}})$, magnetic hopping integral $\tilde{T}_{\eta,\xi}^{a_j,a_i}\{\mathbf{T}_W(d_j)\}$ and magnetic overlap integral $S_{\eta,\xi}^{a_j,a_i}\{\mathbf{T}_W(d_j)\}$. The term $(\varepsilon_{\eta}^{a_j,\mathbf{0}}+\Delta\varepsilon_{\eta}^{a_j,\mathbf{d_j}})$ can be estimate either by using perturbative MFRTB method [38] or nonperturbative MFRTB method [43]. The magnetic hopping integral $\tilde{T}_{\eta,\xi}^{a_j,a_i}\{\mathbf{T}_W(d_j)\}$ and magnetic overlap integral $S_{\eta,\xi}^{a_j,a_i}\{\mathbf{T}_W(d_j)\}$ which can be expressed as linear combination of hopping and overlap integrals in the absence of magnetic field are obtained from Table II of Ref. [43]. The non-relativistic hopping integral $t_{n'l'J'M'+\frac{1}{2},nlJM-\frac{1}{2}}^{a_j,a_i}(\mathbf{R})$ and non-relativistic overlap integral $s_{n'l'J'M'+\frac{1}{2},nlJM-\frac{1}{2}}^{a_j,a_i}(\mathbf{R})$ involved in Rashba Hamiltonian can be expressed in terms of several TB parameters and can be obtained by using "Slater-Koster table" [101].

Chapter 6

Conclusion

The nonperturbative MFRTB method is applied to graphene immersed in a magnetic field in order to elucidate the mechanism of the reduced g-factor in graphene that has recently been observed in the ESR experiments [28, 29]. It is found that there is no dependence of the bulk SO interaction on the external magnetic field. This implies that the bulk SO interaction does not effect on the effective g-factor. It is also shown that the magnetic field induced by strong orbital diamagnetism is one of the reasons for reduction of the effective g-factor. Specifically, the estimated g-factor of graphene is 1.986 when the external magnetic field is 1 T, which is a reduction of about 0.7 percent. This, however, does not fully account for the magnitude of the reduction in the g-factor of graphene observed in previous experiments [28, 29].

In the calculations by the nonperturbative MFRTB method, the existence of the substrate, which causes the Rashba effect due to the breaking of the space inversion symmetry, is ignored. So, we carried out our calculation on g-factor using empty lattice model in order to investigate the effect of Rashba effect on the reduction in effective g-factor. We derive an expression for the HOS-LUS gap and then energy splitting to evaluate the effective g-factor. The calculation from our model system shows that the reduction in effective g-factor is 3.6 percent. This means that the Rashba effect is the primary cause for the reduction in the g-factor. Due to Rashba effect, the spin magnetic moment tilts towards the in-plane direction of the graphene sheet. As a result, the external magnetic field appreciably decreases the energy splitting. This leads to a reduction in the observed g-factor in the graphene sheet. Furthermore, we have reformulated the MFRTB method so as to incorporate the Rashba effect. We just accomplished the formulation part which is presented in Chap. 5. Numerical calculations are our future work. It is expected that we may estimate the reduction in g-factor of graphene more correctly. This could be a gateway to enhance the calculation scheme to re-evaluate the diamagnetism of graphene and to get near numerical agreement with the experimentally recorded value of the g-factor of graphene.

We shall give a brief comment on the Rashba effect in graphene. It is well-known that the potential gradient of the nucleus of a heavy atom enhances the Rashba effect. Therefore, the Rashba effect in the materials composed by light atoms (such as carbon) is expected to be weak [95]. Despite of small effect, the experimental results of the g-factor is well explained by Rashba effect. Therefore, we may say that ESR could be a worthwhile method for the estimation of small Rashba effect to measure the g-factor.

In Chap. 4, it is assumed that the surface potential on the substrate side (V_{sub}) is negligibly small compared to potential on the vacuum side (V_{vac}). Hence, even though the calculation from our scheme is in agreement with the experimental ones, there exist some room to amend the quantitative errors in obtaining effective g-factor. Particularly, for the overestimation of the reduction of the g-factor that is by 0.5 percent from our scheme in comparison with experimental value [28, 29]. It could be the future work to include the effect of V_{sub} for the improvement of Rashba effect. Apart from Rashba effect, there might be other effects which are likely to alter the effective g-factor.

Next we shall give a brief comment on the effect of electron-electron interaction on the effective g-factor. While discussing effect of diamagnetism in effective g-factor of graphene by means of nonperturbative method and empty lattice model, effects of the electron-electron interaction is not considered. It is reported that the cyclotron resonance frequency is independent of the interaction for two-dimensional electron gas [102]. Therefore, it is appropriate to compare the calculation results from diamagnetism of graphene with experimental results [28, 29]. But, in the experiments of the Shubnikov-de Haas (SdH) oscillations, the g-factor is affected by the electron-electron interaction [103–105]. So, we can not neglect electron-electron interaction in SdH oscillations experiments while discussing effective g-factor. The density functional theory [58, 64] and its extensions [88–90, 106–113] also incorporate effects of the electron-electron interaction.

Finally, we shall give a comment on the significance of this work. Since the g-factor determines the spin relaxation time [28, 29], it has been a major topic of interest in the field of spintronics. As a result, our findings can be used as a guideline when designing spintronics devices. In addition, the Rashba effect may produce g-factor reduction in various atomic layer materials. For instance, the opening of the energy band gap in bilayer graphene makes it appealing for application areas [114]. The work function of bilayer graphene, according to the experiment [115], is roughly 4.4-4.5 [eV], which is somewhat higher than that of monolayer graphene. Because the difference is minimal, the Rashba effect induced by the surface potential in bilayer graphene may be similar to that in monolayer graphene. Therefore, the results of this research can be used as a general reference when looking into the g-factor of atomic layer materials.

Appendix A

Estimation of $T^{a_j,a_i}_{\eta,\xi}(\mathbf{R_l}+\mathbf{d_i}-\mathbf{d_j})$ and $S^{a_j,a_i}_{\eta,\xi}(\mathbf{R_l}+\mathbf{d_i}-\mathbf{d_j})$

From Eqs.(2.38) and (2.39), we have

$$T^{a_j,a_i}_{\eta,\xi}(\mathbf{R_l}+\mathbf{d_i}-\mathbf{d_j}) = \int \psi^{a_j,0}_{\eta}(\mathbf{r})^{\dagger}\left(\frac{V_{a_j}(\mathbf{r})+V_{a_i}(\mathbf{r}-\mathbf{R_l}-\mathbf{d_i}+\mathbf{d_j})}{2}\right)\psi^{a_i,\mathbf{R_l}+\mathbf{d_i}-\mathbf{d_j}}_{\xi}(\mathbf{r})d^3r, \tag{A.1}$$

$$S^{a_j,a_i}_{\eta,\xi}(\mathbf{R_l}+\mathbf{d_i}-\mathbf{d_j}) = \int \psi^{a_j,0}_{\eta}(\mathbf{r})^{\dagger}\psi^{a_i,\mathbf{R_l}+\mathbf{d_i}-\mathbf{d_j}}_{\xi}(\mathbf{r})d^3r. \tag{A.2}$$

Since, $\psi^{a_j,0}_{\eta}(\mathbf{r})$ and $\psi^{a_i,\mathbf{R_l}+\mathbf{d_i}-\mathbf{d_j}}_{\xi}(\mathbf{r})$ are wave functions of Landau gauge, they can be estimated using the symmetric gauge through following transformations:

$$\psi^{a_j,0}_{\eta}(\mathbf{r}) = e^{-i\frac{eB}{2\hbar}xy}\psi^{a_j,0}_{\eta}(\mathbf{r})_{sym}, \tag{A.3}$$

$$\psi^{a_j,\mathbf{R_l}+\mathbf{d_i}-\mathbf{d_j}}_{\xi}(\mathbf{r}) = e^{-i\frac{eB}{2\hbar}xy}\psi^{a_j,\mathbf{R_l}+\mathbf{d_i}-\mathbf{d_j}}_{\xi}(\mathbf{r})_{sym}, \tag{A.4}$$

where $\frac{Bxy}{2}$ denotes the gauge transformation from symmetric gauge to Landau gauge.

Since, $\psi^{a_j,0}_{\eta}(\mathbf{r})_{sym}$ is localized around origin, the phase factor $e^{-i\frac{eB}{2\hbar}xy}$ of Eq.(A.3) would be approximated to unity, i.e.,

$$\psi^{a_j,0}_{\eta}(\mathbf{r}) = \psi^{a_j,0}_{\eta}(\mathbf{r})_{sym}. \tag{A.5}$$

In the vicinity of origin, the relativistic atomic orbital, $\psi^{a_j,0}_{\eta}(\mathbf{r})_{sym}$ in the uniform magnetic field can be approximated as the unperturbed wave function $\phi^{a_j}_{\eta}(\mathbf{r})$ [38]. Thus,

$$\psi^{a_j,0}_{\eta}(\mathbf{r})_{sym} = \phi^{a_j}_{\eta}(\mathbf{r}). \tag{A.6}$$

This implies that,

$$\psi^{a_j,0}_{\eta}(\mathbf{r}) = \psi^{a_j,0}_{\eta}(\mathbf{r})_{sym} = \phi^{a_j}_{\eta}(\mathbf{r}). \tag{A.7}$$

Similar to Eq.(2.31), symmetric gauge $\psi^{a_j,\mathbf{R_l}+\mathbf{d_i}-\mathbf{d_j}}_{\eta}(\mathbf{r})_{sym}$ is related with $\psi^{a_j,0}_{\eta}(\mathbf{R_l}+\mathbf{d_i}-\mathbf{d_j})_{sym}$ by

$$\psi^{a_i,0}_{\xi}(\mathbf{r}-\mathbf{R_l}-\mathbf{d_i}+\mathbf{d_j})_{sym} = e^{-\frac{ieB}{2\hbar}\{(R_{ly}+d_{iy}-d_{jy})x-(R_{lx}+d_{ix}-d_{jx})y\}}\psi^{a_i,\mathbf{R_l}-\mathbf{d_i}+\mathbf{d_j}}_{\xi}(\mathbf{r})_{sym}, \tag{A.8}$$

where, we have used the relation

$$\chi(\mathbf{r}, \mathbf{R_l} - \mathbf{d_i} + \mathbf{d_j}) = \frac{B}{2} \left\{ (R_{ly} + d_{iy} - d_{jy})x - (R_{lx} + d_{ix} - d_{jx})y \right\}. \tag{A.9}$$

From Eq.(A.4) and (A.8), we have

$$\psi_\xi^{a_i, \mathbf{R_l}+\mathbf{d_i}-\mathbf{d_j}}(\mathbf{r}) = e^{-i\frac{eB}{2\hbar}\left\{(R_{lx}+d_{ix}-d_{jx})y-(R_{ly}+d_{iy}-d_{jy})x+xy\right\}} \psi_\xi^{a_i,0}(\mathbf{r} - \mathbf{R_l} - \mathbf{d_i} + \mathbf{d_j})_{sym}. \tag{A.10}$$

The phase factor in Eq.(A.10) can be approximated by the phase factor at $\mathbf{r} = \mathbf{R_l} + \mathbf{d_i} - \mathbf{d_j}$ because wavefuction $\psi_\xi^{a_i,0}(\mathbf{r} - \mathbf{R_l} - \mathbf{d_i} + \mathbf{d_j})_{sym}$ is localized around $\mathbf{r} = \mathbf{R_l} + \mathbf{d_i} - \mathbf{d_j}$. Then, Eq.(A.10) is given by

$$\psi_\xi^{a_i, \mathbf{R_l}+\mathbf{d_i}-\mathbf{d_j}}(\mathbf{r}) = e^{-i\frac{eB}{2\hbar}(R_{lx}+d_{ix}-d_{jx})(R_{ly}+d_{iy}-d_{jy})} \psi_\xi^{a_i,0}(\mathbf{r} - \mathbf{R_l} - \mathbf{d_i} + \mathbf{d_j})_{sym}. \tag{A.11}$$

Using Eq.(A.7), we rewrite Eq.(A.10) either as

$$\psi_\xi^{a_i, \mathbf{R_l}+\mathbf{d_i}-\mathbf{d_j}}(\mathbf{r}) = e^{-i\frac{eB}{2\hbar}(R_{lx}+d_{ix}-d_{jx})(R_{ly}+d_{iy}-d_{jy})} \psi_\xi^{a_i,0}(\mathbf{r} - \mathbf{R_l} - \mathbf{d_i} + \mathbf{d_j}) \tag{A.12}$$

or as

$$\psi_\xi^{a_i, \mathbf{R_l}+\mathbf{d_i}-\mathbf{d_j}}(\mathbf{r}) = e^{-i\frac{eB}{2\hbar}(R_{lx}+d_{ix}-d_{jx})(R_{ly}+d_{iy}-d_{jy})} \phi_\xi^{a_i}(\mathbf{r} - \mathbf{R_l} - \mathbf{d_i} + \mathbf{d_j}). \tag{A.13}$$

From Eqs.(A.7) and (A.13), magnetic hopping and overlap integrals given by Eqs.(A.1) and (A.2) are expressed as

$$T^{a_j,a_i}_{n'l'J'M',nlJM}(\mathbf{R}) = e^{-i\frac{eB}{2\hbar}R_X R_Y} \int \psi_\eta^{a_j,0}(\mathbf{r})^\dagger \left(\frac{V_{a_j}(\mathbf{r}) + V_{a_i}(\mathbf{r} - \mathbf{R})}{2} \right) \psi_\xi^{a_i,0}(\mathbf{r} - \mathbf{R}) d^3r, \tag{A.14}$$

$$S^{a_j,a_i}_{n'l'J'M',nlJM}(\mathbf{R}) = e^{-i\frac{eB}{2\hbar}R_X R_Y} \int \psi_\eta^{a_j,0}(\mathbf{r})^\dagger \psi_\xi^{a_i,0}(\mathbf{r} - \mathbf{R})(\mathbf{r}) d^3r, \tag{A.15}$$

where $R_X = R_{lx} + d_{ix} - d_{jx}$ and $R_Y = R_{ly} + d_{iy} - d_{jy}$ are x and y-components of $\mathbf{R} = \mathbf{R_l} + \mathbf{d_i} - \mathbf{d_j}$, respectively.

Now we take Eq.(2.93) and rewrite the expression of wave function in an uniform magnetic field which is given by

$$\psi_\xi^{a_i,0}(\mathbf{r}) = \begin{cases} \dfrac{\phi^{a_i}_{nlJM}(\mathbf{r}) + \eta^{a_i}_{nlJM}\phi^{a_i}_{nlJ-1M}(\mathbf{r})}{\sqrt{1 + (\eta^{a_i}_{nlJM})^2}} & \text{for } (n, l, J, M), M \neq J \\ \dfrac{\phi^{a_i}_{nlJ-1M}(\mathbf{r}) + \eta^{a_i}_{nlJ-1M}\phi^{a_i}_{nlJM}(\mathbf{r})}{\sqrt{1 + (\eta^{a_i}_{nlJ-1M})^2}} & \text{for } (n, l, J-1, M). \end{cases} \tag{A.16}$$

Now, let us calculate the magnetic hopping integral $T^{a_j,a_i}_{n'l'J'M',nlJM}(\mathbf{R})$ taking the following cases into consideration:

(i) For the combination of unperturbed atomic states (n', l', J', M') and (n, l, J, M) with $M \neq \pm J$.

From, Eqs.(A.14) and (A.16), we have

$$
\begin{aligned}
&T^{a_j,a_i}_{n'l'J'M',nlJM}(\mathbf{R}) \\
&= e^{-i\frac{eB}{2\hbar}R_X R_Y} \int \left\{ \frac{\phi^{a_j}_{n'l'J'M'}(\mathbf{r}) + \eta^{a_j}_{n'l'J'M'}\phi^{a_j}_{n'l'J'-1M'}(\mathbf{r})}{\sqrt{1+(\eta^{a_j}_{n'l'J'M'})^2}} \right\}^{\dagger} \left(\frac{V_{a_j}(\mathbf{r}) + V_{a_i}(\mathbf{r}-\mathbf{R})}{2} \right) \\
&\qquad \times \left\{ \frac{\phi^{a_i}_{nlJM}(\mathbf{r}-\mathbf{R}) + \eta^{a_i}_{nlJM}\phi^{a_i}_{nlJ-1M}(\mathbf{r}-\mathbf{R})}{\sqrt{1+(\eta^{a_i}_{nlJM})^2}} \right\} d^3r \\
&= \frac{e^{-i\frac{eB}{2\hbar}R_X R_Y}}{\sqrt{(1+\eta^{{a_j}^2}_{n'l'J'M'})(1+\eta^{{a_i}^2}_{nlJM})}} \int \left\{ \phi^{a_j}_{n'l'J'M'}(\mathbf{r}) + \eta^{a_j}_{n'l'J'M'}\phi^{a_j}_{n'l'J'-1M'}(\mathbf{r}) \right\}^{\dagger} \\
&\qquad \times \left(\frac{V_{a_j}(\mathbf{r}) + V_{a_i}(\mathbf{r}-\mathbf{R})}{2} \right) \left\{ \phi^{a_i}_{nlJM}(\mathbf{r}-\mathbf{R}) + \eta^{a_i}_{nlJM}\phi^{a_i}_{nlJ-1M}(\mathbf{r}-\mathbf{R}) \right\} \\
&= \frac{e^{-i\frac{eB}{2\hbar}R_X R_Y}}{\sqrt{(1+\eta^{{a_j}^2}_{n'l'J'M'})(1+\eta^{{a_i}^2}_{nlJM})}} \\
&\qquad \times \int \left\{ \phi^{a_j}_{n'l'J'M'}(\mathbf{r})^{\dagger} \left(\frac{V_{a_j}(\mathbf{r}) + V_{a_i}(\mathbf{r}-\mathbf{R})}{2} \right) \phi^{a_i}_{nlJM}(\mathbf{r}-\mathbf{R}) \right. \\
&\qquad + \eta^{a_i}_{nlJM} \left[\phi^{a_j}_{n'l'J'M'}(\mathbf{r})^{\dagger} \left(\frac{V_{a_j}(\mathbf{r}) + V_{a_i}(\mathbf{r}-\mathbf{R})}{2} \right) \phi^{a_i}_{nlJ-1M}(\mathbf{r}-\mathbf{R}) \right] \\
&\qquad + \eta^{a_j}_{n'l'J'M'} \left[\phi^{a_j}_{n'l'J'-1M'}(\mathbf{r})^{\dagger} \left(\frac{V_{a_j}(\mathbf{r}) + V_{a_i}(\mathbf{r}-\mathbf{R})}{2} \right) \phi^{a_i}_{nlJM}(\mathbf{r}-\mathbf{R}) \right] \\
&\qquad \left. + \eta^{a_j}_{n'l'J'M'}\eta^{a_i}_{nlJM} \left[\phi^{a_j}_{n'l'J'-1M'}(\mathbf{r})^{\dagger} \left(\frac{V_{a_j}(\mathbf{r}) + V_{a_i}(\mathbf{r}-\mathbf{R})}{2} \right) \phi^{a_i}_{nlJ-1M}(\mathbf{r}-\mathbf{R}) \right] \right\} d^3r \\
&= \frac{e^{-i\frac{eB}{2\hbar}R_X R_Y}}{\sqrt{(1+\eta^{{a_j}^2}_{n'l'J'M'})(1+\eta^{{a_i}^2}_{nlJM})}} \left\{ t^{a_j,a_i}_{n'l'J'M',nlJM}(\mathbf{R}) + \eta^{a_i}_{nlJM} t^{a_j,a_i}_{n'l'J'M',nlJ-1M}(\mathbf{R}) \right. \\
&\qquad \left. + \eta^{a_j}_{n'l'J'M'} t^{a_j,a_i}_{n'l'J'-1M',nlJM}(\mathbf{R}) + \eta^{a_j}_{n'l'J'M'}\eta^{a_i}_{nlJM} t^{a_j,a_i}_{n'l'J'-1M',nlJ-1M}(\mathbf{R}) \right\}. \quad \text{(A.17)}
\end{aligned}
$$

(ii) For the combination of unperturbed atomic states $(n', l', J'-1, M')$ and $(n, l, J-1, M)$ with $M \neq \pm J$.

From, Eqs.(A.14) and (A.16), we have

$$
\begin{aligned}
&T^{a_j,a_i}_{n'l'J'M',nlJM}(\mathbf{R}) \\
&= e^{-i\frac{eB}{2\hbar}R_X R_Y} \int \left\{ \frac{\phi^{a_j}_{n'l'J'-1M'}(\mathbf{r}) + \eta^{a_j}_{n'l'J'-1M'}\phi^{a_j}_{n'l'J'M'}(\mathbf{r})}{\sqrt{1+(\eta^{a_j}_{n'l'J'-1M'})^2}} \right\}^{\dagger} \left(\frac{V_{a_j}(\mathbf{r}) + V_{a_i}(\mathbf{r}-\mathbf{R})}{2} \right) \\
&\qquad \times \left\{ \frac{\phi^{a_i}_{nlJ-1M}(\mathbf{r}-\mathbf{R}) + \eta^{a_i}_{nlJ-1M}\phi^{a_i}_{nlJM}(\mathbf{r}-\mathbf{R})}{\sqrt{1+(\eta^{a_i}_{nlJ-1M})^2}} \right\} d^3r
\end{aligned}
$$

$$= \frac{e^{-i\frac{eB}{2\hbar}R_X R_Y}}{\sqrt{(1+{\eta^{a_j}_{n'l'J'-1M'}}^2)(1+{\eta^{a_i}_{nlJ-1M}}^2)}} \int \left\{\phi^{a_j}_{n'l'J'-1M'}(\mathbf{r}) + \eta^{a_j}_{n'l'J'-1M'}\phi^{a_j}_{n'l'J'M'}(\mathbf{r})\right\}^\dagger$$

$$\times \left(\frac{V_{a_j}(\mathbf{r}) + V_{a_i}(\mathbf{r}-\mathbf{R})}{2}\right) \left\{\phi^{a_i}_{nlJ-1M}(\mathbf{r}-\mathbf{R}) + \eta^{a_i}_{nlJ-1M}\phi^{a_i}_{nlJM}(\mathbf{r}-\mathbf{R})\right\}$$

$$= \frac{e^{-i\frac{eB}{2\hbar}R_X R_Y}}{\sqrt{(1+{\eta^{a_j}_{n'l'J'-1M'}}^2)(1+{\eta^{a_i}_{nlJ-1M}}^2)}}$$

$$\times \int \left\{ \phi^{a_j}_{n'l'J'-1M'}(\mathbf{r})^\dagger \left(\frac{V_{a_j}(\mathbf{r}) + V_{a_i}(\mathbf{r}-\mathbf{R})}{2}\right) \phi^{a_i}_{nlJ-1M}(\mathbf{r}-\mathbf{R}) \right.$$

$$+\eta^{a_i}_{nlJ-1M}\left[\phi^{a_j}_{n'l'J'-1M'}(\mathbf{r})^\dagger \left(\frac{V_{a_j}(\mathbf{r}) + V_{a_i}(\mathbf{r}-\mathbf{R})}{2}\right) \phi^{a_i}_{nlJM}(\mathbf{r}-\mathbf{R})\right]$$

$$+\eta^{a_j}_{n'l'J'-1M'}\left[\phi^{a_j}_{n'l'J'M'}(\mathbf{r})^\dagger \left(\frac{V_{a_j}(\mathbf{r}) + V_{a_i}(\mathbf{r}-\mathbf{R})}{2}\right) \phi^{a_i}_{nlJ-1M}(\mathbf{r}-\mathbf{R})\right]$$

$$\left. +\eta^{a_j}_{n'l'J'-1M'}\eta^{a_i}_{nlJ-1M}\left[\phi^{a_j}_{n'l'J'M'}(\mathbf{r})^\dagger \left(\frac{V_{a_j}(\mathbf{r}) + V_{a_i}(\mathbf{r}-\mathbf{R})}{2}\right) \phi^{a_i}_{nlJM}(\mathbf{r}-\mathbf{R})\right]\right\} d^3r$$

$$= \frac{e^{-i\frac{eB}{2\hbar}R_X R_Y}}{\sqrt{(1+{\eta^{a_j}_{n'l'J'-1M'}}^2)(1+{\eta^{a_i}_{nlJ-1M}}^2)}} \left\{ t^{a_j,a_i}_{n'l'J'-1M',nlJ-1M}(\mathbf{R}) \right.$$

$$+\eta^{a_i}_{nlJ-1M} t^{a_j,a_i}_{n'l'J'-1M',nlJM}(\mathbf{R}) + \eta^{a_j}_{n'l'J-1'M'} t^{a_j,a_i}_{n'l'J'M',nlJ-1M}(\mathbf{R})$$

$$\left. +\eta^{a_j}_{n'l'J'-1M'}\eta^{a_i}_{nlJ-1M} t^{a_j,a_i}_{n'l'J'M',nlJM}(\mathbf{R})\right\}. \quad \text{(A.18)}$$

(iii) For the combination of unperturbed atomic states (n', l', J', M') and $(n, l, J-1, M)$ with $M \neq \pm J$.

From, Eqs.(A.14) and (A.16), we have

$$T^{a_j,a_i}_{n'l'J'M',nlJM}(\mathbf{R})$$

$$= e^{-i\frac{eB}{2\hbar}R_X R_Y} \int \left\{ \frac{\phi^{a_j}_{n'l'J'M'}(\mathbf{r}) + \eta^{a_j}_{n'l'J'M'}\phi^{a_j}_{n'l'J'-1M'}(\mathbf{r})}{\sqrt{1+(\eta^{a_j}_{n'l'J'M'})^2}} \right\}^\dagger \left(\frac{V_{a_j}(\mathbf{r}) + V_{a_i}(\mathbf{r}-\mathbf{R})}{2}\right)$$

$$\times \left\{ \frac{\phi^{a_i}_{nlJ-1M}(\mathbf{r}-\mathbf{R}) + \eta^{a_i}_{nlJ-1M}\phi^{a_i}_{nlJM}(\mathbf{r}-\mathbf{R})}{\sqrt{1+(\eta^{a_i}_{nlJ-1M})^2}} \right\} d^3r$$

$$= \frac{e^{-i\frac{eB}{2\hbar}R_X R_Y}}{\sqrt{(1+{\eta^{a_j}_{n'l'J'M'}}^2)(1+{\eta^{a_i}_{nlJ-1M}}^2)}} \int \left\{\phi^{a_j}_{n'l'J'M'}(\mathbf{r}) + \eta^{a_j}_{n'l'J'M'}\phi^{a_j}_{n'l'J'-1M'}(\mathbf{r})\right\}^\dagger$$

$$\times \left(\frac{V_{a_j}(\mathbf{r}) + V_{a_i}(\mathbf{r}-\mathbf{R})}{2}\right) \left\{\phi^{a_i}_{nlJ-1M}(\mathbf{r}-\mathbf{R}) + \eta^{a_i}_{nlJ-1M}\phi^{a_i}_{nlJM}(\mathbf{r}-\mathbf{R})\right\} d^3r$$

$$
\begin{aligned}
&= \frac{e^{-i\frac{eB}{2\hbar}R_X R_Y}}{\sqrt{(1+\eta^{a_j\,2}_{n'l'J'M'})(1+\eta^{a_i\,2}_{nlJ-1M})}} \\
&\qquad \int \left\{ \phi^{a_j}_{n'l'J'M'}(\mathbf{r})^\dagger \left(\frac{V_{a_j}(\mathbf{r}) + V_{a_i}(\mathbf{r}-\mathbf{R})}{2} \right) \phi^{a_i}_{nlJ-1M}(\mathbf{r}-\mathbf{R}) \right. \\
&\quad + \eta^{a_i}_{nlJ-1M} \left[\phi^{a_j}_{n'l'J'M'}(\mathbf{r})^\dagger \left(\frac{V_{a_j}(\mathbf{r}) + V_{a_i}(\mathbf{r}-\mathbf{R})}{2} \right) \phi^{a_i}_{nlJM}(\mathbf{r}-\mathbf{R}) \right] \\
&\quad + \eta^{a_j}_{n'l'J'M'} \left[\phi^{a_j}_{n'l'J'-1M'}(\mathbf{r})^\dagger \left(\frac{V_{a_j}(\mathbf{r}) + V_{a_i}(\mathbf{r}-\mathbf{R})}{2} \right) \phi^{a_i}_{nlJ-1M}(\mathbf{r}-\mathbf{R}) \right] \\
&\quad \left. + \eta^{a_j}_{n'l'J'M'} \eta^{a_i}_{nlJ-1M} \left[\phi^{a_j}_{n'l'J'-1M'}(\mathbf{r})^\dagger \left(\frac{V_{a_j}(\mathbf{r}) + V_{a_i}(\mathbf{r}-\mathbf{R})}{2} \right) \phi^{a_i}_{nlJM}(\mathbf{r}-\mathbf{R}) \right] \right\} d^3r \\
&= \frac{e^{-i\frac{eB}{2\hbar}R_X R_Y}}{\sqrt{(1+\eta^{a_j\,2}_{n'l'J'M'})(1+\eta^{a_i\,2}_{nlJ-1M})}} \left\{ t^{a_j,a_i}_{n'l'J'M',nlJ-1M}(\mathbf{R}) + \eta^{a_i}_{nlJ-1M} t^{a_j,a_i}_{n'l'J'M',nlJM}(\mathbf{R}) \right. \\
&\qquad \left. + \eta^{a_j}_{n'l'J'M'} t^{a_j,a_i}_{n'l'J'-1M',nlJ-1M}(\mathbf{R}) + \eta^{a_j}_{n'l'J'M'} \eta^{a_i}_{nlJ-1M} t^{a_j,a_i}_{n'l'J'-1M',nlJM}(\mathbf{R}) \right\}.
\end{aligned}
\tag{A.19}
$$

(iv) For the combination of unperturbed atomic states $(n', l', J'-1, M')$ and (n, l, J, M) with $M \neq \pm J$.

From, Eqs.(A.14) and (A.16), we have

$$
\begin{aligned}
&T^{a_j,a_i}_{n'l'J'M',nlJM}(\mathbf{R}) \\
&= e^{-i\frac{eB}{2\hbar}R_X R_Y} \int \left\{ \frac{\phi^{a_j}_{n'l'J'-1M'}(\mathbf{r}) + \eta^{a_j}_{n'l'J'-1M'} \phi^{a_j}_{n'l'J'M'}(\mathbf{r})}{\sqrt{1+(\eta^{a_j}_{n'l'J'-1M'})^2}} \right\}^\dagger \left(\frac{V_{a_j}(\mathbf{r}) + V_{a_i}(\mathbf{r}-\mathbf{R})}{2} \right) \\
&\qquad \times \left\{ \frac{\phi^{a_i}_{nlJM}(\mathbf{r}-\mathbf{R}) + \eta^{a_i}_{nlJM} \phi^{a_i}_{nlJ-1M}(\mathbf{r}-\mathbf{R})}{\sqrt{1+(\eta^{a_i}_{nlJM})^2}} \right\} d^3r \\
&= \frac{e^{-i\frac{eB}{2\hbar}R_X R_Y}}{\sqrt{(1+\eta^{a_j\,2}_{n'l'J'-1M'})(1+\eta^{a_i\,2}_{nlJM})}} \int \left\{ \phi^{a_j}_{n'l'J'-1M'}(\mathbf{r}) + \eta^{a_j}_{n'l'J'-1M'} \phi^{a_j}_{n'l'J'M'}(\mathbf{r}) \right\}^\dagger \\
&\qquad \times \left(\frac{V_{a_j}(\mathbf{r}) + V_{a_i}(\mathbf{r}-\mathbf{R})}{2} \right) \left\{ \phi^{a_i}_{nlJM}(\mathbf{r}-\mathbf{R}) + \eta^{a_i}_{nlJM} \phi^{a_i}_{nlJ-1M}(\mathbf{r}-\mathbf{R}) \right\} d^3r \\
&= \frac{e^{-i\frac{eB}{2\hbar}R_X R_Y}}{\sqrt{(1+\eta^{a_j\,2}_{n'l'J'-1M'})(1+\eta^{a_i\,2}_{nlJM})}} \\
&\qquad \times \int \left\{ \phi^{a_j}_{n'l'J'-1M'}(\mathbf{r})^\dagger \left(\frac{V_{a_j}(\mathbf{r}) + V_{a_i}(\mathbf{r}-\mathbf{R})}{2} \right) \phi^{a_i}_{nlJM}(\mathbf{r}-\mathbf{R}) \right. \\
&\quad + \eta^{a_i}_{nlJM} \left[\phi^{a_j}_{n'l'J'-1M'}(\mathbf{r})^\dagger \left(\frac{V_{a_j}(\mathbf{r}) + V_{a_i}(\mathbf{r}-\mathbf{R})}{2} \right) \phi^{a_i}_{nlJ-1M}(\mathbf{r}-\mathbf{R}) \right] \\
&\quad + \eta^{a_j}_{n'l'J'-1M'} \left[\phi^{a_j}_{n'l'J'M'}(\mathbf{r})^\dagger \left(\frac{V_{a_j}(\mathbf{r}) + V_{a_i}(\mathbf{r}-\mathbf{R})}{2} \right) \phi^{a_i}_{nlJM}(\mathbf{r}-\mathbf{R}) \right] \\
&\quad \left. + \eta^{a_j}_{n'l'J'-1M'} \eta^{a_i}_{nlJM} \left[\phi^{a_j}_{n'l'J'M'}(\mathbf{r})^\dagger \left(\frac{V_{a_j}(\mathbf{r}) + V_{a_i}(\mathbf{r}-\mathbf{R})}{2} \right) \phi^{a_i}_{nlJ-1M}(\mathbf{r}-\mathbf{R}) \right] \right\} d^3r
\end{aligned}
$$

$$= \frac{e^{-i\frac{eB}{2\hbar}R_X R_Y}}{\sqrt{(1+\eta_{n'l'J'-1M'}^{a_j\,2})(1+\eta_{nlJM}^{a_i\,2})}} \left\{ t_{n'l'J'-1M',nlJM}^{a_j,a_i}(\mathbf{R}) + \eta_{nlJM}^{a_i} t_{n'l'J'-1M',nlJ-1M}^{a_j,a_i}(\mathbf{R}) \right.$$
$$\left. + \eta_{n'l'J'-1M'}^{a_j} t_{n'l'J'M',nlJM}^{a_j,a_i}(\mathbf{R}) + \eta_{n'l'J'-1M'}^{a_j} \eta_{nlJM}^{a_i} t_{n'l'J'M',nlJ-1M}^{a_j,a_i}(\mathbf{R}) \right\}. \quad \text{(A.20)}$$

(v) For the combination of unperturbed atomic states (n', l', J', M') and (n, l, J, M) with $M = \pm J$.

From, Eqs.(A.14) and (A.16), we have

$$\begin{aligned} & T_{n'l'J'M',nlJM}^{a_j,a_i}(\mathbf{R}) \\ & = e^{-i\frac{eB}{2\hbar}R_X R_Y} \int \phi_{n'l'J'\pm J'}(\mathbf{r})^\dagger \left(\frac{V_{a_j}(\mathbf{r}) + V_{a_i}(\mathbf{r}-\mathbf{R})}{2} \right) \phi_{nlJ\pm J}(\mathbf{r}) d^3r \\ & = e^{-i\frac{eB}{2\hbar}R_X R_Y} t_{n'l'J'\pm J',nlJ\pm J}^{a_j,a_i}(\mathbf{R}) \\ & = e^{-i\frac{eB}{2\hbar}R_X R_Y} t_{n'l'J'M',nlJM}^{a_j,a_i}(\mathbf{R}). \end{aligned} \quad \text{(A.21)}$$

(vi) For the combination of unperturbed atomic states (n', l', J', M') with $M' = \pm J'$ and (n, l, J, M) with $M \neq \pm J$.

From, Eqs.(A.14) and (A.16), we have

$$\begin{aligned} & T_{n'l'J'M',nlJM}^{a_j,a_i}(\mathbf{R}) \\ & = e^{-i\frac{eB}{2\hbar}R_X R_Y} \int \phi_{n'l'J'M'}^{a_j}(\mathbf{r})^\dagger \left(\frac{V_{a_j}(\mathbf{r}) + V_{a_i}(\mathbf{r}-\mathbf{R})}{2} \right) \\ & \qquad \times \left\{ \frac{\phi_{nlJM}^{a_i}(\mathbf{r}-\mathbf{R}) + \eta_{nlJM}^{a_i} \phi_{nlJ-1M}^{a_i}(\mathbf{r}-\mathbf{R})}{\sqrt{1+(\eta_{nlJM}^{a_i})^2}} \right\} d^3r \\ & = \frac{e^{-i\frac{eB}{2\hbar}R_X R_Y}}{\sqrt{1+\eta_{nlJM}^{a_i\,2}}} \int \phi_{n'l'J'M'}^{a_j}(\mathbf{r})^\dagger \left(\frac{V_{a_j}(\mathbf{r}) + V_{a_i}(\mathbf{r}-\mathbf{R})}{2} \right) \\ & \qquad \times \left\{ \phi_{nlJM}^{a_i}(\mathbf{r}-\mathbf{R}) + \eta_{nlJM}^{a_i} \phi_{nlJ-1M}^{a_i}(\mathbf{r}-\mathbf{R}) \right\} d^3r \end{aligned}$$

$$\begin{aligned} & = \frac{e^{-i\frac{eB}{2\hbar}R_X R_Y}}{\sqrt{1+\eta_{nlJM}^{a_i\,2}}} \int \left\{ \phi_{n'l'J'M'}^{a_j}(\mathbf{r})^\dagger \left(\frac{V_{a_j}(\mathbf{r}) + V_{a_i}(\mathbf{r}-\mathbf{R})}{2} \right) \phi_{nlJM}^{a_i}(\mathbf{r}-\mathbf{R}) + \right. \\ & \qquad \left. \times \eta_{nlJM}^{a_i} \left[\phi_{n'l'J'M'}^{a_j}(\mathbf{r})^\dagger \left(\frac{V_{a_j}(\mathbf{r}) + V_{a_i}(\mathbf{r}-\mathbf{R})}{2} \right) \phi_{nlJ-1M}^{a_i}(\mathbf{r}-\mathbf{R}) \right] \right\} d^3r \\ & = \frac{e^{-i\frac{eB}{2\hbar}R_X R_Y}}{\sqrt{1+\eta_{nlJM}^{a_i\,2}}} \left\{ t_{n'l'J'M',nlJM}^{a_j,a_i}(\mathbf{R}) + \eta_{nlJM}^{a_i} t_{n'l'J'M',nlJ-1M}^{a_j,a_i}(\mathbf{R}) \right\}. \end{aligned} \quad \text{(A.22)}$$

(vii) For the combination of unperturbed atomic states (n', l', J', M') with $M' \neq \pm J'$ and (n, l, J, M) with $M = \pm J$.

From, Eqs.(A.14) and (A.16), we have

$$
\begin{aligned}
&T^{a_j,a_i}_{n'l'J'M',nlJM}(\mathbf{R}) \\
&= e^{-i\frac{eB}{2\hbar}R_X R_Y} \int \left\{ \frac{\phi^{a_j}_{n'l'J'M'}(\mathbf{r}) + \eta^{a_j}_{n'l'J'M'}\phi^{a_j}_{n'l'J'-1M'}(\mathbf{r})}{\sqrt{1+(\eta^{a_j}_{n'l'J'M'})^2}} \right\}^\dagger \\
&\qquad\qquad \times \left(\frac{V_{a_j}(\mathbf{r}) + V_{a_i}(\mathbf{r}-\mathbf{R})}{2} \right) \phi^{a_i}_{nlJM}(\mathbf{r}-\mathbf{R}) d^3r \\
&= \frac{e^{-i\frac{eB}{2\hbar}R_X R_Y}}{\sqrt{1+\eta^{a_i\,2}_{n'l'J'M'}}} \int \left\{ \phi^{a_j}_{n'l'J'M'}(\mathbf{r})^\dagger \left(\frac{V_{a_j}(\mathbf{r}) + V_{a_i}(\mathbf{r}-\mathbf{R})}{2} \right) \phi^{a_i}_{nlJM}(\mathbf{r}-\mathbf{R}) \right. \\
&\qquad\qquad \left. + \eta^{a_j}_{n'l'J'M'} \left[\phi^{a_j}_{n'l'J'-1M'}(\mathbf{r})^\dagger \left(\frac{V_{a_j}(\mathbf{r}) + V_{a_i}(\mathbf{r}-\mathbf{R})}{2} \right) \phi^{a_i}_{nlJM}(\mathbf{r}-\mathbf{R}) \right] \right\} d^3r \\
&= \frac{e^{-i\frac{eB}{2\hbar}R_X R_Y}}{\sqrt{1+\eta^{a_j\,2}_{n'l'J'M'}}} \left\{ t^{a_j,a_i}_{n'l'J'M',nlJM}(\mathbf{R}) + \eta^{a_j}_{n'l'J'M'} t^{a_j,a_i}_{n'l'J'-1M',nlJM}(\mathbf{R}) \right\}.
\end{aligned}
\tag{A.23}
$$

(viii) For the combination of unperturbed atomic states (n', l', J', M') with $M' = \pm J'$ and $(n, l, J-1, M)$ with $M \neq \pm J$.

From, Eqs.(A.14) and (A.16), we have

$$
\begin{aligned}
&T^{a_j,a_i}_{n'l'J'M',nlJM}(\mathbf{R}) \\
&= e^{-i\frac{eB}{2\hbar}R_X R_Y} \int \phi^{a_j}_{n'l'J'M'}(\mathbf{r})^\dagger \left(\frac{V_{a_j}(\mathbf{r}) + V_{a_i}(\mathbf{r}-\mathbf{R})}{2} \right) \\
&\qquad\qquad \times \left\{ \frac{\phi^{a_i}_{nlJ-1M}(\mathbf{r}-\mathbf{R}) + \eta^{a_i}_{nlJ-1M}\phi^{a_i}_{nlJM}(\mathbf{r}-\mathbf{R})}{\sqrt{1+(\eta^{a_i}_{nlJ-1M})^2}} \right\} d^3r \\
&= \frac{e^{-i\frac{eB}{2\hbar}R_X R_Y}}{\sqrt{1+\eta^{a_i\,2}_{nlJ-1M}}} \int \left\{ \phi^{a_j}_{n'l'J'M'}(\mathbf{r})^\dagger \left(\frac{V_{a_j}(\mathbf{r}) + V_{a_i}(\mathbf{r}-\mathbf{R})}{2} \right) \phi^{a_i}_{nlJ-1M}(\mathbf{r}-\mathbf{R}) \right. \\
&\qquad\qquad \left. + \eta^{a_i}_{nlJ-1M} \left[\phi^{a_j}_{n'l'J'M'}(\mathbf{r})^\dagger \left(\frac{V_{a_j}(\mathbf{r}) + V_{a_i}(\mathbf{r}-\mathbf{R})}{2} \right) \right] \phi^{a_i}_{nlJM}(\mathbf{r}-\mathbf{R}) \right\} d^3r \\
&= \frac{e^{-i\frac{eB}{2\hbar}R_X R_Y}}{\sqrt{1+\eta^{a_i\,2}_{nlJ-1M}}} \left\{ t^{a_j,a_i}_{n'l'J'M',nlJ-1M}(\mathbf{R}) + \eta^{a_i}_{nlJ-1M} t^{a_j,a_i}_{n'l'J'M',nlJM}(\mathbf{R}) \right\}.
\end{aligned}
\tag{A.24}
$$

(ix) For the combination of unperturbed atomic states $(n', l', J'-1, M')$ with $M' \neq \pm J'$ and (n, l, J, M) with $M = \pm J$.

From, Eqs.(A.14) and (A.16), we have

$$
\begin{aligned}
&T^{a_j,a_i}_{n'l'J'M',nlJM}(\mathbf{R}) \\
&= e^{-i\frac{eB}{2\hbar}R_XR_Y}\int\left\{\frac{\phi^{a_j}_{n'l'J'-1M'}(\mathbf{r})+\eta^{a_j}_{n'l'J'-1M'}\phi^{a_j}_{n'l'J'M'}(\mathbf{r})}{\sqrt{1+(\eta^{a_j}_{n'l'J'-1M'})^2}}\right\}^{\dagger} \\
&\qquad\qquad\times\left(\frac{V_{a_j}(\mathbf{r})+V_{a_i}(\mathbf{r}-\mathbf{R})}{2}\right)\phi^{a_i}_{nlJM}(\mathbf{r}-\mathbf{R})d^3r \\
&= \frac{e^{-i\frac{eB}{2\hbar}R_XR_Y}}{\sqrt{1+\eta^{a_j\,2}_{n'l'J'-1M'}}}\int\left\{\phi^{a_j}_{n'l'J'-1M'}(\mathbf{r})^{\dagger}\left(\frac{V_{a_j}(\mathbf{r})+V_{a_i}(\mathbf{r}-\mathbf{R})}{2}\right)\phi^{a_i}_{nlJM}(\mathbf{r}-\mathbf{R})\right. \\
&\qquad\left.+\eta^{a_j}_{n'l'J'-1M'}\left[\phi^{a_j}_{n'l'J'M'}(\mathbf{r})^{\dagger}\left(\frac{V_{a_j}(\mathbf{r})+V_{a_i}(\mathbf{r}-\mathbf{R})}{2}\right)\phi^{a_i}_{nlJM}(\mathbf{r}-\mathbf{R})\right]\right\}d^3r \\
&= \frac{e^{-i\frac{eB}{2\hbar}R_XR_Y}}{\sqrt{1+\eta^{a_j\,2}_{n'l'J'-1M'}}}\left\{t^{a_j,a_i}_{n'l'J'-1M',nlJM}(\mathbf{R})+\eta^{a_j}_{n'l'J'-1M'}t^{a_j,a_i}_{n'l'J'M',nlJM}(\mathbf{R})\right\}.
\end{aligned}
\tag{A.25}
$$

The corresponding magnetic overlap integrals are obtained in the same way and by replacing relativistic hopping integral $t^{a_j,a_i}_{n'l'J'M',nlJM}(\mathbf{R})$ by relativistic overlap integral $s^{a_j,a_i}_{n'l'J'M',nlJM}(\mathbf{R})$.

Now let's calculate the magnetic hopping and overlap integral in the case of $l = 0$ and 1. Following eight unperturbed atomic orbitals should be taken in to consideration to calculate the magnetic hopping integrals and magnetic overlap integrals.

$$
(n,l,J,M) = \left(n,0,\frac{1}{2},\pm\frac{1}{2}\right),\left(n,1,\frac{1}{2},\pm\frac{1}{2}\right),\left(n,1,\frac{3}{2},\pm\frac{1}{2}\right),\left(n,1,\frac{3}{2},\pm\frac{3}{2}\right). \tag{A.26}
$$

From Eq.(3.1), we have,

$$
\begin{aligned}
&\eta_\alpha = \eta_{n1\frac{3}{2}\frac{1}{2}} = -\eta_{n1\frac{1}{2}\frac{1}{2}} \\
\text{and}\qquad &\eta_\beta = \eta_{n1\frac{3}{2}-\frac{1}{2}} = -\eta_{n1\frac{1}{2}-\frac{1}{2}}.
\end{aligned}
\tag{A.27}
$$

Now, we can calculate the magnetic Hopping and overlap integrals using Eqs.(A.17)-(A.25). Only few of them are calculated to illustrate the derivation techniques. They are calculated as follows:

(i) Combination of $(n,0,\frac{1}{2},\frac{1}{2})$ and $(n,1,\frac{1}{2},\frac{1}{2})$.

This is the case defined by Eq.(A.24). Hence, magnetic hopping integral is given by

$$
\begin{aligned}
T^{a_j,a_i}_{n0\frac{1}{2}\frac{1}{2},n1\frac{1}{2}\frac{1}{2}}(\mathbf{R}) &= \frac{e^{-i\frac{eB}{2\hbar}R_XR_Y}}{\sqrt{1+\eta^{a_i\,2}_{n1\frac{1}{2}\frac{1}{2}}}}\left\{t^{a_j,a_i}_{n0\frac{1}{2}\frac{1}{2},n1\frac{1}{2}\frac{1}{2}}(\mathbf{R})+\eta^{a_i}_{n1\frac{1}{2}\frac{1}{2}}t^{a_j,a_i}_{n0\frac{1}{2}\frac{1}{2},n1\frac{3}{2}\frac{1}{2}}(\mathbf{R})\right\} \\
&= \frac{e^{-i\frac{eB}{2\hbar}R_XR_Y}}{\sqrt{1+\eta^2_\alpha}}\left\{t^{a_j,a_i}_{n0\frac{1}{2}\frac{1}{2},n1\frac{1}{2}\frac{1}{2}}(\mathbf{R})-\eta_\alpha t^{a_j,a_i}_{n0\frac{1}{2}\frac{1}{2},n1\frac{3}{2}\frac{1}{2}}(\mathbf{R})\right\}.
\end{aligned}
\tag{A.28}
$$

(ii) Combination of $(n,1,\frac{1}{2},\frac{1}{2})$ and $(n,1,\frac{1}{2},\frac{1}{2})$.

This is the case defined by Eq.(A.18). Hence, magnetic hopping integral is given by

$$\begin{aligned}
T^{a_j,a_i}_{n1\frac{1}{2}\frac{1}{2},n1\frac{1}{2}\frac{1}{2}}(\mathbf{R}) &= \frac{e^{-i\frac{eB}{2\hbar}R_XR_Y}}{\sqrt{(1+{\eta^{a_j}_{n1\frac{1}{2}\frac{1}{2}}}^2)(1+{\eta^{a_i}_{n1\frac{1}{2}\frac{1}{2}}}^2)}}\Big\{t^{a_j,a_i}_{n1\frac{1}{2}\frac{1}{2},n1\frac{1}{2}\frac{1}{2}}(\mathbf{R})+\eta^{a_i}_{n1\frac{1}{2}\frac{1}{2}}t^{a_j,a_i}_{n1\frac{1}{2}\frac{1}{2},n1\frac{3}{2}\frac{1}{2}}(\mathbf{R}) \\
&\qquad +\eta^{a_j}_{n1\frac{1}{2}\frac{1}{2}}t^{a_j,a_i}_{n1\frac{3}{2}\frac{1}{2},n1\frac{1}{2}\frac{1}{2}}(\mathbf{R})+\eta^{a_j}_{n1\frac{1}{2}\frac{1}{2}}\eta^{a_i}_{n1\frac{1}{2}\frac{1}{2}}t^{a_j,a_i}_{n1\frac{3}{2}\frac{1}{2},n1\frac{3}{2}\frac{1}{2}}(\mathbf{R})\Big\} \\
&= \frac{e^{-i\frac{eB}{2\hbar}R_XR_Y}}{\sqrt{(1+\eta_\alpha^2)(1+\eta_\alpha^2)}}\Big\{t^{a_j,a_i}_{n1\frac{1}{2}\frac{1}{2},n1\frac{1}{2}\frac{1}{2}}(\mathbf{R})-\eta_\alpha t^{a_j,a_i}_{n1\frac{1}{2}\frac{1}{2},n1\frac{3}{2}\frac{1}{2}}(\mathbf{R}) \\
&\qquad -\eta_\alpha t^{a_j,a_i}_{n1\frac{3}{2}\frac{1}{2},n1\frac{1}{2}\frac{1}{2}}(\mathbf{R})+\eta_\alpha^2 t^{a_j,a_i}_{n1\frac{3}{2}\frac{1}{2},n1\frac{3}{2}\frac{1}{2}}(\mathbf{R})\Big\} \\
&= \frac{e^{-i\frac{eB}{2\hbar}R_XR_Y}}{(1+\eta_\alpha^2)}\Big\{t^{a_j,a_i}_{n1\frac{1}{2}\frac{1}{2},n1\frac{1}{2}\frac{1}{2}}(\mathbf{R})-\eta_\alpha t^{a_j,a_i}_{n1\frac{1}{2}\frac{1}{2},n1\frac{3}{2}\frac{1}{2}}(\mathbf{R}) \\
&\qquad -\eta_\alpha t^{a_j,a_i}_{n1\frac{3}{2}\frac{1}{2},n1\frac{1}{2}\frac{1}{2}}(\mathbf{R})+\eta_\alpha^2 t^{a_j,a_i}_{n1\frac{3}{2}\frac{1}{2},n1\frac{3}{2}\frac{1}{2}}(\mathbf{R})\Big\}.
\end{aligned} \tag{A.29}$$

(iii) Combination of $(n,1,\frac{1}{2},\frac{1}{2})$ and $(n,1,\frac{3}{2},-\frac{1}{2})$.

This is the case defined by Eq.(A.20). Hence, magnetic hopping integral is given by

$$\begin{aligned}
T^{a_j,a_i}_{n1\frac{1}{2}\frac{1}{2},n1\frac{3}{2}-\frac{1}{2}}(\mathbf{R}) &= \frac{e^{-i\frac{eB}{2\hbar}R_XR_Y}}{\sqrt{(1+{\eta^{a_j}_{n1\frac{1}{2}\frac{1}{2}}}^2)(1+{\eta^{a_i}_{n1\frac{3}{2}-\frac{1}{2}}}^2)}}\Big\{t^{a_j,a_i}_{n1\frac{1}{2}\frac{1}{2},n1\frac{3}{2}-\frac{1}{2}}(\mathbf{R}) \\
&\qquad +\eta^{a_i}_{n1\frac{3}{2}-\frac{1}{2}}t^{a_j,a_i}_{n1\frac{1}{2}\frac{1}{2},n1\frac{1}{2}-\frac{1}{2}}(\mathbf{R})+\eta^{a_j}_{n1\frac{1}{2}\frac{1}{2}}t^{a_j,a_i}_{n1\frac{3}{2}\frac{1}{2},n1\frac{3}{2}-\frac{1}{2}}(\mathbf{R}) \\
&\qquad +\eta^{a_j}_{n1\frac{1}{2}\frac{1}{2}}\eta^{a_i}_{n1\frac{3}{2}-\frac{1}{2}}t^{a_j,a_i}_{n1\frac{3}{2}\frac{1}{2},n1\frac{1}{2}-\frac{1}{2}}(\mathbf{R})\Big\} \\
&= \frac{e^{-i\frac{eB}{2\hbar}R_XR_Y}}{\sqrt{(1+\eta_\alpha^2)(1+\eta_\beta^2)}}\Big\{t^{a_j,a_i}_{n1\frac{1}{2}\frac{1}{2},n1\frac{3}{2}-\frac{1}{2}}(\mathbf{R})+\eta_\beta t^{a_j,a_i}_{n1\frac{1}{2}\frac{1}{2},n1\frac{1}{2}-\frac{1}{2}}(\mathbf{R}) \\
&\qquad -\eta_\alpha t^{a_j,a_i}_{n1\frac{3}{2}\frac{1}{2},n1\frac{3}{2}-\frac{1}{2}}(\mathbf{R})-\eta_\alpha\eta_\beta t^{a_j,a_i}_{n1\frac{3}{2}\frac{1}{2},n1\frac{1}{2}-\frac{1}{2}}(\mathbf{R})\Big\}.
\end{aligned} \tag{A.30}$$

(iv) Combination of $(n,1,\frac{1}{2},-\frac{1}{2})$ and $(n,1,\frac{3}{2},-\frac{1}{2})$.

This is the case defined by Eq.(A.20). Hence, magnetic hopping integral is given by

$$\begin{aligned}
T^{a_j,a_i}_{n1\frac{1}{2}-\frac{1}{2},n1\frac{3}{2}-\frac{1}{2}}(\mathbf{R}) &= \frac{e^{-i\frac{eB}{2\hbar}R_XR_Y}}{\sqrt{(1+{\eta^{a_j}_{n1\frac{1}{2}-\frac{1}{2}}}^2)(1+{\eta^{a_i}_{n1\frac{3}{2}-\frac{1}{2}}}^2)}}\Big\{t^{a_j,a_i}_{n1\frac{1}{2}-\frac{1}{2},n1\frac{3}{2}-\frac{1}{2}}(\mathbf{R}) \\
&\qquad +\eta^{a_i}_{n1\frac{3}{2}-\frac{1}{2}}t^{a_j,a_i}_{n1\frac{1}{2}-\frac{1}{2},n1\frac{1}{2}-\frac{1}{2}}(\mathbf{R})+\eta^{a_j}_{n1\frac{1}{2}-\frac{1}{2}}t^{a_j,a_i}_{n1\frac{3}{2}-\frac{1}{2},n1\frac{3}{2}-\frac{1}{2}}(\mathbf{R}) \\
&\qquad +\eta^{a_j}_{n1\frac{1}{2}-\frac{1}{2}}\eta^{a_i}_{n1\frac{3}{2}-\frac{1}{2}}t^{a_j,a_i}_{n1\frac{3}{2}-\frac{1}{2},n1\frac{1}{2}-\frac{1}{2}}(\mathbf{R})\Big\}
\end{aligned}$$

$$= \frac{e^{-i\frac{eB}{2\hbar}R_X R_Y}}{\sqrt{(1+\eta_\beta^2)(1+\eta_\beta^2)}} \Big\{ t^{a_j,a_i}_{n1\frac{1}{2}-\frac{1}{2},n1\frac{3}{2}-\frac{1}{2}}(\mathbf{R}) + \eta_\beta t^{a_j,a_i}_{n1\frac{1}{2}-\frac{1}{2},n1\frac{1}{2}-\frac{1}{2}}(\mathbf{R}) - \eta_\beta t^{a_j,a_i}_{n1\frac{3}{2}-\frac{1}{2},n1\frac{3}{2}-\frac{1}{2}}(\mathbf{R}) - \eta_\beta^2 t^{a_j,a_i}_{n1\frac{3}{2}-\frac{1}{2},n1\frac{1}{2}-\frac{1}{2}}(\mathbf{R}) \Big\}$$

$$= \frac{e^{-i\frac{eB}{2\hbar}R_X R_Y}}{(1+\eta_\beta^2)} \Big\{ t^{a_j,a_i}_{n1\frac{1}{2}-\frac{1}{2},n1\frac{3}{2}-\frac{1}{2}}(\mathbf{R}) + \eta_\beta t^{a_j,a_i}_{n1\frac{1}{2}-\frac{1}{2},n1\frac{1}{2}-\frac{1}{2}}(\mathbf{R}) - \eta_\beta t^{a_j,a_i}_{n1\frac{3}{2}-\frac{1}{2},n1\frac{3}{2}-\frac{1}{2}}(\mathbf{R}) - \eta_\beta^2 t^{a_j,a_i}_{n1\frac{3}{2}-\frac{1}{2},n1\frac{1}{2}-\frac{1}{2}}(\mathbf{R}) \Big\}. \tag{A.31}$$

(v) Combination of $(n,1,\frac{3}{2},\frac{1}{2})$ and $(n,1,\frac{3}{2},\frac{1}{2})$.

This is the case defined by Eq.(A.17). Hence, magnetic hopping integral is given by

$$T^{a_j,a_i}_{n1\frac{3}{2}\frac{1}{2},n1\frac{3}{2}\frac{1}{2}}(\mathbf{R}) = \frac{e^{-i\frac{eB}{2\hbar}R_X R_Y}}{\sqrt{(1+\eta^{{a_j}^2}_{n1\frac{3}{2}\frac{1}{2}})(1+\eta^{{a_i}^2}_{n1\frac{3}{2}\frac{1}{2}})}} \Big\{ t^{a_j,a_i}_{n1\frac{3}{2}\frac{1}{2},n1\frac{3}{2}\frac{1}{2}}(\mathbf{R}) + \eta^{a_i}_{n1\frac{3}{2}\frac{1}{2}} t^{a_j,a_i}_{n1\frac{3}{2}\frac{1}{2},n1\frac{1}{2}\frac{1}{2}}(\mathbf{R}) + \eta^{a_j}_{n1\frac{3}{2}\frac{1}{2}} t^{a_j,a_i}_{n1\frac{1}{2}\frac{1}{2},n1\frac{3}{2}\frac{1}{2}}(\mathbf{R}) + \eta^{a_j}_{n1\frac{3}{2}\frac{1}{2}} \eta^{a_i}_{n1\frac{3}{2}\frac{1}{2}} t^{a_j,a_i}_{n1\frac{1}{2}\frac{1}{2},n1\frac{1}{2}\frac{1}{2}}(\mathbf{R}) \Big\}$$

$$= \frac{e^{-i\frac{eB}{2\hbar}R_X R_Y}}{\sqrt{(1+\eta_\alpha^2)(1+\eta_\alpha^2)}} \Big\{ t^{a_j,a_i}_{n1\frac{3}{2}\frac{1}{2},n1\frac{3}{2}\frac{1}{2}}(\mathbf{R}) + \eta_\alpha t^{a_j,a_i}_{n1\frac{3}{2}\frac{1}{2},n1\frac{1}{2}\frac{1}{2}}(\mathbf{R}) + \eta_\alpha t^{a_j,a_i}_{n1\frac{1}{2}\frac{1}{2},n1\frac{3}{2}\frac{1}{2}}(\mathbf{R}) + \eta_\alpha^2 t^{a_j,a_i}_{n1\frac{1}{2}\frac{1}{2},n1\frac{1}{2}\frac{1}{2}}(\mathbf{R}) \Big\}. \tag{A.32}$$

In the similar way, the rest of the magnetic hopping integrals can be calculated. The list of the magnetic hopping integrals which are used in our calculation is depicted in Table I of Ref. [43]. The magnetic overlap integrals are obtained simply by replacing $t^{a_i,a_j}_{n'l'J'M',nlJM}(\mathbf{R})$ with $s^{a_i,a_j}_{n'l'J'M',nlJM}(\mathbf{R})$ in each equations.

Appendix B

Estimation of $\varepsilon_{\xi}^{a_i,0}$ and $\psi_{\xi}^{a_i,0}(\mathbf{r})$ using nonperturbative MFRTB method

Under the approximation of neglecting orbitals other than outermost one, following eight unperturbed atomic orbitals for $s(l=0)$ and $p(l=1)$ are taken in to consideration for our calculation.

$$(n,l,J,M) = \left(n,0,\frac{1}{2},\pm\frac{1}{2}\right), \left(n,1,\frac{1}{2},\pm\frac{1}{2}\right), \left(n,1,\frac{3}{2},\pm\frac{1}{2}\right), \left(n,1,\frac{3}{2},\pm\frac{3}{2}\right). \quad \text{(B.1)}$$

Considering all possible interaction of these eight unperturbed atomic orbitals, the matrix elements of Hamiltonian matrix $H_{n'l'J'M',nlJM}(\mathbf{R})$ are calculated by using Eqs.(2.60), (2.64), (2.67) and (2.70). The 8×8 Hamiltonian matrix $H_{n'l'J'M',nlJM}(\mathbf{R})$ is obtained as shown in Table (B.1). where

Table B.1: Matrix elements of Hamiltonian matrix $H_{n'l'J'M',nlJM}(\mathbf{R})$

	$(20\frac{1}{2}\frac{1}{2})$	$(20\frac{1}{2}\text{-}\frac{1}{2})$	$(21\frac{1}{2}\frac{1}{2})$	$(21\frac{3}{2}\frac{1}{2})$	$(21\frac{1}{2}\text{-}\frac{1}{2})$	$(21\frac{3}{2}\text{-}\frac{1}{2})$	$(21\frac{3}{2}\frac{3}{2})$	$(21\frac{3}{2}\text{-}\frac{3}{2})$
$(20\frac{1}{2}\frac{1}{2})$	$\bar{\varepsilon}^{a_i}_{n0\frac{1}{2}}+Z$	0	0	0	0	0	0	0
$(20\frac{1}{2}\text{-}\frac{1}{2})$	0	$\bar{\varepsilon}^{a_i}_{n0\frac{1}{2}}\text{-}Z$	0	0	0	0	0	0
$(21\frac{1}{2}\frac{1}{2})$	0	0	$\bar{\varepsilon}^{a_i}_{n1\frac{1}{2}}+\frac{1}{3}Z$	$\text{-}\frac{\sqrt{2}}{3}S_{n1}Z$	0	0	0	0
$(21\frac{3}{2}\frac{1}{2})$	0	0	$\text{-}\frac{\sqrt{2}}{3}S^{*}_{n1}Z$	$\bar{\varepsilon}^{a_i}_{n1\frac{3}{2}}+\frac{2}{3}Z$	0	0	0	0
$(21\frac{1}{2}\text{-}\frac{1}{2})$	0	0	0	0	$\bar{\varepsilon}^{a_i}_{n1\frac{1}{2}}\text{-}\frac{1}{3}Z$	$\text{-}\frac{\sqrt{2}}{3}S_{n1}Z$	0	0
$(21\frac{3}{2}\text{-}\frac{1}{2})$	0	0	0	0	$\text{-}\frac{\sqrt{2}}{3}S^{*}_{n1}Z$	$\bar{\varepsilon}^{a_i}_{n1\frac{3}{2}}\text{-}\frac{2}{3}Z$	0	0
$(21\frac{3}{2}\frac{3}{2})$	0	0	0	0	0	0	$\bar{\varepsilon}^{a_i}_{n1\frac{3}{2}}+2Z$	0
$(21\frac{3}{2}\text{-}\frac{3}{2})$	0	0	0	0	0	0	0	$\bar{\varepsilon}^{a_i}_{n1\frac{3}{2}}\text{-}2Z$

$$Z = \frac{e\hbar B}{2m}, \tag{B.2}$$

$$S_{n1} = \int F^{a_i}_{n1\frac{1}{2}}(\mathbf{r})^\dagger F^{a_i}_{n1\frac{3}{2}}(\mathbf{r}) d^3r, \tag{B.3}$$

$$S^*_{n1} = \int F^{a_i}_{n1\frac{3}{2}}(\mathbf{r})^\dagger F^{a_i}_{n1\frac{1}{2}}(\mathbf{r}) d^3r. \tag{B.4}$$

The diagonalization can be performed in each diagonal block matrix. Each diagonal block matrix is 2×2 matrix and therefore are given by

$$H_\alpha = \begin{pmatrix} \bar{\varepsilon}^{a_i}_{n1\frac{1}{2}} + \frac{1}{3}Z & -\frac{\sqrt{2}}{3}S_{n1}Z \\ -\frac{\sqrt{2}}{3}S^*_{n1}Z & \bar{\varepsilon}^{a_i}_{n1\frac{3}{2}} + \frac{2}{3}Z \end{pmatrix} \tag{B.5}$$

and

$$H_\beta = \begin{pmatrix} \bar{\varepsilon}^{a_i}_{n1\frac{1}{2}} - \frac{1}{3}Z & -\frac{\sqrt{2}}{3}S_{n1}Z \\ -\frac{\sqrt{2}}{3}S^*_{n1}Z & \bar{\varepsilon}^{a_i}_{n1\frac{3}{2}} - \frac{2}{3}Z \end{pmatrix}. \tag{B.6}$$

Now, let us calculate the eigenvalues and eigenfunctions corresponding to both H_α and H_β, respectively.

(a) Eigenvalues and eigenfunctions corresponding to H_α.

Diagonalizing H_α, we have

$$|H_\alpha - \lambda I| = 0$$

or

$$\begin{vmatrix} \bar{\varepsilon}^{a_i}_{n1\frac{1}{2}} + \frac{1}{3}Z & -\frac{\sqrt{2}}{3}S_{n1}Z \\ -\frac{\sqrt{2}}{3}S^*_{n1}Z & \bar{\varepsilon}^{a_i}_{n1\frac{3}{2}} + \frac{2}{3}Z \end{vmatrix} = 0.$$

Then, we obtain

$$\lambda^2 - \lambda\left(\bar{\varepsilon}^{a_i}_{n1\frac{1}{2}} + \bar{\varepsilon}^{a_i}_{n1\frac{3}{2}} + Z\right) + \bar{\varepsilon}^{a_i}_{n1\frac{1}{2}}\bar{\varepsilon}^{a_i}_{n1\frac{3}{2}} + \frac{Z}{3}\left(\bar{\varepsilon}^{a_i}_{n1\frac{3}{2}} + 2\bar{\varepsilon}^{a_i}_{n1\frac{1}{2}}\right) + \frac{2}{9}Z^2\left(1 - |S_{nl}|^2\right) = 0. \tag{B.7}$$

The solutions of Eq.(B.7) are given by

$$\lambda = \frac{\left(\bar{\varepsilon}^{a_i}_{n1\frac{1}{2}} + \bar{\varepsilon}^{a_i}_{n1\frac{3}{2}} + Z\right)}{2} \pm \frac{1}{2}\sqrt{\left(\bar{\varepsilon}^{a_i}_{n1\frac{1}{2}} + \bar{\varepsilon}^{a_i}_{n1\frac{3}{2}} + Z\right)^2 - 4\bar{\varepsilon}^{a_i}_{n1\frac{1}{2}}\bar{\varepsilon}^{a_i}_{n1\frac{3}{2}} - \frac{4}{3}\left(\bar{\varepsilon}^{a_i}_{n1\frac{3}{2}} + 2\bar{\varepsilon}^{a_i}_{n1\frac{1}{2}}\right) - \frac{8}{9}Z^2(1 - |S_{nl}|^2)}$$

$$= \frac{\left(\bar{\varepsilon}^{a_i}_{n1\frac{1}{2}} + \bar{\varepsilon}^{a_i}_{n1\frac{3}{2}} + Z\right)}{2} \pm \frac{1}{2}\sqrt{\left(\bar{\varepsilon}^{a_i}_{n1\frac{3}{2}} - \bar{\varepsilon}^{a_i}_{n1\frac{1}{2}}\right)^2 + \frac{2}{3}Z\left(\bar{\varepsilon}^{a_i}_{n1\frac{3}{2}} - \bar{\varepsilon}^{a_i}_{n1\frac{1}{2}}\right) + \frac{1}{9}Z^2(1+8|S_{nl}|^2)}$$

$$= \frac{\bar{\varepsilon}^{a_i}_{n1\frac{1}{2}} + \bar{\varepsilon}^{a_i}_{n1\frac{3}{2}}}{2} + \frac{Z}{2} \pm \frac{\bar{\varepsilon}^{a_i}_{n1\frac{3}{2}} - \bar{\varepsilon}^{a_i}_{n1\frac{1}{2}}}{2}\sqrt{1 + \frac{2}{3}\left(\frac{Z}{\bar{\varepsilon}^{a_i}_{n1\frac{3}{2}} - \bar{\varepsilon}^{a_i}_{n1\frac{1}{2}}}\right) + \frac{1}{9}(1+8|S_{nl}|^2)\left(\frac{Z}{\bar{\varepsilon}^{a_i}_{n1\frac{3}{2}} - \bar{\varepsilon}^{a_i}_{n1\frac{1}{2}}}\right)^2}$$

$$= \frac{\bar{\varepsilon}^{a_i}_{n1\frac{1}{2}} + \bar{\varepsilon}^{a_i}_{n1\frac{3}{2}}}{2} + \frac{Z}{2} \pm \frac{\bar{\varepsilon}^{a_i}_{n1\frac{3}{2}} - \bar{\varepsilon}^{a_i}_{n1\frac{1}{2}}}{2}\sqrt{1 + \frac{2}{3}x_{nl} + \frac{1}{9}(1+8S^2_{nl})x^2_{nl}}.$$

Hence, the eigenvalues corresponding to H_α are given by

$$\lambda = \frac{\bar{\varepsilon}^{a_i}_{n1\frac{1}{2}} + \bar{\varepsilon}^{a_i}_{n1\frac{3}{2}}}{2} + \frac{e\hbar B}{4m} \pm \frac{\bar{\varepsilon}^{a_i}_{n1\frac{3}{2}} - \bar{\varepsilon}^{a_i}_{n1\frac{1}{2}}}{2}\sqrt{1 + \frac{2}{3}x_{nl} + \frac{1}{9}(1+8S^2_{nl})x^2_{nl}}, \tag{B.8}$$

with

$$x_{nl} = \frac{e\hbar B/2m}{\bar{\varepsilon}^{a_i}_{n1\frac{3}{2}} - \bar{\varepsilon}^{a_i}_{n1\frac{1}{2}}}. \tag{B.9}$$

Let, $\begin{pmatrix} a \\ b \end{pmatrix}$ is the eigenvectors of H_α, then the characteristics equation is given by

$$\begin{pmatrix} \bar{\varepsilon}^{a_i}_{n1\frac{1}{2}} + \frac{1}{3}Z - \lambda & -\frac{\sqrt{2}}{3}S_{n1}Z \\ -\frac{\sqrt{2}}{3}S^*_{n1}Z & \bar{\varepsilon}^{a_i}_{n1\frac{3}{2}} + \frac{2}{3}Z - \lambda \end{pmatrix} \begin{pmatrix} a \\ b \end{pmatrix} = 0.$$

Then, we obtain

$$\left(\bar{\varepsilon}^{a_i}_{n1\frac{1}{2}} + \frac{1}{3}Z\right)a - \frac{\sqrt{2}}{3}S_{n1}Z \;\; b = \lambda a \tag{B.10}$$

and

$$-\frac{\sqrt{2}}{3}S^*_{n1}Z \;\; a + \left(\bar{\varepsilon}^{a_i}_{n1\frac{3}{2}} + \frac{2}{3}Z\right)b = \lambda b. \tag{B.11}$$

Let us consider plus sign in Eq.(B.8), then Eq.(B.11) becomes

$$\frac{a}{b} = \frac{3}{\sqrt{2}S_{nl}Z}\left(\bar{\varepsilon}^{a_i}_{n1\frac{3}{2}} + \frac{2}{3}Z - \lambda\right). \tag{B.12}$$

From Eqs.(B.8) and (B.12), we have

$$\begin{aligned}\frac{a}{b} &= \frac{3}{\sqrt{2}S_{nl}Z}\left\{\bar{\varepsilon}^{a_i}_{n1\frac{3}{2}} + \frac{2}{3}Z - \frac{\bar{\varepsilon}^{a_i}_{n1\frac{1}{2}} + \bar{\varepsilon}^{a_i}_{n1\frac{3}{2}}}{2} - \frac{Z}{2} - \frac{\bar{\varepsilon}^{a_i}_{n1\frac{3}{2}} - \bar{\varepsilon}^{a_i}_{n1\frac{1}{2}}}{2}\sqrt{1+\frac{2}{3}x_{nl}+\frac{1+8S^2_{nl}}{9}x^2_{nl}}\right\} \\ &= \frac{3}{\sqrt{2}S_{nl}Z}\left\{\frac{\bar{\varepsilon}^{a_i}_{n1\frac{3}{2}} - \bar{\varepsilon}^{a_i}_{n1\frac{1}{2}}}{2} + \frac{Z}{6} - \frac{\bar{\varepsilon}^{a_i}_{n1\frac{3}{2}} - \bar{\varepsilon}^{a_i}_{n1\frac{1}{2}}}{2}\sqrt{1+\frac{2}{3}x_{nl}+\frac{1+8S^2_{nl}}{9}x^2_{nl}}\right\} \\ &= \frac{3}{\sqrt{2}S_{nl}Z}\left(\frac{\bar{\varepsilon}^{a_i}_{n1\frac{3}{2}} - \bar{\varepsilon}^{a_i}_{n1\frac{1}{2}}}{2}\right)\left\{1+\frac{x_{nl}}{3} - \sqrt{1+\frac{2}{3}x_{nl}+\frac{1+8S^2_{nl}}{9}x^2_{nl}}\right\} \\ &= \frac{3}{2\sqrt{2}S_{nl}x_{nl}}\left\{1+\frac{x_{nl}}{3} - \sqrt{1+\frac{2}{3}x_{nl}+\frac{1+8S^2_{nl}}{9}x^2_{nl}}\right\}.\end{aligned} \tag{B.13}$$

Here, we introduce the symbol $\eta^{a_i}_{+}$ which is given by

$$\eta^{a_i}_{+} = \frac{3}{2\sqrt{2}S_{nl}x_{nl}}\left\{1+\frac{x_{nl}}{3} - \sqrt{1+\frac{2}{3}x_{nl}+\frac{1+8S^2_{nl}}{9}x^2_{nl}}\right\}. \tag{B.14}$$

Then, from Eqs.(B.13) and (B.14), we get

$$a = \eta^{a_i}_{+} b. \tag{B.15}$$

Hence, the standardized eigenvectors which are obtained as

$$\begin{pmatrix} a \\ b \end{pmatrix} = \frac{1}{\sqrt{1+\eta^{a_i^2}_{+}}}\begin{pmatrix} \eta^{a_i}_{+} \\ 1 \end{pmatrix}. \tag{B.16}$$

Finally, we obtain the eigenfunctions corresponding to H_α considering plus sign in Eq.(B.8) as

$$\psi^{a_i,0}_{\xi}(\mathbf{r}) = \frac{1}{\sqrt{1+\eta^{a_i^2}_{+}}}\left[\phi^{a_i}_{n1\frac{3}{2}\frac{1}{2}}(\mathbf{r}) + \eta^{a_i}_{+}\phi^{a_i}_{n1\frac{1}{2}\frac{1}{2}}(\mathbf{r})\right]. \tag{B.17}$$

Now, let us consider minus sign in Eq.(B.8). Then Eqs. (B.10) becomes

$$\frac{b}{a} = \frac{3}{\sqrt{2}S_{nl}Z}\left(\bar{\varepsilon}^{a_i}_{n1\frac{3}{2}} + \frac{2}{3}Z - \lambda\right). \tag{B.18}$$

From Eqs.(B.8) and (B.18), we have

$$\begin{aligned}\frac{b}{a} &= \frac{3}{\sqrt{2}S_{nl}Z}\left\{\bar{\varepsilon}^{a_i}_{n1\frac{1}{2}} + \frac{Z}{3} - \frac{\bar{\varepsilon}^{a_i}_{n1\frac{3}{2}} + \bar{\varepsilon}^{a_i}_{n1\frac{1}{2}}}{2} - \frac{Z}{2} + \frac{\bar{\varepsilon}^{a_i}_{n1\frac{3}{2}} - \bar{\varepsilon}^{a_i}_{n1\frac{1}{2}}}{2}\sqrt{1+\frac{2}{3}x_{nl}+\frac{1+8S^2_{nl}}{9}x^2_{nl}}\right\} \\ &= \frac{3}{\sqrt{2}S_{nl}Z}\left\{\frac{\bar{\varepsilon}^{a_i}_{n1\frac{1}{2}} - \bar{\varepsilon}^{a_i}_{n1\frac{3}{2}}}{2} - \frac{Z}{6} + \frac{\bar{\varepsilon}^{a_i}_{n1\frac{3}{2}} - \bar{\varepsilon}^{a_i}_{n1\frac{1}{2}}}{2}\sqrt{1+\frac{2}{3}x_{nl}+\frac{1+8S^2_{nl}}{9}x^2_{nl}}\right\}\end{aligned}$$

$$= -\frac{3}{\sqrt{2}S_{nl}Z}\left(\frac{\bar{\varepsilon}^{a_i}_{n1\frac{3}{2}} - \bar{\varepsilon}^{a_i}_{n1\frac{1}{2}}}{2}\right)\left\{1 + \frac{x_{nl}}{3} - \sqrt{1 + \frac{2}{3}x_{nl} + \frac{1+8S^2_{nl}}{9}x^2_{nl}}\right\}$$
$$= -\frac{3}{2\sqrt{2}S_{nl}x_{nl}}\left\{1 + \frac{x_{nl}}{3} - \sqrt{1 + \frac{2}{3}x_{nl} + \frac{1+8S^2_{nl}}{9}x^2_{nl}}\right\}$$
$$= -\eta^{a_i}_{+}. \tag{B.19}$$

$$b = -\eta^{a_i}_{+}a. \tag{B.20}$$

Hence, the standardized eigenvectors which are obtained as

$$\begin{pmatrix} a \\ b \end{pmatrix} = \frac{1}{\sqrt{1+\eta^{a_i^2}_{+}}}\begin{pmatrix} 1 \\ -\eta^{a_i}_{+} \end{pmatrix}. \tag{B.21}$$

Hence, the corresponding eigenfunction of H_α considering minus sign in Eq.(B.8) is given by

$$\psi^{a_i,0}_{\xi}(\mathbf{r}) = \frac{1}{\sqrt{1+\eta^{a_i}_{+}{}^2}}\left[-\eta^{a_i}_{+}\phi^{a_i}_{n1\frac{3}{2}\frac{1}{2}}(\mathbf{r}) + \phi^{a_i}_{n1\frac{1}{2}\frac{1}{2}}(\mathbf{r})\right]. \tag{B.22}$$

(b) Eigenvalues and eigenfunctions corresponding to H_β.

Diagonalizing H_β, we have

$$|H_\beta - \lambda I| = 0$$

or

$$\begin{vmatrix} \bar{\varepsilon}^{a_i}_{n1\frac{1}{2}} - \frac{1}{3}Z - \lambda & -\frac{\sqrt{2}}{3}S_{n1}Z \\ -\frac{\sqrt{2}}{3}S^*_{n1}Z & \bar{\varepsilon}^{a_i}_{n1\frac{3}{2}} - \frac{2}{3}Z - \lambda \end{vmatrix} = 0.$$

Thus, we obtain

$$\lambda^2 - \lambda\left(\bar{\varepsilon}^{a_i}_{n1\frac{1}{2}} + \bar{\varepsilon}^{a_i}_{n1\frac{3}{2}} - Z\right) + \bar{\varepsilon}^{a_i}_{n1\frac{1}{2}}\bar{\varepsilon}^{a_i}_{n1\frac{3}{2}} - \frac{Z}{3}\left(\bar{\varepsilon}^{a_i}_{n1\frac{3}{2}} + 2\bar{\varepsilon}^{a_i}_{n1\frac{1}{2}}\right) + \frac{2}{9}Z^2\left(1 - S^2_{nl}\right) = 0. \tag{B.23}$$

We have the solutions of Eq.(B.23) as

$$\lambda = \frac{\left(\bar{\varepsilon}^{a_i}_{n1\frac{1}{2}} + \bar{\varepsilon}^{a_i}_{n1\frac{3}{2}} - Z\right)}{2} \pm \frac{1}{2}\sqrt{\left(\bar{\varepsilon}^{a_i}_{n1\frac{1}{2}} + \bar{\varepsilon}^{a_i}_{n1\frac{3}{2}} - Z\right)^2 - 4\bar{\varepsilon}^{a_i}_{n1\frac{1}{2}}\bar{\varepsilon}^{a_i}_{n1\frac{3}{2}} + \frac{4}{3}\left(\bar{\varepsilon}^{a_i}_{n1\frac{3}{2}} + 2\bar{\varepsilon}^{a_i}_{n1\frac{1}{2}}\right) - \frac{8}{9}Z^2(1 - S^2_{nl})}}$$

$$
\begin{aligned}
&= \frac{\left(\bar{\varepsilon}^{a_i}_{n1\frac{1}{2}} + \bar{\varepsilon}^{a_i}_{n1\frac{3}{2}} - Z\right)}{2} \pm \frac{1}{2}\sqrt{\left(\bar{\varepsilon}^{a_i}_{n1\frac{3}{2}} - \bar{\varepsilon}^{a_i}_{n1\frac{1}{2}}\right)^2 + \frac{2}{3}Z\left(\bar{\varepsilon}^{a_i}_{n1\frac{3}{2}} - \bar{\varepsilon}^{a_i}_{n1\frac{1}{2}}\right) + \frac{1}{9}Z^2(1+8|S_{nl}|^2)} \\
&= \frac{\bar{\varepsilon}^{a_i}_{n1\frac{1}{2}} + \bar{\varepsilon}^{a_i}_{n1\frac{3}{2}}}{2} - \frac{Z}{2} \pm \frac{\bar{\varepsilon}^{a_i}_{n1\frac{3}{2}} - \bar{\varepsilon}^{a_i}_{n1\frac{1}{2}}}{2}\sqrt{1 - \frac{2}{3}\left(\frac{Z}{\bar{\varepsilon}^{a_i}_{n1\frac{3}{2}} - \bar{\varepsilon}^{a_i}_{n1\frac{1}{2}}}\right)} \\
&\qquad\qquad \overline{+\frac{(1+8S^2_{nl})}{9}\left(\frac{Z}{\bar{\varepsilon}^{a_i}_{n1\frac{3}{2}} - \bar{\varepsilon}^{a_i}_{n1\frac{1}{2}}}\right)^2} \\
&= \frac{\bar{\varepsilon}^{a_i}_{n1\frac{1}{2}} + \bar{\varepsilon}^{a_i}_{n1\frac{3}{2}}}{2} - \frac{Z}{2} \pm \frac{\bar{\varepsilon}^{a_i}_{n1\frac{3}{2}} - \bar{\varepsilon}^{a_i}_{n1\frac{1}{2}}}{2}\sqrt{1 - \frac{2}{3}x_{nl} + \frac{(1+8S^2_{nl})}{9}x^2_{nl}}.
\end{aligned}
\tag{B.24}
$$

Hence, the eigenvalues corresponding to H_β are given by

$$
\lambda = \frac{\bar{\varepsilon}^{a_i}_{n1\frac{1}{2}} + \bar{\varepsilon}^{a_i}_{n1\frac{3}{2}}}{2} - \frac{e\hbar B}{4m} \pm \frac{\bar{\varepsilon}^{a_i}_{n1\frac{3}{2}} - \bar{\varepsilon}^{a_i}_{n1\frac{1}{2}}}{2}\sqrt{1 - \frac{2}{3}x_{nl} + \frac{(1+8S^2_{nl})}{9}x^2_{nl}}. \tag{B.25}
$$

Again, let us take $\begin{pmatrix} a \\ b \end{pmatrix}$ is the eigenvectors of H_β, then the characteristics equation is given by

$$
\begin{pmatrix}
\bar{\varepsilon}^{a_i}_{n1\frac{1}{2}} - \frac{1}{3}Z - \lambda & -\frac{\sqrt{2}}{3}S_{n1}Z \\
-\frac{\sqrt{2}}{3}S^*_{n1}Z & \bar{\varepsilon}^{a_i}_{n1\frac{3}{2}} - \frac{2}{3}Z - \lambda
\end{pmatrix}
\begin{pmatrix} a \\ b \end{pmatrix} = 0.
$$

Then, we have following sets of equation:

$$
\left(\bar{\varepsilon}^{a_i}_{n1\frac{1}{2}} - \frac{1}{3}Z\right)a - \frac{\sqrt{2}}{3}S_{n1}Z\ \ b = \lambda a \tag{B.26}
$$

and

$$
-\frac{\sqrt{2}}{3}S^*_{n1}Z\ \ a + \left(\bar{\varepsilon}^{a_i}_{n1\frac{3}{2}} - \frac{2}{3}Z\right)b = \lambda b. \tag{B.27}
$$

Let's consider a plus sign in Eq.(B.25), then from Eq.(B.27) we have

$$
\frac{a}{b} = \frac{3}{\sqrt{2}S_{nl}Z}\left(\bar{\varepsilon}^{a_i}_{n1\frac{3}{2}} - \frac{2}{3}Z - \lambda\right). \tag{B.28}
$$

From Eqs.(B.25) and (B.28), we have

$$
\frac{a}{b} = \frac{3}{\sqrt{2}S_{nl}Z}\left\{\bar{\varepsilon}^{a_i}_{n1\frac{3}{2}} - \frac{2}{3}Z - \frac{\bar{\varepsilon}^{a_i}_{n1\frac{1}{2}} + \bar{\varepsilon}^{a_i}_{n1\frac{3}{2}}}{2} + \frac{Z}{2} - \frac{\bar{\varepsilon}^{a_i}_{n1\frac{3}{2}} - \bar{\varepsilon}^{a_i}_{n1\frac{1}{2}}}{2}\sqrt{1 - \frac{2}{3}x_{nl} + \frac{1+8S^2_{nl}}{9}x^2_{nl}}\right\}
$$

$$
\begin{aligned}
&= \frac{3}{\sqrt{2}S_{nl}Z}\left\{\frac{\bar{\varepsilon}^{a_i}_{n1\frac{3}{2}} - \bar{\varepsilon}^{a_i}_{n1\frac{1}{2}}}{2} - \frac{Z}{6} - \frac{\bar{\varepsilon}^{a_i}_{n1\frac{3}{2}} - \bar{\varepsilon}^{a_i}_{n1\frac{1}{2}}}{2}\sqrt{1-\frac{2}{3}x_{nl}+\frac{1+8S^2_{nl}}{9}x^2_{nl}}\right\} \\
&= \frac{3}{\sqrt{2}S_{nl}Z}\left(\frac{\bar{\varepsilon}^{a_i}_{n1\frac{3}{2}} - \bar{\varepsilon}^{a_i}_{n1\frac{1}{2}}}{2}\right)\left\{1-\frac{x_{nl}}{3}-\sqrt{1-\frac{2}{3}x_{nl}+\frac{1+8S^2_{nl}}{9}x^2_{nl}}\right\} \\
&= \frac{3}{2\sqrt{2}S_{nl}x_{nl}}\left\{1-\frac{x_{nl}}{3}-\sqrt{1-\frac{2}{3}x_{nl}+\frac{1+8S^2_{nl}}{9}x^2_{nl}}\right\}.
\end{aligned}
\tag{B.29}
$$

Again, we introduce the symbol $\eta^{a_i}_-$ which is given by

$$
\eta^{a_i}_- = \frac{3}{2\sqrt{2}S_{nl}x_{nl}}\left\{1-\frac{x_{nl}}{3}-\sqrt{1-\frac{2}{3}x_{nl}+\frac{1+8S^2_{nl}}{9}x^2_{nl}}\right\}. \tag{B.30}
$$

Then, from Eq.(B.29) and (B.30), we have

$$
a = \eta^{a_i}_- b. \tag{B.31}
$$

Hence, the standardized eigenvectors corresponding to H_β are obtained as

$$
\begin{pmatrix} a \\ b \end{pmatrix} = \frac{1}{\sqrt{1+\eta^{a_i^2}_-}}\begin{pmatrix} \eta^{a_i}_- \\ 1 \end{pmatrix}. \tag{B.32}
$$

Hence, the corresponding eigenfunction of H_β considering plus sign in Eq.(B.26)is given by

$$
\psi^{a_i,0}_\xi = \frac{1}{\sqrt{1+\eta^{a_i\,2}_-}}\left[\phi^{a_i}_{n1\frac{3}{2}-\frac{1}{2}}(\mathbf{r}) + \eta^{a_i}_-\phi^{a_i}_{n1\frac{1}{2}-\frac{1}{2}}(\mathbf{r})\right]. \tag{B.33}
$$

Let's consider a minus sign in Eq.(B.25). Then, from Eqs.(B.26), we have

$$
\frac{b}{a} = \frac{3}{\sqrt{2}S_{nl}Z}\left(\bar{\varepsilon}^{a_i}_{n1\frac{1}{2}} - \frac{1}{3}Z - \lambda\right). \tag{B.34}
$$

From Eqs.(B.25) and (B.34), we have

$$
\begin{aligned}
\frac{b}{a} &= \frac{3}{\sqrt{2}S_{nl}Z}\left\{\bar{\varepsilon}^{a_i}_{n1\frac{1}{2}} - \frac{Z}{3} - \frac{\bar{\varepsilon}^{a_i}_{n1\frac{3}{2}} + \bar{\varepsilon}^{a_i}_{n1\frac{1}{2}}}{2} + \frac{Z}{2} + \frac{\bar{\varepsilon}^{a_i}_{n1\frac{3}{2}} - \bar{\varepsilon}^{a_i}_{n1\frac{1}{2}}}{2}\sqrt{1-\frac{2}{3}x_{nl}+\frac{1+8S^2_{nl}}{9}x^2_{nl}}\right\} \\
&= \frac{3}{\sqrt{2}S_{nl}Z}\left\{\frac{\bar{\varepsilon}^{a_i}_{n1\frac{1}{2}} - \bar{\varepsilon}^{a_i}_{n1\frac{3}{2}}}{2} + \frac{Z}{6} + \frac{\bar{\varepsilon}^{a_i}_{n1\frac{3}{2}} - \bar{\varepsilon}^{a_i}_{n1\frac{1}{2}}}{2}\sqrt{1-\frac{2}{3}x_{nl}+\frac{1+8S^2_{nl}}{9}x^2_{nl}}\right\} \\
&= -\frac{3}{\sqrt{2}S_{nl}Z}\left(\frac{\bar{\varepsilon}^{a_i}_{n1\frac{3}{2}} - \bar{\varepsilon}^{a_i}_{n1\frac{1}{2}}}{2}\right)\left\{1-\frac{x_{nl}}{3}-\sqrt{1-\frac{2}{3}x_{nl}+\frac{1+8S^2_{nl}}{9}x^2_{nl}}\right\} \\
&= -\frac{3}{2\sqrt{2}S_{nl}x_{nl}}\left\{1-\frac{x_{nl}}{3}-\sqrt{1-\frac{2}{3}x_{nl}+\frac{1+8S^2_{nl}}{9}x^2_{nl}}\right\} \\
&= -\eta^{a_i}_-.
\end{aligned}
\tag{B.35}
$$

This implies that

$$b = -\eta_-^{a_i} a. \tag{B.36}$$

Hence, the standardized eigenvectors corresponding to H_β are obtained as

$$\begin{pmatrix} a \\ b \end{pmatrix} = \frac{1}{\sqrt{1+\eta_-^{a_i^2}}} \begin{pmatrix} 1 \\ -\eta_-^{a_i} \end{pmatrix}. \tag{B.37}$$

Hence, we obtain the eigenfunction corresponding to H_β considering minus sign in Eq.(B.26) is given by

$$\psi_\xi^{a_i,0} = \frac{1}{\sqrt{1+\eta_-^{a_i^2}}} \left[-\eta_-^{a_i} \phi^{a_i}_{n1\frac{3}{2}-\frac{1}{2}}(\mathbf{r}) + \phi^{a_i}_{n1\frac{1}{2}-\frac{1}{2}}(\mathbf{r}) \right]. \tag{B.38}$$

Finally, summarizing the results, the eigenvalues of Hamiltonian matrix $H_{n'l'J'M',nlJM}$ are given by

$$\bar{\varepsilon}_\xi^{a_i,0} = \begin{cases} \bar{\varepsilon}^{a_i}_{n0\frac{1}{2}} \pm \dfrac{e\hbar B}{2m} \\ \dfrac{\bar{\varepsilon}^{a_i}_{n1\frac{3}{2}} + \bar{\varepsilon}^{a_i}_{n1\frac{1}{2}}}{2} + \dfrac{e\hbar B}{4m} + \dfrac{\bar{\varepsilon}^{a_i}_{n1\frac{3}{2}} - \bar{\varepsilon}^{a_i}_{n1\frac{1}{2}}}{2} \sqrt{1 + \dfrac{2}{3}x_{nl} + \dfrac{1+8S_{nl}^2}{9}x_{nl}^2} \\ \dfrac{\bar{\varepsilon}^{a_i}_{n1\frac{3}{2}} + \bar{\varepsilon}^{a_i}_{n1\frac{1}{2}}}{2} + \dfrac{e\hbar B}{4m} - \dfrac{\bar{\varepsilon}^{a_i}_{n1\frac{3}{2}} - \bar{\varepsilon}^{a_i}_{n1\frac{1}{2}}}{2} \sqrt{1 + \dfrac{2}{3}x_{nl} + \dfrac{1+8S_{nl}^2}{9}x_{nl}^2} \\ \dfrac{\bar{\varepsilon}^{a_i}_{n1\frac{3}{2}} + \bar{\varepsilon}^{a_i}_{n1\frac{1}{2}}}{2} - \dfrac{e\hbar B}{4m} + \dfrac{\bar{\varepsilon}^{a_i}_{n1\frac{3}{2}} - \bar{\varepsilon}^{a_i}_{n1\frac{1}{2}}}{2} \sqrt{1 - \dfrac{2}{3}x_{nl} + \dfrac{1+8S_{nl}^2}{9}x_{nl}^2} \\ \dfrac{\bar{\varepsilon}^{a_i}_{n1\frac{3}{2}} + \bar{\varepsilon}^{a_i}_{n1\frac{1}{2}}}{2} - \dfrac{e\hbar B}{4m} - \dfrac{\bar{\varepsilon}^{a_i}_{n1\frac{3}{2}} - \bar{\varepsilon}^{a_i}_{n1\frac{1}{2}}}{2} \sqrt{1 - \dfrac{2}{3}x_{nl} + \dfrac{1+8S_{nl}^2}{9}x_{nl}^2} \\ \bar{\varepsilon}^{a_i}_{n1\frac{3}{2}} \pm \dfrac{e\hbar B}{m} \end{cases}, \tag{B.39}$$

and corresponding eigenfunctions are given by

$$\psi_\xi^{a_i,0} = \begin{cases} \phi^{a_i}_{n0\frac{1}{2}\pm\frac{1}{2}}(\mathbf{r}) \\ \dfrac{\phi^{a_i}_{n1\frac{3}{2}\frac{1}{2}}(\mathbf{r}) + \eta_+^{a_i}\phi^{a_i}_{n1\frac{1}{2}\frac{1}{2}}(\mathbf{r})}{\sqrt{1+\eta_+^{a_i^2}}} \\ \dfrac{-\eta_+^{a_i}\phi^{a_i}_{n1\frac{3}{2}\frac{1}{2}}(\mathbf{r}) + \phi^{a_i}_{n1\frac{1}{2}\frac{1}{2}}(\mathbf{r})}{\sqrt{1+\eta_+^{a_i^2}}} \\ \dfrac{\phi^{a_i}_{n1\frac{3}{2}-\frac{1}{2}}(\mathbf{r}) + \eta_-^{a_i}\phi^{a_i}_{n1\frac{1}{2}-\frac{1}{2}}(\mathbf{r})}{\sqrt{1+\eta_-^{a_i^2}}} \\ \dfrac{-\eta_-^{a_i}\phi^{a_i}_{n1\frac{3}{2}-\frac{1}{2}}(\mathbf{r}) + \phi^{a_i}_{n1\frac{1}{2}-\frac{1}{2}}(\mathbf{r})}{\sqrt{1+\eta_-^{a_i^2}}} \\ \phi^{a_i}_{n1\frac{3}{2}\pm\frac{1}{2}}(\mathbf{r}) \end{cases}, \tag{B.40}$$

with

$$\eta_{\pm}^{a_i} = \frac{3}{2\sqrt{2}S_{nl}x_{nl}} \left\{ 1 \pm \frac{x_{nl}}{3} - \sqrt{1 \pm \frac{2}{3}x_{nl} + \frac{1+8S_{nl}^2}{9}x_{nl}^2} \right\} \tag{B.41}$$

and

$$x_{nl} = \frac{e\hbar B/2m}{\bar{\varepsilon}_{n1\frac{3}{2}}^{a_i} - \bar{\varepsilon}_{n1\frac{1}{2}}^{a_i}}. \tag{B.42}$$

Appendix C

Effective thickness and r_s parameter of graphene

In this appendix, We present the effective thickness of graphene by taking graphene magnetization into consideration. We also use it to determine the r_s parameter of graphene, i.e., the electron density of graphene.

First, we derive the effective thickness of graphene which is referred to as l. In our previous work, the sheet magnetization, which corresponds to the magnetization per unit ares, is defined as

$$M_{sheet} = -\frac{dE_{total}}{dB_{ext}}, \tag{C.1}$$

where E_{total} is the total energy of graphene per unit area. If the magnetic dipole moment per one carbon atom in graphene is denoted as m_{carbon}, it is given by

$$m_{carbon} = \mu_0 S_{carbon} M_{sheet}, \tag{C.2}$$

where S_{carbon} is the area occupied by one carbon atom in graphene which is given by

$$S_{carbon} = \frac{\sqrt{3}}{4} a^2, \tag{C.3}$$

with a being lattice constant of graphene.

Since the magnetic dipole moment of current carrying loop is also current times area enclosed by the loop, then m_{carbon} can also be defined as

$$m_{carbon} = \mu_0 I_{carbon} S_{carbon}, \tag{C.4}$$

where I_{carbon} is the electrical current flowing along the edge of the triangular cell which contains one carbon atom.

Comparing Eqs.(C.2) and (C.4), we get the relation

$$M_{sheet} = I_{carbon}. \tag{C.5}$$

Since electric current I_{carbon} is flowing along triangular loop, it induces the magnetic field B_{ind} at the center of the loop. That is given by

$$B_{ind} = \frac{9\mu_0 I_{carbon}}{2\pi a}, \tag{C.6}$$

Considering the fact that B_{ind} originates from M_{sheet}, we may write

$$B_{ind} = \mu_0 \frac{M_{sheet}}{l}. \tag{C.7}$$

From Eqs. (C.5), (C.6) and (C.7), we have

$$\frac{\mu_0 I_{carbon}}{l} = \frac{9\mu_0 I_{carbon}}{2\pi a}.$$

Hence, the effective thickness of graphene is given by

$$l = \frac{2\pi a}{9}. \tag{C.8}$$

Using the effective thickness of the graphene, we can calculate the electron density. In graphene, one conduction electron (sometimes referred as π-electron) is supplied per carbon atom. The volume occupied by one carbon atom is given by $\Omega_{carbon} = S_{carbon} l$. The electron density of graphene is give by $n = 1/\Omega_{carbon}$. Substituting values of S_{carbon} and l from Eqs.(C.3) and (C.8) into this equation, we get

$$n = \frac{6\sqrt{3}}{\pi a^3}. \tag{C.9}$$

The r_s parameter (Wigner-Seitz radius for an electron) is defined as

$$r_s = \frac{1}{a_B} \left(\frac{3}{4\pi n} \right)^{\frac{1}{3}}, \tag{C.10}$$

where a_B is the Bohr radius. Substituting eq.(C.9) into eq.(C.10), and using lattice constant of graphene: $a = 2.46 \times 10^{-10}$m, we finally get the r_s parameter of graphene: $r_s = 1.93548$

Bibliography

[1] J. W. McClure. *Phys. Rev.* , **104**, 666 (1956).

[2] J. W. McClure. *Phys. Rev.* , **119**, 666 (1960).

[3] S. A. Safran and F.J. DiSalvo. *Phys. Rev. B* , **20**, 4889 (1979).

[4] R. Saito and H. Kamimura. *Phys. Rev. B* , **33**, 7218 (1986).

[5] H. Fukuyama. *J. Phys. Soc. Jpn.*, **76**, 043711 (2007).

[6] M. Koshino and T. Ando. *Phys. Rev. B* , **75**, 235333 (2007).

[7] M. Sepioni, R. R. Nair, S. Rablen, J. Narayanan, F. Tuna, R. Winpenny, A. K. Geim, and I. V. Grigorieva . *Phys. Rev. Lett.* , **105**, 207205 (2010).

[8] A. Raoux, F. Piechon, J. N. Fuchs, and G. Montambaux. *Phys. Rev. B* , **91**, 085120 (2015).

[9] Y. Gao, S. A. Yang, and Q. Niu. *Phys. Rev. B* , **91**, 214405 (2015).

[10] G. Gomez-Santos and T. Stauber. *Phys. Rev. Lett.* , **106**, 045504 (2011).

[11] S. A. Safran. *Phys. Rev. B* , **30**, 421 (1984).

[12] M. Koshino, Y. Arimura, and T. Ando. *Phys. Rev. Lett.* , **102**, 177203 (2009).

[13] M. Ogata and H. Fukuyama. *J. Phys. Soc. Jpn.* , **84**, 124708 (2015).

[14] S. G. Sharapov, V. P. Gusynin, and H. Beck. *Phys. Rev. B*, **69**, 075104 (2004).

[15] K. Kishigi, and Y. Hasegawa. *Phys. Rev. B*, **90**, 085427 (2014).

[16] F. Escudero, J. S. Ardenghi, L. Sourrouille, and P. Jasen. *J. Magn. Matter*, **429**, 294 (2017).

[17] Y. Zheng and T. Ando. *Phys. Rev. B*, **65**, 245420 (2002).

[18] C. L. Kane and E. J. Mele. *Phys. Rev. Lett.*, **95**, 226801 (2005).

[19] Y. Zhang. Y. W. Tan, H. L. Stormer, and P. Kim. *Nature*, **438**, 201 (2005).

[20] Y. Zhang, Z. Jiang, J. P. Small, M. S. Purewal, Y. W. Tan, M. Fazlollahi, J. D. Chudow, J. A. Jaszczak, H. L. Stormer, and P. Kim. *Phys. Rev. Lett.*, **96**, 136806 (2006).

[21] D. J. Thouless, M. Kohmoto, M. P. Nightingale, and M. den Nijs. *Phys. Rev. Lett.*, **49**, 405 (1982).

[22] P. Streda. *J. Phys. C* **15**, L1299 (1982).

[23] A. H. McDonald. *Phys. Rev. B* **28**, 6713 (1983).

[24] M. Koshino, H. Aoki, K. Kuroki, S. Kagoshima, and T. Osada. *Phys. Rev. Lett.* **86**, 1062 (2001).

[25] Y. Hasegawa and M. Kohomoto. *Phys. Rev. B* **74**, 155415 (2006).

[26] Y. Hatsugai, T. Fukui, and H. Aoki. *Phys. Rev. B* **74**, 205414 (2006).

[27] M. Koshino and T. Ando. *Phys. Rev. B* **73**, 155304 (2006).

[28] R. G. Mani, J. Hankinson, C. Berger, and W. A. de Heer. *Nat. Commun.* **3**, 996 (2012).

[29] T. J. Lyon, J. Sichau, A. Dorn, A. Centeno, A. Pesquera, A. Zurutuza, and R. H. Blick. *Phys. Rev. Lett.* **119**, 066802 (2017).

[30] K. S. Novoselov, A. K. Geim, S. V. Morozov, D. Jiang, M. I. Katsnelson, I. V. Grigorieva, S. V. Dubonos, and A. A. Firsov. *Nature*, **438**, 197 (2005).

[31] K. S. Novoselov, A. K. Geim, S. V. Morozov, D. Jiang, M. I. Katsnelson, I. V. Grigorieva, S. V. Dubonos, and A. A. Firsov. *Nature*, **306**, 666 (2004).

[32] A. K. Geim, and K. S. Novoselov. *Nature Mat.*, **6**, 183 (2007).

[33] P. Avouris, T. F. Heinz, and T. Low. *2D materials: Properties and Devices.* (Cambridge University Press, Cambridge, 2017).

[34] M. Balkanski. *Devices based on Low-dimensional Semiconductor Structures.* (Kluwer Academic Publishers, Dordrecht, 1996).

[35] K. Higuchi, H. Matsumoto, T. Mishima, and T. Nakamura. *IEEE Trans. Elec. Dev.*, **46**, 1312 (1999).

[36] T. Mishima, M. Kudo, J. Kasai, K. Higuchi, and T. Nakamura. *J. Cryst. Growth.*, **201-202**, 271 (1999).

[37] G. Hellings and K. De Myer. *High mobility and Quantum Well Transistors*, Springer, New York, 2013).

[38] K. Higuchi, D. B. Hamal, and M. Higuchi. *Physical Review B*, **91**, 075122 (2015).

[39] D. B. Hamal, M. Higuchi, and K. Higuchi. *Physical Review B*, **91**, 245101 (2015).

[40] M. Higuchi, D. B. Hamal, and K. Higuchi. *Physical Review B*, **95**, 195153 (2017).

[41] K. Higuchi, D. B. Hamal, and M. Higuchi. *Physical Review B*, **96**, 235125 (2017).

[42] I. M. Lifshiz, and A. M. Kosevich. *Sov. Phys. JETP 2*, 636 (1956).

[43] K. Higuchi, D. B. Hamal, and M. Higuchi. *Physical Review B*, **97**, 195135 (2018).

[44] P. R. Wallace. *Phys. Rev.* , **71**, 622 (1947).

[45] G. S. Painter and D. E. Ellis. *Phys. Rev. B*, **1**, 4747 (1970).

[46] M. Gmitra, S. Konschuh, C. Ertler, C. Ambrosch-Draxl, and J. Fabian. *Phys. Rev. B*, **80**, 235431 (2009).

[47] H. Min, J. E. Hill, N. A. Sinitsyn, B. R. Sahu, L. kleinman, and A. H. MacDonald. *Phys. Rev. B*, **74**, 165310 (2006).

[48] M. Higuchi, D. B. Hamal, A. Shrestha, and M. Higuchi. *J. Phys. Soc. Jpn.*, **88**, 094707 (2019).

[49] K. S. Krishnan. *Nature*, **133**, 174 (1934).

[50] A. K. Geim, and I. V. Grigorieva. *Phys. Rev. Lett.*, **105**, 207205 (2010).

[51] E. I. Rashba. *Sov. Phys. Solid State* **2**. 1109 (1960).

[52] Y. A. Bychkov and E. I. Rashba. *JETP Lett.*, **39**, 78 (1984).

[53] Yu. S. Dedkov, M. Fonin, U. Rudiger, and C. Laubschat . *Phys. Rev. Lett.* , **100**, 107602 (2008).

[54] A. Messiah. *Quantum Mechanics.* (North-Holland, Amsterdam, 1966), Chap. 20.

[55] H. Friedrich. *Theoretical atomic Physics.* 3rd ed. (Springer, Berlin, 2006) , Chap. 3.

[56] E. Brown. *Phys. Rev.*, **133**, A1038 (1964).

[57] D. R. Hofstadter. *Physical Review B*, **14**, 2239 (1976).

[58] P. Hohenberg and W. Kohn. *Phys. Rev.*, **136**, B864 (1964).

[59] R. M. Martin. *Electronic Structure.* (Cambridge University Press, Cambridge, 2004), Chap. 14.

[60] T. Inui. *Electronic Structure.* (Cambridge University Press, Cambridge, 2004), Chap. 14.

[61] M. Higuchi, D. B. Hamal, A. Shrestha, and K. Higuchi . *J. Phys. Soc. Jpn.*, **88**, 094707 (2019).

[62] P. Blaha, K. Schwarz, G. K. H. Madsen, D. Kvasnicka, and J. Luitz. *WIEN2K* ed. K. Schwarz (Technische Universitat Wien, Vieenna, 2001).

[63] J. Yafet. *Solid State Phys.* **14**, 1 (1963).

[64] W. Kohn and L. J. Sham. *Phys. Rev.*, **140**, A1133 (1965).

[65] M. Levy. *Proc. Natl. Acad. Sci. U.S.A.*, **76**, 6062 (1979).

[66] M. Levy. *Phys. Rev. A*, **26**, 1200 (1982).

[67] M. Higuchi and A. Hasegawa. *J. Phys. Soc. Jpn.*, **64**, 830 (1995).

[68] H. Sugawara, M. Higuchi, O. Inoue, T. Nishigaki, Y. Aoki, H. Sato, R. Setti, Y. Onuki, and A Hasegawa. *J. Phys. Soc. Jpn.*, **65**, 1744 (1996).

[69] K. Higuchi and M. Higuchi. *J. Mag. Mag. Matter.*, **272-276**, 659 (2004).

[70] K. Higuchi and M. Higuchi. *Phys. Rev. A*, **79**, 0022113 (2009).

[71] P. Ziesche. *Phys. Lett. A*, **195**, 213 (1994).

[72] A. Gonis, T. C. Schulthess, J. van Ek, and P. E. A. Turchi. *Phys. Rev. Lett.*, **77**, 2981 (1996).

[73] M. Levy and P. Ziesche. *J. Chem. Phys.*, **115**, 9110 (2001).

[74] A. Nagy. *Phys. Rev. A*, **66**, 022505 (2002).

[75] N. H. March and R. Santamaria. *Int. J. Quantum Chem.*, **39**, 585 (1991).

[76] P. W. Ayers. *J. Math, Phys.*, **46**, 062107 (2005).

[77] M. Higuchi, M. Miyasita, M. Kodera, and K. Higuchi. *J. Magn. Magn. Matter*, **310**, 990 (2007).

[78] P. W. Ayers and S. Liu. *Phys. Rev. A*, **75**, 022514 (2007).

[79] B. Hetenyi and A. W. Hauser. *Phys. Rev. B*, **77**, 155110 (2008).

[80] M. Higuchi and K. Higuchi. *Phys. Rev.B*, **78**, 125101 (2008).

[81] K. Higuchi and M. Higuchi. *J. Phys. Condens. Matter* , **21**, 064206 (2009).

[82] K. Higuchi and M. Higuchi. *Phys. Rev. B*, **82**, 155135 (2010).

[83] M. Higuchi and K. Higuchi. *Phys. Rev. A*, **84**, 044502 (2011).

[84] M. Higuchi and K. Higuchi. *Comput. Theor. Chem*, **1003**, 91 (2013).

[85] A. Nagy. *Phys. Rev. A*, **90**, 022505 (2014).

[86] D. Chakraborty and P. W. Ayers. *J. Math. Chem.*, **49**, 1810 (2011).

[87] R. Cuev-Saavedra and P. W. Ayers.

[88] G. Vignale and M. Rasolt. *Phys. Rev. Lett.*, **59**, 2360 (1987).

[89] G. Vignale and M. Rasolt. *Phys. Rev. B*, **37**, 10685 (1988).

[90] M. Higuchi and K. Higuchi. *Phys. Rev. A*, **81**, 042505 (2010).

[91] K. Higuchi and M. Higuchi. *J. Phys. Condens. Matter* , **19**, 365216 (2007).

[92] If we consider graphene that is placed in a vacuum, then the surface potential caused by the work function is symmetric with respect to the z-axis. In this case, the SO interaction caused by the surface potential vanishes because of the parity of the wave function.

[93] S. LaShell, B. A. McDougall, and E. Jensen. *Phys. Rev.Lett.*, **77**, 3419 (1996).

[94] M. Nagano, A. Kodama, T. Shishidou, and T. Oguchi. *J. Phys.: Condens. Matter*, **21**, 064239 (2009).

[95] Y. Liu, A. Goswami, F. Liu, D. L. Smith, and P. P. Ruden. *J. Appl. Phys.*, **116**, 234301 (2014).

[96] N. D. Lang and W. Kohn. *Phys. Rev. B*, **1**, 4555 (1970).

[97] A. Shrestha, K. Higuchi, S. Yoshida, and M. Higuchi. *J. of Appl. Phys.*, **130**, 124303 (2021).

[98] H. Hibino, H. Kageshima, M. Kotsugi, F. Maeda, F. Z. Guo, and Y. Watanabe. *Phys. Rev. B*, **79**, 125437 (2009).

[99] K. Matsubara, T. Tsuzuku, and K. Sugihara. *Phys. Rev. B*, **44**, 11845 (1991).

[100] D. L. Huber, R. R. Urbano, M. S. Sercheli and C. Rettori. *Phys. Rev. B*, **70**, 125417 (2004).

[101] J.C. Slater and G.F. Koster. *Phys. Rev.*, **94**, 1498 (1954).

[102] W. Kohn. *Phys. Rev.*, **123**, 1242 (1961).

[103] T. Ando and Y. Uemura. *J. Phys. Soc. Jpn.*, **37**, 1044 (1974).

[104] E. V. kurganova, H. J. vanElferen, A. McCollam, L. A. Ponomarenko, K. S. Novoselov, A. Veligura, B. J. van Wees, J. C. Maan, and U. Zeitler. *Phys. Rev. B*, **84**, 121407(R) (2011).

[105] A. V. Volkov, A. A. Shylau and I. V. Zozoulenko. *Phys. Rev.*, **86**, 155440 (2012).

[106] M. Higuchi and K. Higuchi. *Phys. Rev.B*, **69**, 035113 (2004).

[107] K. Higuchi and M. Higuchi. *Phys. Rev.B*, **69**, 165118 (2004).

[108] K. Higuchi, E. Miki and M. Higuchi. *J. Phys. Soc. Jpn.*, **86**, 064704 (2017).

[109] K. Higuchi, H. Niwa and M. Higuchi. *J. Phys. Soc. Jpn.*, **86**, 104705 (2017).

[110] K. Higuchi and M. Higuchi. *Phys. Rev.B*, **74**, 195122 (2006).

[111] K. Higuchi and M. Higuchi. *Phys. Rev.B*, **75**, 159902 (2007).

[112] M. Higuchi and A. Hasegawa. *J. Phys. Soc. Jpn.*, **66**, 149 (1997).

[113] M. Higuchi and A. Hasegawa. *J. Phys. Soc. Jpn.*, **67**, 2037 (1998).

[114] E. McCann and M. Koshino. *Rep. Prog. Phys.*, **76**, 056503 (2013).

[115] Y. Murata, S. Nie, A. Ebnonnasir, E. Starodub, B. B. Kappes, K. F. McCarty, C. V. Ciobanu and S. Kodambaka. *Phys. Rev. B*, **85**, 20543 (2012).

公表論文
(Articles)

(1) **Reduction of g-factor due to Rashba effect in graphene.** A. Shrestha, K. Higuchi, S. Yoshida, and M. Higuchi,. *Journal of Applied Physics*, **130**, 124303-1–124303-9 (2021).

(2) **Reduced effective g-factor in graphene.** M. Higuchi, D. B. Hamal, A. Shrestha, and K. Higuchi. *Journal of the Physical Society of Japan*, **88**, 094707-1–094707-2 (2019).